THE POSITIONING OF A LOW FRICTION PNEUMATIC ACTUATOR USING ON-OFF CONTROL

M C SMITH

Ph.D
University of Edinburgh
1987

ABSTRACT

This thesis describes the development of an accurate, fast, pneumatic position control system driving an inertia load which uses a low friction, linear, symmetric, double-acting actuator controlled by a BBC microcomputer and on-off valves. The supply pressures used were approximately 5.5 *bar gauge* and masses of up to 37 *kg* were driven by an actuator of around 60 *mm* diameter.

A review of the previous work in the area is presented and this highlights the potential benefits of the use of a low friction actuator in a pneumatic control system. Two new designs of actuator using air bearings are proposed and the measurement of the friction in each is compared to a standard actuator of similar dimensions. The best design gave a 90% reduction in friction compared to the standard design; as a percentage of the maximum driving force of the actuator with a 6 *bar gauge* supply then this represents a value of less than 0.2% compared to the 2% for the standard design. This actuator almost eliminated one of the major non-linearities in the system and allowed the quasi-linear root locus and phase plane techniques to provide accurate predictions of the system behaviour under various feedback control schemes.

A non-linear computer model of the system has also been developed and this is successfully used to simulate the system behaviour under the control schemes considered. The model is theoretically based and so can be generally applied thus enabling the accurate analysis of future systems to be undertaken.

Further analysis of the actuator and load friction indicated that the friction forces at around 4 to 5 *bar gauge* can be represented to a good degree of accuracy by and empirical function of piston velocity, acceleration and differential pressure in the actuator.

Step inputs to the position control system were considered. A dual mode controller was used with the initial mode following an approximately 'time-optimal' path using feedback of position and velocity. Various feedback schemes were investigated for the second mode of control which was to complete the step. Good response using position, velocity and differential pressure feedback was achieved with an appropriate choice of feedback gains. Tests also showed that the step response was considerably worse when a friction load was applied. Finally, the various possibilities for the future development of the system are discussed.

ABSTRACT

This thesis describes the development of an accurate, fast, pneumatic position control system driving an inertia load which uses a low friction, linear, symmetric, double-acting actuator controlled by a BBC microcomputer and on-off valves. The supply pressures used were approximately 5.5 *bar gauge* and masses of up to 37 *kg* were driven by an actuator of around 60 *mm* diameter.

A review of the previous work in the area is presented and this highlights the potential benefits of the use of a low friction actuator in a pneumatic control system. Two new designs of actuator using air bearings are proposed and the measurement of the friction in each is compared to a standard actuator of similar dimensions. The best design gave a 90% reduction in friction compared to the standard design; as a percentage of the maximum driving force of the actuator with a 6 *bar gauge* supply then this represents a value of less than 0.2% compared to the 2% for the standard design. This actuator almost eliminated one of the major non-linearities in the system and allowed the quasi-linear root locus and phase plane techniques to provide accurate predictions of the system behaviour under various feedback control schemes.

A non-linear computer model of the system has also been developed and this is successfully used to simulate the system behaviour under the control schemes considered. The model is theoretically based and so can be generally applied thus enabling the accurate analysis of future systems to be undertaken.

Further analysis of the actuator and load friction indicated that the friction forces at around 4 to 5 *bar gauge* can be represented to a good degree of accuracy by and empirical function of piston velocity, acceleration and differential pressure in the actuator.

Step inputs to the position control system were considered. A dual mode controller was used with the initial mode following an approximately 'time-optimal' path using feedback of position and velocity. Various feedback schemes were investigated for the second mode of control which was to complete the step. Good response using position, velocity and differential pressure feedback was achieved with an appropriate choice of feedback gains. Tests also showed that the step response was considerably worse when a friction load was applied. Finally, the various possibilities for the future development of the system are discussed.

CONTENTS

NOMENCLATURE i

1 INTRODUCTION 1
1.1 Applications of Pneumatics 1
1.2 The Limitations of Pneumatic Systems 2
1.3 Possible Areas of Research 3
1.3.1 Conventional Linear or Rotary Actuators 3
1.3.2 Actuators For Prosthetic Applications 4
1.3.3 Defining the Area of Research 5
1.4 Review of Literature 6
1.5 Research Objectives 11
1.6 Summary 13

2 REDUCTION OF FRICTION 15
2.1 Introduction 15
2.2 Actuator Designs 16
2.2.1 Standard Actuator 16
2.2.2 Proposed Designs 16
2.2.3 Specifications 19
2.3 Test Equipment 21
2.3.1 Interface Unit 23
2.3.2 Pneumatic Circuit 24
2.4 Test Methods 25
2.4.1 Static Friction Measurement 25
2.4.2 Dynamic Friction Measurement 25
2.5 Results 26
2.5.1 Static Friction 26
2.5.2 Dynamic Friction 28
2.6 Summary 29

3 MODELLING THE PNEUMATIC SYSTEM 30
3.1 Introduction 30
3.2 Pneumatic System and Mode of Operation 32
3.3 Model Development 35
3.3.1 Cylinder Chamber Equations 35
3.3.2 Valve Equations 38
3.3.3 Equations of Motion 39
3.4 Test Equipment 41
3.4.1 Loading System 41
3.4.2 Pneumatic Circuit 45
3.4.3 Data Acquisition 45
3.5 Comparison of System and Model for the Switching of the Exhaust Valve 47
3.5.1 Improvement of Model Constants 49
3.5.2 Variation of System Initial Conditions 59
3.6 Comparison of System and Model for Motion in Two Directions 66
3.6.1 Investigation of Actuator and Load Friction 70
3.7 Summary 78

4 CONTROL SYSTEM ANALYSIS 79
4.1 Introduction 79
4.2 System Specification 80
4.3 System Synthesis 82
4.3.1 Determination of Switching Criteria for Mode 1 82
4.3.2 Root Locus Analysis for Mode 2 86
4.3.3 State Space Analysis for Mode 2 95
4.4 Computer Simulation of the Control Scheme Proposals 100
4.5 Summary 110

5 EXPERIMENTAL EVALUATION OF CONTROL STRATEGIES 111
5.1 Introduction 111
5.2 Test Equipment 111
5.3 Test Procedure 113
5.4 Scheme 1 - Position Feedback Only 116
5.5 Scheme 2 - Position Plus Velocity Feedback 116

5.6 Scheme 3 - Position Plus Velocity Plus Differential
Pressure Feedback 119
5.7 System Response With Added Friction Load 124
5.8 Summary 127

6 CONCLUSIONS 128
6.1 Summary of Research 128
6.2 Achievements 130
6.3 Future Work 130
6.3.1 Applications Development 131
6.3.2 System Development 131
6.3.3 Modelling and Analysis 133
6.4 Summary 134

BIBLIOGRAPHY 135

APPENDICES
Appendix 1 Circuit Diagram of Interface Unit.
Appendix 2 Model Programme Flowchart.
Appendix 3a System Programme Flowchart - Single Step.
Appendix 3b System Programme Flowchart - Motion in Two Directions.
Appendix 4 Simulation Programme Flowchart.
Appendix 5 System Programme Flowchart - Dual Mode Controller.
Appendix 6 Data Store Format on Disc.
Appendix 7 Publication - Low Friction Pneumatic Actuators For Accurate Robot Control.

ACKNOWLEDGEMENT

DECLARATION

NOMENCLATURE

A_O	=	Orifice effective area
A_P	=	Actuator piston area
b	=	Critical pressure ratio
c	=	Computer command (± 1)
C	=	Constant of Integration
C_{FA}	=	Constant of acceleration related friction
C_{FP}	=	Constant of differential pressure related friction
C_{FV}	=	Constant of velocity related friction
e	=	Error
f_S	=	Sanville flow function
F	=	Force
F_C	=	Coulomb friction force
F_F	=	Total friction force
F_L	=	Piston pressure force
$G(s)$	=	Forward path transfer function
j	=	$\sqrt{-1}$
k_p	=	Rate of change of pressure
K	=	Constant
K_E	=	Equivalent gain
K_p	=	Differential pressure feedback gain
K_{SW}	=	Switch function constant
K_γ	=	Constant function of specific heats and gas constant
m	=	Mass
$\dot{m}$	=	Mass flow rate
n	=	Polytropic exponent
p	=	Absolute pressure
Δp	=	Pressure difference across piston
R	=	Universal gas constant (287 Nm/KgK for air)
s	=	Laplace operator

t	=	Time
T	=	Absolute temperature
v	=	Specific volume
V	=	Volume
x	=	Piston position
$\dot{x}$	=	Piston velocity
$\ddot{x}$	=	Piston acceleration
y	=	State variables
γ	=	Ratio of specific heats
ω_n	=	Undamped natural frequency
τ_s	=	System time constant
τ_c	=	Velocity feedback gain
ζ	=	Damping ratio

SUBSCRIPTS

1	=	Supply side of actuator
2	=	Exhaust side of actuator
d	=	Desired value
e	=	Exhaust condition
i	=	Initial state
M	=	Maximum value
s	=	Supply condition

1 : INTRODUCTION

1.1 Applications of Pneumatics

The use of compressed air as a power source is widespread. It is used

- in industry; where the movement of a load or the application of a force is required.
- in aircraft and missiles; as a means of controlling flight.
- in prosthetics; to provide motion for artificial limbs.

When selecting a drive for a particular task a choice is made between electrical, hydraulic or pneumatic power. Each has its own advantages and disadvantages and these will determine the best choice for any particular task.

The advantages of using pneumatic systems are :

a) Pneumatic systems in general cost considerably less than comparable electric or hydraulic systems.

b) Pneumatic systems are very reliable. They have a high life expectancy and resist physical damage due to load vibration and shock. In addition they are superior in their resistance to contamination in wet, dirty environments. Failure is usually gradual and not catastrophic as in some electro-mechanical systems.

c) The maintenance of pneumatic systems is less complex and generally requires a lower degree of specialised training than similar hydraulic or electric systems.

d) The compressibility of air makes energy storage with a receiver easy, cheap, convenient and relatively efficient.

e) Pneumatic actuators and motors can operate consistently at full load. They can also stall indefinitely at full load without overheating. Thus the selection of the appropriate size of actuator can be made to optimise the size and cost of the unit.

f) Pneumatic devices provide high power/weight and power/size ratios across a broad range of load force.

g) Pneumatic equipment works well over a broad range of operating temperatures.

h) Compressed air presents no spark or electrical shock hazard. It is well suited to potentially flammable or explosive environments.

The ability to store high pressure air (or carbon-dioxide) and the good power/weight ratio makes pneumatic systems very attractive in prosthetics.

In industry a large number of 'pick and place' devices use pneumatic drives because of their low cost, good reliability and easy maintenance. It is even common for small factory units to have a compressed air ring main so adding new pneumatic devices is usually straightforward and economical.

For aircraft and missile controls high pressure pneumatic systems are used ($\approx$ 70 *bar*). The small variation in gas properties with temperature, the good power/weight and power/size ratios and the ability to allow the actuator exhaust to leak to atmosphere are the most significant benefits in this application.

1.2 The Limitations of Pneumatic Systems

The low bulk modulus and the low natural damping of air makes the position control of pneumatic systems difficult. Any pneumatic control system will also include significant inherent non-linearities such as actuator friction and stiction. In aircraft and missile controls, the use of high pressure gas goes some way to overcoming these problems. However, at the lower pressures that are used for safety reasons in prosthetics and industrial applications these effects are significant.

In prosthetics the advantages of energy storage and small size have outweighed the disadvantages of compressibility and non-linearity, and pneumatic systems are the most common choice. For many of these systems the control loop is closed by the human operator and many benefits can be gained from this. However, low stiffness and slow response are problems that have been the subject of much research effort in this area.

The disadvantages of pneumatics have restricted their use in industry to applications where compressibility and low damping are not important. In applications which require the control of the speed and acceleration during the move, pneumatic servo-systems are unable to provide the necessary quality of control to compete with the well developed electric and hydraulic servos. For example, there are no pneumatically driven continuous path industrial robots available today. However, a large number of industrial applications require the attainment of a new position without continuous control throughout the move. Many of these operations consist of simple movements that can be achieved by actuators working between two pre-set extremes and they are part of a continuous production process which is changed very rarely. In these cases pneumatics are generally the best choice because the control of position between the extremes is not required. In fact, pneumatic systems dominate this sector of the market. However, when a programming ability is desirable (for frequently changing work cycles) or where various positions are to be achieved during one work cycle (*eg.* palletising parts) then accurate positioning of the actuator at any point along the stroke is necessary and pneumatics are far more rarely used. Only one or two

pneumatic servo drives are commercially available and these are not widely used at present; electric and hydraulic alternatives, or the use of pneumatics with regular resetting of the mechanical end stops, tends to be preferred.

1.3 Possible Areas of Research

There has been much research effort directed at the development of pneumatic systems that can provide controllable motion. Overcoming the problems of compressibility and non-linearity would lead to a more widespread use of pneumatic drives. The many advantages of pneumatics could then be exploited in areas that require the positioning or motion of a load (*eg.* programmable 'pick and place' robots, variable pitch turbine blades *etc.*).

The initial research objective was intentionally broad and could be stated as "the investigation of the problems in the accurate positioning of a load using pneumatic actuation." First of all a general investigation into the many ways in which motion can be achieved using pneumatic power was carried out, with emphasis on the methods that are most suitable for positioning. The overall aim was to include the broadest range of ideas possible.

1.3.1 Conventional Linear or Rotary Actuators.

The most common method of obtaining motion is with a linear actuator; a cylinder and piston assembly operating with either one pressurised chamber (single acting) or two pressurised chambers (double acting). Motion of the piston and rod assembly is transmitted directly to the load. A similar method of using pressurised air to drive a load uses a radial vane in a circular chamber to provide a rotary actuator for, say, a quarter or half turn. Control of position for these actuators requires

either - controlled application of the compressed air to the actuator chambers.

or - controlled braking of the driven assembly.

These methods differ considerably. Methods involving the controlled braking of the actuator to achieve a desired end position require a detailed study of the characteristics of the braking mechanism and the combined effect of the surrounding pneumatic components. Research work in this area has been reported by Huhne (1) and Belforte (2). Variations in load mass and speed affect the positioning accuracy and so good repeatability is difficult to achieve. This has restricted the application of these systems.

Methods where the controlled application of pressurised air causes the piston and load to take up the desired position have also been the subject of research. The control system can use on-off valves which switch rapidly to pulse the air into the chambers thus moving the piston to the desired position. The valve is either fully open or fully closed, the flow of air in and out of the chambers is determined only by the upstream and downstream pressures

around the valve when it is open.

Work by Drazan (**3,4,5,6,7,8**) on computer controlled pneumatic actuators used on-off valves and this led to the marketing of a pneumatic robot capable of point to point motion. The various limitations on the use of this robot and the poor quality of the drive system meant that the system was not a commercial success. Details of this system are discussed later in this chapter.

One novel method of controlling position using on-off valves was reported by Harada (**9**) and was originally proposed by Kaiho (**10**). A number of on-off valves are placed in series at both the inlet and the outlet of the cylinder. A small volume of pressurised air is trapped between the valves and with the correct sequence of switching the piston can be pulsed a small distance. The minimum pulse distance was a function of the actuator friction and, by reducing the friction, positioning was achieved to within ±0.02 *mm*. However, positioning times for the 50 *mm* stroke actuator were sometimes as much as 20 *s*.

An alternative to the on-off valve is a servo-valve where the rate of air flow is determined by the position of a solenoid operated spool. Publications by researchers at Loughborough University of Technology (**11,12,13,14**) have described a computer controlled pneumatic position control system using servo-valves which was marketed in 1985 as a family of robot modules. At present there are only a few areas in which this system has been applied, although the performance of the drive and its positioning accuracy are very much better than the system developed by Drazan.

1.3.2 Actuators For Prosthetic Applications.

Most of the actuators used for prostheses are of the conventional linear or rotary type. However, the review of the actuators used revealed a very unusual and novel method of obtaining motion from compressed air. The actuator consists of a highly elastic 'bladder' which has around it a helically woven tube (similar to braiding on electrical cables). The load is attached to one end of this tube, the other end is rigidly mounted. When the pressure inside the bladder is increased its volume increases which causes the diameter of the woven tube to increase. Due to the helical winding of the tube the diameter increase causes the tube to decrease in length and thus the application of a force to the load is achieved. This unidirectional actuator is known as McKibben Muscle and is usually operated as an antagonistic pair. A positional servo-mechanism using these actuators for prosthesis control is described in Gavrilovic (**15**). The main advantage of this actuator is that it exhibits no static friction, it suffers no alignment problems and it is very light and inexpensive. However, the muscle does exhibit considerable viscous friction and has a poor stroke to length ratio.

Another method of obtaining motion from compressed air used a rotary pouch actuator for prosthesis motion, and this was described by Bousso (16). A number of interconnecting inflatable pouches are radially restrained at a hinge. When the pouches are inflated they cause the rotation of the hinge. Very low values of friction and stiction and an excellent size/stroke ratio can be obtained using this actuator. Again the applied force is in a single direction and so this actuator is used in pairs or requires a return spring.

Finally a useful idea came from the review of prosthetics. It arose after viewing the method by which 'perfect' cushion shape is obtained for wheelchair patients. Small expanded polystyrene beads partially fill a large polythene bag. When the pressure in the bag is reduced using a vacuum pump, the bag contents gradually solidify. This could be adapted to be a tubular 'bag' positioned alongside a pneumatic actuator and coupled to the piston rod. When open to atmosphere the actuator would move almost unrestrained by the coupled tube. When evacuated the particles in the tube would lock the actuator in position. With the appropriate choice of particle material and size, geometry and pressure within the tube, the effective viscosity of the actuator/tube assembly could be varied thus introducing stiffness and damping to the system.

1.3.3 Defining the Area of Research.

This review of the general area of pneumatic actuation showed the broad range of devices that could be used for motion control. The solution to the problems of positioning the actuator will depend upon the type of actuator used and that choice is determined mainly by the use that is to be made of it. The specialist requirement of efficient energy storage and small size and weight have stimulated some novel developments in the area of prosthetics which may be applicable in some industrial areas too. There is undoubtedly considerable scope for research in the use of McKibben muscle, variable viscosity damping and rotary pouch actuators for pneumatic positioning systems, but this is not to be investigated in this thesis.

The largest group of actuators, used for the majority of applications in industry, are the linear and rotary types using a piston or vane. Research leading to a positioning capability for this type of actuator using computer control has enabled the development of some small to medium sized robots. These have had only limited commercial success which suggests that there are still some problems to be overcome. The objective of this research was therefore narrowed to be in the area of linear or rotary actuators positioned using pneumatic valves under computer control, that may be used as a programmable point to point drive for a small to medium sized industrial robot.

1.4 Review of Literature

A review of the previous work in the area of pneumatic position control of linear or rotary actuators was carried out in order to assess the performance capabilities of pneumatic systems already developed. In this way the difficulties of pneumatic position control could be understood and the outstanding problems identified so that a more specific area of research could be established.

The research work looked at could be split into two main groups which were sometimes reported on concurrently.

- Implementation studies; the testing and evaluation of system proposals, the effect of various system parameters and good system design.
- Simulation studies; the modelling of pneumatic systems, the evaluation of the accuracy of the model and the analysis of system non-linearities.

Most of the literature refers to the early work by Shearer (**17,18**). A four-way pneumatic servo-valve was used to control a double acting symmetrical actuator driving an inertia load against a constant force. The analysis of the system made a number of assumptions to simplify the mathematical treatment of the non-linearities. For example :

- the equations relating the pressures and the volumes of the cylinder chambers were linearised by assuming only small changes about the centre stroke position.
- friction was assumed to be viscous only (no static friction).
- the load force and the load mass were small so that only small changes to the chamber pressures occurred.

As a result of an analogue computer simulation of the simplified system, a scheme using transient pressure feedback was proposed and was shown to successfully stabilise the system for large values of feedback time constant. A practical realisation of this scheme was achieved by using two 'stabilising tanks' or plenum chambers connected to the supply lines between valve and cylinder (one in each line) via capillary resistances. Shearer later developed a more complex non-linear analogue computer simulation of a high pressure pneumatic servo (**19**) which included coulomb friction and this was shown to be an effective tool in attaining optimum designs of the system using stabilising tanks. This work also showed that the simplified linear analysis was not able to predict the actual system response accurately.

Davies (**20**) made gross linearising assumptions to represent a pneumatic position control system as a third order system. This could be stabilised by using velocity, acceleration or transient pressure feedback (assuming constant applied load force), or a combination of

these. Burrows (**21**) and Lord (**22**) demonstrated the benefit of stabilising tanks but comment that the excessive bulk of the tanks make them unsuitable for applications with restricted availability of space.

Eun (**23**) used fixed volume tanks to stabilise a pneumatic system but he also evaluated a means of achieving transient pressure feedback using a cylinder orifice (the two cylinder chambers were connected via an orifice). He concludes that positioning accuracy for the system using a cylinder orifice is superior to that using stabilising tanks, but that the output stiffness is reduced. Eun also suggested the use of velocity feedback to improve the system accuracy but this was found to be less effective than transient pressure feedback using tanks or a cylinder orifice. Burrows (**24,25**) also demonstrated the stabilising effect of velocity feedback combined with acceleration feedback in an analogue computer simulation of a pneumatic position control system.

Most of the above work applies to systems with servo-valves, which enable small quantities of compressed air to enter the cylinder for small system errors. The work by Burrows (**21,24,25**) and Eun (**23**) used on-off valves, where the valve is either fully open or fully closed. There are a number of advantages in using on-off valves over using servo-valves. Servo-valves are expensive to produce as they require accurate machining and are generally of complex design. Another important consideration in the use of on-off control is that this form of control provides the theoretical time-optimum response of the system; the valve reacts to an error signal by applying the maximum flow of air to correct it. Also it is a simpler task to interface an on-off valve to a digital computer system than the analogue driven servo-valve.

It is for these reasons that the first major effort to produce a low-cost pneumatically controlled robot utilised on-off valving. Drazan built what is thought to be the first pneumatically driven programmable robot in 1975. The robot was controlled by a digital computer and was fitted with an optical sensor. It was capable of following a light source, but its speed of response and stability were poor. The system in its original state used linear actuators with each one driven by a single 5-way on-off valve. Drazan demonstrated the stabilising effect of restricting the peak velocity of the actuator when the position error was within a pre-defined band. He also reports (**3,4**) considerable difficulties in controlling the robot arm due to :

- the compressibility of air and large pneumatic volumes.
- the delays in the pneumatic system.

- the friction in the cylinder.
- the delays in the response of the valve.
- the high ratio of the static to dynamic friction.
- the limited resolution of the 8 bit analogue to digital converter.
- the high inertia forces and near zero viscous forces.

In order to overcome these difficulties the rate of supply of air to the cylinder was considerably reduced by throttling and the output response was consequently very slow. Experimental results for a step displacement of 70% of the maximum shows that the time taken to reach ±2% of the target was 14 *s* (**4**). Later developments of the robot included counterbalancing the weight of the arms, replacing the linear actuators with rotary actuators and the careful reduction of the amount of friction in the robot arm structure. A linearised analysis of the system was carried out and this suggested the use of velocity feedback. An improved step response was obtained using this feedback scheme but a limit cycle existed. This was overcome by the use of a 'controlled friction' operating in the vicinity of the target (**6**). An improved speed of response was also demonstrated using a dual mode controller; two different control schemes were used depending on the system error. For large position errors (caused initially by a step input to the system) the error is reduced at the maximum rate. When the system is detected to be less than a set distance from the target the second mode of control is entered and the velocity feedback scheme is used. In this way the stabilising effect of velocity feedback is gained near to the target, together with fast response initially that rapidly removes large system errors. Quantitative examples of the benefit of the dual mode controller were not given, although for high velocity feedback gain a decrease in positioning time is clearly obtained. The last reported work on the pneumatic robot system concentrated on the difficulties encountered with the quasi-continuous control of motion of the arm between successive set points (**7**). A control algorithm was developed that was able to smooth the continuous motion of the robot between these points. However the methods used were specific to the system analysed and so were not widely applicable.

Drazan used various models of the on-off controlled pneumatic system through the period of his work. The most complex model was an empirical one where the characteristics of the highly non-linear valve-motor pair were experimentally measured and then modelled by fitting a polynomial of degree 10 (**8**). The model is again specific to the system under consideration, but it was able to show that the friction in the actuator is significant and can be quite accurately modelled as a stiction term, a constant term and a term dependent on the

differential pressure. The main drawback of this approach to modelling is that it cannot be directly applied to other systems. Changes to parameters such as cylinder diameter or valve size cannot be accommodated in the model without resorting to further experimental measurements. Drazan had also been quite specific in the way that the performance of the system had been improved; a general approach had not been taken and work had been directed at improving the performance of the robot arm rather than to improve the positioning ability of the actuator itself.

A theoretical model of the dynamic behaviour of a linear pneumatic actuator was developed from first principles by Bowns (**26**). The model was constructed to simulate the motion of a linear actuator over a complete stroke when loaded with an inertia and operated with a pair of on-off valves. No attempt was made to model the dynamics of stopping the actuator at a position on the stroke. However, the reported work on the development of the model gave a good indication of the parameters which are most important in establishing a good model.

Bowns split the problem into three parts:

a) The determination of the airflow through the valve.

b) The charging and discharging of the actuator.

c) The motion of the piston and load.

The valve was modelled as a series of orifices and an empirical formula first proposed by Sanville (**27**) was used to improve the mass flow prediction for pressures below the critical pressure ratio. Representation of the charging and discharging process was similar to the model by Burrows (**24,25**) and was developed from the early work by Horlock (**28**). The motion of the piston and load was modelled as an inertia plus friction force.

A digital computer was used to evaluate the model predictions and experimental tests were carried out to assess its accuracy. It was found that the main obstacle to accurate prediction was the friction characteristic of the actuator and load. With careful measurement of the friction force the results of the simulation were shown to give a high degree of agreement with the experimental results. Friction was represented by an empirical formula made up of a constant, a velocity related friction and a friction proportional to the pressure difference across the actuator. Bowns continued the work by investigating the effect of seal friction on the stroking time of the actuator, and how the seal friction varies with a change in system parameter such as supply pressure or cylinder barrel surface finish (**29**). The many variables that can effect the friction levels in the actuator made it difficult to draw conclusions from the large number of tests carried out. In a later paper (**30**) the simulation was

used to examine the behaviour of the actuator when under various operating conditions. The effect of the inlet and outlet port sizes were investigated and it was shown that the ratio of these sizes is an important criteria in obtaining smooth operation of the actuator; a poor choice could cause oscillatory motion. Another interesting result was that the stroking time was basically insensitive to changes in load inertia; it was found that the speed of motion was limited by the choked conditions in the exhaust port.

The digital computer simulation proposed by Bowns can be used to predict the behaviour of pneumatic valve and cylinder combinations over a wide variety of operating conditions. It is a model that is theoretically based, although the good accuracy obtained does rely on empirical relationships for mass flow through the valve and for actuator and load friction. The valve relationship is well proven and it takes account of a reduced mass flow through the valve when the pressure ratio around it is not sufficient to cause sonic conditions. Friction remained the most important, and the most difficult, parameter to model.

The second development of a pneumatically powered robot device was carried out by Weston and Moore (**11,12,13,14**). A single electrically operated servo-valve was chosen to control the linear actuator in place of the single on-off valve used by Drazan. A linearised model of the servo-valve, actuator and load was developed from the early work by Burrows (**24,25**). It was assumed that the valve could be represented by a linear characteristic and that the actuator and load friction effects were negligible. The analysis suggested the use of position, velocity and acceleration feedback (**13**). The gain of the feedback signal was chosen to be a function of load position so that an improved dynamic performance could be achieved for different types of move. It was also found that a variation in the position loop gain with position error was beneficial in reducing the dead-band and increasing the static stiffness whilst retaining stability for large position errors. In the system tested the variation in position gain was linear and a decrease in loop gain occurred with an increase in position error. The variation in velocity loop gain with error was non-linear; below a certain set value of error the gain was increased with a decrease in position error, above the set value the velocity gain took a constant value. The use of this non-linear gain allows the control damping to increase as the target position is reached which ensures stability, and it allows a fast dynamic response when the position error is large (**11,13,14**).

Weston also describes the use of 'front end' control schemes to improve the system response and to overcome some of the problems experienced with the drive (**11,12**). Front end control is based on an outer decision loop which modifies the command issued to the existing closed loop drive. In the first scheme, called saturation control, a maximum command signal is generated in the inner control system at the start of the move in order to

overcome stiction in the piston and load assembly. A return to the normal control scheme occurs when the first movement of the actuator is detected. A significant improvement in response for short moves was achieved using the saturation front end scheme. Two further front end schemes were also investigated. These were used in addition to the saturation control and were termed set-point modification schemes. Immediately after saturation control a command signal equal to twice the original command signal is applied until the system error is half of the original error. Following this a negative saturation signal is applied for a set time period to decelerate the drive as it approaches the target position. Finally the normal control scheme (without front end adjustment) completes the move. Again this front end control scheme is shown to significantly improve the performance of the drive (**11**).

Most of the experimental tests on the servo-system developed by Weston and Moore had only the intrinsic inertia load of the piston and slide-way, ie about 3.5 *kg*. Some tests were carried out for higher masses (8 and 13 *kg*) (**11**) and these showed a marked increase in overshoot and rise-time. It was concluded that the system parameters should be chosen to suit the loading condition in any particular application so as to retain an acceptable dynamic response.

A development of a similar system was reported by Nguyen (**31**). Positioning accuracy was attained to within 0.1 *mm* although this was not possible for a wide variety of loads and step sizes. It was observed that one limitation on the attainment of an improved positional accuracy was the friction within the actuator and slide-way and that a reduction in this would offer many benefits.

1.5 Research Objectives

The most successful development of a position controlled pneumatic actuator has been carried out by Weston and Moore in collaboration with an industrial sponsor, and this has led to the marketing of a range of 'programmable actuator' modules capable of being positioned at any point on the stroke to within ±0.1 *mm*. This positioning capability is achieved only after the 'setting up' of the drive for a particular loading condition. The system, although cheaper than a comparable electric or hydraulic drive, is an expensive alternative to the traditional pneumatic device which uses pre-set mechanical end stops, because it uses a servo-valve to control the air flow into the cylinder. The ability to allow small quantities of air into the cylinder when near to the target position is the main advantage of the servo-valve. Computer control of this valve means that an expensive digital to analogue converter is also required. The cost of the system is one reason why it has not found widespread use to date. A system using a servo-valve does not provide the speed of response of an on-off system because the air flow through the servo-valve is not as high

unless it is saturated. In order to retain a good speed of response, a front end control scheme is used to cause saturation of the valve until quite near to the target position. This type of operation moves the system towards the category of on-off control but an expensive servo-valve is used to provide this.

It may be possible to develop a system which uses an on-off valve to control the air flow. The valve would be much less costly, would allow fast response of the system and, with computer control, it may be able to provide a sufficient level of positioning accuracy.

As discussed, a positioning system controlled by a computer using an on-off valve was developed by Drazan in 1977/78. The main problems that halted the work were the difficulties in overcoming the complex friction and compressibility effects. The computer systems available at that time did not allow the processing of very complex control algorithms in real time and so only simple feedback schemes were evaluated. Also, the use of rotary actuators (dictated by the installation requirements of the robot) would have worsened the effects of friction because of their large seals and poor geometry.

It is clear that, with the improvements in computer technology, there is scope for further development of on-off computer controlled pneumatic systems particularly if combined with pneumatic components that minimise the problems of friction and compressibility. A linear actuator with low friction piston seals and rod bearings would reduce the problems of friction in the actuator. Low friction could be achieved at the expense of some leakage as it has been reported that the presence of leakage will return some damping to the system (**23**). One of the main effects of compressibility is the significant time delays in transmitting pulses along the supply and exhaust lines. If the control system requires the measurement of chamber pressure there may be another time delay along the transmission lines to the pressure transducer. These problems can be minimised by using two on-off valves and two pressure transducers one at each end of the actuator.

In order for the system to be developed for use as a drive for a small to medium 'pick and place' programmable robot, it will be necessary to achieve positioning with a medium load, therefore the system will be developed to drive an inertia load of up to 40 kg.

It is likely that a model of the system will be required in order to aid the synthesis of an appropriate control algorithm. Drazan had developed an empirical model but this had only limited use to the specific system developed. The most accurate model that was theoretically based was presented by Bowns but this had not been extended to be used in a control system simulation. The main difficulty with modelling was the determination of the friction characteristic of the actuator and load. With the development of a low friction actuator this problem should be reduced and a more accurate model obtained. The model, together with

a linearised analysis of the system, can be used to develop an appropriate control scheme. Detailed analysis of the control system can follow, with investigations into other feedback schemes and system designs. Feedback schemes similar to that tried by Weston and Moore can be investigated in the on-off system. ie :

- Non-linear feedback schemes; to compensate for variations in system response with piston position or chamber pressure.
- Learning schemes (adaptive control); to compensate for variations in system response with load mass and force.

The effect of variations in the system components can be assessed by simulation or testing. Optimisation of the cost/performance of the valves and transducers can be carried out when a more thorough understanding of the important parameters is gained. It will also be possible to reduce the cost of the low friction seals and bearings in the actuator when the benefits of low friction are quantified.

1.6 Summary

The use of compressed air as a power source has many advantages. Pneumatics are generally fast, reliable, clean and inexpensive. The use of pneumatics in industry is widespread but the area of application has so far been limited to tasks which do not require the accurate positioning of a load at any position on the stroke. The compressibility of air and the existence of high levels of static friction in the actuator/load make the task of accurate positioning difficult at present.

A low cost computer controlled pneumatic position control system would be an attractive alternative to the more established electric and hydraulic drives for applications where a very high degree of positional accuracy is not required but some level of programmability is necessary. It will also be possible to take advantage of some of the many benefits of pneumatics (*eg.* safety, reliability *etc.*) in new areas that were previously served only by electric or hydraulic systems.

The development of a computer controlled pneumatic position control system is described in this thesis. The positioning problems caused by the typically high levels of friction in the actuator (seals and bearings) are overcome by the design of a low friction linear actuator which is described in Chapter 2. Chapter 3 describes the development of a mathematical model of the on-off valve, low friction actuator and load system. A more thorough understanding of the friction forces in the actuator is obtained and this is included in the model as an empirical function of velocity and pressure difference across the actuator. Correlation of the model output with experimental measurement of the system response is

carried out to evaluate its accuracy and its suitability for use as a tool for the analysis of various system proposals.

Analysis of the control system proposals is described in Chapter 4. Linearising assumptions are made in order to assess the stability of the system using the root locus technique. Velocity and differential pressure feedback schemes are proposed by the analysis and these are further analysed in the state space, assuming a piecewise linear system. The non-linear computer model is then extended to simulate the control scheme proposals, and this provides a means of tuning the feedback parameters to obtain improved system response.

Chapter 5 describes the experimental tests carried out using the feedback schemes considered and the accuracy of the computer simulation is confirmed. Tests with an added friction load are also described and these enable a comparison to be made between a system using a low friction actuator and one using an actuator with more typical friction levels.

A summary of the research described is given in Chapter 6, together with a discussion of some of the work that is required to continue the development of the system towards particular areas of application. There are a number of possible routes for development, and it is hoped that these will lead to a variety of pneumatic position control systems that can be more widely applied and can offer significant benefits over systems available at present.

2 : REDUCTION OF FRICTION

2.1 Introduction

All of the points of sliding contact in a pneumatic actuator are sources of friction. In a linear actuator the points of contact are between the piston and cylinder and between the rod and cylinder at the end of the actuator. In a typical design bronze or acetal resin bearings locate the rod and piston assembly and nitrile rings provide an air seal. These materials offer good wear resistance and minimise leakage from the cylinder and across the piston, but in order to achieve this they cause a considerable amount of friction.

In normal use a typical pneumatic actuator is driven from one extreme of its motion to the other. Different stroke lengths are obtained with mechanical stops and the amount of friction is not of vital importance to the function of the actuator, the only cost of high friction in most cases is a slight reduction in power. Because of this, and because low friction, durability and low leakage are conflicting requirements of the design, bronze bearings and nitrile rubber seals have been found to be a good compromise after many years of development, despite their high friction.

If the position of the actuator between the end stops is to be controlled by the appropriate application of pressurised air to the two chambers, then friction is of far greater importance. Movement will only begin after a pressure difference is established that is great enough to overcome the static friction. Dynamic friction is likely to be lower than static and this, combined with the low bulk modulus of air, will cause significant problems when making small movements or when attempting to stop accurately at a target position. The standard design with its high friction would suffer these problems if it was used in a servo system. In order to overcome these problems it was decided to attempt a re-design of the sealing methods to develop a system more suited to servo control applications.

Many different methods of reducing friction were considered. They were assessed on their likelihood to offer significant reductions in friction and on their ease of manufacture and cost.

Following a survey of the types of piston seal available, two types were selected for further investigation; a PTFE composite seal and a pair of rubber rolling diaphragm seals. At the piston rod, the application of an air bearing offered the greatest reduction in friction. Consideration was given to installing an air bearing at the piston too, but this was rejected on the basis of design complexity and cost.

Two low friction symmetrical actuators were designed. Both designs used air bearings at the ends of the cylinder but they differed in their method of piston seal. These were compared to a conventional actuator of comparable size bought 'off the shelf'.

Two methods of measuring friction were used. The first measured the static friction or stiction, the second measured the dynamic friction (that force required to maintain constant velocity motion of the actuator). The friction of each actuator design was then compared to determine which of the sealing methods was the most effective at reducing the friction. This design could then be used in the development of an accurate position control system.

2.2 Actuator Designs

2.2.1 Standard Actuator

The asymmetric actuator, referred to as Type 0, is shown in figures 2.1 and 2.2. It utilises rubber seals and bronze piston rod bearings and a piston seal of two nitrile U cups with a central acetal resin wear strip.

Being of asymmetrical design the radial loads and torque on the piston and rod assembly are transmitted to the cylinder by the rod bearing and piston wear strip. The bronze rod bearing has been designed to have sufficient length to support some torque loading and the acetal wear ring prevents the piston scuffing the cylinder wall and removes radial load from the U cups. Air leakage around the rod is prevented by rubber seals housed in the cylinder end cap.

2.2.2 Proposed Designs

Two symmetrical, double acting actuators of similar size were designed to evaluate two methods for reducing friction. A symmetrical actuator may seem a bad choice for a low friction design because there is an extra point of sliding contact in a symmetrical actuator compared to an asymmetrical one. However, the method by which axial moments on the rod and piston are transmitted is improved, particularly on a long stroke actuator, as the moment is now transmitted through the two rod bearings which have a greater spacing than the piston wear strip and rod bearing in the asymmetric design. This reduces the radial load for a given moment and this would therefore reduce the axial friction force.

Both designs (Types 1 and 2) incorporated almost identical air bearings at the cylinder ends to locate the piston rod and piston assembly and seal the cylinder. A drawing of the air bearing arrangement is given in figure 2.3.

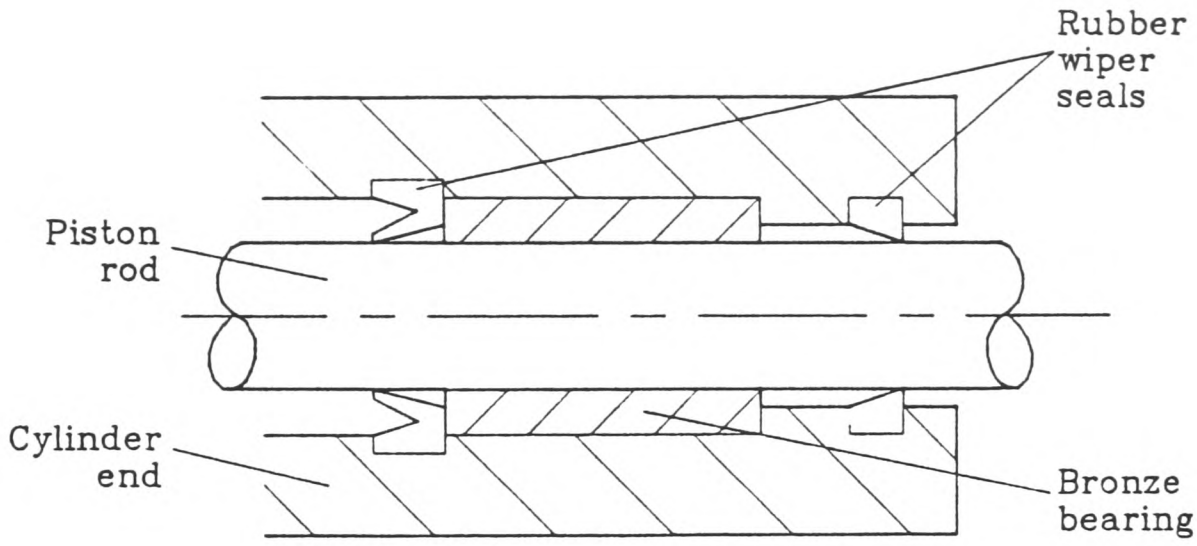

FIGURE 2.1 Piston rod seal and bearing. Actuator Type 0.

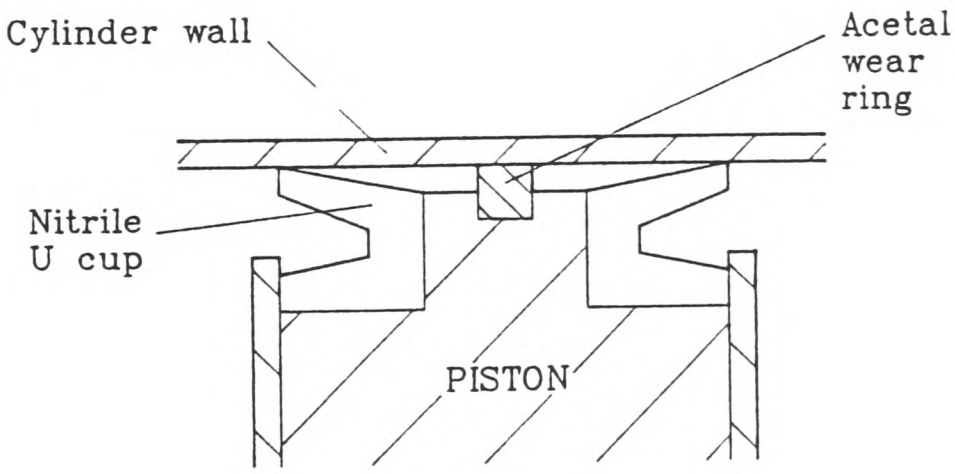

FIGURE 2.2 Piston seal. Actuator Type 0.

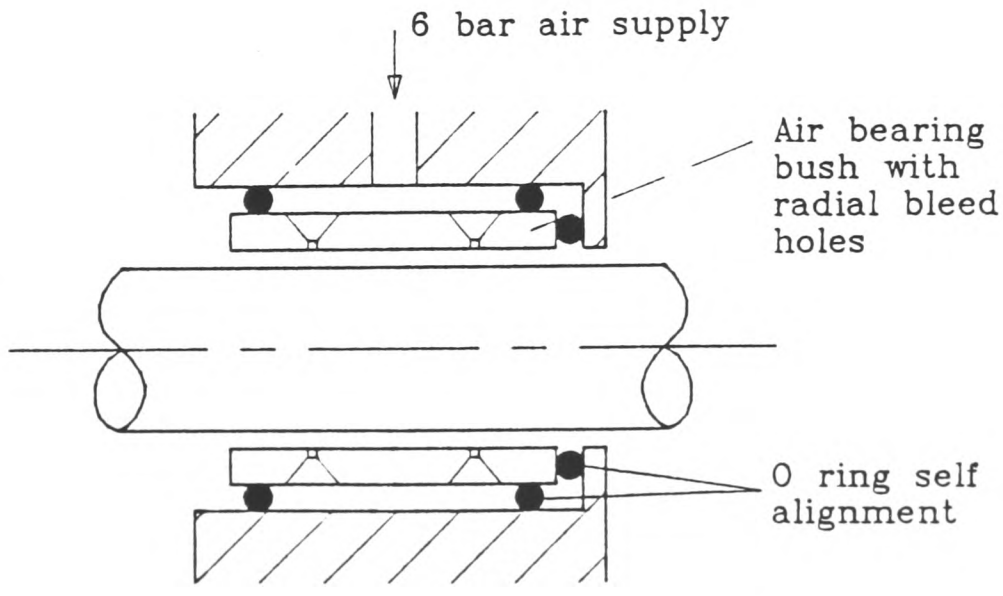

FIGURE 2.3 Air bearing arrangement for Types 1 and 2.

The air bearing consists of the piston rod as the inner member and a static brass bush with radial bleed holes as the outer member. To allow for some variation of straightness and concentricity of the piston and rod assembly and the cylinder bore, the mounting of the two air bearing bushes has been designed to allow self alignment.

A 6 *bar gauge* air supply pressurises an annular chamber around the bush and forces air through the radial bleed holes. The air flows axially along the rod in both directions to lubricate the bearing and form an air gap between rod and bush. The bleed holes act as restrictors to the air flow. The role of these restrictors is to provide a pressure drop between the supply pressure and the film pressure so that the latter can compensate for changes in radial load - ie the bearing has stiffness. There is an optimum restrictor geometry for which bearing stiffness is a maximum. For practical purposes the lower limit on the bleed hole diameter was set to 0.2 *mm* and the bearing diameter was set by the piston rod. Empirical tables (**32**) were then consulted to set the other parameters.

It is important that the installation of the actuator is such that the driving force is transmitted to the load in an axial direction. This will ensure that the radial load on the air bearings is less than the design maximum.

The two designs of low friction actuator differed in their method of piston sealing. The first design, Type 1, uses a PTFE compound composite seal at the piston mounted as shown in figure 2.4.

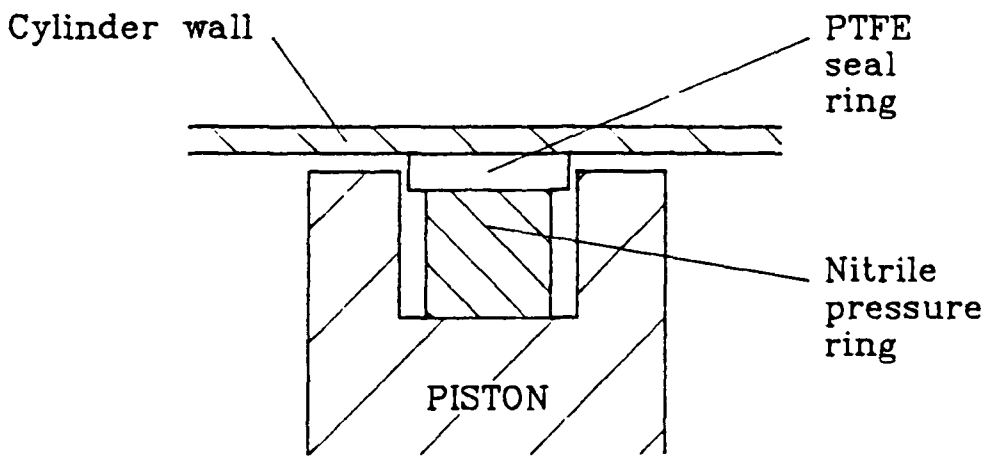

FIGURE 2.4 Piston seal. Actuator Type 1.

The seal comprises of two parts, a guide ring of PTFE and a contact seal ring of elastic Acrylonitrile-Butadiene. The PTFE compound contains a glass fibre filler to improve its wear resistance without significant effects on the coefficient of friction or elasticity. A typical value of the coefficient of friction for this material is 0.14.

The second design, Type 2, uses a rubber diaphragm seal on the piston mounted back to back as shown in figure 2.5.

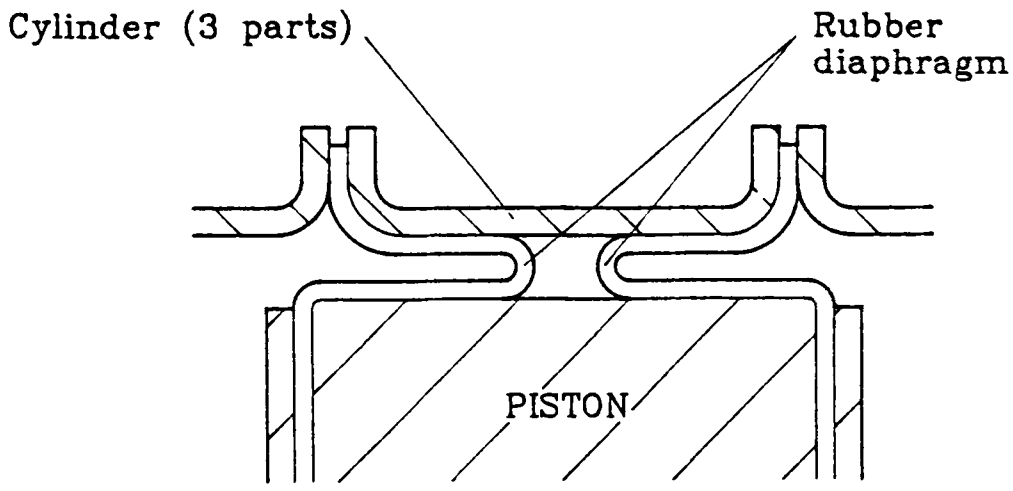

FIGURE 2.5 Piston seal. Actuator Type 2.

The seals are manufactured from a layer of woven fabric impregnated with a thin layer of elastomer. They are formed as a 'top hat' and are installed with a convolution between the cylinder and piston. As the pressure forces the piston to move, the diaphragms roll up and down the piston providing a smooth low friction seal.

2.2.3 Specifications.

The specifications of the three actuator types are given in table 2.1. The air bearing specification is given in table 2.2.

ACTUATOR	TYPE 0	TYPE 1	TYPE 2
Design	Double acting, asymmetric	Double acting, symmetric	Double acting, symmetric
Bore (*mm nom*)	57	64	76
Stroke (*mm*)	204	295	120
Max force. *N* (nom. at 6 *bar*)	1400	1750	2600
Cylinder material	Al. alloy	Al. alloy	Al. alloy
Piston	One piece Al. alloy	Split Al. alloy	Split Al. alloy
Rod material	Chrome plated mild steel	Silver steel	Silver steel
Piston seals	Acetal resin and 2 nitrile U cups	PTFE compo-site seal	Rubber diaphragm
Rod bearings	Bronze bearing and nitrile wipers	Air bearing	Air bearing

TABLE 2.1 Actuator specifications.

Diameter	18 *mm nom*
Stroke	300 *mm max*
Length	19 *mm*
Radial clearance	0.02 *mm*
Supply Pressure	6 *bar gauge*
Orifice type	Inherent restriction
Number of planes of air entry	2
Positions of planes	5 *mm* and 14 *mm*
Number of holes in each plane	10 equally spaced
Bleed hole diameter	0.2 *mm*

TABLE 2.2 Air bearing specification.

2.3 Test Equipment.

For all of the tests the actuators were mounted horizontally in a rigid space frame which allowed quick interchanging of the three actuator designs.

A BBC 'B' microcomputer was used to record all data from the rig and to control the pneumatic circuit. The choice of digital storage of data and control of the pneumatics was made so that the equipment could easily be adapted for the later work on computer control.

Measurements of the piston position and the two chamber pressures were required. Details of the transducers are given in table 2.3.

The analogue signals from the three transducers were recorded by the BBC computer via a 12 bit analogue to digital converter (ADC) housed in a purpose-built interface unit. The unit also housed the circuitry required for the on-off valve which controlled the air supply. A schematic drawing of the arrangement is given in figure 2.6.

INPUT	TRANSDUCER	INPUT RANGE	OUTPUT RANGE(*V*)
Piston position	Linear variable differential transformer device	0 to 400 *mm*	-1.5 to 1.5
Chamber 1 pressure	Piezoelectric signal conditioned device	0 to 6 *bar gauge*	0 to 10
Chamber 2 pressure	Piezoelectric signal conditioned device	0 to 6 *bar gauge*	0 to 10

TABLE 2.3 Details of Transducers used.

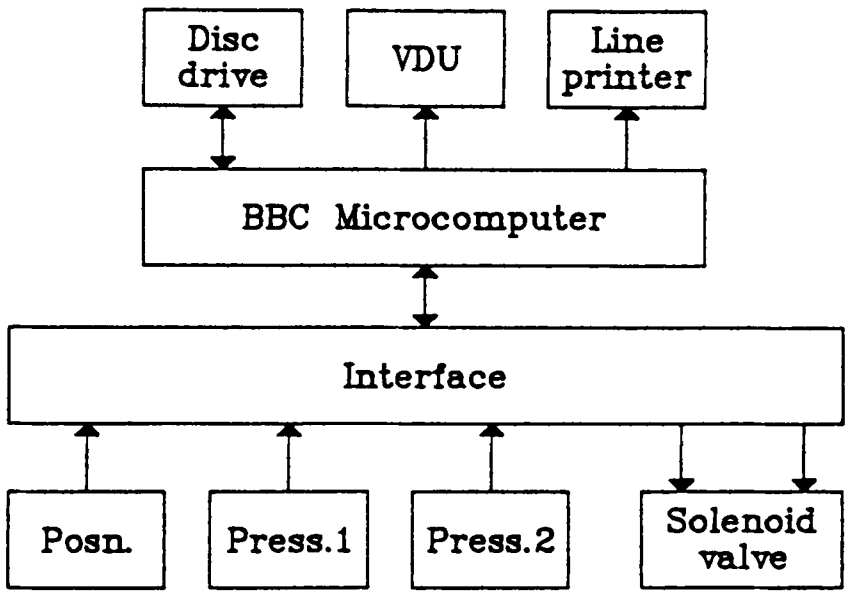

FIGURE 2.6 Schematic of the hardware arrangement.

2.3.1 Interface Unit

The layout of the components of the interface unit is shown in figure 2.7. A circuit diagram for the final unit is given in Appendix 1.

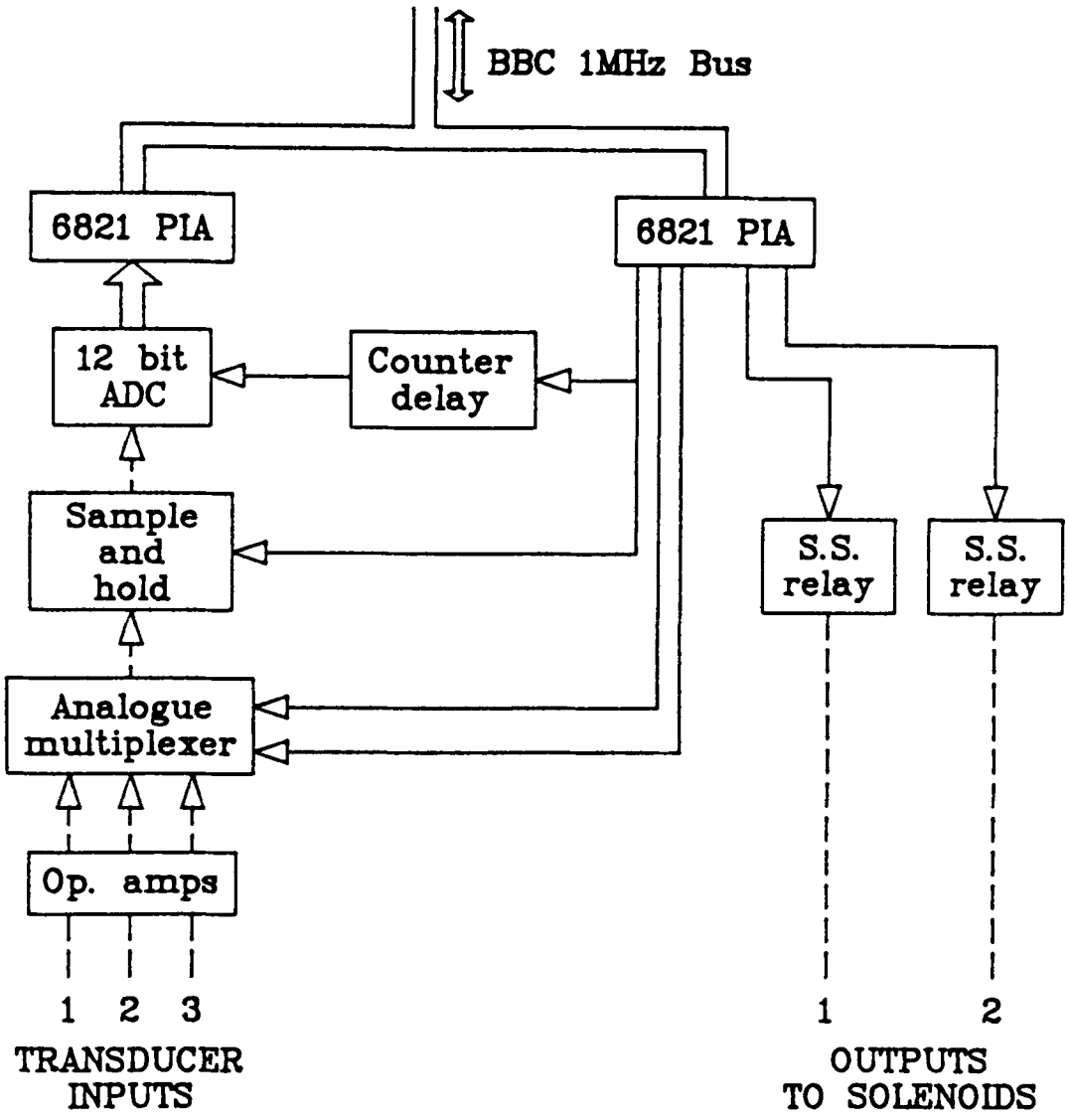

FIGURE 2.7 Schematic of the interface.

Two 6821 programmable interface adaptors (PIA's) are connected to the BBC 1 *MHz* bus. These act as memory mapped input/output devices and are directly addressable by the computer. In order to simplify the connections and the programming, one PIA is used for all of the input channels, another for all outputs.

Three analogue inputs enter the unit; two pressure signals and the linear potentiometer signal. The position signal is amplified to match the maximum input range of the ADC. Any one of the three signals can be selected using the analogue multiplexer switch. It is then passed through the sample and hold circuit to the ADC. The sample and hold is important as the ADC sets the 12 bits sequentially over a period of around 25 *micro-s* starting from the high bit, and a large error could occur on a rapidly changing analogue input. This 12

bits of data are then passed onto the BBC computer by the PIA which is used exclusively for inputs.

Two digital outputs to control the pneumatic valve originate as a software command to the BBC 1 *MHz* bus and these are passed on by the output PIA to the solid state relays. The relays use the 0/5 *V* digital signals to switch the two output signals of 0/250 *V* ac which supply the solenoids on the pneumatic valve.

A further three digital output signals from the output PIA are required to control the multiplexer, sample and hold and the ADC. Two lines control the multiplexer switch, the third activates the hold of the analogue signal and initialises a counter delay circuit. The delay circuit is driven by the 1 *MHz* clock on the BBC bus and after a 32 *micro-s* count a pulse is sent to the ADC to begin the conversion. This delay is provided to allow the sample and hold circuit to charge the hold capacitors and to stabilise its output.

2.3.2 Pneumatic Circuit.

Two of the actuators required an air supply to the air bearings. Type 0 did not. Thus two different circuits were used for the friction tests. The circuit for the Type 0 actuator is shown in figure 2.8. A 6 *bar gauge* pressure line is filtered through a 5 *micron* filter and regulator unit. This feeds a solenoid operated spool valve which controls the direction of air flow to the actuator.

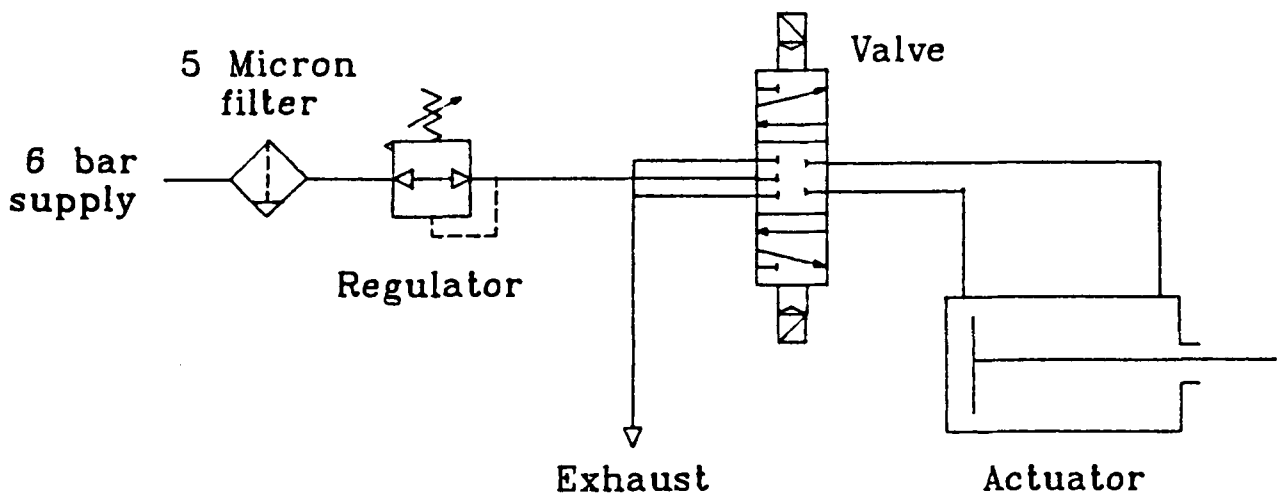

FIGURE 2.8 Pneumatic circuit for actuator Type 0.

The circuit for the Type 1 and 2 designs is shown in figure 2.9. A 6 *bar gauge* supply is again filtered by a 5 *micron* filter unit. It is then supplied direct to the air bearings. The bleed air from the bearing that enters the cylinder chamber is exhausted through a variable restrictor. Thus the pressure on each side of the piston can be controlled by varying the

amount of restriction of the air flow out of each chamber.

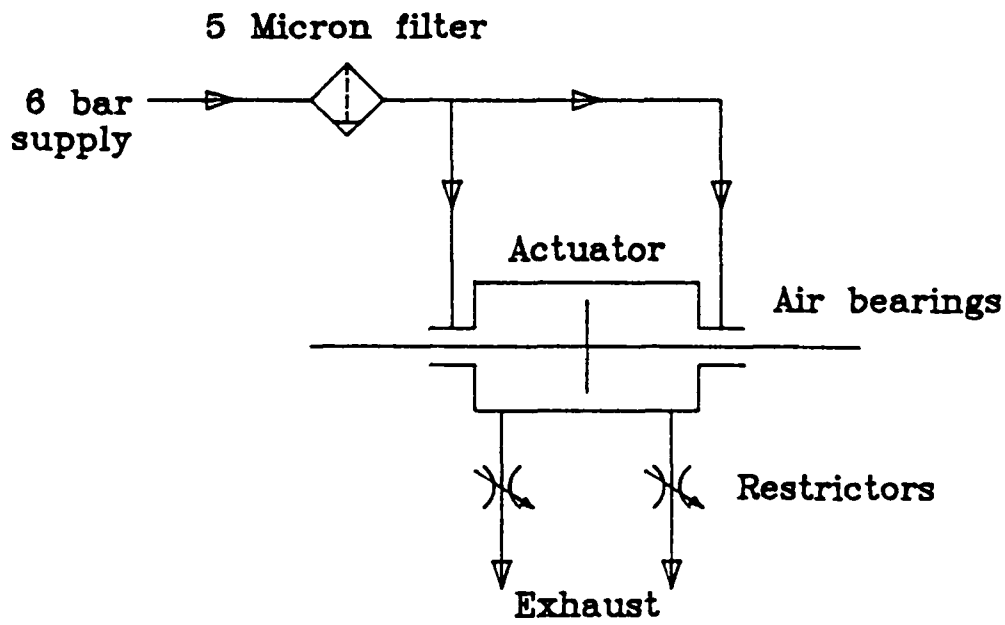

FIGURE 2.9 Pneumatic circuit for actuator Types 1 and 2.

2.4 Test Methods.

Before carrying out any friction tests each actuator was cycled between the two extremes of its motion 2000 times in order to bed in the seals. The orientation of the piston and rod assembly relative to the cylinder was kept constant throughout.

2.4.1 Static Friction Measurement.

With the piston stationary in a known position the computer continuously monitored the outputs from the three transducers. The chamber pressure was then slowly increased using the regulator for Type 0 or the restrictor for Types 1 and 2. The two chamber pressure readings, taken immediately prior to the detection of movement of the piston, were used to calculate the net driving force. This was repeated along the stroke of the actuator for motion in both directions.

The frequency of the software loop was greater than 50 *Hz*, the resolution of the linear motion was < 0.15 *mm* and that of the driving force < 1.0 *N*.

2.4.2 Dynamic Friction Measurement.

The piston was driven at a constant velocity of around 40 *mm/s* from one extreme of its motion to the other. The two chamber pressures were recorded at various positions along the stroke for motion in both directions. These pressures were then used to calculate the net driving force and, as no appreciable acceleration exists, this was equivalent to the dynamic friction force.

2.5 Results

2.5.1 Static Friction.

The results of the static friction tests are shown in figure 2.10.

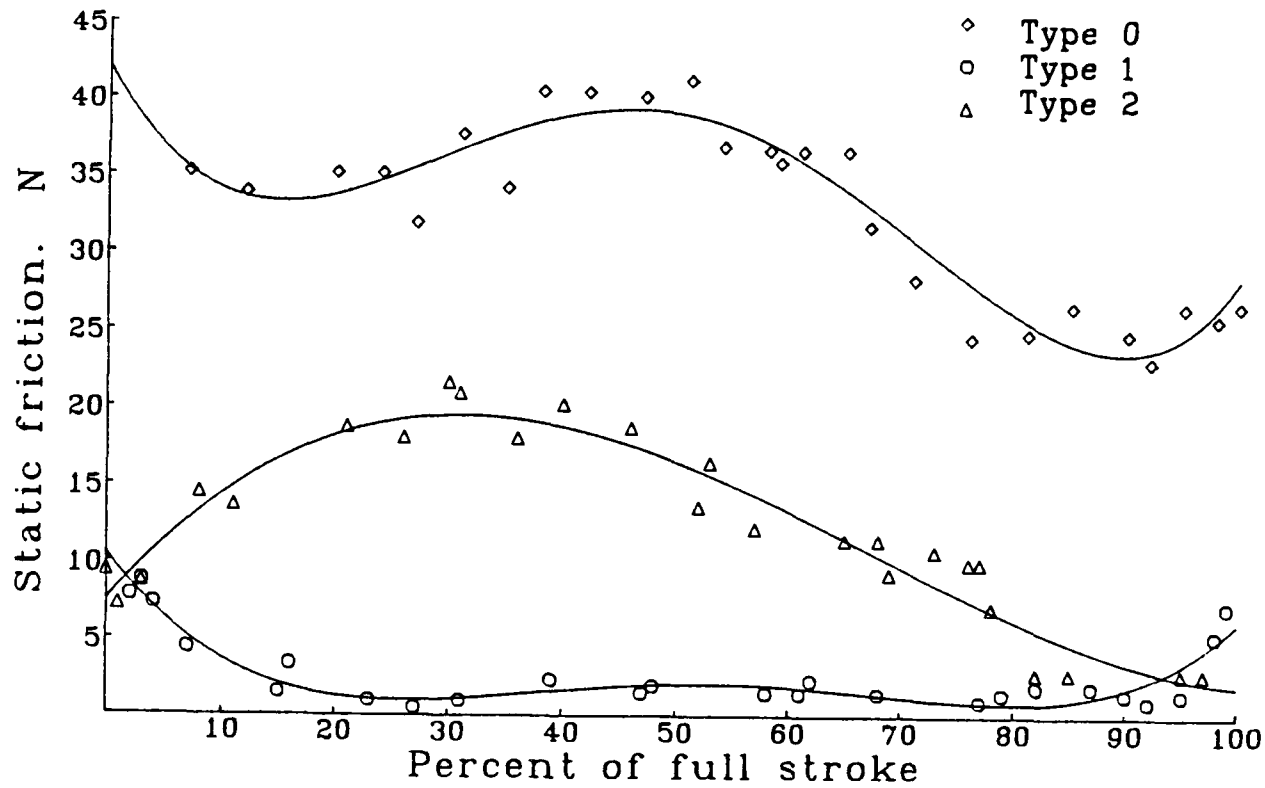

FIGURE 2.10 Variation of static friction with piston position.

On average the Type 1 low friction design is seen to have the lowest friction while the standard design, Type 0, has the highest.

There is a variation in friction of over 15 *N* along the stroke for both Type 0 and Type 2 designs. In Type 0 the cause of this variation is probably due to dimensional differences along the stroke of the actuator; the friction at the sliding contacts will vary with a change in the contact force caused itself by the varying geometrical tolerances inside the cylinder. It is likely therefore that there will be significant variations in this characteristic between actuators of the same design.

In the Type 2 actuator there is an increase of friction towards the centre of the stroke. This may be explained by the behaviour of the rubber seal as the piston begins to move. At the ends of the stroke, as shown in figure 2.11, the seals are folded back on themselves only over a small distance, allowing one seal to 'ripple' as the piston starts to move which will require only a small force. At the centre stroke position shown in figure 2.5, both seals are fully convoluted within the clearance between piston and cylinder and the rippling cannot so easily take place. This effect is emphasised because of the low pressures used in these tests.

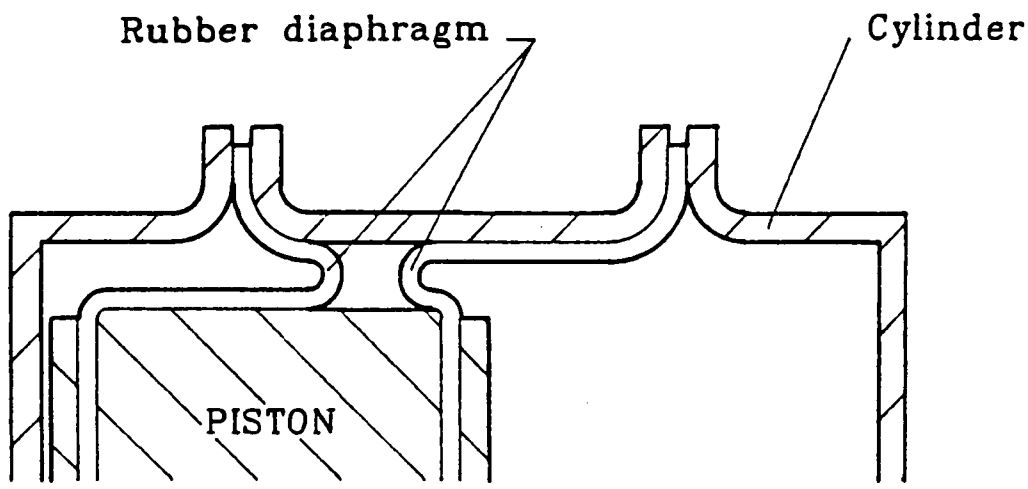

FIGURE 2.11 Operation of the rolling seal for Type 2 design.

The results for Type 1 show a much flatter friction characteristic with a rise at each end. This rise was due to the misalignment of the end caps, cylinder bore and piston rods. It would be caused by a breakdown of the air bearing film where the 'O' ring self-alignment is not sufficient.

The flatness of the friction curve over most of the stroke length for Type 1 may well prove to be a significant factor for servo applications as a variation of friction along the stroke (exhibited in Types 0 and 2) would add a large non-linearity to the system.

2.5.2 Dynamic Friction.

The results of the dynamic friction tests are shown in figure 2.12.

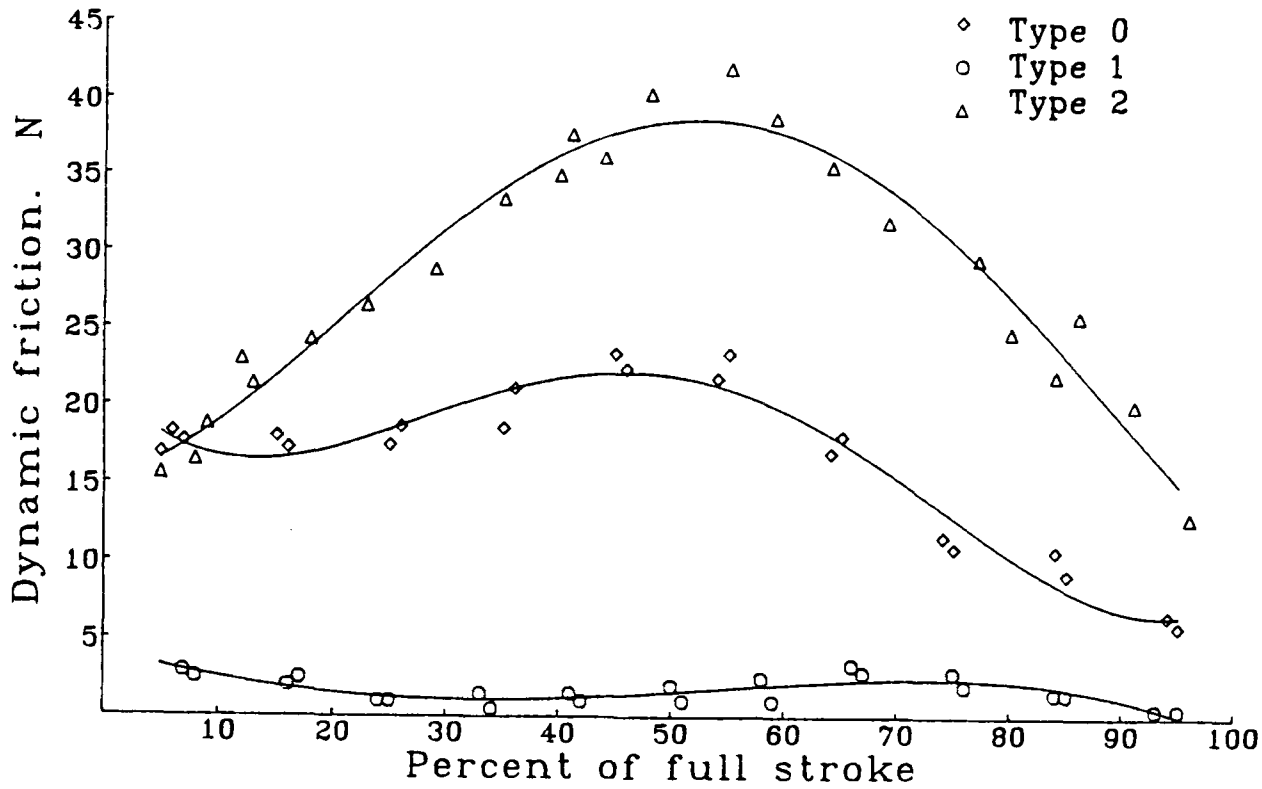

FIGURE 2.12 Variation of dynamic friction with piston position.

Again actuator Type 1 is seen to have the lowest friction, but this time it is Type 2 which has the highest. Furthermore, the friction levels for Type 2 are larger than those obtained in the static test, which is contrary to the normal Coulomb friction characteristic. The explanation must be due to the dynamic behaviour of the rubber seal as the piston is moving.

There are two main causes for the increase. The first is the hysteresis in the rubber seal. The total length of fold in the 1 *mm* reinforced rubber diaphragm is approximately 460 *mm*. These convolutions require some work to roll them up and down the piston. This would account for an overall increase in friction level when the piston is in motion. The second is due to the position of the diaphragm in the small gap between the piston and the cylinder, the size of which was set following design rules specified for hydraulic actuators. The two sides of the convolution are in contact where they are 'trapped' in this gap. Although the seal is lubricated, some friction will exist between these surfaces which have to move relative to each other as the piston moves. This will account for a rise in friction in the centre of the stroke as the area of contact is a maximum at this point. Figures 2.5 and 2.11 show the condition of maximum and minimum contact area respectively.

Dynamic friction for Type 0 is slightly lower than its static friction as expected. The variation along the length is similar to the static test and can be explained in the same way.

Dynamic friction for Type 1 is at the same level of around 3 *N* as the static test. Any difference between them was within the error bound of the test measuring equipment. Table 2.1 listed the actuator specifications and this gave the maximum net driving force for each actuator with a nominal 6 *bar gauge* pressure difference across the piston. If the approximate overall friction level is expressed as a percentage of this maximum driving force, then for the Type 1 design a value of less than 0.2% is obtained compared to 2% for the Type 0 standard design. It is difficult to make a general statement for the Type 2 actuator as the level of friction varied widely between the static and dynamic tests.

2.6 Summary

The Type 1 actuator, using a combination of air bearings as piston rod seals and a PTFE composite piston seal, has a considerably lower friction level than either the standard Type 0 actuator or the Type 2 actuator which also had air bearings but used a rolling piston seal.

Results for the rolling piston seal were particularly disappointing in the dynamic friction case, where the friction level was higher than the standard actuator. This was due mainly to the low pressures used in the tests and the design of the piston and cylinder assembly which did not successfully prevent contact between the two surfaces of the seal. It should be possible to improve the results from this method of sealing with a re-design that takes account of these findings.

The performance of the Type 1 actuator was very impressive. Its friction level was only 10% of that of the standard actuator over the central 90% of the stroke. Furthermore, the friction level is almost constant over this length. As a percentage of the maximum driving force of the actuator with a 6 *bar gauge* supply then this represents a value of less than 0.2% compared to the 2% for the Type 0 standard design.

Although the Type 2 design may offer similar benefits after a further period of development, the Type 1 actuator with its more simple design and proven performance met the requirements specified for this part of the research project and was the actuator used in the development of the accurate position control system described in subsequent chapters.

3 : MODELLING THE PNEUMATIC SYSTEM

3.1 Introduction

The position of the Type 1 low friction pneumatic actuator that was described in Chapter 2 was to be controlled by the application of pressurised air to the two cylinder chambers. This was to be achieved by switching pneumatic on-off valves with a BBC microcomputer through an interface unit. The most simple level of control would be to provide the pressurised air for a set time duration that is known to achieve the desired piston displacement. This would be known as 'open loop' control as no information about the actual piston displacement is fed back to the computer to inform it of the outcome of the opening of the valve. Many system parameters such as supply pressure, load, step size etc. affect the amount of displacement of the piston for a certain duration of valve opening, so open loop control would be highly inaccurate. Feedback of one or more of the output parameters, such as position, will provide information on the current state of the drive to the computer which can then adjust the control input to the valves to achieve the desired displacement. This would be known as closed loop control.

The task of synthesis is the determination of which types of feedback are desirable and how these should be used to adjust the air input to obtain a satisfactory response.

In order to carry out synthesis a mathematical model of each component is required. These individual component models can then be combined to obtain a set of differential equations that describe the system behaviour. Many commonly used system elements can be represented by a linear model because their output varies linearly with a variation in the input parameter and their output is not affected by other variables. The response of these elements is never perfectly linear but for the purposes of analysis, and over the range of values that are likely to occur, the assumption of linearity usually holds well and provides a very good predictions of the actual response. There are many general methods of synthesis for these linear systems, however, there are no general methods for the analysis and synthesis of non-linear systems and the system under consideration here includes elements that have large non-linearities.

The pneumatic actuator that is to be used in the system is the Type 1 design described in Chapter 2, and, although it is of low friction design, it is still likely to exhibit non-linear behaviour. The response of the actuator will be affected by even the low amount of friction within it, and this friction has a discontinuity when the piston motion changes direction. Therefore the output (piston position) is affected by a parameter that cannot be

expressed easily as a continuous function of the input variable (pressure difference), and its response is said to be non-linear. Other non-linearities will also affect the response of the actuator, some of these are listed below :

- The variation of bulk modulus with pressure
- The choking of inlet or outlet ports
- The coulomb friction and stiction in the actuator.

The on-off valve is another non-linear element of this control system. It is either fully open, when it will supply its maximum flow for those conditions, or it will be fully open in the other direction when the maximum flow of exhaust air will be passed. It is also likely to include a dead-time delay and hysteresis in its response which also contribute to its non-linearity.

Although there are no general methods of analysis and synthesis of non-linear systems, many methods have been developed that can be applied, but each method is limited in one way or another depending on the system analysed, the input size and range, and the particular performance characteristics that are of interest. Some of these methods such as the state-space concept, harmonic linearisation and the describing function are discussed in Chapter 4. However, a digital computer can be used to solve the set of non-linear differential equations that describe the behaviour of the non-linear system, thus avoiding a highly complex direct mathematical solution which may be impossible to solve for the range of inputs considered. This method is generally applicable to non-linear systems and it can provide considerable information on the dynamic behaviour of the system for a number of different parameter values, over a range which may not be easily realised on the actual system. The digital computer model is therefore a useful tool in the development of the control system, and it will complement the other methods of analysis that are available.

This chapter will describe the development of a computer model. The theoretical basis of the equations of the system and an explanation of the digital computer solution are given. An experimental rig is described which was a development of the equipment used in the friction tests of Chapter 2. The rig was used to obtain the actual response of the system for

1. A step change to the system causing motion in one direction.
2. A step change as in 1), followed by another step change to cause motion reversal.

In the first series of tests an initial correlation was carried out between the actual system response and the model output to improve the accuracy of some of the assumptions made about the system constants. This model was then used in a variety of conditions in order to gain a more thorough understanding of some of the more significant parameters.

Finally the model was extended to include motion in both directions and these results of the model output were compared to the measured response of the system in the second series of tests. As part of these, a more detailed investigation into the friction forces of the actuator and load was carried out.

3.2 Pneumatic System and Mode of Operation

Before a model could be developed the specification of the pneumatic system and its mode of operation was established.

The system was built up from the equipment used in the friction tests of Chapter 2. The first modification was to include a method of loading. This was added for the following reasons :

i) The large piston area and low intrinsic moving mass of the actuator made possible accelerations in the order of 300 ms^{-2} with a 6 *bar gauge* supply.

ii) Moore (11) had reported a large variation in system response with inertia load and this would provide the possibility of investigating this at a later date.

iii) A more realistic control system is created as every application of the position control system would require a load to be driven.

Secondly a different type of valve was used to control the air flow. Mannetje (33) had suggested that time delays caused by wave propagation along the transmission pipes between valve and cylinder were detrimental to the performance of the system and that a good system design should minimise the distance between valve and cylinder chamber. A single valve controlling both chambers was used for the friction tests of Chapter 2, but if this type of valve is used the minimum transfer pipe length is equal to half the stroke of the actuator. If this valve is 'split' into a pair of two-way valves, perhaps incorporated into the cylinder ends, the transfer pipe length can be just a few millimetres. This is shown schematically in figure 3.1.

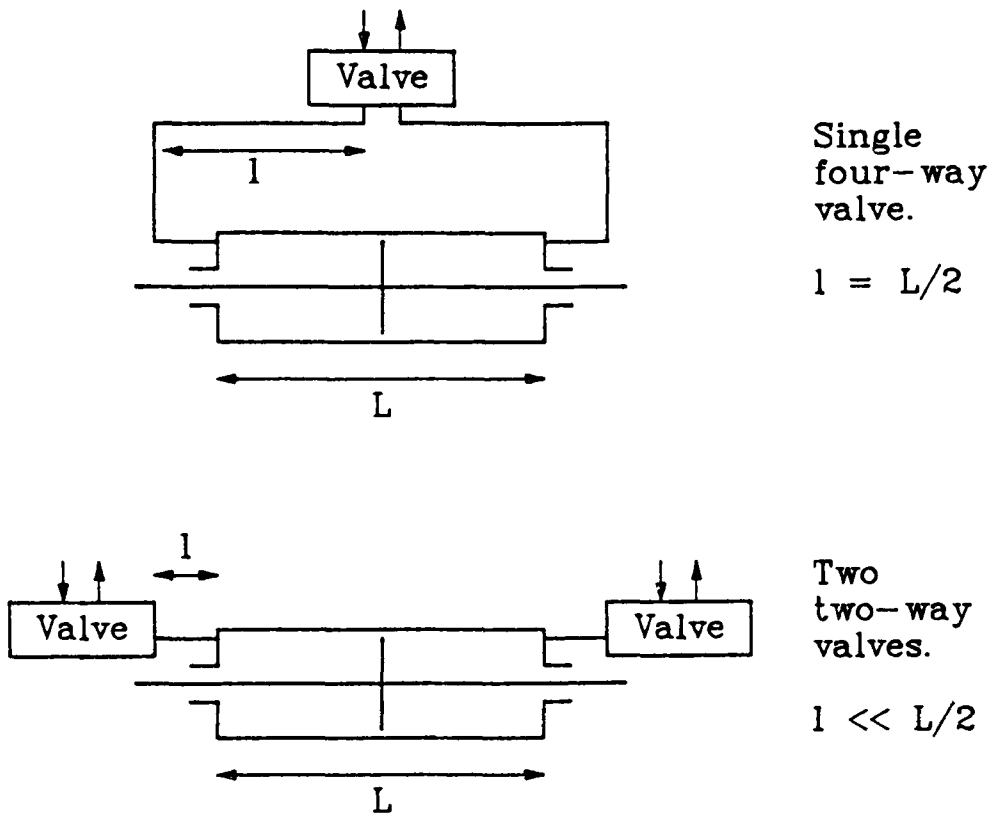

FIGURE 3.1. Minimum transmission pipe lengths for different valve arrangement.

In order to allow an investigation of the effect of transmission pipe length, the single on-off valve used for the friction tests was exchanged for a pair of two way on-off valves.

The motion of the piston can be controlled in one of three ways using these valves. The three modes are shown in figure 3.2.

The first method, termed *binary mode* is shown in figure 3.2 a. The piston can be at rest only at the ends of the stroke. One chamber is held at the supply pressure, the other at atmospheric pressure. Movement is affected by a simultaneous switching of both valves.

The two other modes require the switching of only one of the valves and the piston can be stationary at any position on its stroke. In the *open mode* of operation shown in figure 3.2 b, both chambers are initially at atmospheric pressure. In the *closed mode* shown in figure 3.2 c, both chambers are initially at supply pressure.

Bowns (**30**) has presented results for tests on a pneumatic actuator driven from end stop to end stop in the open and binary modes of operation. A large difference in the dynamic behaviour between these two modes was shown. During operation in the binary mode the actuator has to work against a higher pressure in the exhausting end of the cylinder than in the open mode. The response was therefore slower in the binary mode than in the open mode and it was also found to be less oscillatory.

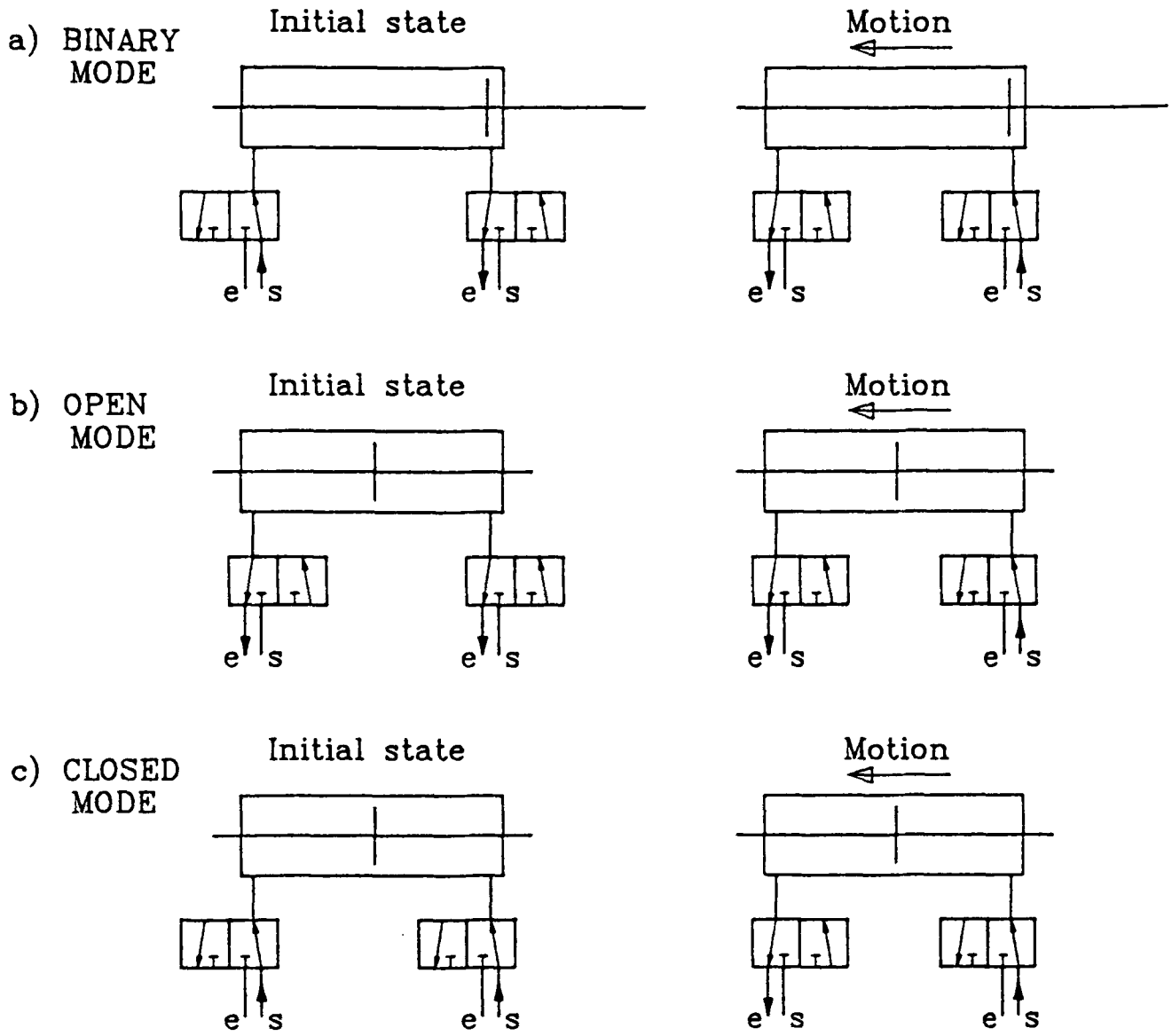

FIGURE 3.2. Modes of operation of the valves and actuator.

For this first stage of development of a position control system, the benefit of a slower and less oscillatory motion of the piston which was shown by the binary mode of operation would be desirable as it would reduce the likelihood of overshoot and oscillations in the position control system. However, the binary mode of operation will only allow the piston to be stationary at the ends of the stroke so it is not suitable for the position control system. No previous results for the closed mode of operation were available but Bowns had also shown the limitation of the velocity of the piston in the binary mode was dependent mainly on the exhausting conditions. The initial conditions in the exhausting chamber are the same in the closed mode and the binary mode so this suggested that the dynamics of these modes would be similar. Therefore the closed mode of operation was chosen.

3.3 Model Development.

A block diagram of the system to be modelled is shown in figure 3.3.

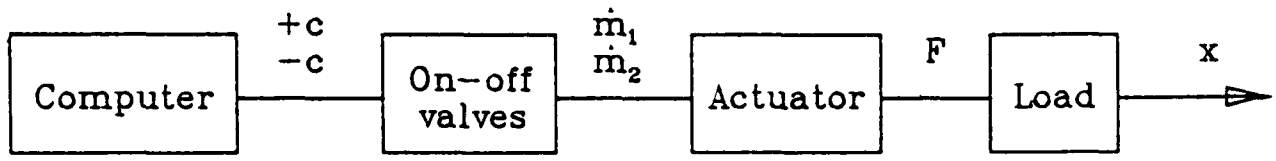

FIGURE 3.3. System block diagram.

The closed mode of operation of the valves shown in figure 3.2 c fixed the initial pressure in the cylinder chambers to be equal to the supply pressure. The step input to the model is an instantaneous command to switch the exhaust valve. This valve then opens the chamber to atmospheric pressure, beginning the flow of air out of the chamber and causing a pressure difference across the piston. This applies a force to the load which then begins to move. As the piston moves, flow into the supply side and out of the exhausting side of the actuator continues until the end of the stroke is reached.

In order to obtain mathematical expressions for the whole process the problem can be first divided into three parts :

1) The charging process from the supply reservoir through the supply valve to one cylinder chamber.
2) The discharging process of the pressurised air in the other cylinder chamber through the exhaust valve to the atmosphere.
3) The motion of the piston and load.

Parts 1) and 2) can be further subdivided thus :

a) Establishing the instantaneous conditions of the air in the cylinder chamber.
b) Determination of the instantaneous mass flow of air through the valve.

3.3.1 Cylinder Chamber Equations.

The supply side of the actuator can be represented by the thermodynamic control volume shown in figure 3.4.

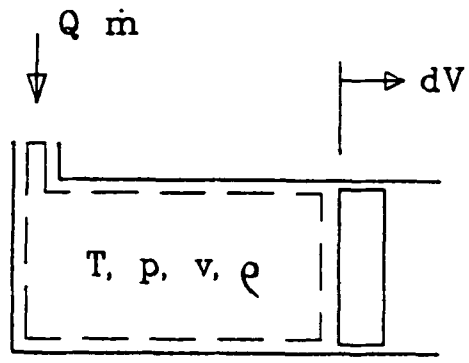

FIGURE 3.4. Thermodynamic system for the supply side of the actuator.

The chamber can be considered as a variable volume vessel, doing work on a moving boundary and being charged with a mass flow of air.

The following assumptions are made about the process to simplify the analysis :

- That the air is a perfect gas.
- That the process is adiabatic and isentropic (reversible).
- That the air in the chamber is homogeneous.
- That there is no expansion of the cylinder or supply line walls.
- That the kinetic energy of the air inflow is negligible.

It can be shown that for an adiabatic reversible process,

$$p_1 v_1^{\gamma} = constant$$

In this system both the pressure, p_1 and the specific volume v_1 will vary with time. Differentiating with respect to time and dividing through by v_1^{γ},

$$\frac{dp_1}{dt} + \frac{p_1 \gamma}{v_1} \cdot \frac{dv_1}{dt} = 0 \qquad [1]$$

Specific volume is defined as

$$v_1 = \frac{V_1}{m_1} \qquad [2]$$

There will be a net mass flow into the cylinder chamber so m_1 will not be constant. Differentiating and rearranging,

$$\frac{dv_1}{dt} = \frac{1}{m_1}\left[\frac{dV_1}{dt} - v_1 \frac{dm_1}{dt}\right] \qquad [3]$$

Substituting [3] and [2] into [1] gives

$$\frac{dp_1}{dt} + \frac{p_1\gamma}{V_1}\left[\frac{dV_1}{dt} - \frac{V_1}{m_1}\cdot\frac{dm_1}{dt}\right] = 0 \qquad [4]$$

The equation of state for a perfect gas can be written as

$$m_1 = \frac{p_1 V_1}{RT_1} \qquad [5]$$

Substituting [5] into [4] and rearranging gives

$$p_1 = \frac{1}{V_1}\left[\dot{m}_1 RT_1 - \frac{V_1\,\dot{p}_1}{\gamma}\right] \qquad [6]$$

The same procedure can be applied to the discharge process to obtain the following

$$p_2 = \frac{1}{V_2}\left[\dot{m}_2 RT_2 - \frac{V_2\,\dot{p}_2}{\gamma}\right] \qquad [7]$$

Equations [6] and [7] were also developed in slightly different ways by Shearer (**17.18**), Burrows (**24**) and Bowns (**26**). Both equations show that the mass flow rate ($\dot{m}$) is a function of cylinder temperature (T). Because an adiabatic process is assumed, the supply side temperature T_1 can be expressed as

$$T_1 = T_s\left[\frac{p_1}{p_s}\right]^{\frac{\gamma-1}{\gamma}} \qquad [8]$$

and for the exhaust side

$$T_2 = T_e\left[\frac{p_2}{p_e}\right]^{\frac{\gamma-1}{\gamma}} \qquad [9]$$

If these equations for chamber temperature were substituted into [6] and [7] respectively, then non-linear equations in p would result and these would require iterative solution on the digital computer.

The assumption of an adiabatic process is an idealisation, the actual process is likely to lie somewhere between an adiabatic and an isothermal change. Equations [8] and [9] give the variation of temperature with pressure for a perfectly adiabatic process so this will be the maximum temperature change possible. The true extent of the temperature change and its effect on the mass flow rate is therefore not clear. Since the cylinder chamber temperatures are not of direct interest, and the initial objective is for a simple computer model of the

system, an assumption of constant temperature throughout the process was taken. ie

$$T_s = T_1 = T_2 = T_e$$

Burrows had made this assumption with reasonable results. Bowns had assumed constant temperature only for the supply side, and had incorporated equation [9] into [7] to obtain a non-linear expression in p_2. However, $\gamma = 1.4$ was replaced by the polytropic exponent n and this had been set equal to 1.0. This had the effect of reducing equation [9] to a constant temperature assumption in any case. Bowns had presented good results with these assumptions.

3.3.2 Valve Equations.

During the charging and the discharging process the on-off valves used in the system act as restrictors to the flow of air. The amount of air passed by the valve will be a function of the pressures either side of it. In this system the switching of the valve on the exhausting side of the actuator will initially cause a large pressure difference across the valve. As the chamber empties, this pressure difference will slowly reduce causing a reduction in the mass flow through the valve. If the valve is considered as a perfect orifice the initial high pressure difference across the orifice will cause sonic conditions through the orifice. The standard nozzle flow equations can be applied to the choked orifice to obtain the mass flow rate. However, a valve does not consist of a single orifice, it is more accurately described as series of orifices and this affects the standard mass flow/pressure relationship such that it can no longer be applied with success. Sanville (**27**) developed an empirical formula which modified the standard orifice mass flow/pressure relationship by reducing the critical pressure ratio as a function of the upstream and downstream pressures.

The Sanville formula for the supply valve can be expressed as

$$\dot{m}_1 = \frac{f_{s_1} K_\gamma A_{O_1} p_s}{\sqrt{T_s}} \qquad [10]$$

where :

$$K_\gamma = \left[\frac{\gamma}{R}\left[\frac{2}{\gamma+1}\right]^{\frac{\gamma+1}{\gamma-1}}\right]^{1/2}$$

$$f_{s_1} = \left[1 - \left[\frac{\frac{p_1}{p_s} - b}{1-b}\right]^2\right]^{1/2} \qquad \text{for} \quad \frac{p_1}{p_s} > b$$

$$f_{s_1} = 1 \qquad \text{for} \quad \frac{p_1}{p_s} \leq b$$

Similarly for the exhaust valve,

$$\dot{m}_2 = \frac{f_{s_2} K_\gamma A_{O_2} p_2}{\sqrt{T_s}} \qquad [11]$$

where :

$$f_{s_2} = \left[1 - \left[\frac{\frac{p_e}{p_2} - b}{1-b}\right]^2\right]^{1/2} \qquad \text{for} \quad \frac{p_e}{p_2} > b$$

$$f_{s_2} = 1 \qquad \text{for} \quad \frac{p_e}{p_2} \leq b$$

The instantaneous mass flow rate for the charging and discharging processes can be calculated using equations [10] and [11].

3.3.3 Equations of Motion.

The loading system to be modelled can be represented as an inertia plus friction. The driving force due to the pressure difference across the actuator will be equal to the sum of the inertia force and the friction force, where the friction force always opposes the direction of motion :

$$A_p (p_1 - p_2) = m\ddot{x} + F_F \, sgn \, \dot{x} \qquad [12]$$

Burrows (24) assumed that the friction force consisted only of coulomb friction, ie a constant term, but Bowns (26) has shown good results by assuming that friction is made up of the sum of three parts :

$$F_F = F_C + C_{FV} |\dot{x}| + C_{FP} |p_1 - p_2| \qquad [13]$$

Bowns (29) had measured friction for an actuator of similar size to the one used in this system and had found that the fit of the friction curve could not be improved upon when the approximation of equation [13] was replaced with a polynomial of higher order. Equation [13] was therefore used as the friction characteristic for the actuator and load for the model of this system.

3.3.4 Complete Mathematical Model.

The equations derived above for the charging and discharging process of the actuator and for the motion of the piston and load can be combined to obtain an overall mathematical model of the system. The flow diagram of the variables in this system model is shown in figure 3.5. The non-linear character of the equations can clearly be seen by the occurrence of many blocks with multiple input/outputs.

These equations can be solved in a quasi-static way by a digital computer. The flowchart of the digital computer programme is given in Appendix 2.

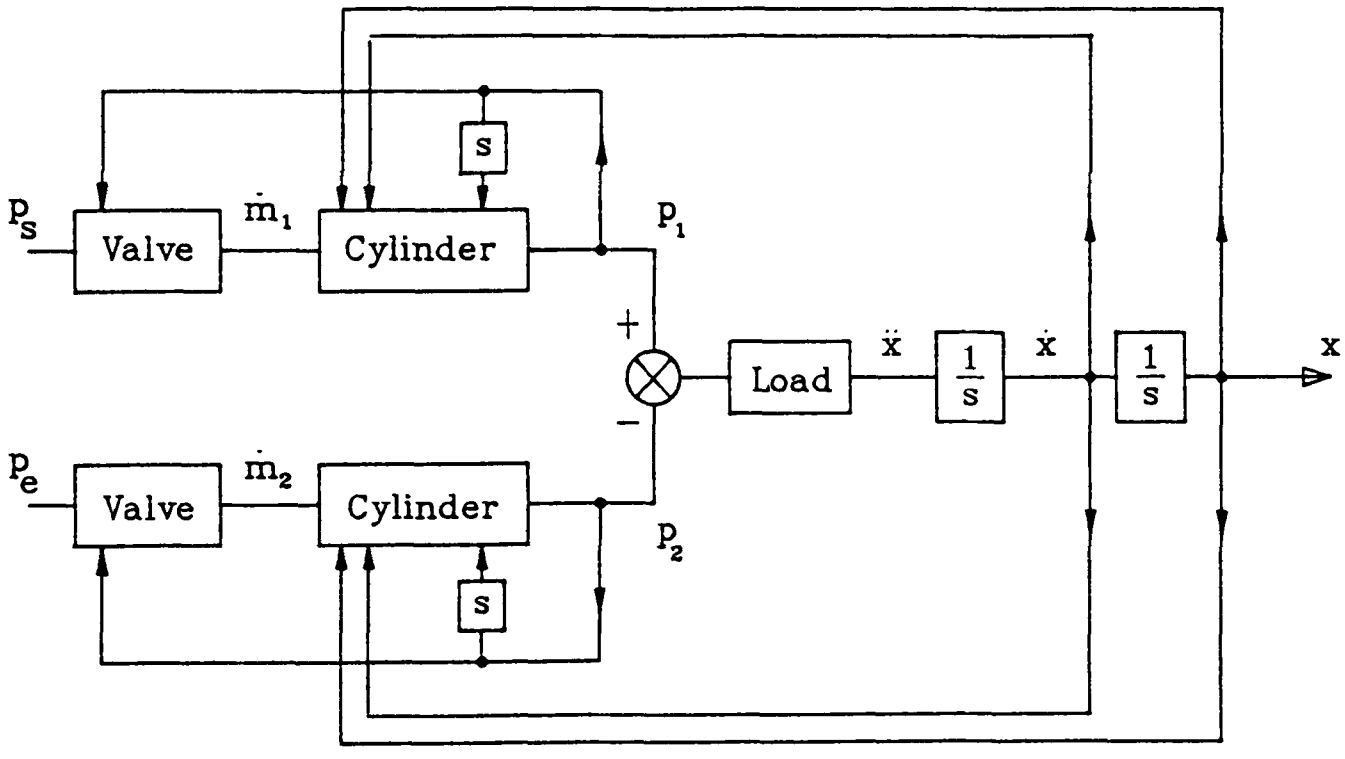

FIGURE 3.5. Flow Diagram of the System Variables.

3.4 Test Equipment

The model of the pneumatic system can provide information on the time response of many system parameters, these are :

1. Piston position
2. Piston velocity
3. Piston acceleration
4. Supply chamber pressure
5. Exhaust chamber pressure
6. Supply air mass flow rate
7. Exhaust air mass flow rate

In order to compare the model response to the actual system response a test rig was constructed so that the variables 1 to 5 above could be directly measured on the actual system during the motion of the piston and load. Both the measured data and the model output were stored on disc in the same format so that a single data processing software package could be used to present the results graphically. The data format on the disc is shown in Appendix 6.

3.4.1 Loading System.

The space frame used in the friction tests of Chapter 2 provided a strong and rigid method of mounting the actuator and valves for this series of tests. The main modification to this equipment was to include a method of loading the actuator. The specification of the loading system was to ;

1) Contribute a minimum amount of friction to the system.
2) Provide inertia loads ranging from 20 *kg* to 60 *kg* in increments of 2 *kg*.
3) Allow easy and quick changing of the inertia load.
4) Securely fix the load without problems of 'backlash' etc..
5) Minimise side loads on the piston/rod assembly.

Various possible designs were considered. These can be broadly split into two main groups; those with a vertical orientation of the piston motion and those with a horizontal orientation. These are shown in figure 3.6.

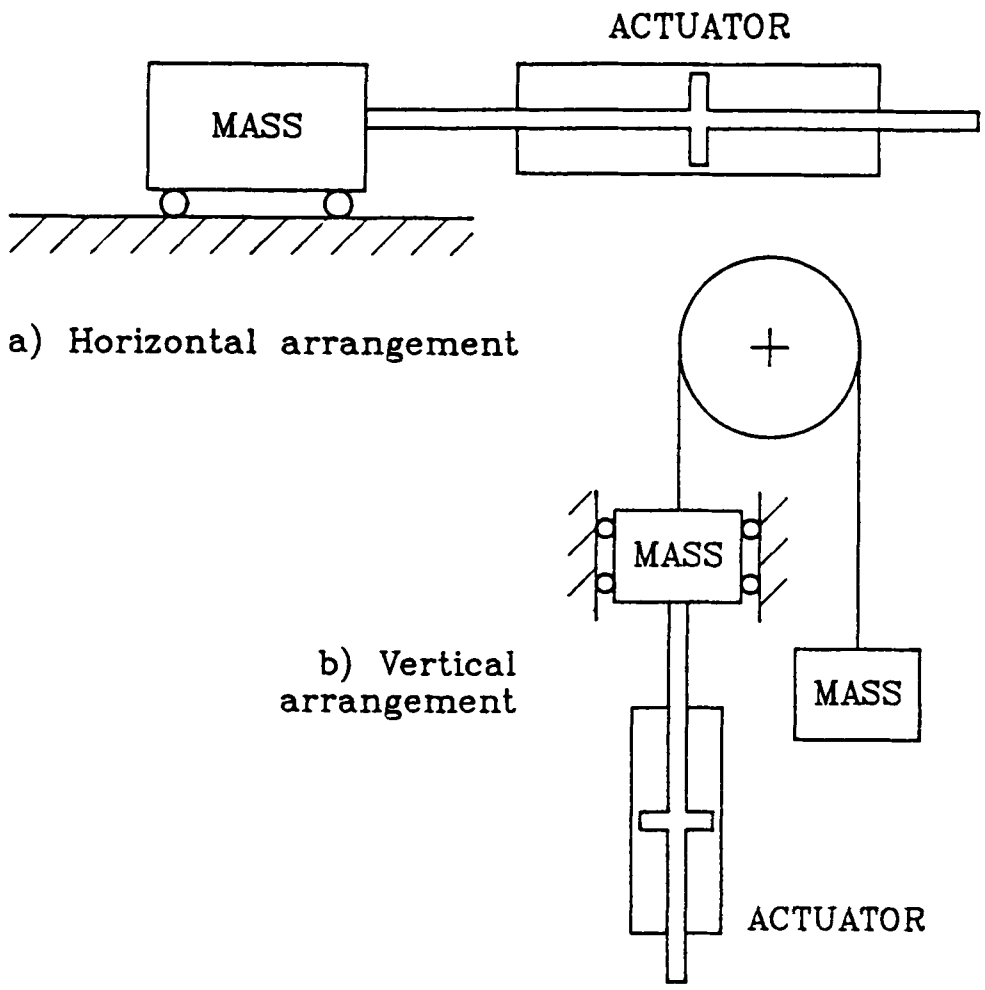

FIGURE 3.6. Possible Orientation of Actuator and Load.

Although all of the possible designs met the requirements of the specification to a greater or lesser degree, there was a large difference between the two groups particularly for the requirement of low friction.

In a horizontal arrangement the weight of the mass must be supported by rollers or some other linear surface bearing shown in figure 3.6a or on rods with linear bearings. To ensure a minimum of friction it was not possible to use a simple greased slideway or greased rods. However, a series of rollers or air bearings could be used.

In a vertical arrangement shown in figure 3.6b, the masses are balanced over a large wheel on roller bearings which supports the weight of the balanced masses. Other bearings are used to guide the mass and reduce side forces on the piston rod although these take only very small horizontal forces.

The best option for low friction would be a horizontal arrangement with air bearings but the design complexity and the resulting increase in the time to manufacture the loading system ruled out this option. A second choice was a vertical arrangement with balanced masses and a single large pulley wheel. The advantages of this option were that ;

- fewer roller bearings were required therefore contributing less friction.
- the effect of friction is reduced by the ratio of the diameter of the wheel to the diameter of the wheel bearing.
- alignment of the motion of the mass and the motion of the piston is simplified.

This option was therefore chosen although the final design used two pulley wheels to overcome the problem of the jumping of the belt when large accelerations of the mass took place. The final arrangement is shown in figure 3.7.

Two masses hang on a steel belt which passes over a large wheel. The first mass is connected via a ball joint to the piston rod of the actuator which is mounted in a vertical plane. The piston rod at the lower end of the actuator is connected to a second steel belt which continues downwards in alignment with the piston rod before turning upward around another large wheel. The belt finally meets the second mass and is attached to the underside of it. A complete loop is thus created ensuring that piston forces in either direction are transmitted efficiently to *both* masses. The masses on either side of the loop are equal so that it is not necessary for the actuator to support weight.

The design utilised standard slotted stackable masses on a purpose-built carrier to allow easy changing of the applied inertia load.

The inertia load on the actuator was calculated from the addition of the mass of the slotted masses, mass carriers, steel belt, connectors and a equivalent mass term for the rotational inertia of the two pulley wheels.

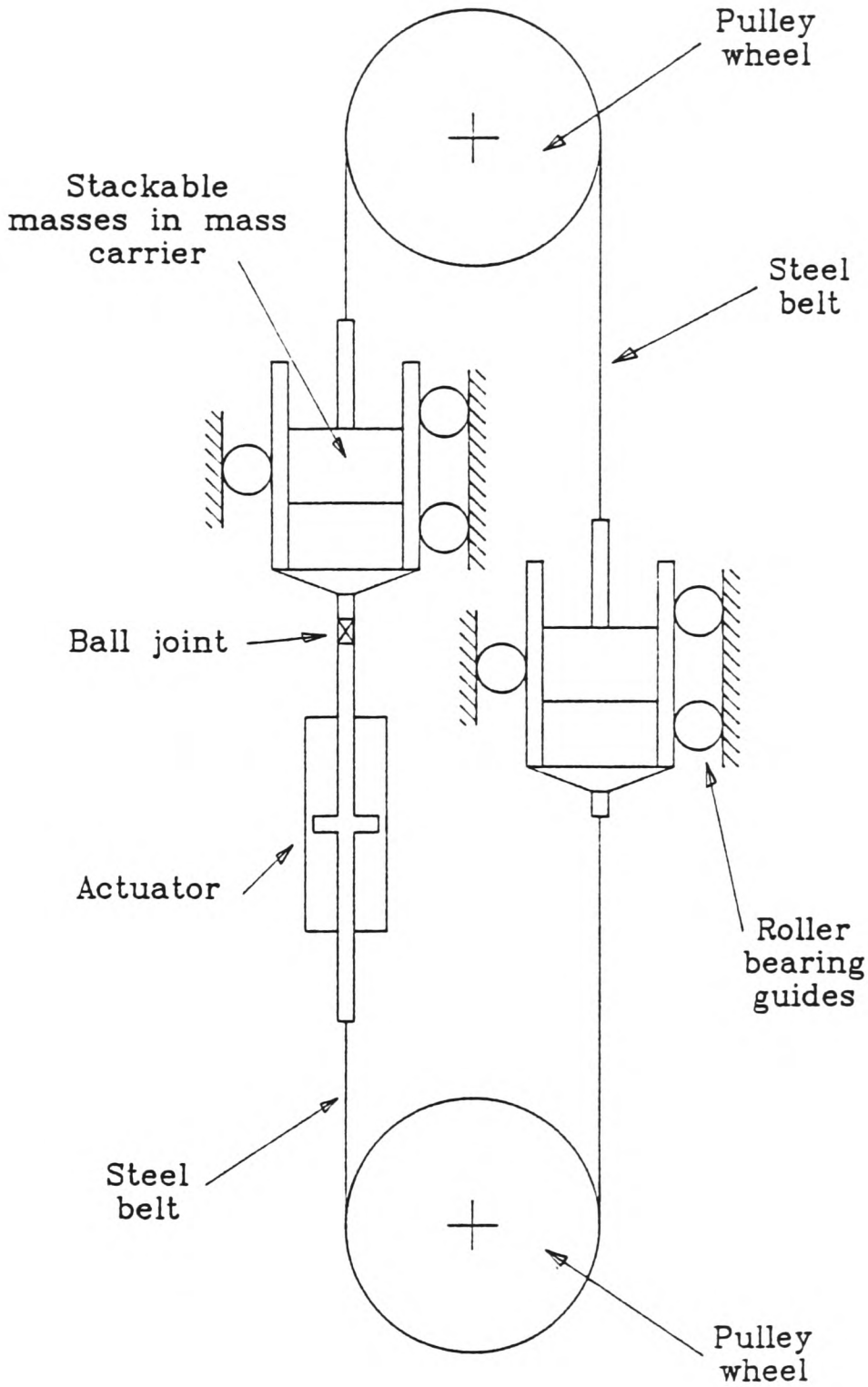

FIGURE 3.7. Schematic Drawing of Final Arrangement of Rig.

3.4.2 Pneumatic Circuit.

The pneumatic circuit used for these tests is shown in figure 3.8.

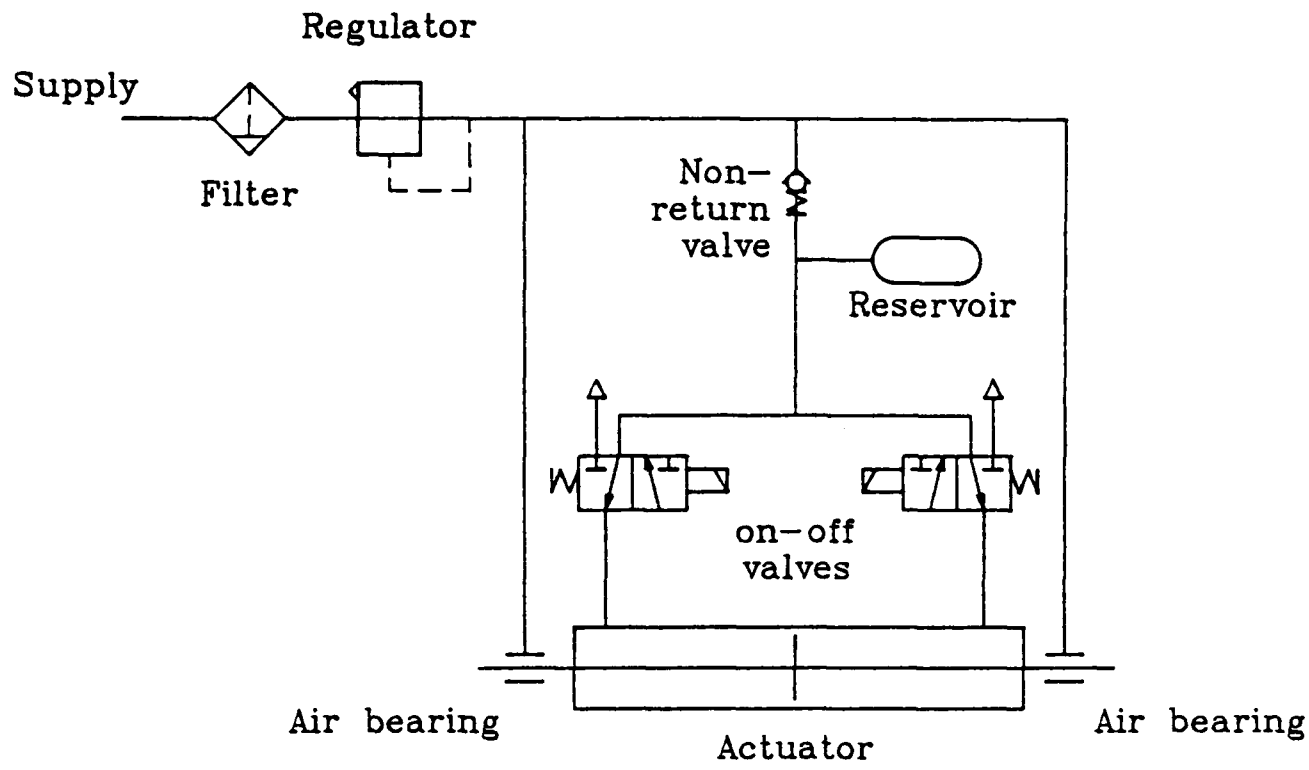

FIGURE 3.8. Pneumatic circuit of Test Equipment.

The Type 1 actuator incorporated air bearings in the cylinder ends, so a filtered 6 bar supply was fed directly to them. A reservoir was included in the system between filter and valves in order to provide a constant air supply to the valves. Direct feed from the laboratory supply line did not maintain pressure during high flow demand and it was effected by other users. Both on-off valves were placed as close as possible to the cylinder ends to reduce the effect of transmission pipe length. Quick release couplings were used for the pneumatic circuit so that pipe lengths could be changed easily.

3.4.3 Data Acquisition.

A BBC microcomputer was used to store the system variables at finite time steps following a disturbance to the system. Flowcharts for the computer programmes used are given in Appendix 3. Data was acquired from various transducers through a purpose built interface unit that was a development of the interface used for the friction tests of Chapter 2. A schematic drawing of the arrangement is given in figure 3.9.

The frequency of the interrupt routine determined the sampling rate of the test equipment and this was set to 200 *Hz*.

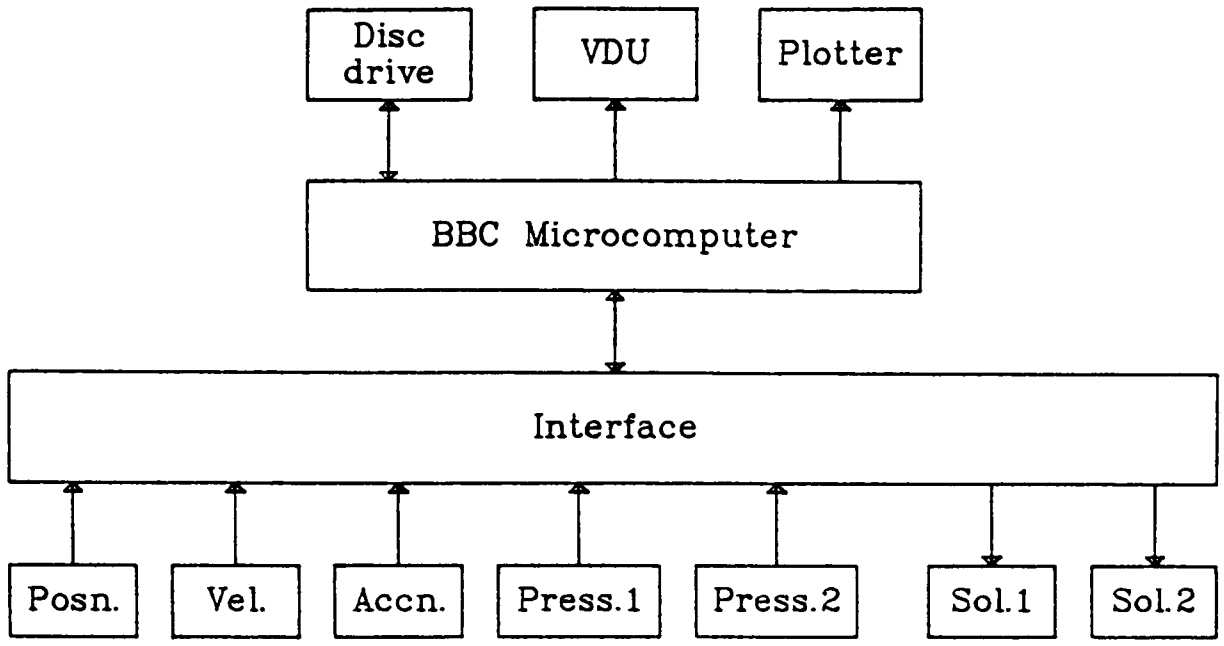

FIGURE 3.9. Schematic drawing of the hardware arrangement.

The design of the interface unit is similar to that described in section 2.3.1. Modifications to it were as follows :

1. Two analogue input channels were added.
2. The LVDT input channel was amplified further to improve resolution as the complete 400 *mm* range of the transducer was not required.
3. Offset circuits for the tachometer and accelerometer inputs were added.

Details of the transducers used are given in table 3.1 together with the overall resolution possible after amplification and conversion to a digital value.

Direct measurement of the piston position with the linear variable differential transformer device was used only for initialisation because its DC to 75 *Hz* bandwidth reduced accuracy on fast moving signals. Integration of the tachometer output was therefore used for the dynamic measurement of position. This was a feasible alternative because at the supply pressures and loads for these tests the complete stroke of the actuator is completed in around one second. Integration of the tachometer signal to obtain the piston position has a maximum drift of approximately 0.5 *mm* over this period, which is acceptable.

INPUT	TRANSDUCER TYPE	INPUT RANGE	OUTPUT RANGE	RESOLUTION (quantisation)
Piston position	Linear variable differential transformer	0 to 400 *mm*	-1.5 to 1.5 *V*	80×10^{-6} *m*
Piston velocity	DC tachometer	-1.0 to +1.0 ms^{-1}	-5 to 5 *V*	0.5×10^{-3} ms^{-1}
Piston accn.	Piezo-ceramic accelerometer plus charge amplifier	-50 to +50 ms^{-2}	-5 to 5 *V*	24×10^{-3} ms^{-2}
Chamber 1 pressure	Piezoelectric signal conditioned device	0 to 6 *bar (g)*	0 to 10 *V*	1.5×10^{-3} *bar*
Chamber 2 pressure	Piezoelectric signal conditioned device	0 to 6 *bar (g)*	0 to 10 *V*	1.5×10^{-3} *bar*

TABLE 3.1. Details of Transducers used for model correlation tests.

3.5 Comparison of System and Model for the Switching of the Exhaust Valve

The mathematical model that has been developed for the pneumatic system relates the variables to each other through equations which contain many parameters which are constant for a given system. In order to compare the results of the model and the response of the actual system the constants must be determined for the real system. For example, the area of the piston will determine the force applied to the load for a given pressure difference. This area is easily measured on the actuator being used. However, other constants are not so easily determined. These are listed below :

1. Coulomb friction. F_C
2. Constant of velocity dependent friction. C_{FV}
3. Constant of differential pressure dependent friction. C_{FP}
4. Supply valve orifice effective area. A_{O_1}
5. Exhaust valve orifice effective area. A_{O_2}

The objective of the work by Bowns (**26**) was to determine the accuracy of this type of model, therefore orifices of known effective area were inserted in the transmission pipes

between valve and cylinder in the actual system and the pressures immediately adjacent to these were taken as the supply and exhaust pressures. This eliminated errors that may have been introduced by estimating an actual *valve* orifice effective area. Bowns also carried out separate tests to determine F_C , C_{FV} and C_{FP} for the actuator used in his tests, in order to evaluate the accuracy of the assumption that the friction can be represented by the characteristic of equation [13].

The model of this position control system was developed to aid the design and analysis of the control system and, although a representative model was required, it was not necessary at this early stage to carry out a thorough investigation of each component to accurately determine the constants listed above. For example, the valve orifice effective areas A_{O_1} and A_{O_2} were initially estimated from the sizes quoted in the manufacturers catalogue. The first tests on the system showed that the maximum velocity predicted by the model was higher than the measured velocity. This velocity is set by the mass flow rate through the valve, in particular on the exhaust side and therefore A_{O_2} is significant in establishing the maximum velocity of the piston. After determination of the exhaust orifice size required in the model, the supply side orifice was set by comparing the pressure difference across the piston with the measured value. It was found that the orifice areas used in the model had to be unequal to achieve reasonable values of maximum velocity and pressure difference.

An initial estimation of the friction constants F_C , C_{FV} and C_{FP} for the low friction actuator was made on the basis of the Bowns results (**26**). The values of C_{FV} and C_{FP} were calculated by scaling down the Bowns figures by the ratio of the coulomb friction in the Bowns actuator to the dynamic friction of the Type 1 actuator. Although the work described in Chapter 2 did not measure friction at higher pressures and velocities, the total friction force (F_F) of the low friction actuator used here is quite low. This small amount of friction will have a smaller effect on the response of the system so, for this first investigation of a model, these rough approximations were sufficiently accurate.

The objective of this series of tests was firstly to attempt to improve the parameter approximations described above by repeated comparisons of the system and the model output, and then to investigate the significance of some of these parameters and some of the assumptions in the model. Finally, the accuracy of the simulation for various system initial states is investigated to determine the range of input conditions over which it can be applied. In this way the process of charging and discharging the actuator under load can be better understood.

A simple step change to the system as described in section 3.2 was used for the experimental tests and the model simulation. This was simply the switching of the exhaust valve when operating in closed mode which opens the exhausting chamber to atmosphere. This was easily achieved on the real system and was modelled as an instantaneous change to the downstream pressure in the exhaust valve equation (p_e in equation [11]). A flowchart of the computer programme used to record the experimental data is shown in Appendix 3a.

3.5.1 Improvement of Model Constants.

Because of the non-linear behaviour of the system the first stage of the improvement of the model parameters used measured results from experimental tests with constant initial conditions. ie :

- Piston positioned at end bump stop.
- Inertia load of 37 *kg*.
- Supply pressure of approximately 5.5 *bar gauge*.

The accurate measurement of the supply pressure for each experiment was used as an input to the simulation.

The first model run, SIM1 used the initial conditions given in table 3.2. Variables in italics are those which were directly set on the test equipment for the comparison real response, EXP1.

The equipment used for the first experiments did not include the pneumatic reservoir and large variations in supply pressure through the stroke were observed. This variation was measured by moving one of the pressure transducers into the supply line. The complex curve obtained from this was modelled with three straight line segments and was used as an input to the model simulation in place of the constant value of supply pressure p_s. Inclusion of the reservoir greatly reduced this variation and enabled it to be quite accurately modelled by the straight line approximation :

$$p_s = - k_{p_s} t + p_{s_0}$$

where t = elapsed time after switching valve

p_{s_0} = initial value of supply pressure

k_{p_s} = rate of change of supply pressure

To complete the input variables, values of coulomb friction (F_C) and the friction coefficients (C_{FV} and C_{FP}) were estimated from the Bowns results as discussed above.

PARAMETER		SIM1	SIM2	SIM3	SIM4	SIM5
Cylinder Length	*mm*	300	300	300	300	300
Piston Area A	m^2	2.9×10^{-3}	2.9×10^{-3}	2.9×10^{-3}	2.9×10^{-3}	2.9×10^{-3}
Valve Orifice Effective Area A_{O_1}	m^2	3.1×10^{-6}	3.1×10^{-6}	3.1×10^{-6}	3.1×10^{-6}	3.1×10^{-6}
Valve Orifice Effective Area A_{O_2}	m^2	4.6×10^{-6}	4.6×10^{-6}	4.6×10^{-6}	4.6×10^{-6}	4.6×10^{-6}
Mass m	*kg*	37	37	37	37	37
Coulomb Friction F_C	N	5	**22**	22	22	22
Coeff of Velocity Related Friction C_{FV}	Nsm^{-1}	140	**34**	34	34	34
Coeff of Diff Press Related Friction C_{FP}	m^{-2}	30×10^{-5}	$\mathbf{0.4\times10^{-5}}$	0.4×10^{-5}	0.4×10^{-5}	0.4×10^{-5}
Solenoid Dead Time	$s\times10^{3}$	0	**75**	75	75	**50**
Polytropic Exp n		1.4	1.4	1.4	**1.1**	**1.27**
Gas Temperature T_s	^0K	293	293	293	293	293
Supply Pressure p_s	*bar*	6.4	6.4	6.4	6.4	6.4
Rate of Change of Supply Pressure k_{P_s}	$bars^{-1}$	0.17	0.17	0.17	0.17	0.17
Exhaust Pressure p_e	*bar*	1.0	1.0	1.0	1.0	1.0
Supply Chamber Pressure p_1	*bar*	6.4	6.4	6.4	6.4	6.4
Exhaust Chamber Pressure p_2	*bar*	6.4	6.4	6.4	6.4	6.4
Piston Position x	*mm*	0	0	0	0	0
Piston Velocity $\dot{x}$	ms^{-1}	0	0	0	0	0
Piston Accn $\ddot{x}$	ms^{-2}	0	0	0	0	0
Time Increment t	$s\times10^{3}$	5	5	**1**	**5**	5
Duration of Model	s	1.0	1.0	1.0	1.0	1.0
Simulation of -		EXP1	EXP1	EXP1	EXP1	EXP1

Note :
Parameter names in italics indicates the variables that were also set as initial conditions on the experimental equipment.
Figures in bold indicate changes from the previous simulation.

TABLE 3.2. Model Input Parameters for Simulation of Single Switch Experiments, SIM1 to SIM5.

A comparison of the simulation results SIM1 and the experimental result EXP1 is shown in figures 3.10.

The position and velocity response comparisons in figures 3.10 a and b show clearly that the simulation matches the shape of the actual response quite closely but that there is a time shift between them of about 75 *ms*. This was initially attributed to a finite time delay between the computer command for the valve opening and the start of the mass flow through the valve. However, the chamber pressure begins to change almost immediately for the real system although at a lower rate than the model, and this suggests that the valve time delay is considerably smaller than 75 *ms*.

The measured friction is seen to be considerably higher than predicted by the model. This will contribute to the discrepancy in the time response of the other variables as the driving forces in the model will not be resisted by friction to the extent that they are in the real system. It also accounts for the higher initial piston acceleration in the model than in the real system. The friction measured in this test is higher than that measured for the Type 1 actuator in Chapter 2. There are two reasons for this discrepancy. Firstly, a load is now being driven which will add to the total friction force. Secondly the actuator chamber pressures are considerably higher than used for the friction tests of Chapter 2 and this may add to the friction of the piston seal.

Two changes were made to the model parameters in an attempt to improve the simulation of the same experiment - EXP1. Firstly, the total friction force was increased by choosing higher values of F_C and C_{FV}. The value of C_{FP} was reduced because it had a detrimental effect on the peak of acceleration which was already higher than seen in the real system. The revised values were determined after a series of model runs to view their effect. Secondly, a valve time delay was included in the model. The duration of this time delay was determined by comparison of the model and experimental position response.

The initial conditions for the simulation in which both of these changes were included - SIM2 - are also given in table 3.2. This simulation is compared to the experimental results for EXP1 in figure 3.11.

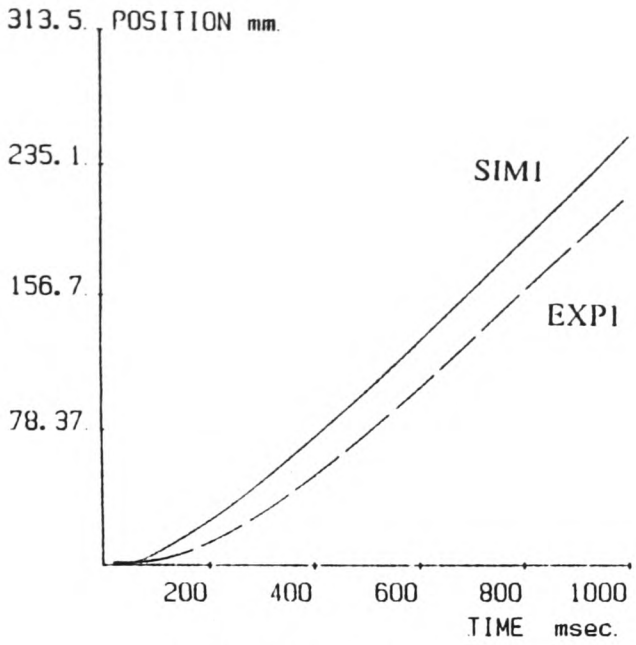

a) Position / time

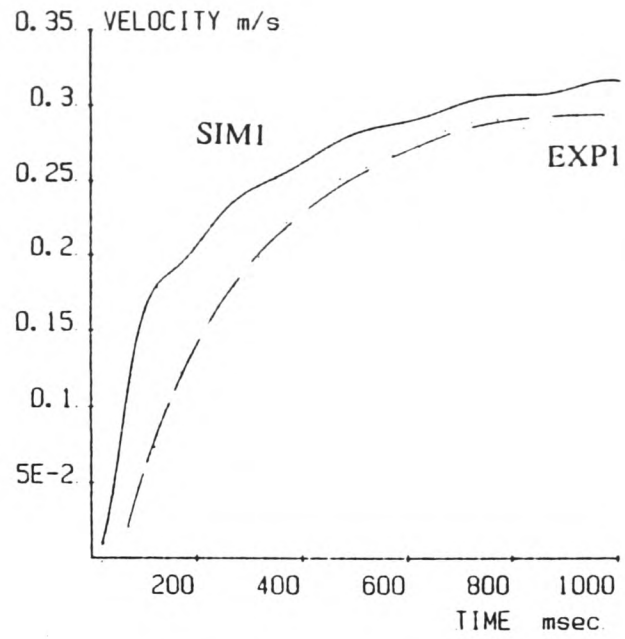

b) Velocity / time

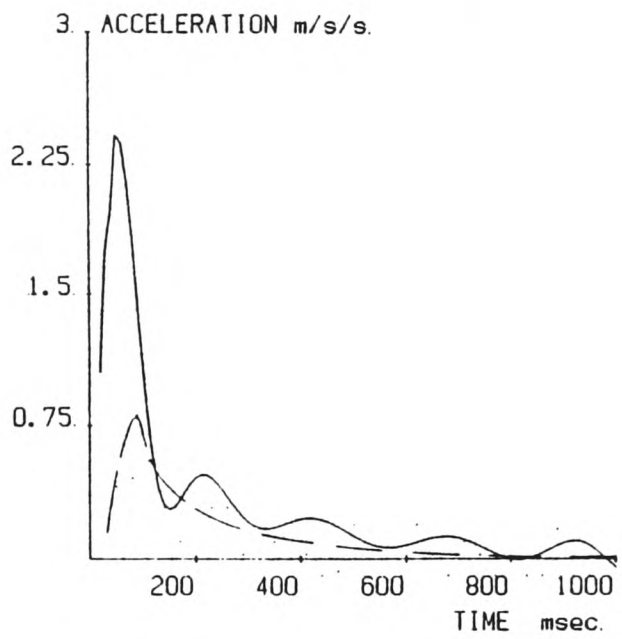

c) Acceleration / time

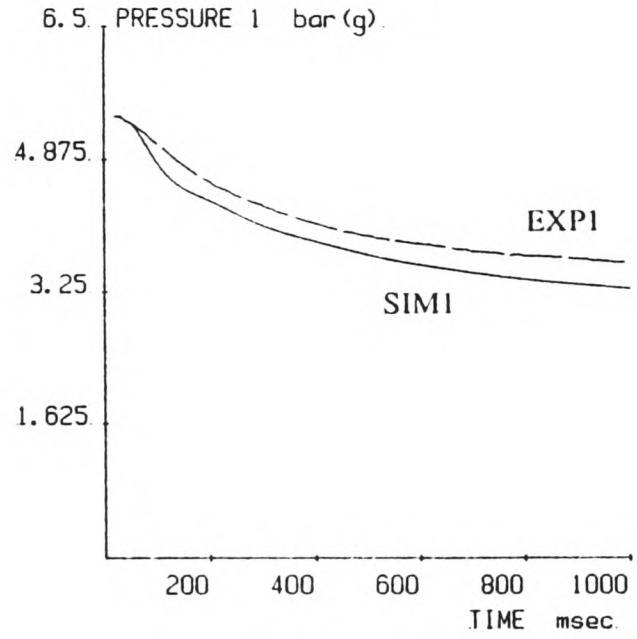

d) Chamber 1 pressure / time

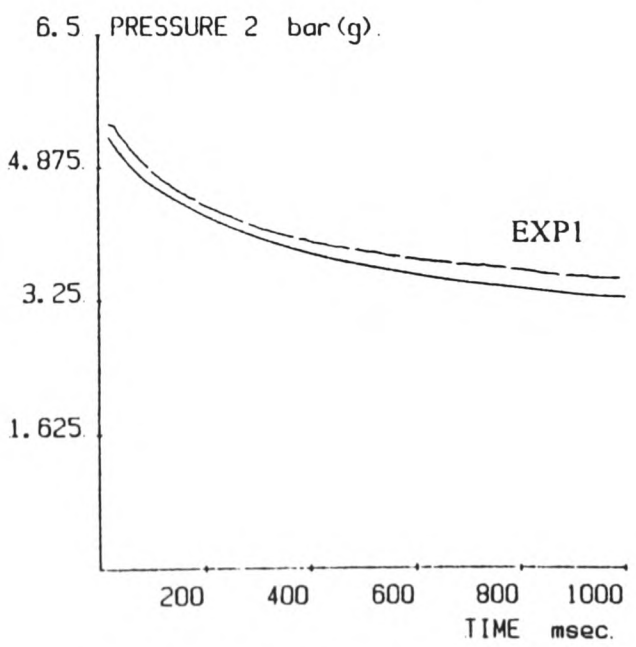

e) Chamber 2 pressure / time

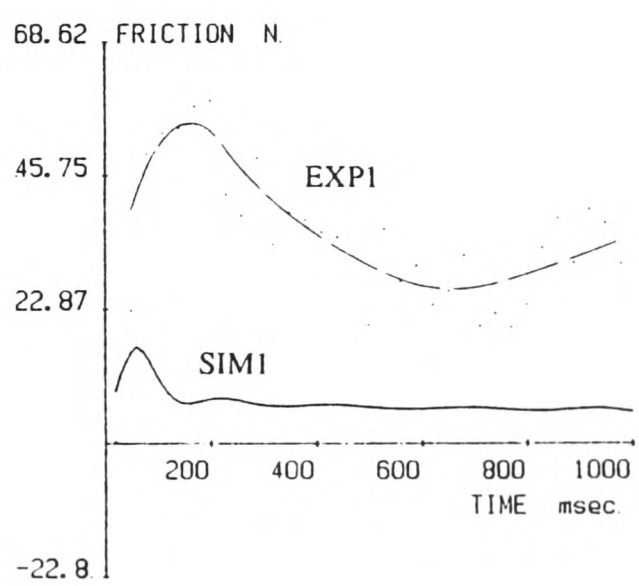

f) Friction /time

FIGURE 3.10. Comparison of Simulation-SIM1 with System Response-EXP1.

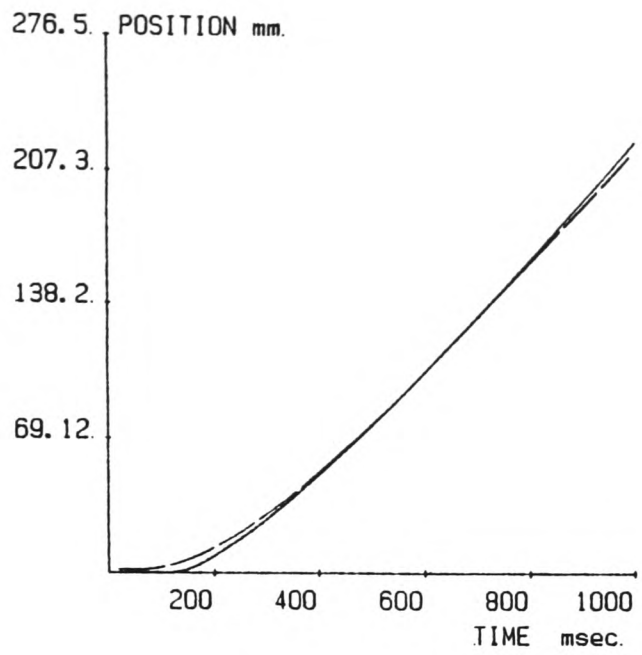

a) Position / time

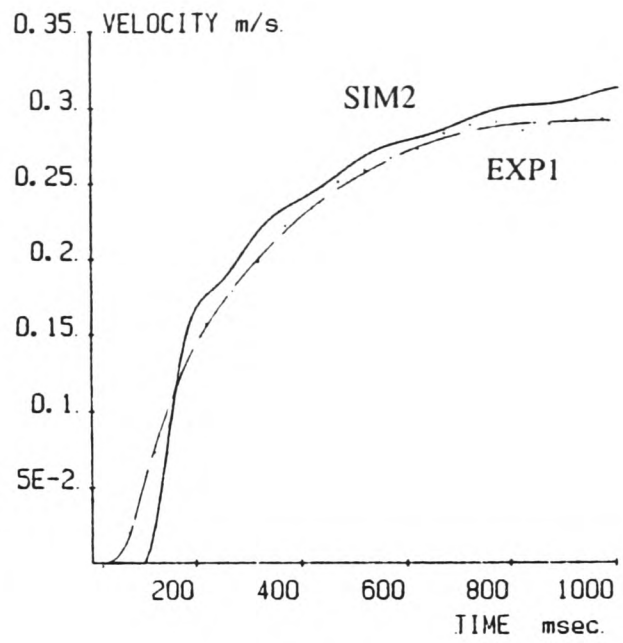

b) Velocity / time

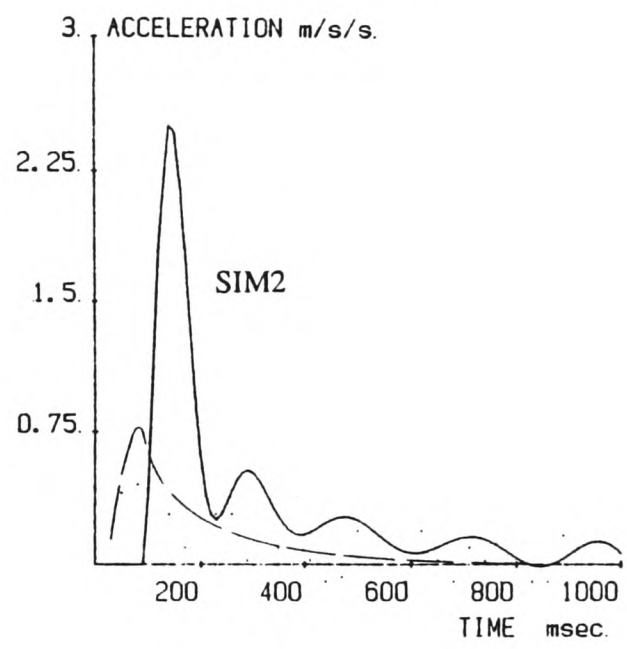

c) Acceleration / time

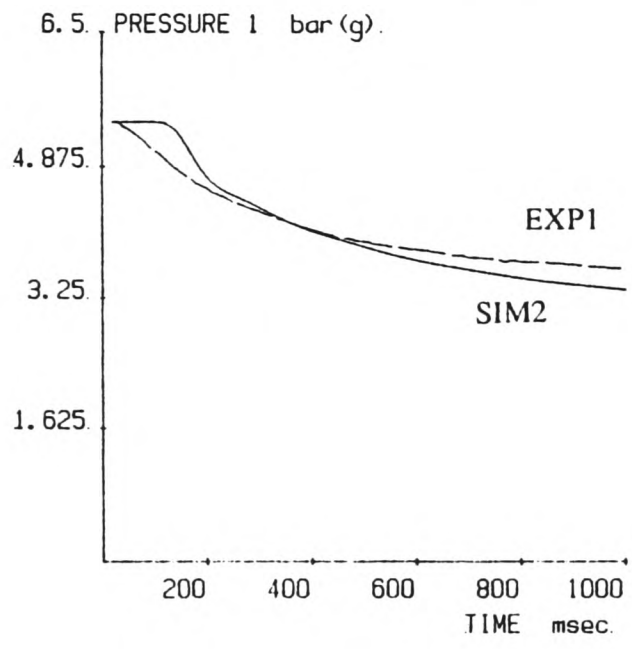

d) Chamber 1 pressure / time

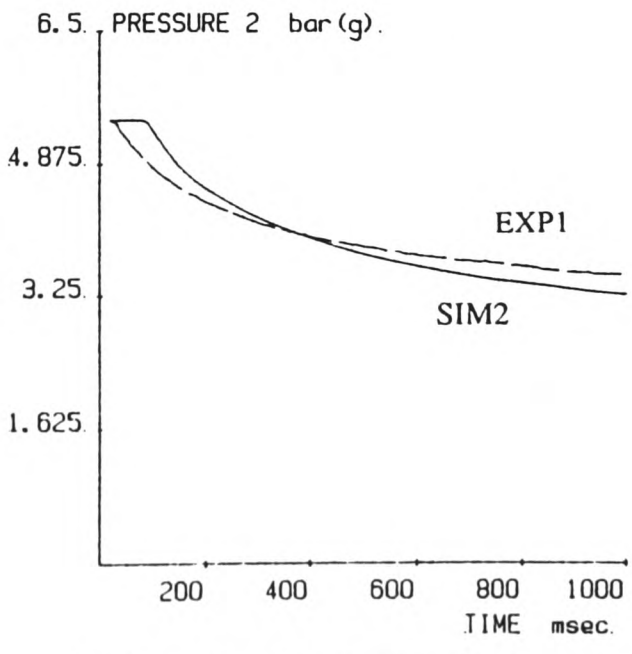

e) Chamber 2 pressure / time

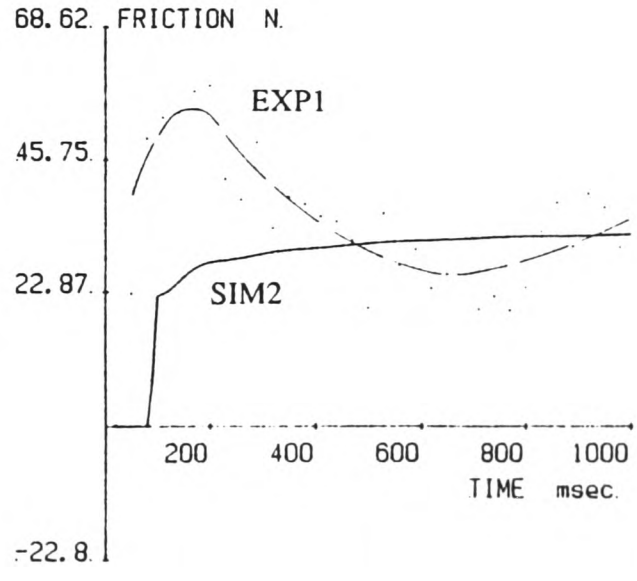

f) Friction /time

FIGURE 3.11. Comparison of Simulation-SIM2 with System Response-EXP1.

The simulation is significantly improved although acceleration remains too high initially. Comparison of chamber pressures exposes the inaccuracy of the model assumption that the time shift between model and experiment can be represented solely by a valve time delay, although this assumption does improve the fit of the position response greatly.

The model input parameters given for SIM2 in table 3.2 could therefore be used as a reasonable simulation of the experimental test EXP1. Before examining how well this model simulates the system response for other *system* initial conditions (shown in italics in table 3.2) a brief investigation of the significance of some of the model constants was carried out.

Firstly, the effect of the model time step was investigated by repeating the simulation above (SIM2) with a reduction in the model time step to 1 *ms*. This simulation was named SIM3 and the full listing of the input parameters is given in table 3.2. A comparison of the model output for the two values of time step is shown in figure 3.12.

No discernible difference is shown in the time response for position or chamber pressures. However, SIM3 which used a 1 *ms* time step shows less oscillatory response for acceleration. The smaller step results in more accurate values being stored for fast moving variables such as acceleration, particularly when near to a maximum or a minimum, and this reduces the overshoot at these points.

The only cost of reducing the time step of the model is the increase in the computing time required. No extra memory or data storage is required as the computer programme allowed the user to specify the maximum number of values to be stored. As a guide, a decrease in the model time step from 5 to 1 *ms* for one second of simulation increased the computing time from approximately 2 minutes to 6 minutes. For the purposes of simulating the tests of the opening of the valve a time step of 5 *ms* was sufficiently accurate.

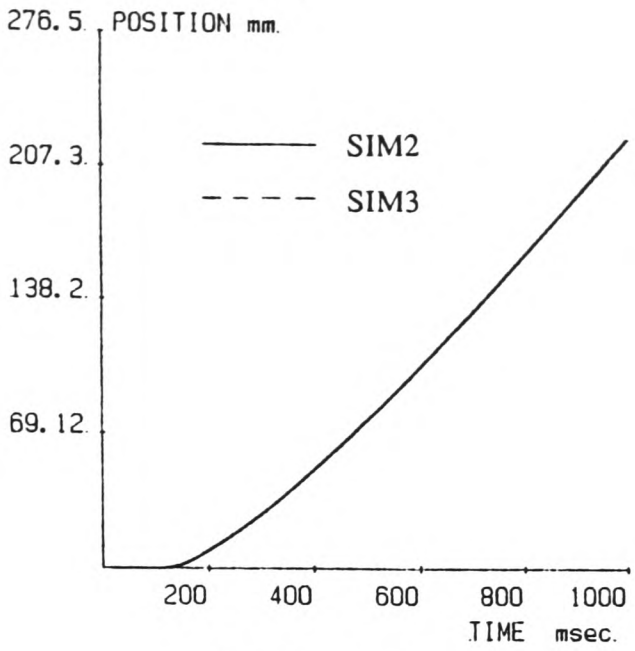

a) Position / time

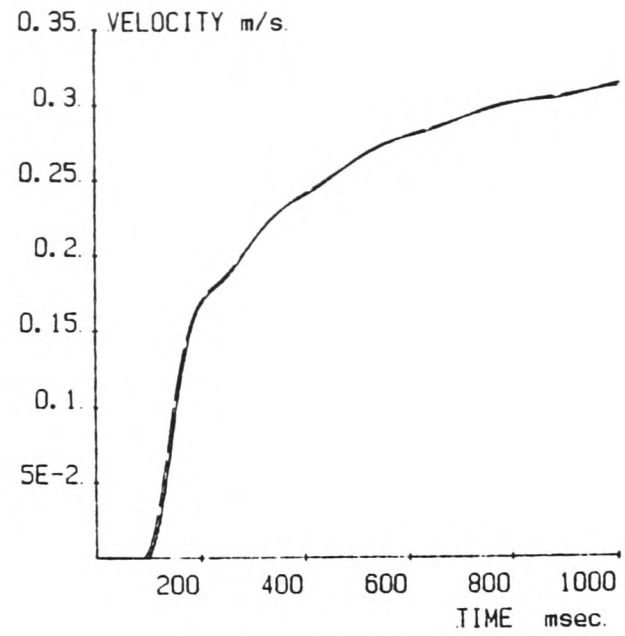

b) Velocity / time

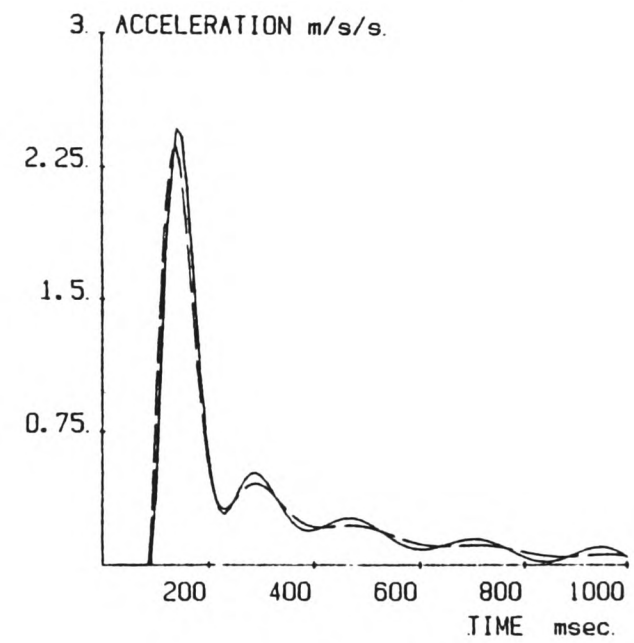

c) Acceleration / time

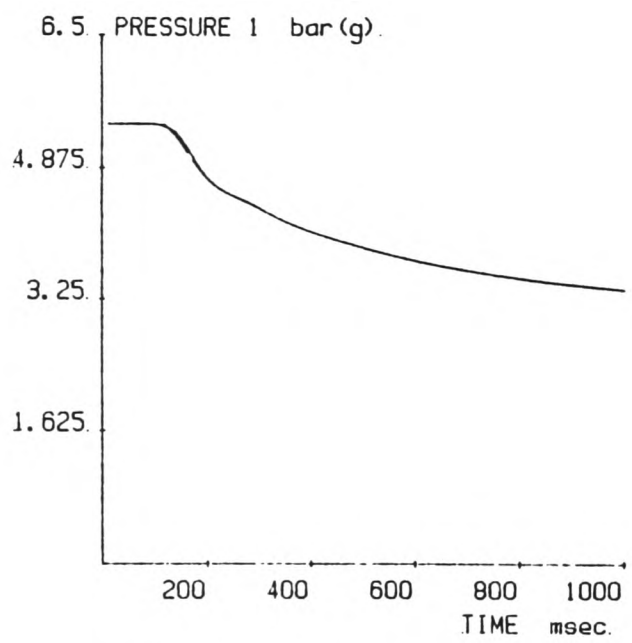

d) Chamber 1 pressure / time

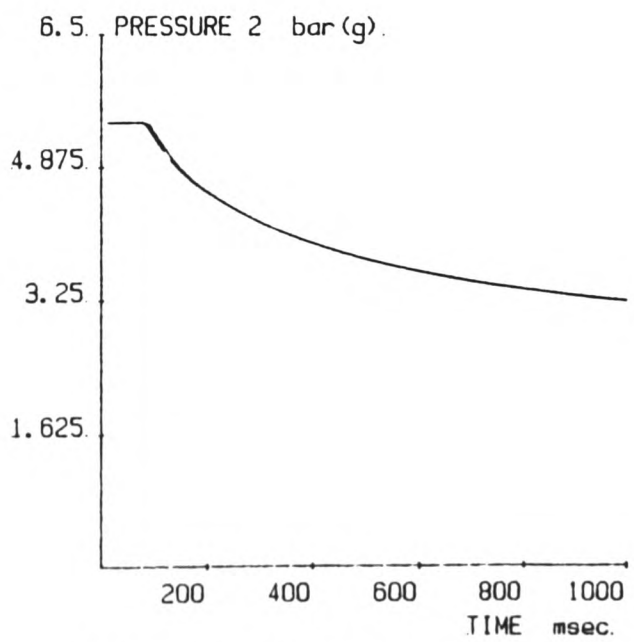

e) Chamber 2 pressure / time

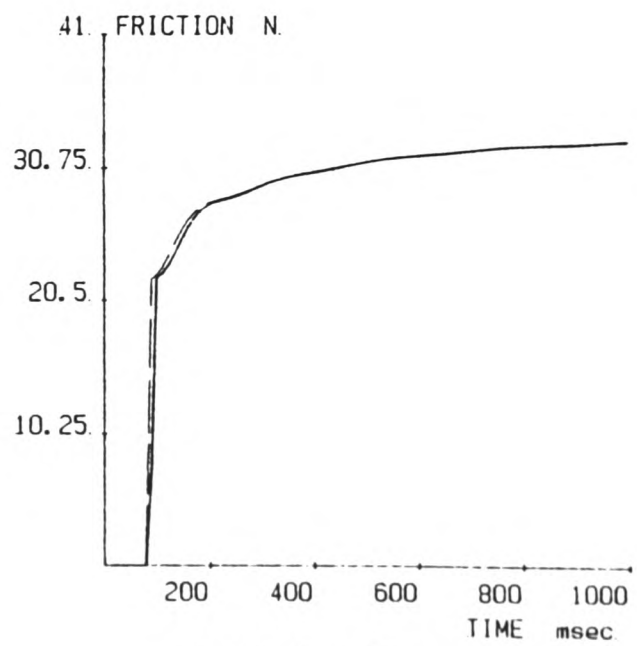

f) Friction /time

FIGURE 3.12. Comparison of Simulations with Different Time Steps-SIM3 and SIM2.

The second parameter investigated was the ratio of specific heats (γ) used in the model equation for an adiabatic gas process. The assumption that the process is adiabatic might be improved by assuming that the same equations hold for a mixed process of adiabatic and isothermal change and by exchanging the exponent γ for the polytropic exponent n. The value of n can lie between two extremes; 1.0 for a totally isothermal change and 1.4 for an adiabatic one. The effect of the exponent n on the output of the simulation was investigated by carrying out a simulation with $n = 1.1$. This simulation was called SIM4 and a listing of the input parameters is given in table 3.2.

Figure 3.13 compares the output of the simulation SIM4 which used $n = 1.1$ to the output from the simulation SIM2 which used $n = 1.4$.

The reduction of the exponent has the effect of reducing the acceleration of the piston and therefore reducing its velocity. Referring back to figure 3.11 the peak in the acceleration in the simulation SIM2 was higher than the experimental test and a reduction in the polytropic exponent from 1.4 to 1.1 would improve this condition. The velocity in the simulation SIM2 in figure 3.11 was also higher than the experimental test and this too would be reduced by a reduction in the polytropic exponent.

A value of $n = 1.27$ was found to give the desired velocity and was also found to reduce the peak acceleration of SIM2 by 12%. This lower initial acceleration allowed the initial time delay to be reduced to 50 *ms*. These values were used in a final run of the simulation - SIM5. A listing of the input parameters for this model simulation is given in table 3.2 and a comparison of the results is shown in figure 3.14. A good match between the experimental results and the simulation is clearly seen. These model parameters produce a good correlation of the mathematical model and the real system.

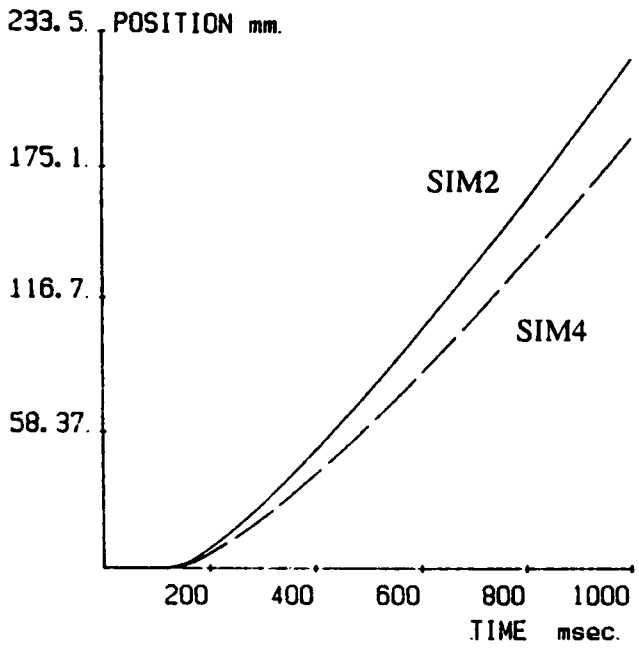

a) Position / time

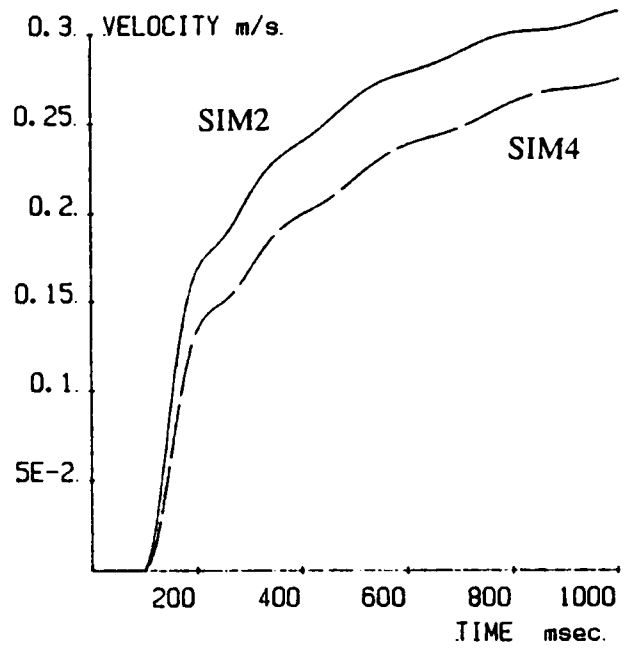

b) Velocity / time

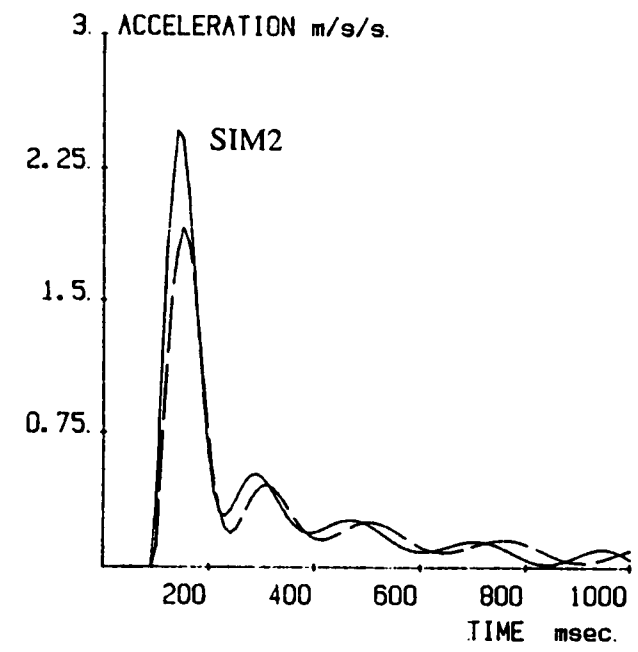

c) Acceleration / time

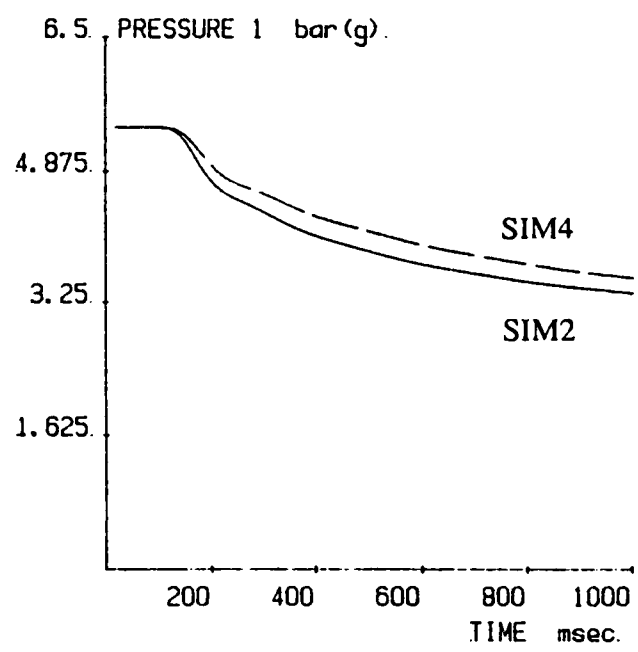

d) Chamber 1 pressure / time

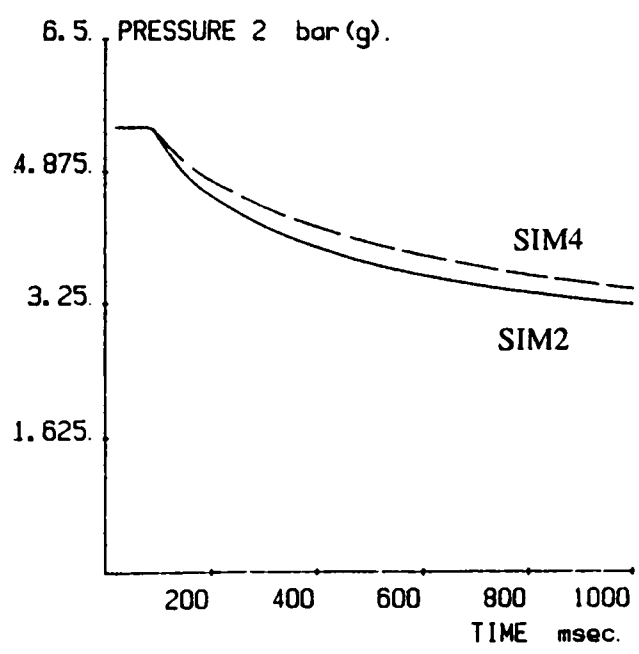

e) Chamber 2 pressure / time

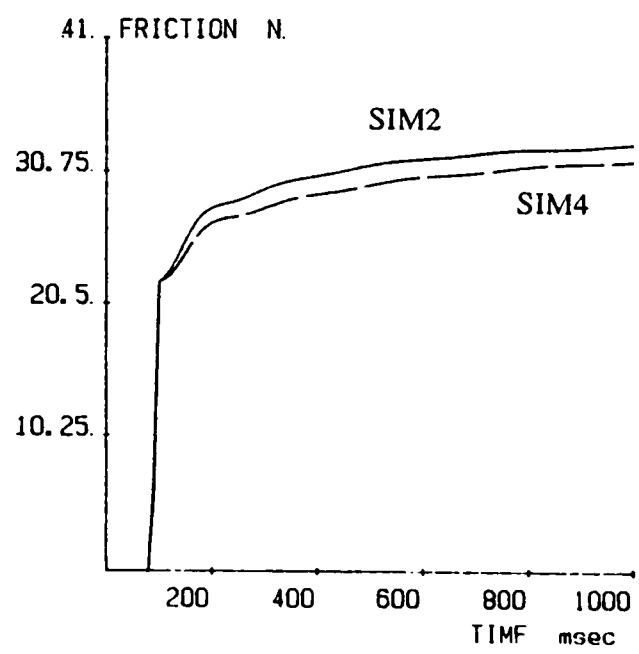

f) Friction /time

FIGURE 3.13. Comparison of Simulations with Varying Polytropic Exponent-SIM4 and SIM2.

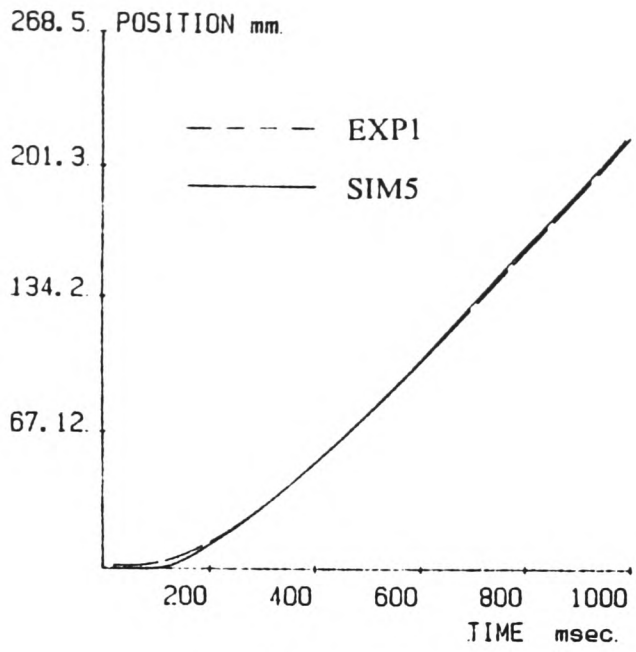

a) Position / time

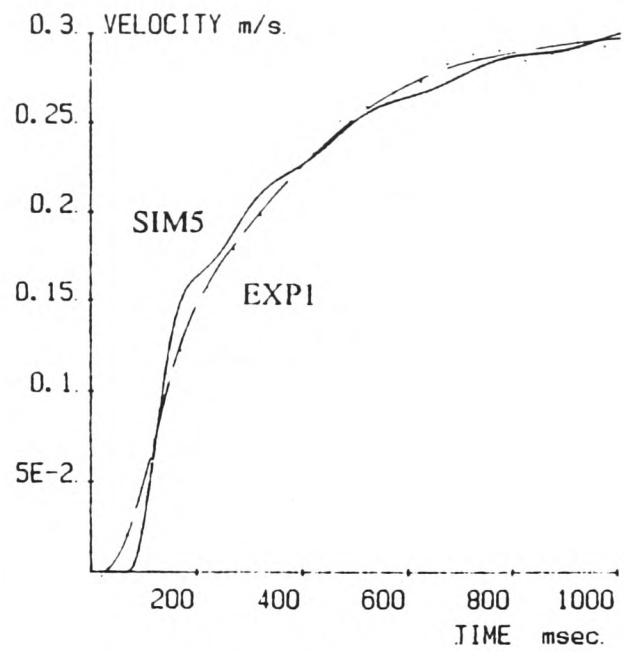

b) Velocity / time

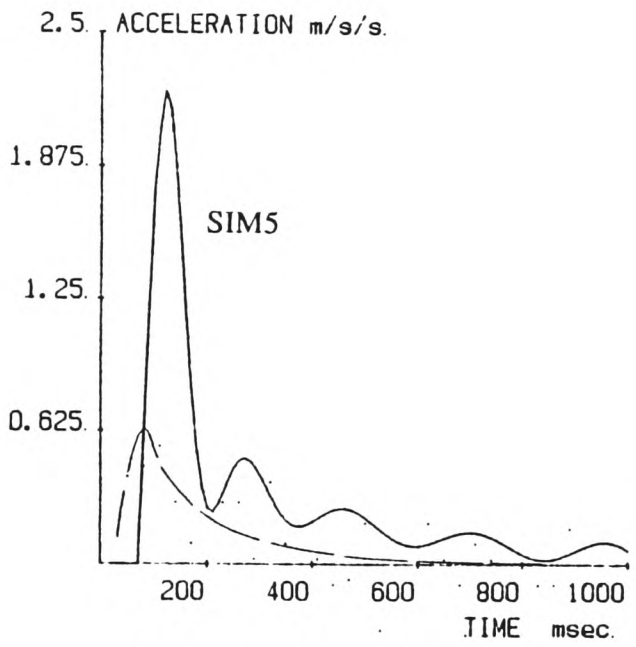

c) Acceleration / time

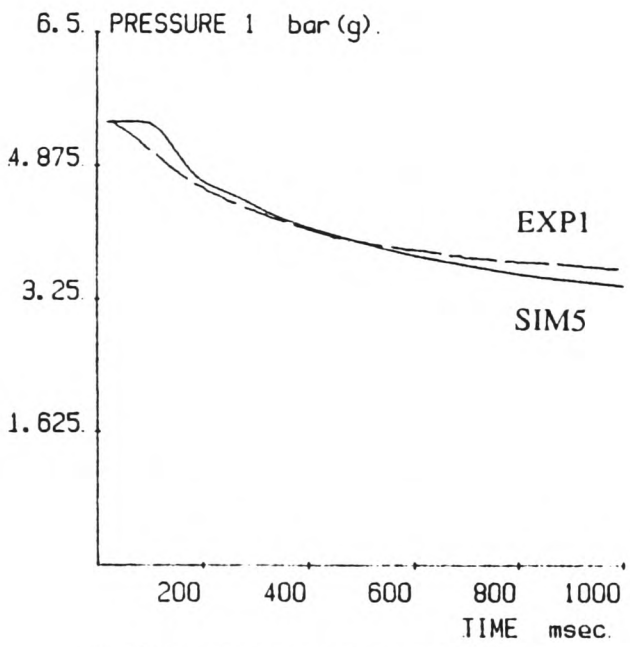

d) Chamber 1 pressure / time

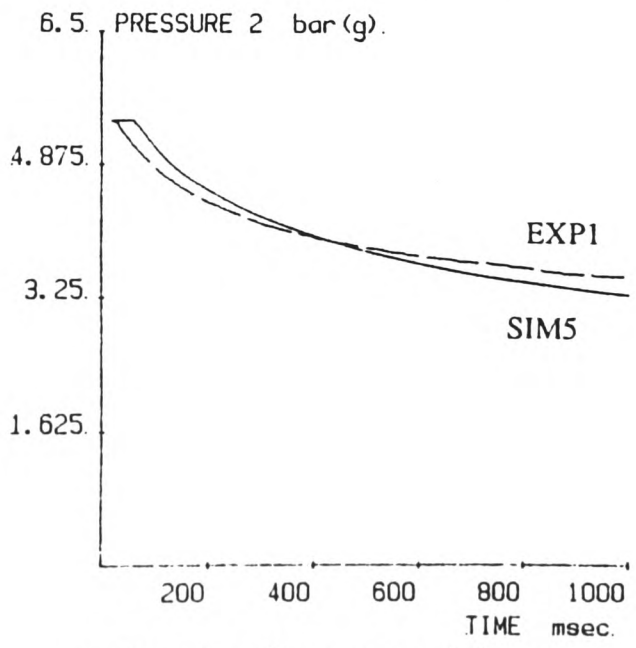

e) Chamber 2 pressure / time

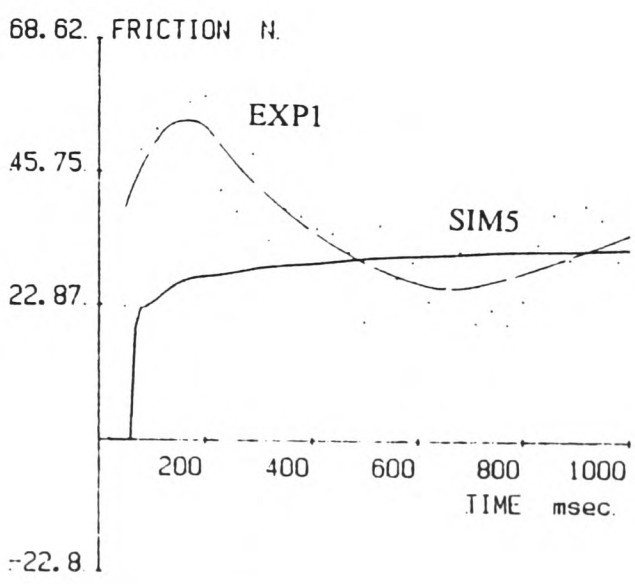

f) Friction /time

FIGURE 3.14. Comparison of Simulation-SIM5 with System Response-EXP1.

3.5.2 Variation of System Initial Conditions.

The model parameters have been established so that they provide a reasonably accurate simulation of the response of the system to a step opening of the valve is achieved but so far this has only been demonstrated for the single set of system initial conditions listed in section 3.5.2.

In this series of tests, each one of these parameters in turn was varied on the real system and then a simulation of this was carried out. The results of the simulation was then compared to the experimental measurements to determine the effect of this variation to the accuracy of the model.

Firstly, the effect of a variation in piston initial position was investigated. An experiment EXP2 was carried out with the piston initially positioned 50 *mm* from the bump stop. This was simulated in SIM6 with the initial conditions listed in table 3.3.

The output of the simulation and experiment are compared in figure 3.15. The simulation does not match the test as well as it did when the piston was initially at the bump stop. The response predicted by the model is considerably more oscillatory than that shown by the experiment and this is particularly clear from the acceleration response in figure 3.15c. The average slope of the position response is a close match to the experiment although the oscillation (clearer on the velocity trace) is markedly different from the smooth response of the system. Although the model does not closely match the the actual system response, the general shape of the position response is a reasonable approximation to the real system therefore it will be of value in predicting the system behaviour following a step change, even if the step is from positions other than the ends of the stroke. However consideration must be given to the poor fit of the velocity and acceleration predictions in these conditions, particularly if the model values of velocity and acceleration are to be used in a computer model of the control system.

PARAMETER		SIM6	SIM7	SIM8	SIM9
Cylinder Length	*mm*	300	300	300	300
Piston Area A	m^2	2.9×10^{-3}	2.9×10^{-3}	2.9×10^{-3}	2.9×10^{-3}
Valve Orifice Effective Area A_{O_1}	m^2	3.1×10^{-6}	3.1×10^{-6}	3.1×10^{-6}	3.1×10^{-6}
Valve Orifice Effective Area A_{O_2}	m^2	4.6×10^{-6}	4.6×10^{-6}	4.6×10^{-6}	4.6×10^{-6}
Mass m	*kg*	37	**47**	17	37
Coulomb Friction F_C	*N*	22	22	22	22
Coeff of Velocity Related Friction C_{FV}	Nsm^{-1}	34	34	34	34
Coeff of Diff Press Related Friction C_{FP}	m^{-2}	0.4×10^{-5}	0.4×10^{-5}	0.4×10^{-5}	0.4×10^{-5}
Solenoid Dead Time	$s\times10^{3}$	50	50	50	50
Polytropic Exp n		1.27	1.27	1.27	1.27
Gas Temperature T_s	^0K	293	293	293	293
Supply Pressure p_s	*bar*	6.24	6.30	6.23	4.80
Rate of Change of Supply Pressure k_{P_s}	*bar/s*	0.17	0.17	0.17	0.17
Exhaust Pressure p_e	*bar*	1.0	1.0	1.0	1.0
Supply Chamber Pressure p_1	*bar*	6.24	6.30	6.23	4.80
Exhaust Chamber Pressure p_2	*bar*	6.24	6.30	6.23	4.80
Piston Position x	*mm*	50	**0**	0	0
Piston Velocity $\dot{x}$	ms^{-1}	0	0	0	0
Piston Accn $\ddot{x}$	ms^{-2}	0	0	0	0
Time Increment t	$s\times10^{3}$	5	5	5	5
Duration of Model Simulation of -	*s*	0.85 EXP2	**1.0** EXP3	1.0 EXP4	1.0 EXP5

Note:
Parameter names in italics indicates the variables that were also set as initial conditions on the experimental equipment.
Figures in bold indicate changes from the previous simulation.

TABLE 3.3. Model Input Parameters for Simulation of Single Switch Experiments, SIM6 to SIM9.

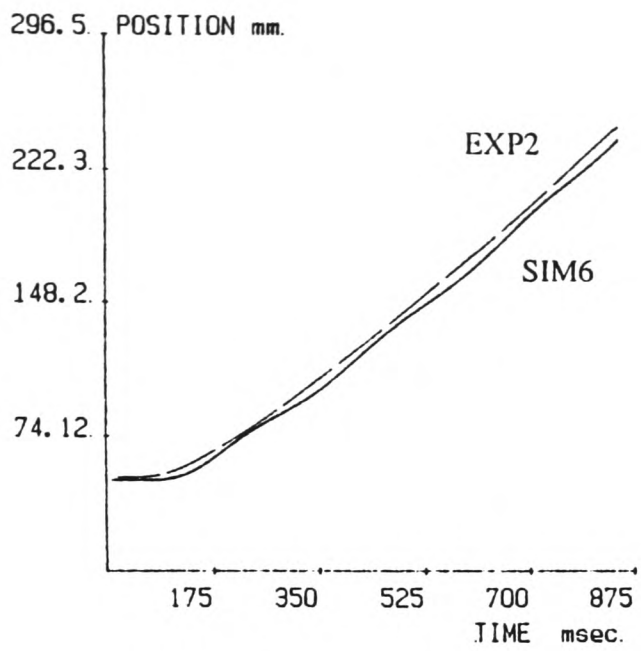

a) Position / time

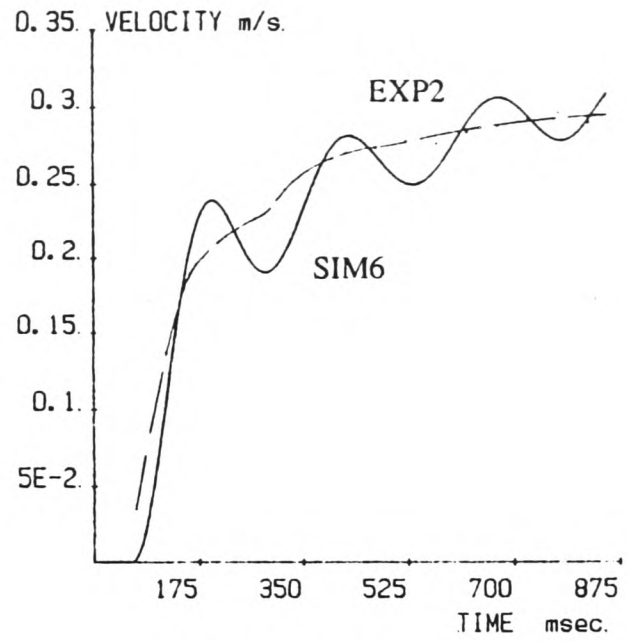

b) Velocity / time

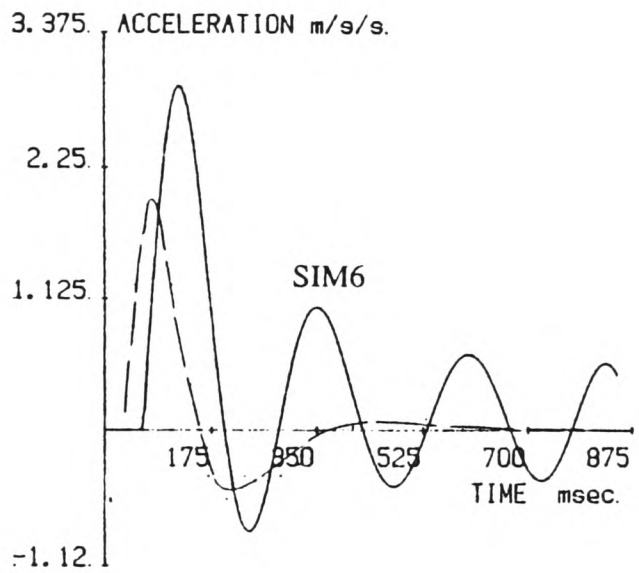

c) Acceleration / time

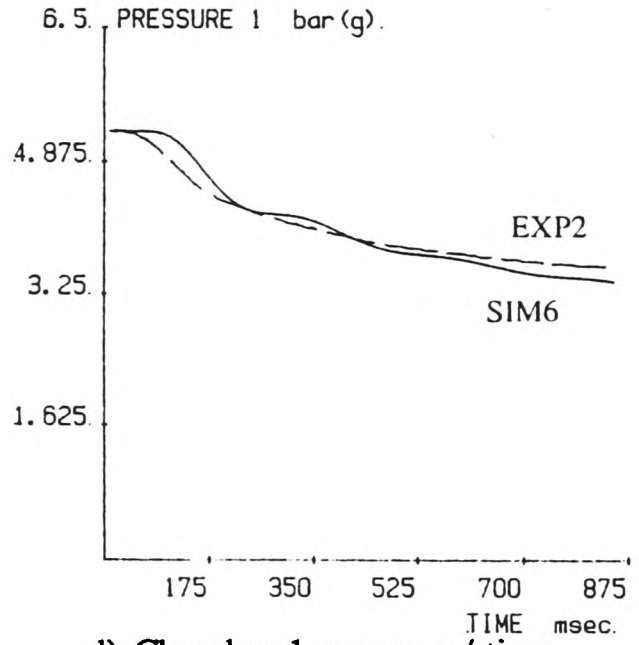

d) Chamber 1 pressure / time

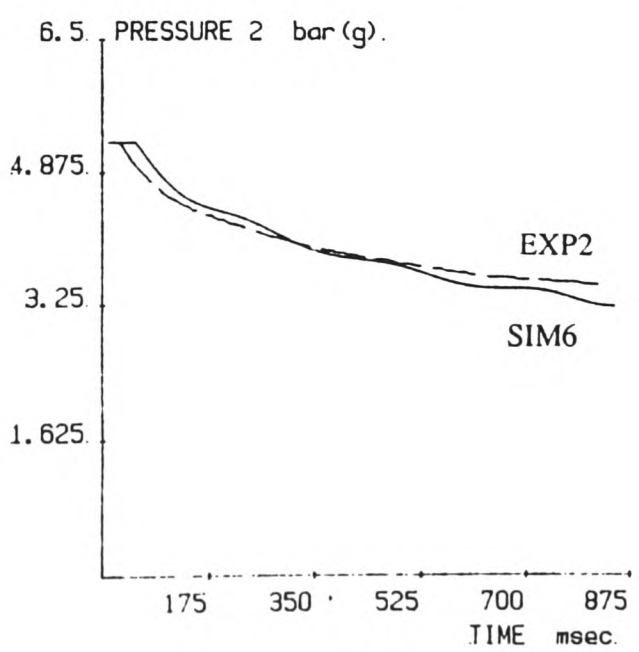

e) Chamber 2 pressure / time

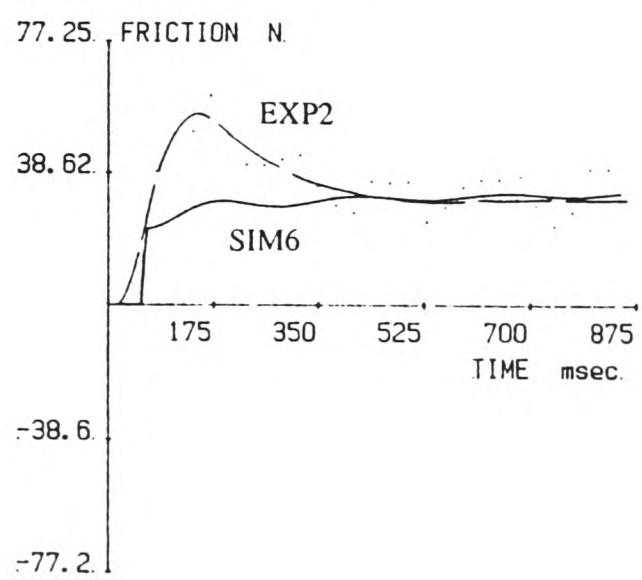

f) Friction /time

FIGURE 3.15. Comparison of Simulation-SIM6 with System Response-EXP2.

For the second investigation, a variation of the inertia load on the actuator was made. Two experimental tests were carried out, EXP3 and EXP4, with loads of 47 *kg* and 17 *kg* respectively. These experiments were modelled in SIM7 and SIM8. The input parameters for the two simulations are given in in table 3.3, and a comparison of the measured values and the simulation output is shown in figure 3.16 for the 47 *kg* inertia and in figure 3.17 for the 17 *kg* inertia.

The simulations are a good match to the measured values for these load inertias although figures 3.17b and c show that the model response is more oscillatory for low inertias than the real system. The model is seen to be more accurate for higher load inertias.

In the third investigation the supply pressure was reduced to approximately 4 *bar gauge* and the measured response was stored in EXP5. The input parameters used for the simulation of this reduced pressure test - SIM9 - are given in table 3.3 . The outputs for the experiment and the simulation are compared in figure 3.18. It can be seen that the accuracy of the simulation has not been effected by the variation of supply pressure and therefore this model is a good representation of the real response at lower supply pressures.

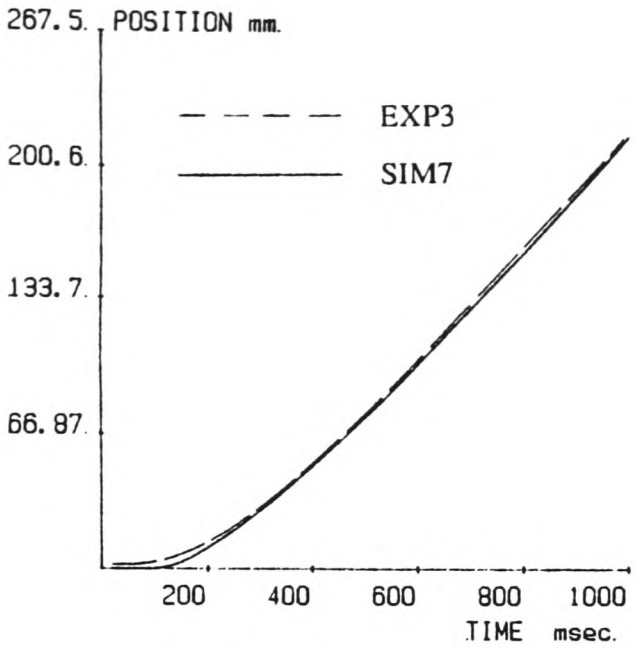

a) Position / time

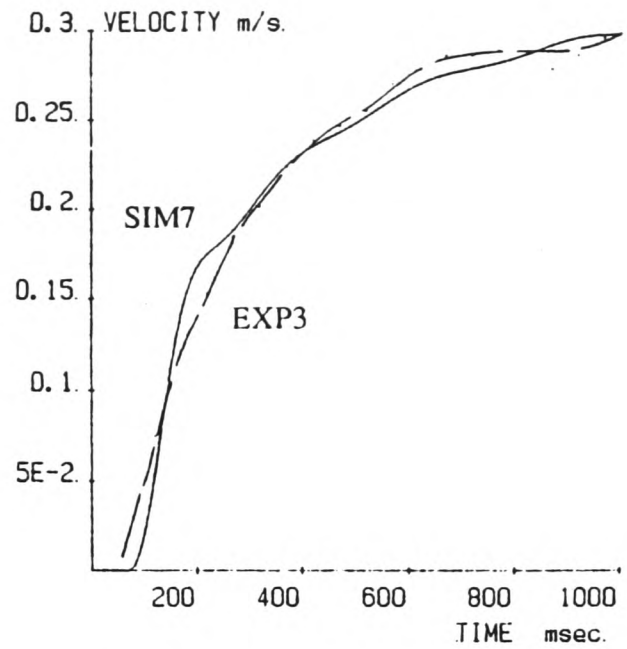

b) Velocity / time

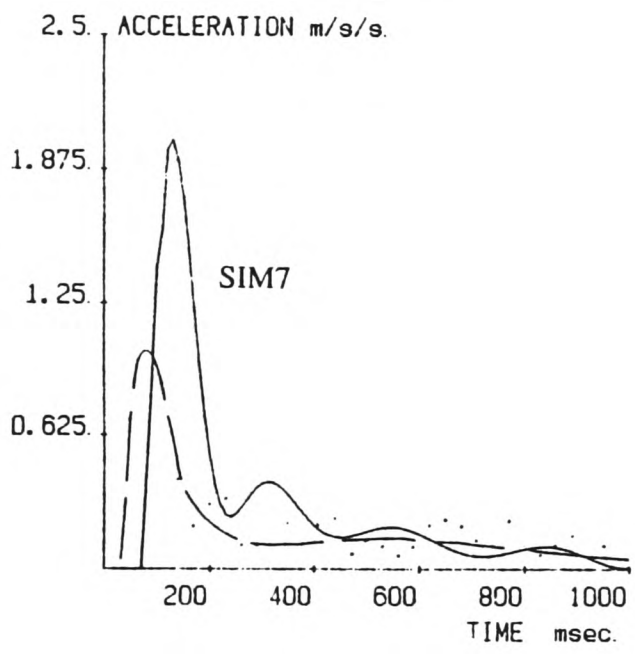

c) Acceleration / time

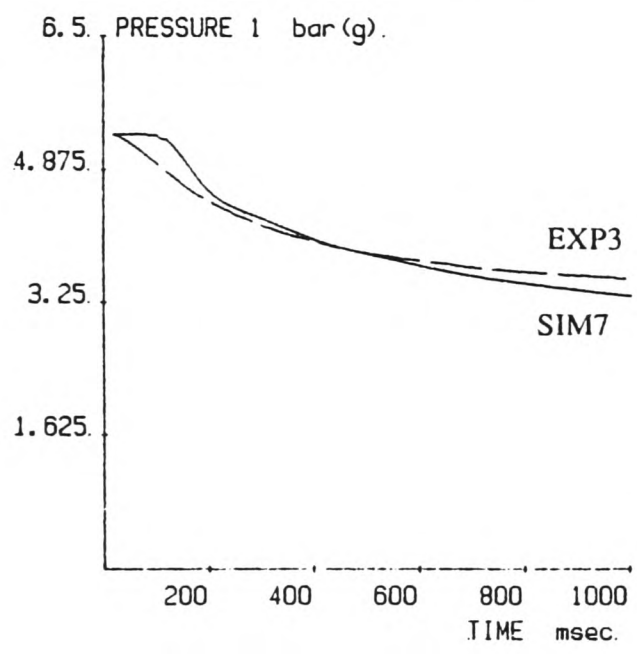

d) Chamber 1 pressure / time

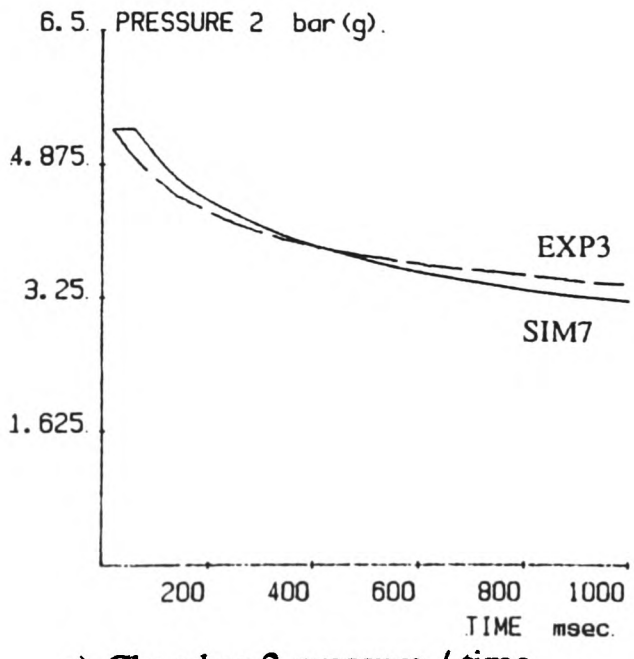

e) Chamber 2 pressure / time

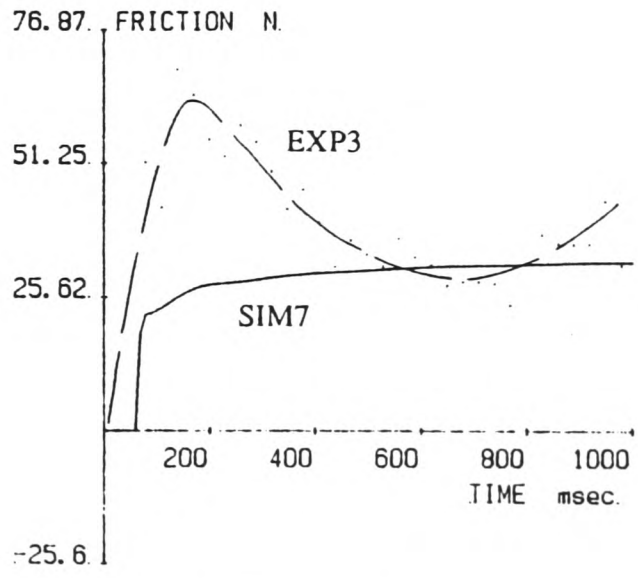

f) Friction /time

FIGURE 3.16. Comparison of Simulation-SIM7 with System Response-EXP3.

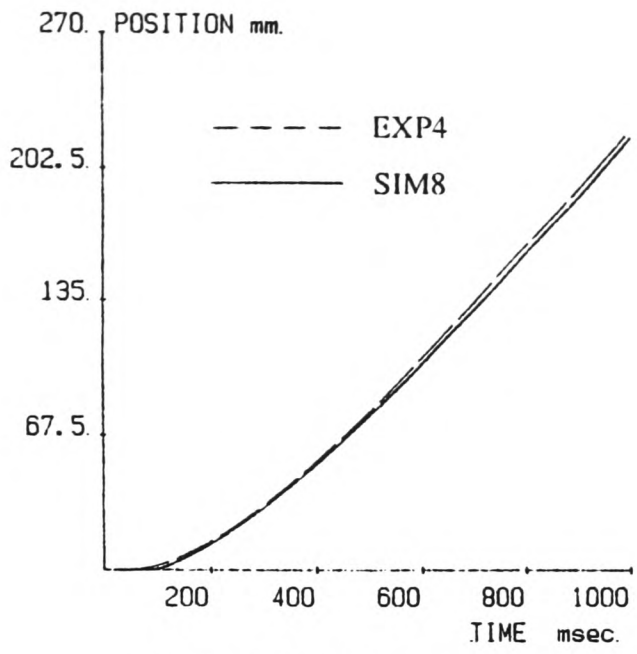

a) Position / time

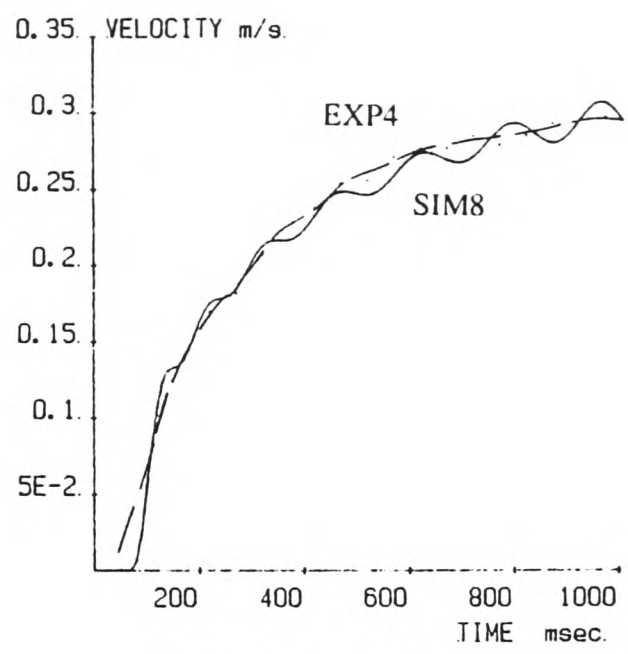

b) Velocity / time

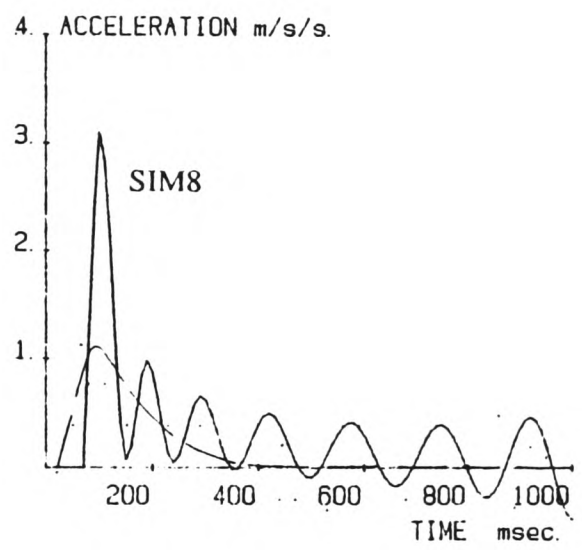

c) Acceleration / time

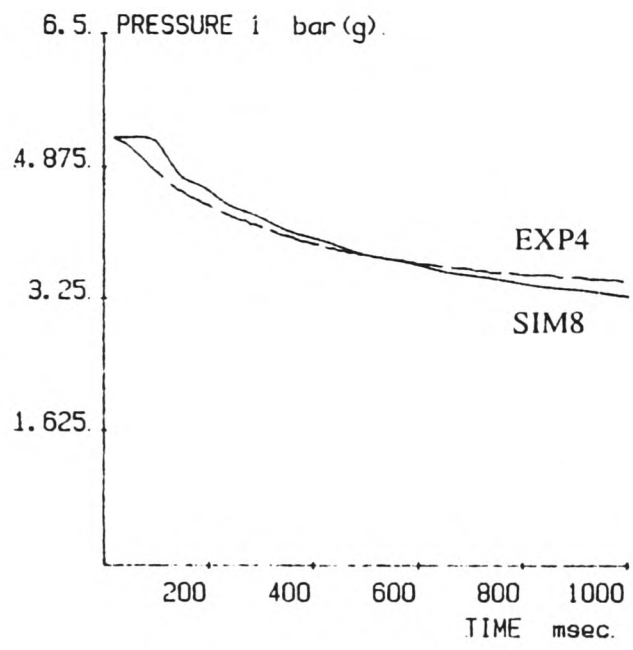

d) Chamber 1 pressure / time

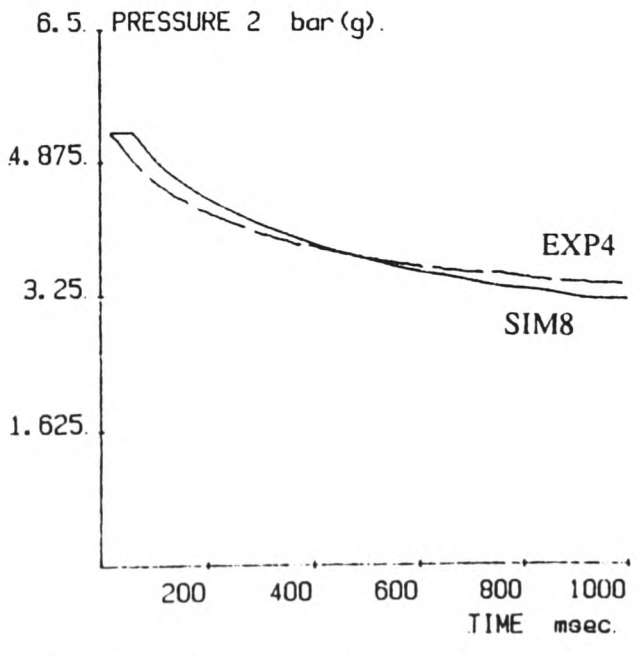

e) Chamber 2 pressure / time

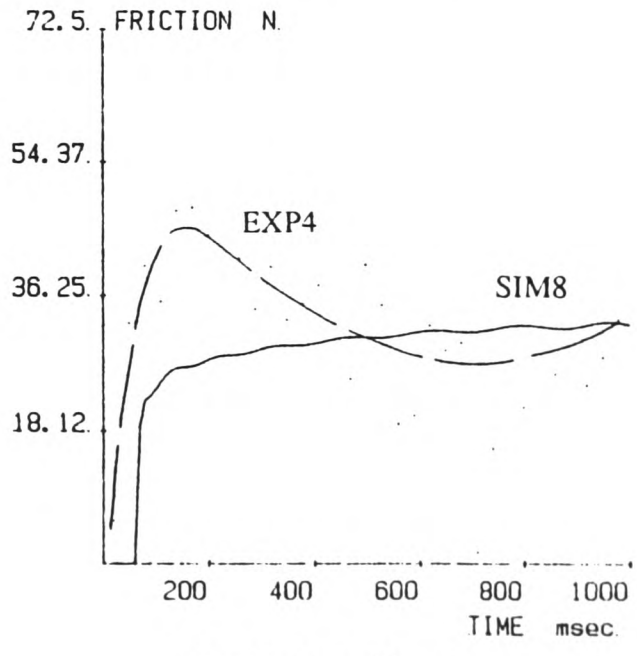

f) Friction /time

FIGURE 3.17. Comparison of Simulation-SIM8 with System Response-EXP4.

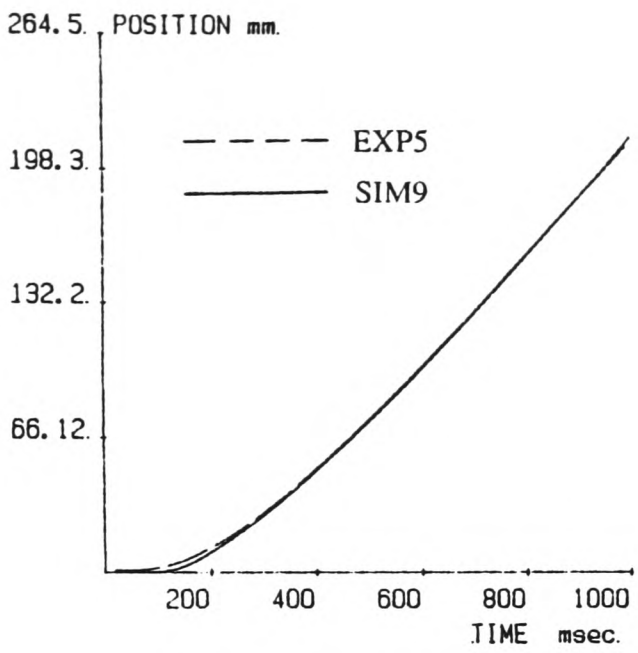

a) Position / time

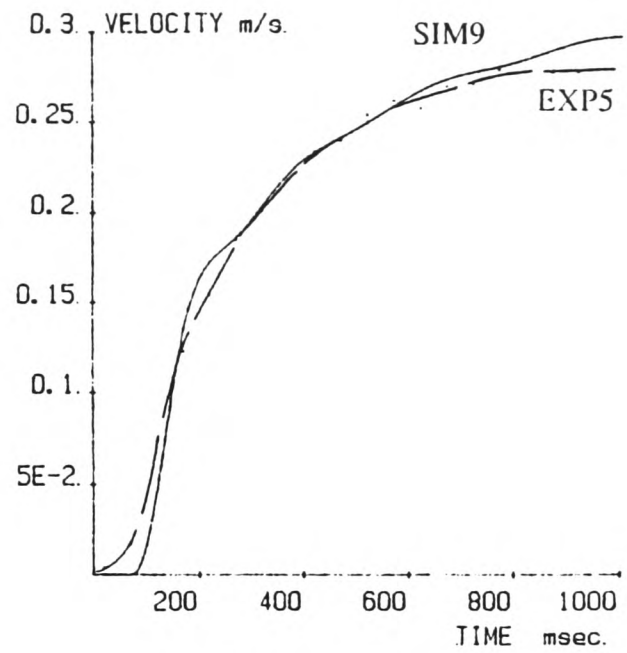

b) Velocity / time

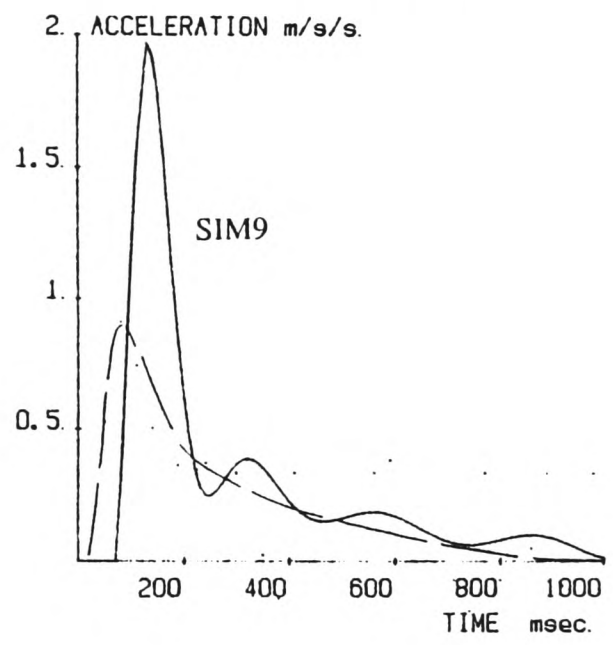

c) Acceleration / time

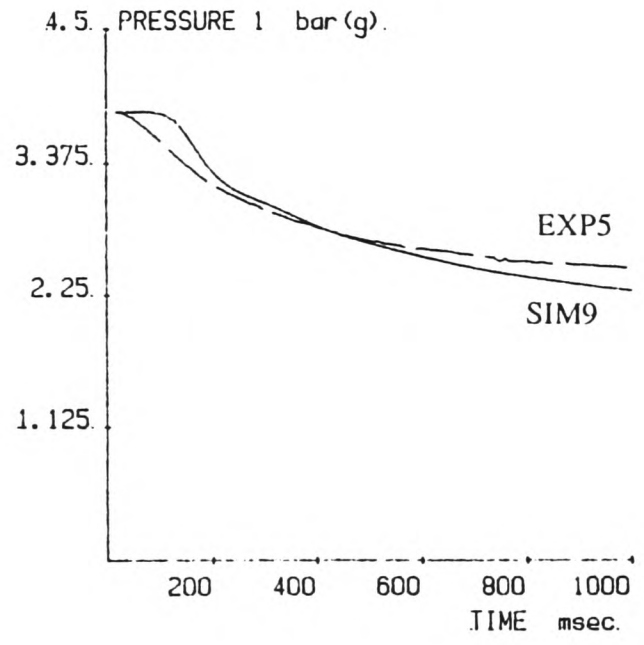

d) Chamber 1 pressure / time

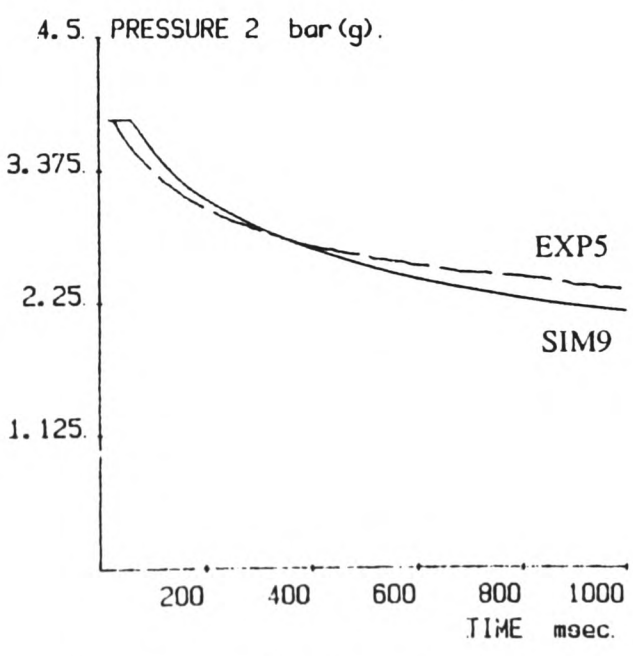

e) Chamber 2 pressure / time

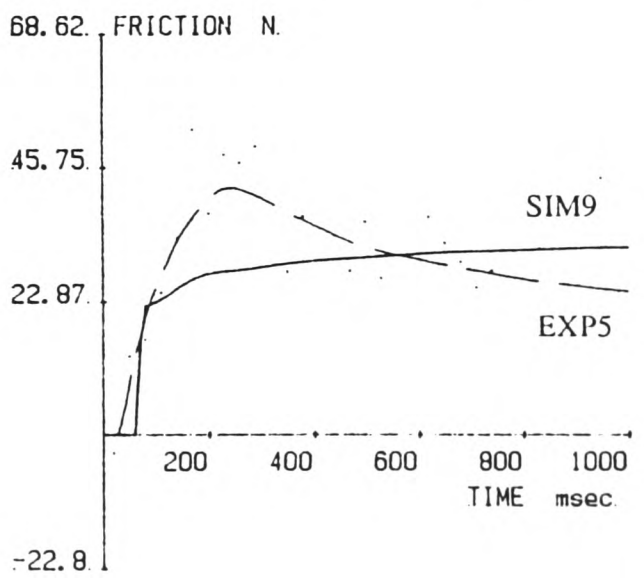

f) Friction /time

FIGURE 3.18. Comparison of Simulation-SIM9 with System Response-EXP5.

3.6 Comparison of System and Model for Motion in Two Directions.

The accuracy of the model has been assessed by comparing its output with the equivalent measured values for a simple single switching of the exhaust valve and the results of this investigation have been presented in section 3.5. Before using the model as a tool for the development of a control system, an assessment of the accuracy of the model for a more complex valve switching scheme was carried out.

The switching scheme was as follows. With the piston positioned at a known point on the stroke, motion is caused by the switching of the exhaust valve as before. The computer monitors the piston position until a specified point on the stroke is reached. At this set point both valves are switched causing a reversal of the motion of the piston and load.

Measurements of the system response are taken in a similar way to that described in section 3.5 but the computer programme was slightly modified so that the switching position can be detected. The flowchart for this programme is given in Appendix 3b.

The switching of both valves simultaneously was easy to achieve on the real system. However in order to obtain this discontinuity in the computer model a variety of changes to the model programme were made. The effect of switching both valves was that the two cylinder chamber equations and the two valve equations were reversed, ie the exhaust side of the actuator became the supply side and vice-versa. Equations [6] and [7] in section 3.3.1 and equations [10] and [11] in section 3.3.2 were now applied to the opposite side of the actuator and the values of p_1 and p_2 used as initial values in these equations were obtained from the p_2 and p_1 of the previous time step.

The first tests using this switching scheme exposed a problem with the original rig design because only one pulley wheel was being used to support the masses. (Refer to section 3.4.1 - Loading System). Jumping of the belt occurred due to the large accelerations when the motion was reversed, and this caused inaccurate measurement of position and velocity. The rig was modified to include a second belt and pulley wheel to overcome this problem.[1]

When the increases in the inertia and the friction forces due to the rig modification were included in the computer model the output of the model was found to match the measured results well, confirming that the model was a good simulation of the real system.

The first experimental test was carried out with the initial conditions of :

- Initial piston position = 50 *mm*
- Position for motion reversal = 150 *mm*

[1] In order to present a consistent set of results in sections 3.5 and 3.6, the results in section 3.5 were obtained from the rig after the addition of the second belt and pulley.

- Inertia load = 37 *kg*
- Supply pressure (approx) = 5.5 *bar gauge*

This test was called EXP6 and the simulation, SIM10, used the the input parameters shown in table 3.4. Output of the results of the experiment and the simulation are compared in figure 3.19.

The most significant difference between the simulation and the measured results is in the position response which shows a large oscillation of the piston on the downward stroke. The velocity graph shows that there is a similar tendency towards an inflection in the measured position response but not to such a large degree. A reason for this difference may be the large and surprising difference between the measured and modelled total friction force (figure 3.19f) after the switch to downward motion. The friction was measured to be approximately 230 *N* whereas the model predicts only around 50 *N*. This lack of friction in the model would not damp out the oscillations of position to such a large degree as that which clearly did occur in the real system.

Because this high friction level was not expected and was difficult to explain, a closer investigation of the friction characteristic of the actuator and load system under test was carried out.

PARAMETER		SIM10	SIM11	SIM12
Cylinder Length	*mm*	300	300	300
Piston Area *A*	m^2	2.9×10^{-3}	2.9×10^{-3}	2.9×10^{-3}
Valve Orifice Effective Area A_{O_1}	m^2	3.1×10^{-6}	3.1×10^{-6}	3.1×10^{-6}
Valve Orifice Effective Area A_{O_2}	m^2	4.6×10^{-6}	4.6×10^{-6}	4.6×10^{-6}
Mass m	*kg*	37	37	37
Coulomb Friction F_C	*N*	22	**10**	10
Coeff of Velocity Related Friction C_{FV}	Nsm^{-1}	34	75	**75/375**
Coeff of Diff Press Related Friction C_{FP}	m^{-2}	0.4×10^{-5}	$\mathbf{30\times10^{-5}}$	30×10^{-5}
Solenoid Dead Time	$s\times10^{3}$	30	30	30
Polytropic Exp *n*		1.27	1.27	1.27
Gas Temperature T_s	^0K	293	293	293
Supply Pressure p_s	*bar*	6.30	6.30	6.30
Rate of Change of Supply Pressure k_{P_s}	$bars^{-1}$	0.17	0.17	0.17
Exhaust Pressure p_e	*bar*	1.0	1.0	1.0
Supply Chamber Pressure p_1	*bar*	6.30	6.30	6.30
Exhaust Chamber Pressure p_2	*bar*	6.30	6.30	6.30
Piston Position x	*mm*	50	50	50
Piston Step	*mm*	100	100	100
Piston Velocity $\dot{x}$	ms^{-1}	0	0	0
Piston Accn $\ddot{x}$	ms^{-2}	0	0	0
Time Increment *t*	$s\times10^{3}$	5	5	5
Duration of Model	*s*	0.9	0.9	0.9
Simulation of -		EXP6	EXP6	EXP6

Note :
Parameter names in italics indicates the variables that were also set as initial conditions on the experimental equipment.
Figures in bold indicate changes from the previous simulation.

TABLE 3.4. Model Input Parameters for Simulation of Motion in Two Directions, SIM10 to SIM12.

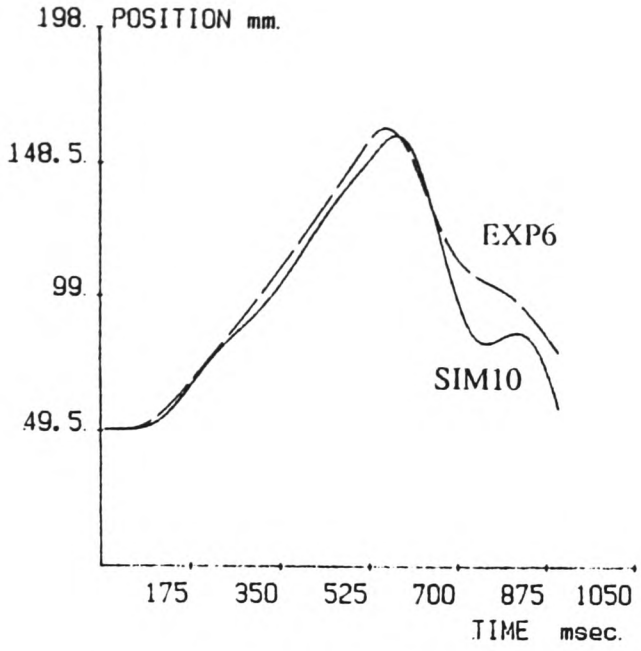

a) Position / time

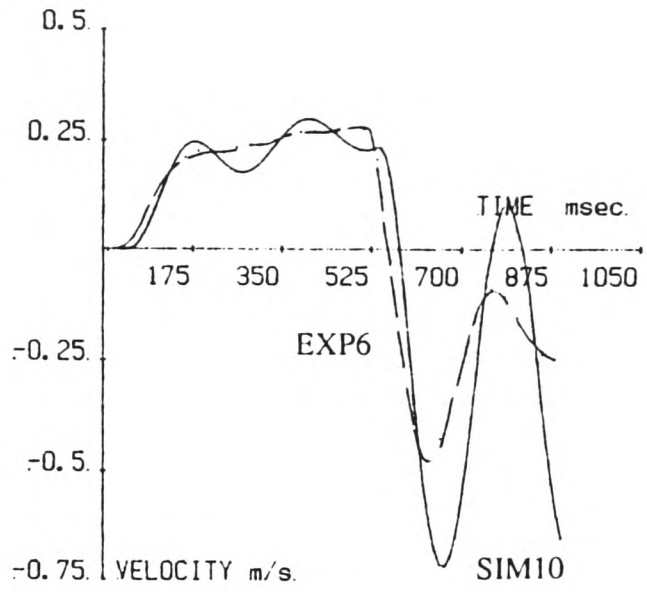

b) Velocity / time

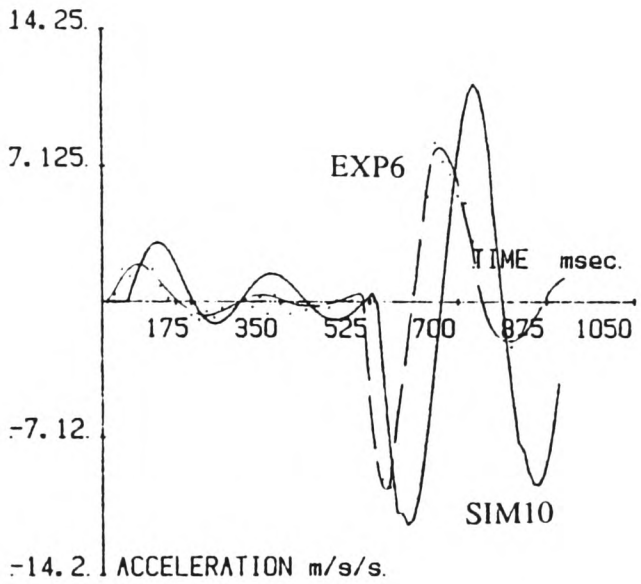

c) Acceleration / time

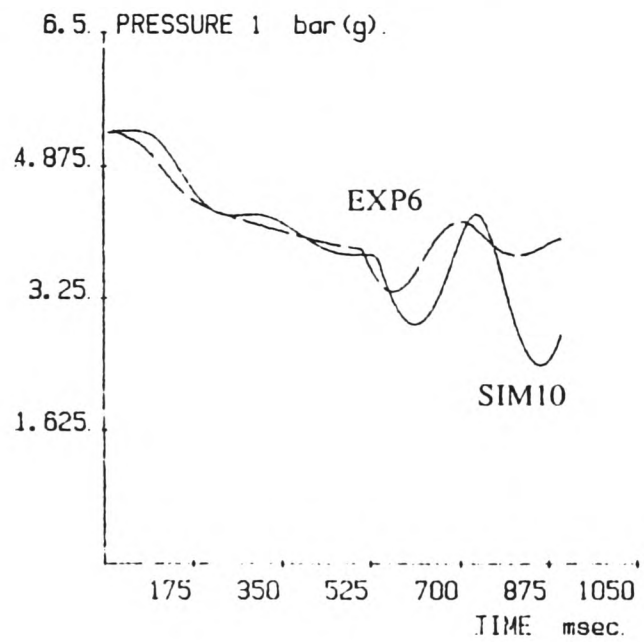

d) Chamber 1 pressure / time

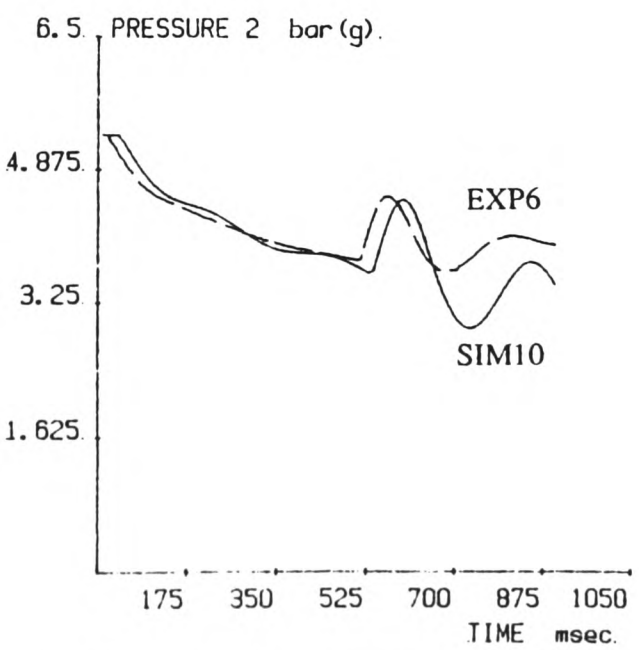

e) Chamber 2 pressure / time

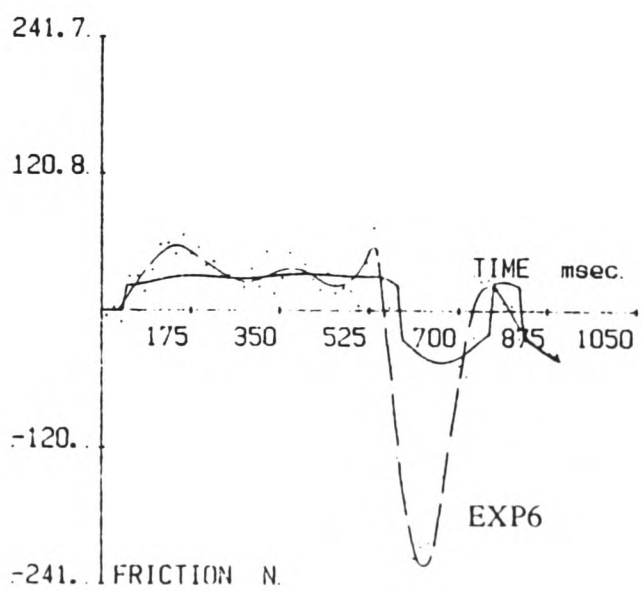

f) Friction /time

FIGURE 3.19. Comparison of Simulation-SIM10 with System Response-EXP6.

3.6.1 Investigation of Actuator and Load Friction

For the first series of tests a single switching of the exhaust valve caused motion of the actuator in one direction only. For this type of test the friction forces of the actuator and load were modelled with the relationship used in the work by Bowns (**26**). The relationship

$$F_F = F_C + C_{FV} |\dot{x}| + C_{FP} |p_2 - p_1| \qquad [13]$$

has been shown to hold reasonably well with $F_C = 22\ N$, $C_{FV} = 34\ Nsm^{-1}$ and $C_{FP} = 0.4{\times}10^{-5} m^2$. These values have been established in an approximate way because it was not felt that highly accurate values were necessary when the total friction force is small compared to the driving forces. However, for the test shown in figure 3.19 above, the friction in the actuator changed considerably when the motion of the piston and load was reversed, and so measurement of F_C, C_{FV} and C_{FP} were now necessary in order to gain a better understanding of the cause of this large change.

This investigation was initially carried out in the following way. The friction equation [13] was rearranged to be of the form :

$$\left| \frac{F_F - F_C}{p_1 - p_2} \right| = C_{FV} \left| \frac{\dot{x}}{p_1 - p_2} \right| + C_{FP} \qquad [15]$$

An estimate of F_C was made from the experimental results as being the friction level when the piston motion has just commenced. This was found to be approximately 10 *N*. The piston force summation :

$$A\ (p_1 - p_2) - F_F = m\ \ddot{x}$$

was then used with the measured values of p_1, p_2 and $\ddot{x}$ to calculate the measured total friction force F_F. Finally, measured values of p_1, p_2 and $\dot{x}$ were used to calculate $\left| \frac{F_F - F_C}{p_1 - p_2} \right|$ and $\left| \frac{\dot{x}}{p_1 - p_2} \right|$ and then these were plotted on a graph to give a straight line of slope C_{FV} and intercept C_{FP}.

Measurements were taken for a test called EXP7 using the following initial conditions :

- Initial piston position = 30 *mm*.
- Position for motion reversal = 220 *mm*.
- Inertia load = 37 *kg*.
- Supply pressure (approx) = 5.5 *bar gauge*.

A large step was chosen so that the friction over the majority of the stroke could be measured. Because there is a large difference in friction between the upward and the downward stroke it was important to distinguish at what time during the motion the values were taken before plotting them. If the values are plotted for the complete duration of the test, ie. for motion upward and for motion downward, then there is a large scatter of points and no clear straight line relationship can be seen. However, figure 3.20 shows the results of this procedure for measured values taken for upward motion only.

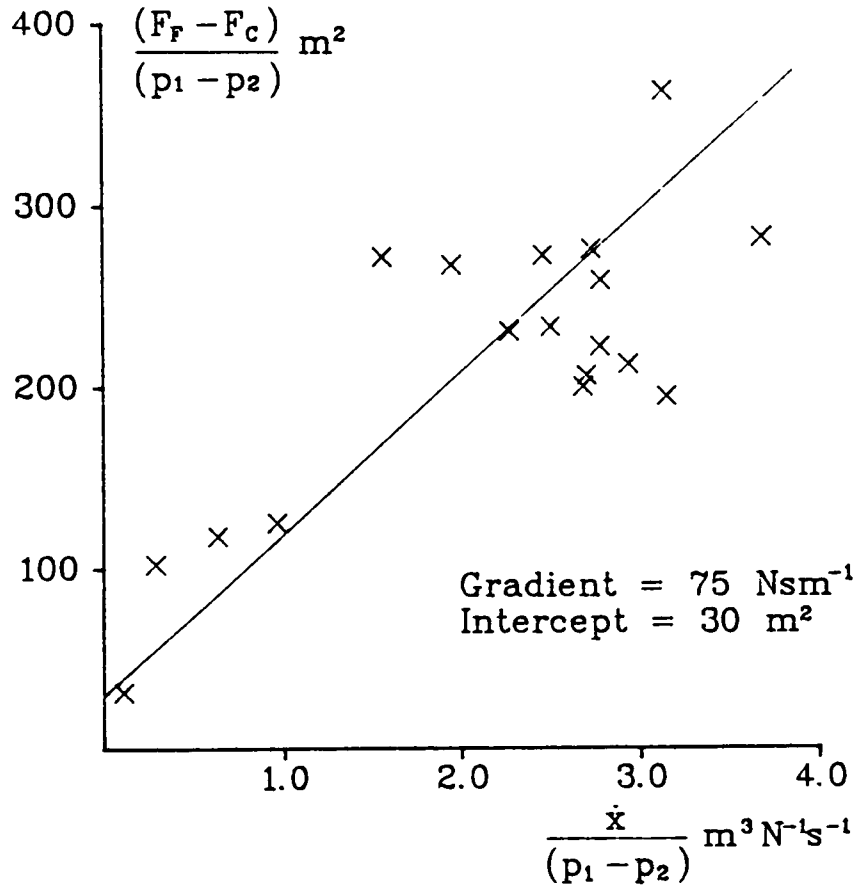

FIGURE 3.20. Graph of $\left|\frac{F_F - F_C}{p_1 - p_2}\right|$ against $\left|\frac{\dot{x}}{p_1 - p_2}\right|$ for EXP7 with F_C = 10 N and for upward motion only.

Although there is still a large scatter of points, an approximate relationship can be obtained for this part of the piston motion. This gives values of $C_{FV} = 75\ Nsm^{-1}$ and $C_{FP} = 30{\times}10^{-5}\ m^2$. The value of C_{FP} established from this graph was substituted back into equation [15] to leave only one unknown - C_{FV}. A computer programme was written to select six sets of measured values of p_1, p_2, $\dot{x}$ and $\ddot{x}$ which had taken over a period of 60 *ms*. For each set the value of C_{FV} was calculated from equation [15], and then the average value of C_{FV} calculated from the six sets was obtained for this 60 *ms* period. This was repeated to cover the duration of the whole test and finally these values of C_{FV} were plotted as a function of time. The result is shown in figure 3.21. The valves were switched at

$t = 1.1\ s$, this is marked as a broken line on the graph.

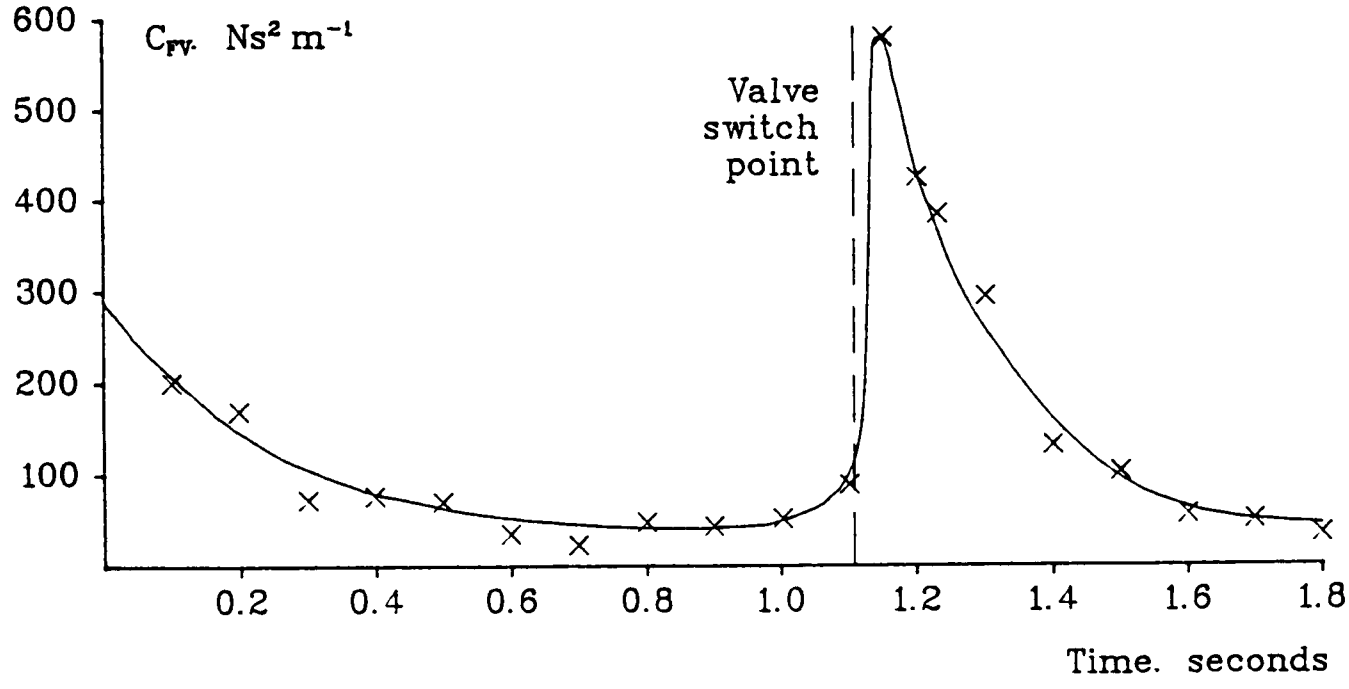

FIGURE 3.21. Graph of C_{FV} against time for EXP7 with $F_C = 10$ N and $C_{FP} = 30\times10^{-5}$ m^2.

Figure 3.21 clearly shows that there is a large variation in C_{FV} with time and that it sharply increases at the switch point. A variation in C_{FV} is also seen from $t = 0$ to $t = 0.3\ s$. It is initially high and then decreases to an approximately constant level of 50 Nsm^{-1} for the rest of the upward motion. The reason for this variation in C_{FV} with time is not clear. However, a comparison was made between it and the measured values of velocity, pressure difference and acceleration for EXP7 are shown in figure 3.22. There is a similarity between the graph of acceleration/time and the graph of C_{FV}/time. The duration of the peaks of acceleration are similar to the peaks seen in figure 3.21. The response of the pressure difference is also similar, but the peaks are of shorter duration. The first conclusion from this might be that the constant of velocity related friction C_{FV} was also a function of acceleration, but this may be an overcomplicated assumption when the accuracy of the measurements is considered. A better approach would be to reconsider the assumption of equation [13] and rewrite it thus :

$$F_F = F_C + C_{FV}\,|\dot{x}| + C_{FA}\,|\ddot{x}| + C_{FP}\,|p_1 - p_2| \qquad [16]$$

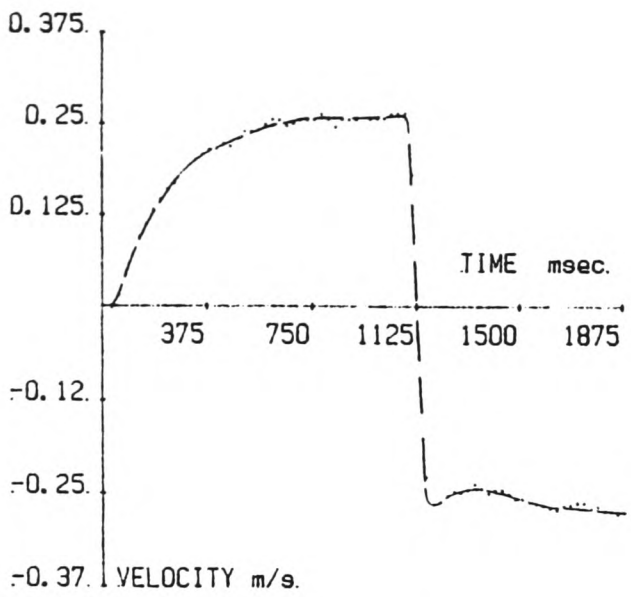

a) Velocity / time

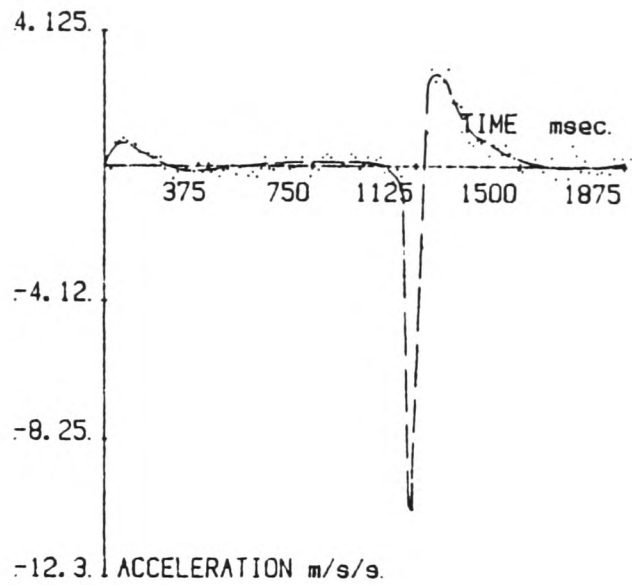

b) Acceleration / time

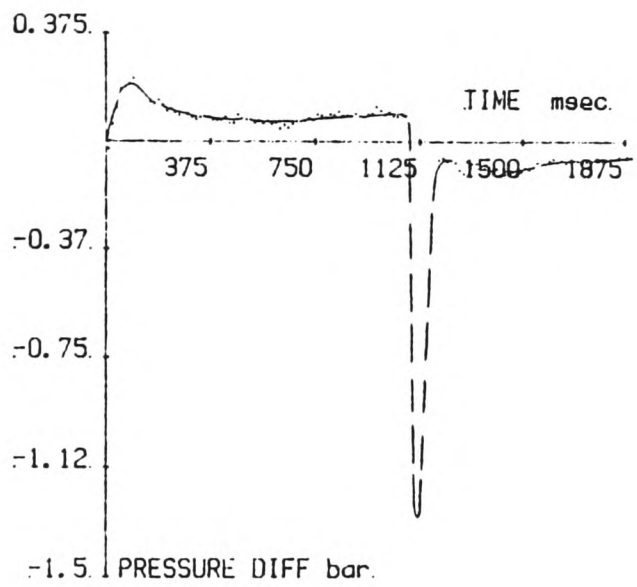

c) Pressure Difference / time

FIGURE 3.22. System Response-EXP7.

This can be rearranged as before to give :

$$\left|\frac{F_F - F_C - C_{FP}\,(p_1 - p_2)}{\dot{x}}\right| = C_{FA}\left|\frac{\ddot{x}}{\dot{x}}\right| + C_{FV}$$

The values of F_C and C_{FP} that were used before were substituted into this to give C_{FA}, the gradient of the straight line and C_{FV}, the intercept. The experimental data obtained from EXP7 described above was used to obtain the graph shown in figure 3.23.

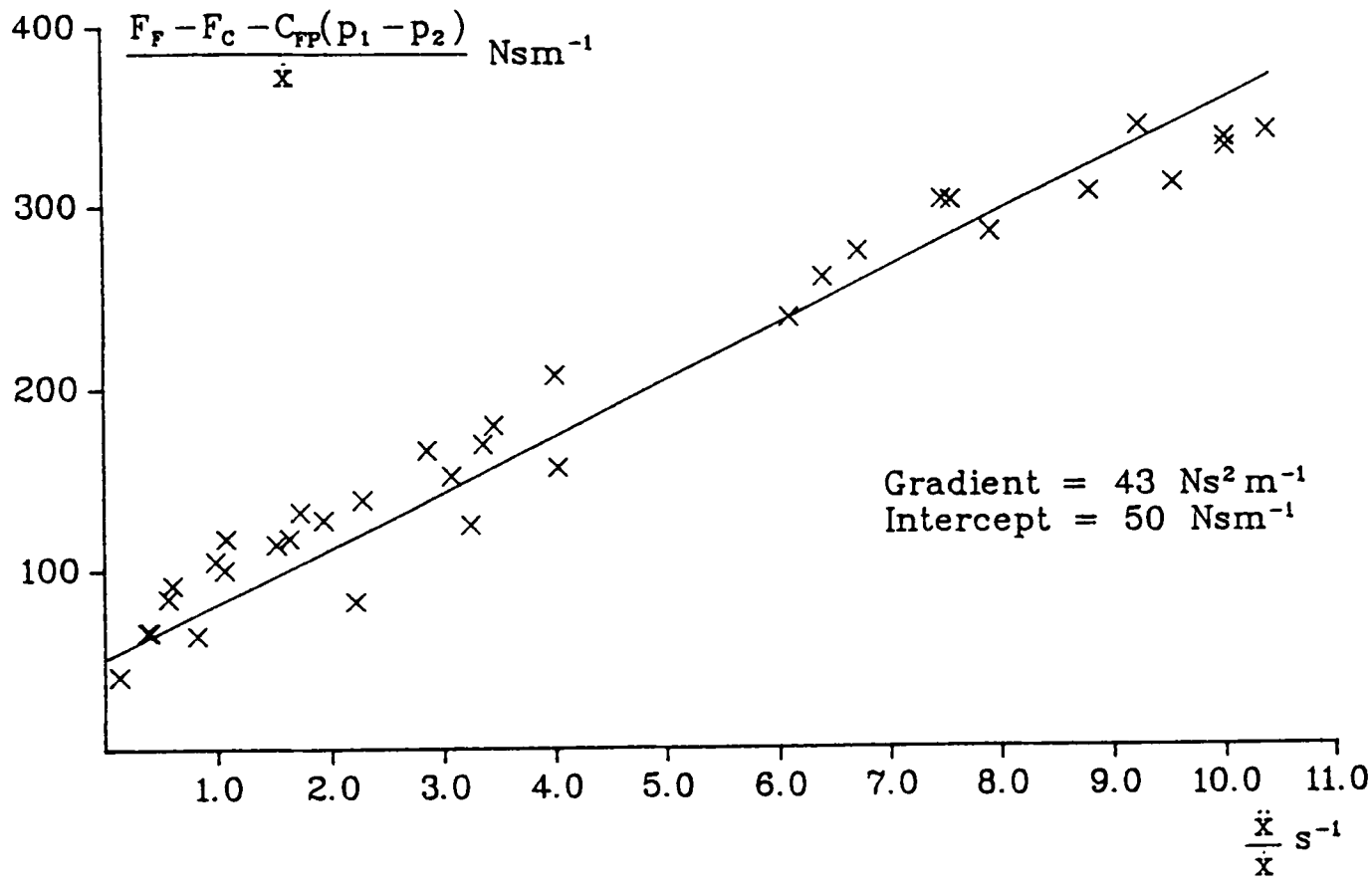

FIGURE 3.23. Graph of $\left|\frac{F_F - F_C - C_{FP}\,(p_1 - p_2)}{\dot{x}}\right|$ against $\left|\frac{\ddot{x}}{\dot{x}}\right|$

for EXP7 with $F_C = 10$ N and $C_{FP} = 30\times10^{-5}$ m^2.

A straight line relationship is shown quite clearly and with less scatter than before. The value of $C_{FV} = 50\ Nsm^{-1}$ obtained from the intercept confirms the findings of figure 3.21 and a value of $C_{FA} = 43\ Ns^2m^{-1}$ is obtained from the gradient of the line. These values suggest that the friction of the actuator can be represented by :

$$F_F = 10 + 50\ |\dot{x}| + 43\ |\ddot{x}| + 30\ .\ 10^{-5}\ |p_1 - p_2|$$

where the units of $\dot{x}$ are ms^{-1}, $\ddot{x}$ are ms^{-2} and p are Nm^{-2}. However, when this relationship is used in the model programme unreliable results are obtained. The modelling of the acceleration of the piston is not accurate for steps of the piston that begin from

intermediate points on the stroke; this was demonstrated in section 3.5. The acceleration error in the model causes a large inaccuracy in the total friction force and this is particularly true near to the switching points. It was at these points where the improvement in the friction modelling was sought so this does not achieve the objectives.

A compromise was reached after consideration of the likely working conditions of the actuator when used in a control system. First of all it was clear that a reasonable model of friction has been achieved for the motion up to the point where the the switching of the two valves occurs. This model uses terms relating to velocity and differential pressure only. It is then, after switching the valves, that a large increase in friction occurs for a relatively short time period. When the system is used for point to point positioning, rapid switching of the valves must occur in order to achieve accurate positioning. As the duration between the changes of flow direction is small then the friction level is likely to be near to the higher values shown in figure 3.20. If an average value of C_{FV} is chosen for the period between 1.1 s and 1.4 s then its value is approximately 375 Nsm^{-1}. Again referring to figure 3.20, an approximate value of C_{FV} for the upward stroke can be obtained too. It would be reasonable then to use $C_{FV} = 75\ Nsm^{-1}$ for the first stroke followed by a change in C_{FV} to 375 Nsm^{-1} for all subsequent motion. This method of modelling was evaluated for the test EXP6. As a comparison to this the same simulation was run without the change in C_{FV} after the first stroke.

SIM11 was the simulation of EXP6 using the friction model

$$F_F = 10 + 75\ |\dot{x}| + 30\times10^{-5}\ |p_1 - p_2|$$

and this is shown in figure 3.24.

SIM12 was the simulation of EXP6 using the friction model

$$F_F = 10 + 75\ |\dot{x}| + 30\times10^{-5}\ |p_1 - p_2| \qquad \text{for } \textit{upward motion}$$

$$F_F = 10 + 375\ |\dot{x}| + 30\times10^{-5}\ |p_1 - p_2| \qquad \text{for } \textit{downward motion}$$

and this is shown in figure 3.25.

Figure 3.24f shows the poor fit of the friction simulation for the period immediately after the valves were switched ($t = 525\ ms$) when only a single value of C_{FV} was used. However, the fit of this simulation is an improvement on the simulation shown in figure 3.19f which used the estimated values of F_C, C_{FV} and C_{FP}. Figure 3.25f shows a significant improvement in the fit of the simulated friction to the measured values when using the pair of equations, each with different values of C_{FV}. The simulation diverges from the measured values a short time after the motion reversal but this was expected because it has been

assumed that the value of C_{FV} remains high for the whole of the downward stroke. As mentioned above, this part of the simulation will not be important in a point to point positioning simulation. This change in the friction simulation has greatly improved the fit of the velocity simulation, particularly in the prediction of the first negative peak immediately after the motion reversal. This again will be more significant in a simulation of the control system than any error introduced by the inaccuracy of the velocity simulation at $t > 800\ ms$.

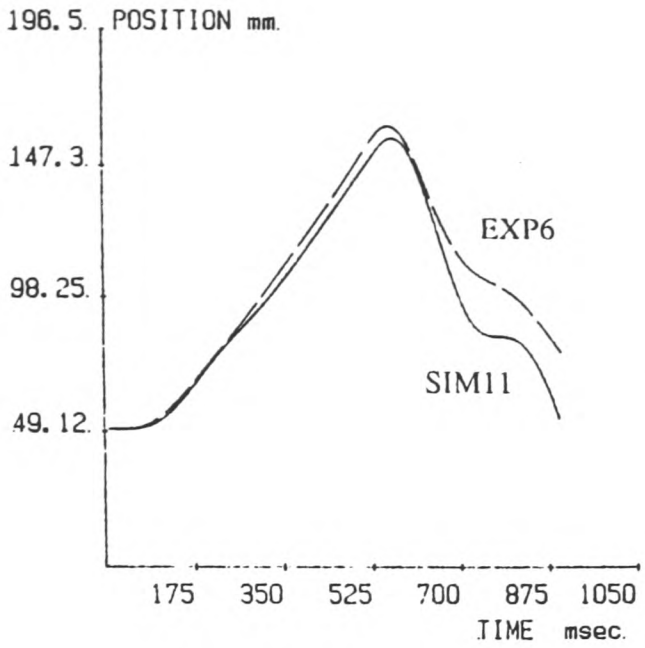

a) Position / time

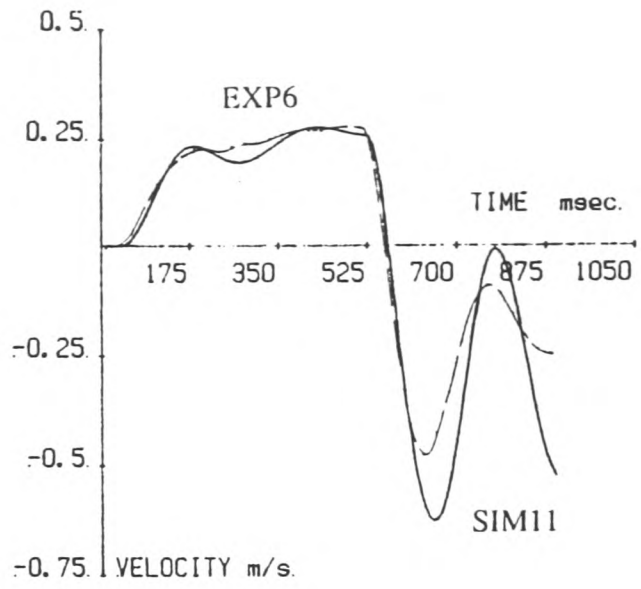

b) Velocity / time

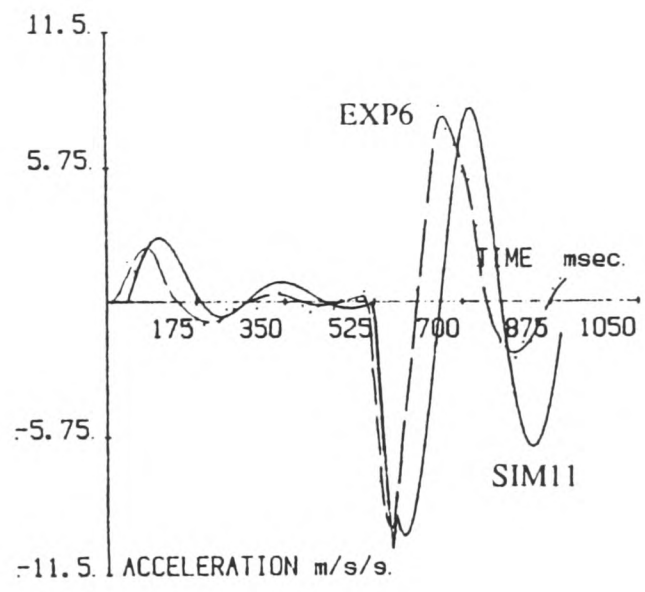

c) Acceleration / time

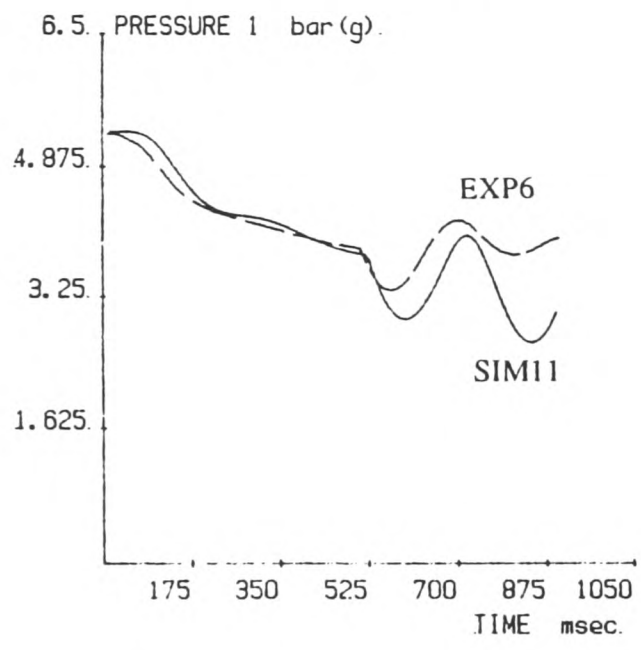

d) Chamber 1 pressure / time

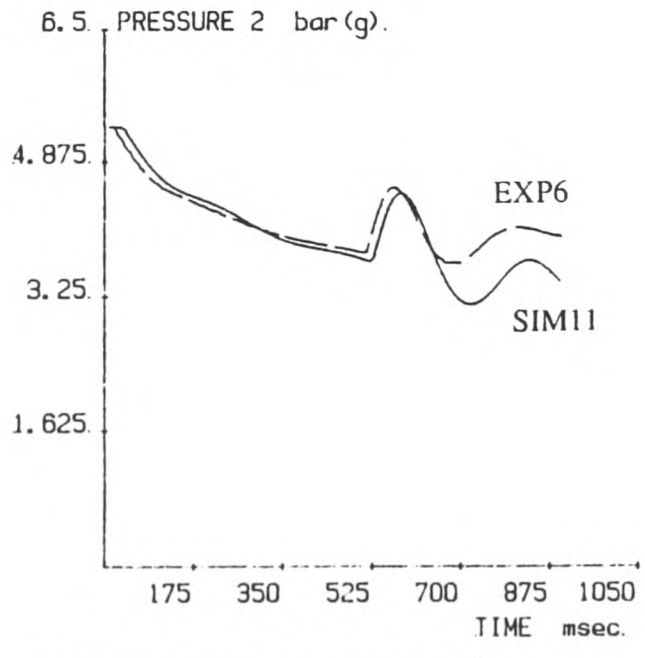

e) Chamber 2 pressure / time

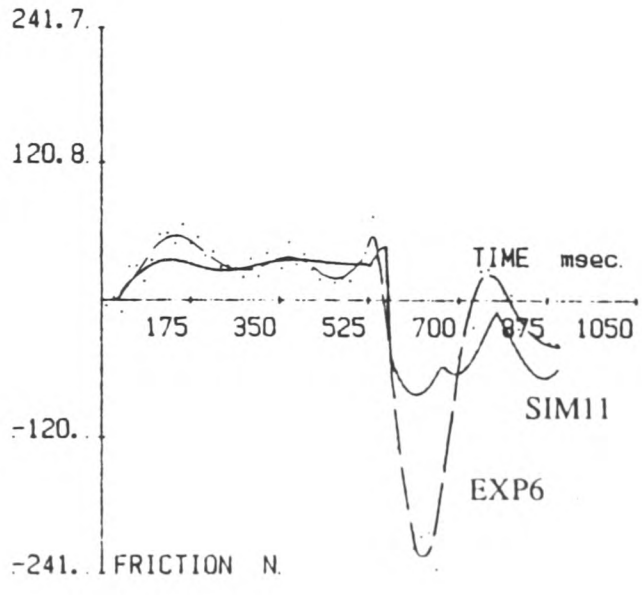

f) Friction /time

FIGURE 3.24. Comparison of Simulation-SIM11 with System Response-EXP6.

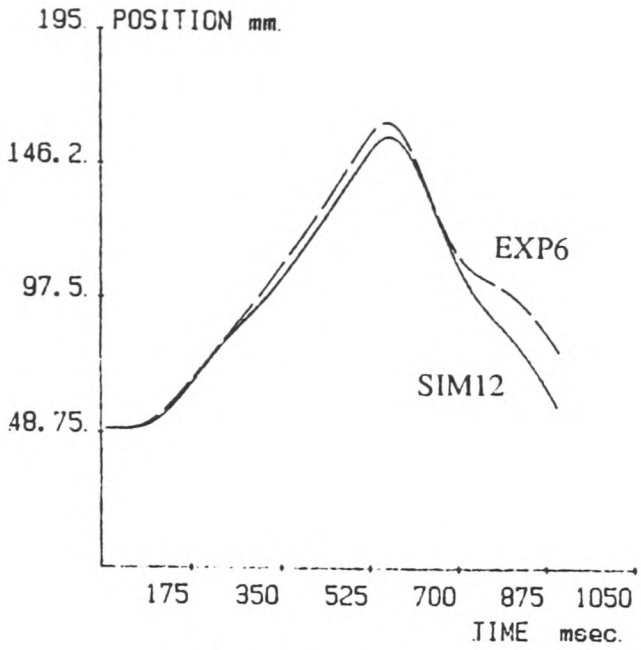

a) Position / time

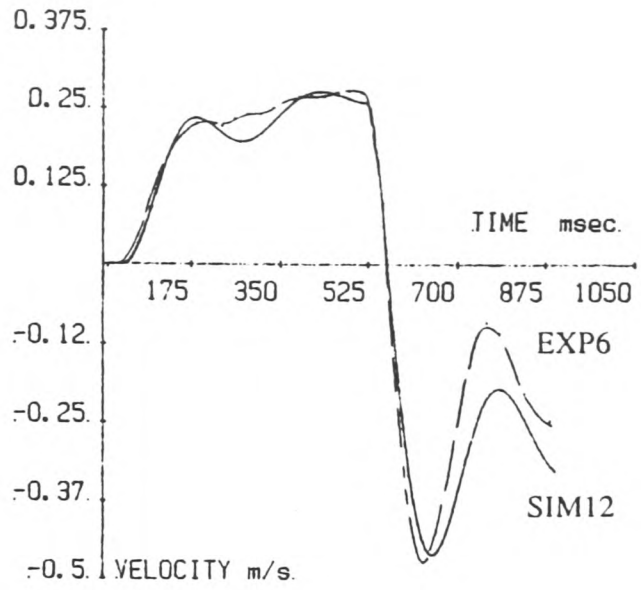

b) Velocity / time

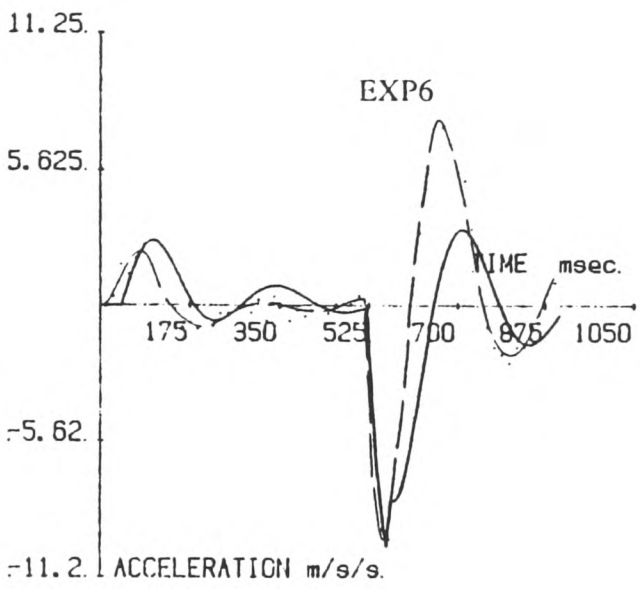

c) Acceleration / time

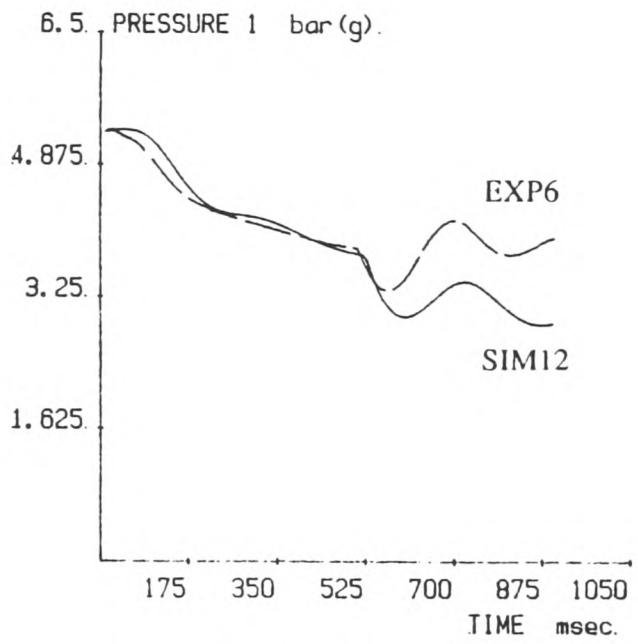

d) Chamber 1 pressure / time

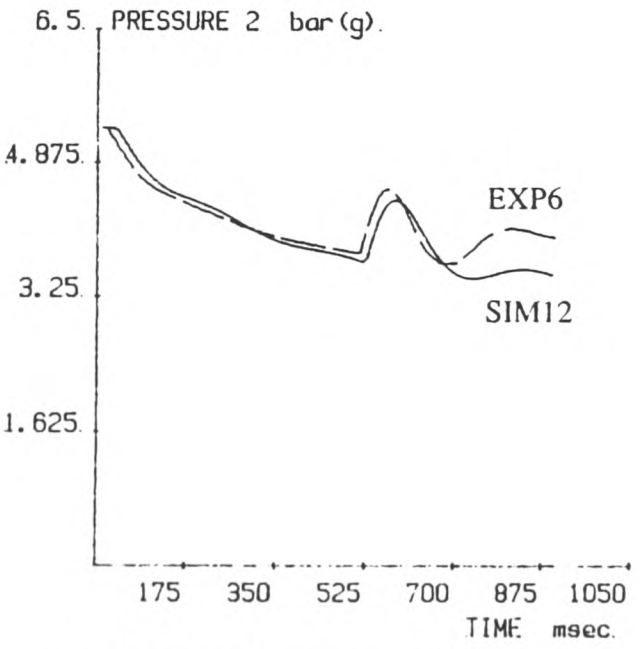

e) Chamber 2 pressure / time

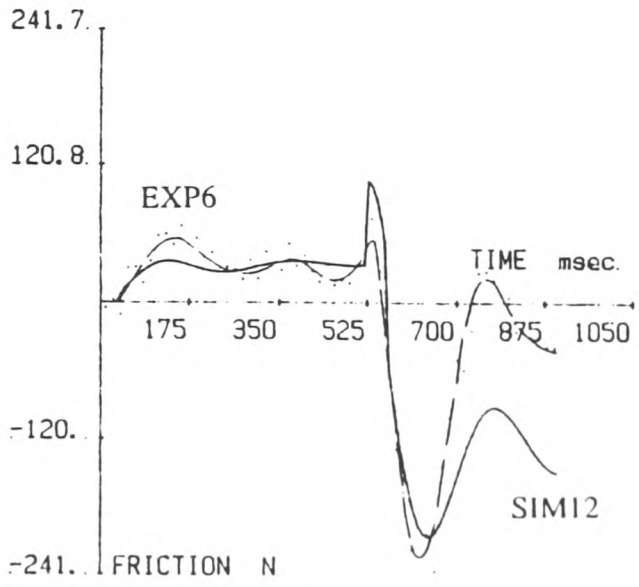

f) Friction /time

FIGURE 3.25. Comparison of Simulation-SIM12 with System Response-EXP6.

3.7 Summary

The pneumatic system has been designed and built and its mode of operation has been established. Two on-off valves control the flow of air into the cylinder chambers. Both chambers are initially held at supply pressure and motion of the piston and load is achieved by switching one valve and thus opening one chamber to atmosphere. The test equipment allows measurements to be taken of the system response for a variety of initial conditions.

A mathematical model of the system has been developed on the basis of the assumption that the filling and venting of the chambers can be approximated by an adiabatic reversible process. Measurements of the friction force of the actuator and the load has led to an empirical model of the total friction of the system and this has been used in the computer model with success. Correlation of the model output with the measured system response has given a high degree of confidence in the model and has shown that the simulation programme will be a useful tool in the development of a position control system.

4 : CONTROL SYSTEM ANALYSIS

4.1 Introduction

The highly non-linear character of some of the system elements makes synthesis of a suitable control scheme for the position control system a difficult task. The methods of synthesis for linear systems that are commonly used can only be applied here with careful consideration of the linearising assumptions made about the system.

In a linear system the shape of the time response is independent of the size of the input or the initial conditions, and stability is a property of the system only. In a non-linear system however, the nature of the time response and stability are likely to be dependent on the initial conditions and the size of the input. The methods of synthesis for non-linear systems can provide information on the likely behaviour of the system for certain inputs, but each method has its limitations; none offers a full description of the system behaviour.

The system was designed to carry out step displacements only and so the range of initial conditions was fairly well known and considerably less varied than a system that must respond to random or sinusoidal inputs. The specification of the control system is presented in section 4.2.

The method of analysis was chosen to suit the system and the range of inputs considered. For example, methods that predict the frequency response of the system are not suitable for this system, which will have only step inputs. As a first attempt at synthesis, the actuator and load were grossly simplified and represented by a linear block in a similar way to that described by Drazan (5). The highly non-linear on-off solenoid valve was replaced by a block of variable gain depending on the size of the system error. The root locus method could then be used to assess the system stability. A better understanding of the time response of the system was then obtained by applying the phase plane technique. The system was considered to be piecewise linear with the state of the solenoids determining in which of two regions the system was operating. For each of the two regions the state space approach gave estimates of the trajectories of the system in the state space. The end conditions in one region just prior to the switching of the valves were used as initial conditions for the motion in the other region, and in this way the response of the system can be pieced together. For the final stage of the analysis, the non-linear computer simulation was used to predict the the behaviour of the system under the various control schemes proposed by the linear analysis. Discussion of this approach to analysis is given in section 4.3.

4.2 System Specification

The specification of the control system can be broadly stated as follows :

a) The piston and load are initially at rest

b) Only step displacements are required

c) The displacements range from a few millimetres to 250 *mm*

d) The piston can be in any stroke position initially

e) The air supply is approximately 5.5 *bar gauge*

f) The load is an inertia of 37 *kg*

g) Pneumatic operation will be the closed mode (refer to section 3.2)

h) The step displacement is to be completed as quickly as possible with minimum overshoot and small deadband

i) Limit cycling is to be avoided

j) The target position is to be held for a sufficient time for a lock to operate on the load

k) The variation of the system response with the displacement size and starting position is to be minimised

Most of the factors in this specification were established after consideration of the likely working conditions of a pneumatic actuator used as a robot module. However, some have been simplified so that a practical solution can be sought more quickly. The effect of the simplifications can be assessed after a suitable control scheme has been developed for the simple system. For example, the supply pressure will be held constant at around 5.5 *bar gauge*. It may be found later that higher or lower pressures are beneficial to obtaining more accurate position control but an investigation into this would complicate the already difficult task of proposing control schemes. A constant inertia load of 37 *kg* will also be used in the control tests for similar reasons.

Finally it is assumed that a lock will be employed in the practical installation of this pneumatic actuator in order to hold the desired position and provide high stiffness, without requiring continuous rapid switching of the on-off valves. Hence it is only necessary to demonstrate accurate positioning for a period of up to 0.1 *s*, during which time a lock can be applied.

Previous work by Drazan (**5**) on an on-off pneumatic system had shown that significant benefits can be obtained by using *dual mode* control. In a dual mode controller, the step displacement is achieved using two separate control strategies depending on the system error size. The first mode of control is entered initially and this moves the system along a

time optimal path towards the desired position. For a simple second order system using on-off valves the time optimal path would be the opening of one valve for maximum acceleration towards the target, followed by the switching of the valves to reverse the applied force and to decelerate at a maximum stopping exactly on the target. For higher order linear systems it has been shown that the number of switchings required for time optimum response is one less than the order of the system (**34**). If the system behaviour is non-linear during the interval between switching then the determination of the switching criteria becomes almost a calibration exercise for the particular system, and so offers little benefit over an open loop control scheme. However, there should be a definite time benefit to be gained from using the time optimum path up to the first switching point, particularly on long step displacements. It is at this valve switching point that the change is made between the first mode of control and the second mode. The initial conditions for the second mode are those of the system at the switching point, ie the end conditions of the first mode of control. The system error at this point varies over a much smaller range than it would if the second mode of control was used throughout the whole step displacement. This has the advantage of reducing the range of input conditions for the second mode of control, and this will aid the synthesis of an appropriate control scheme for this mode. The control scheme can also be tailored to achieve good stability and accurate positioning without such a severe constraint on the positioning time as the step in mode 2 is quite small.

Hence the control scheme developed will be a dual mode controller and the task of synthesis will require :

a) The determination of a suitable switching function for the control mode 1.

b) The determination of a control method to position the piston and load accurately in control mode 2.

Obviously, a reduction in positioning time using this scheme will only be achieved if control mode 2 would have been slower had it been used for the whole step. For any control proposal it will be necessary to demonstrate the time benefit of the more complex dual mode controller.

4.3 System Synthesis

The first step towards the synthesis of an appropriate control system is to greatly simplify the system so that it can be represented by a linear block combining the actuator and load and a non-linear block for the the on-off valve. This would allow more simple analytical treatment in both modes of control and the results of the analysis of the simplified system would complement the results from the non-linear computer model that has been developed in Chapter 3.

4.3.1 Determination of Switching Criteria for Mode 1.

The system can be represented by the block diagram shown in figure 4.1.

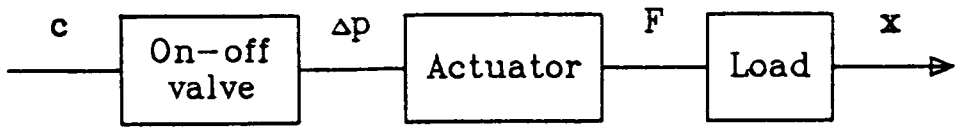

FIGURE 4.1. System Block Diagram.

The computer command (c) controls the on-off valve to switch in one direction or the other. This causes a pressure difference (Δp) to be built up across the actuator which provides a driving force to the load. Motion of the load will cause it to take up a position x.

At the most simple level this process can be assumed to be represented by a perfect switch and an inertial load as shown in figure 4.2.

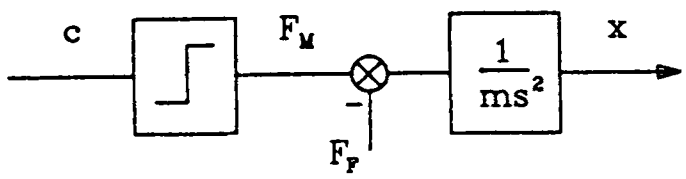

FIGURE 4.2 Simple second-order system representation.

The valve and actuator have been replaced by a switch operated by the computer control command which switches either a positive or a negative driving force (F_M). Subtracted from this is the total friction force of the load and actuator (F_F), resulting in a net driving force which acts on a pure inertia load.

Considering a positive value of c, the equation of motion of the system in this direction is

$$(F_M - F_F) = m \ddot{x}$$

This equation shows that for a given value of $(F_M - F_F)$ a constant acceleration will result. ie,

$$\ddot{x} = K = \frac{F_M - F_F}{m}$$

Thus :

$$\int d\ddot{x} = \int K\, dt$$

So

$$\dot{x} = Kt + C_1 \qquad [4.1]$$

Integrating again

$$x = \frac{Kt^2}{2} + C_1 t + C_2 \qquad [4.2]$$

The initial condition $t = 0$, $\dot{x} = 0$ and $x = x_i$ leads to the determination of $C_1 = 0$ and $C_2 = x_i$. Therefore, eliminating t between [4.1] and [4.2],

$$(x - x_i) = \frac{\dot{x}^2}{2K}$$

Let $\frac{1}{2K} = K_{SW}$ then

$$(x - x_i) = K_{SW}\, \dot{x}^2 \qquad [4.3]$$

This is the equation of a parabola, showing that the phase plane trajectories in x and $\dot{x}$ are parabolic. The decelerating trajectories can be evaluated in the same manner, and because this is assumed to be a second order system the decelerating trajectory will result in stopping exactly on the target. Hence equation [4.3] is also the equation of the switching point and shows the criteria by which the valve switching must occur for the first mode of control. Of course the response is symmetrical for steps in the other direction, and a similar switching line exists for motion in the opposite direction.

From the previous simulation studies in Chapter 3, it was clear that the deceleration after switching was far from being a constant value, and this indicates the extent of the simplification here. However, an approximate value of deceleration can be obtained from the computer simulation of the decelerating trajectory, ($\ddot{x} = 5\ ms^{-2}$), and this can be substituted into [4.3] to establish the switching criteria. This predicts a value of $K_{SW} \approx 100{\times}10^{-3}\ m^{-1}s^2$.

Because the test equipment was available, a series of trajectories for the accelerating and decelerating phases were determined experimentally, and these were plotted out for the actual system. The results of these tests are presented in figure 4.3 and 4.4. A full listing of the system initial conditions for each of the experimental tests is given in table 4.1.

Trajectory	Symbol	Start Position *mm*	Switch Point *mm*	Mass *kg*	Pressure *bar(g)*
a	×	0	150	37	5.5
b	⊗	30	150	37	5.5
c	△	60	150	37	5.5
d	+	90	150	37	5.5
e	•	120	150	37	5.5

TABLE 4.1 Test conditions for trajectory tests shown in figures 4.3 and 4.4.

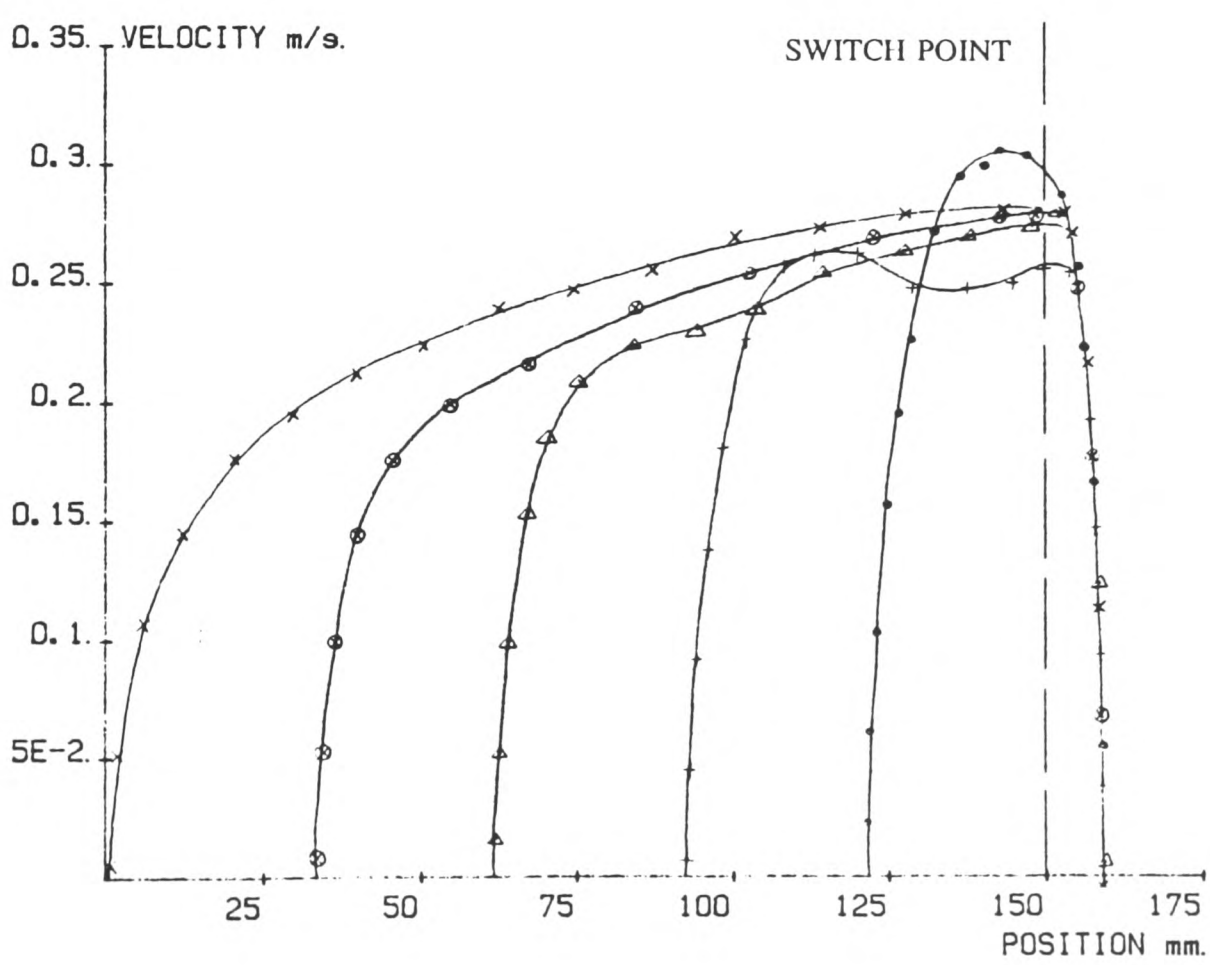

FIGURE 4.3 Position / velocity phase plane trajectories

The trajectories vary with piston start position but they follow a similar trajectory, particularly in the deceleration phase. The accelerating trajectories are of approximately parabolic shape, but they are of very different gradient to the decelerating trajectories. It is not possible to say whether the decelerating trajectories are parabolic on this scale of graph, but each test does follow a similar trajectory as was expected. In order to view the decelerating trajectories in more detail, all of the measured points on the decelerating trajectories were plotted together to a different scale to give an average trajectory that could be used to determine the switching point. This is shown in figure 4.4.

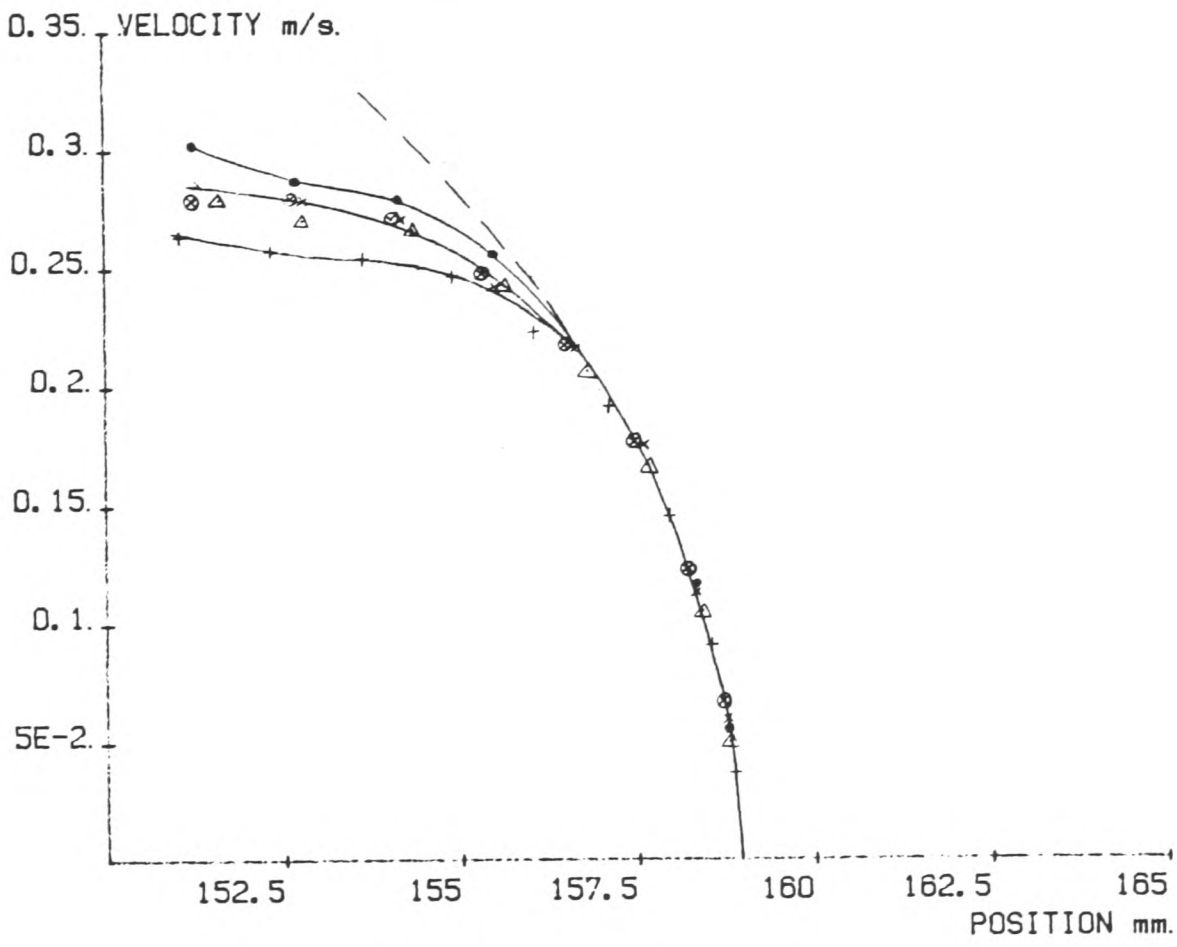

FIGURE 4.4 Decelerating trajectories measured on the test equipment.

Also shown on figure 4.4 is a broken line which is the parabola :

$$(x - x_i) = K_{SW}\, \dot{x}^{\,2}$$

where

$$K_{SW} = 50{\times}10^{-3}\ m^{-1}s^{2}$$

This matches the experimental results very closely, confirming the suitability of the initial assumption that the trajectories can be approximated to parabolas. However, K_{SW} is lower

than the predicted figure of $100\times10^{-3}\ m^{-1}s^2$ obtained from the approximate calculation from the model output that was discussed above.

The omission of both the dead time delay between the computer command to switch the solenoids and their action, and the discrete time period between the sampling of the system state means that there will be a time delay between the true decelerating trajectory and this switching curve. In other words the system will 'overshoot' the switching curve because the valve reversal cannot be effected instantaneously. In this system, 250 *V ac* solenoids are switched by a solid state relay using the ±5 *V* digital command, and the maximum time delay that could occur is up to 10 *ms* (ie half of the supply cycle time). The computer sampling rate is 200 *Hz* and so this could also add another 5 *ms* to the delay. The total delay therefore could be 15 *ms*. The trajectories do not show the time response of the system, but for a velocity of 0.2 ms^{-1} the distance travelled in 15 *ms* is $3\times10^{-3}m$. This can be repeated for other velocities and will lead to a revised switching curve that will operate earlier within the computer, but will still lead to a decelerating trajectory as seen before.

The effect of this procedure has been to include an estimation of the dead time delay between switch curve detection within the controller, and the actual valve reversal. The revised switching curve obtained from this is :

$$(x - x_i) = 150\times10^{-3}\ \dot{x}^2 \qquad [4.4]$$

where the units of x, x_i and $\dot{x}$ are as before. This is the switching curve that will be used in the dual mode controller, with a symmetrically similar one being used for the reverse direction of motion.

4.3.2 Root Locus Analysis for Mode 2.

Referring back to the block diagram of figure 4.1, the system can be simplified to the block diagram of figure 4.5.

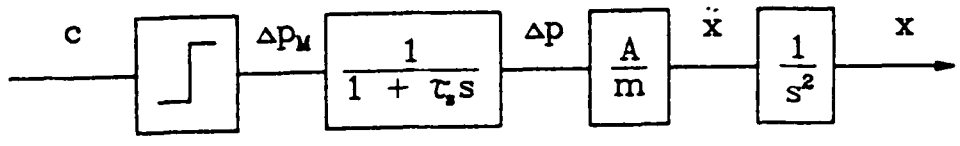

FIGURE 4.5 Third order system representation with non-linear solenoid block.

The solenoids switch on the sign of the computer command *c*. The value of Δp rises exponentially from zero to Δp_M according to the valve/actuator transfer block. The piston area (A_P) and inertia load (m) determines the piston acceleration ($\ddot{x}$) for this value of differential pressure, and finally the integrating block defines the piston position.

The simplest level of closed loop control would be to feed back the current piston position (x) and compare it to the desired value (x_d), using the sign of the comparison to set the control command (c). This scheme will be termed scheme 1, and the block diagram is shown in figure 4.6.

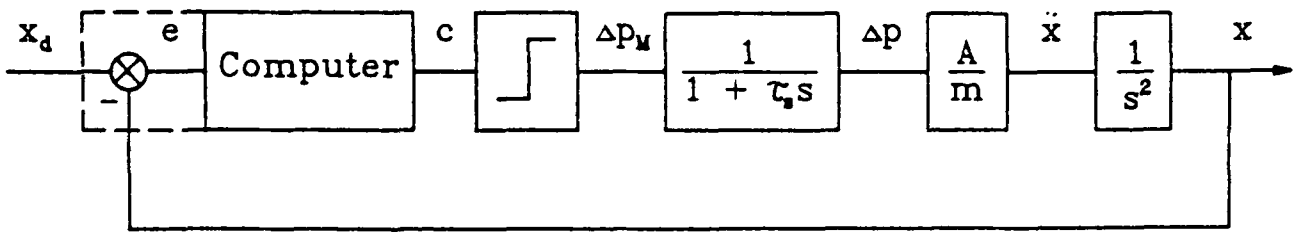

FIGURE 4.6 System block diagram with position feedback.

This block diagram could be linearised by replacing the solenoid and computer blocks with a block of gain K_E, making it possible to analyse the system using root locus technique. The value of the gain K_E can be considered to vary from a low finite value to an infinite one, as the position error ($x_d - x$) varies from a finite value to zero. An explanation of this system representation follows.

Consider the case where the position error is high. The operating point on the non-linear solenoid transfer function is shown as point A in figure 4.7. This operating point is also on the straight line of gradient K_{E_A} shown as a broken line in the figure. Similarly when the position error is small the operating point may be at B which is again a point on a straight line of gradient K_{E_B}. Therefore, as the error decreases the gradient K_E increases until it is infinite when the error is zero.

In the root locus technique, the roots of the system characteristic equation are plotted in the *s–plane* for a variation in another system parameter. If this system parameter is taken as K_E then the plot will show how the roots vary as the error in the system reduces. The transient response of a linear system is dependent on the position of these roots, therefore conclusions can be drawn about the non-linear system by considering certain values of the equivalent gain K_E for the linearised system. The value of $K \rightarrow \infty$ will be of particular importance for stability determination, as the position of these roots will show whether the system is likely to be stable or not as the target is approached. The path of the locus to these points will give an indication of the stability and speed of response of the system for larger position errors.

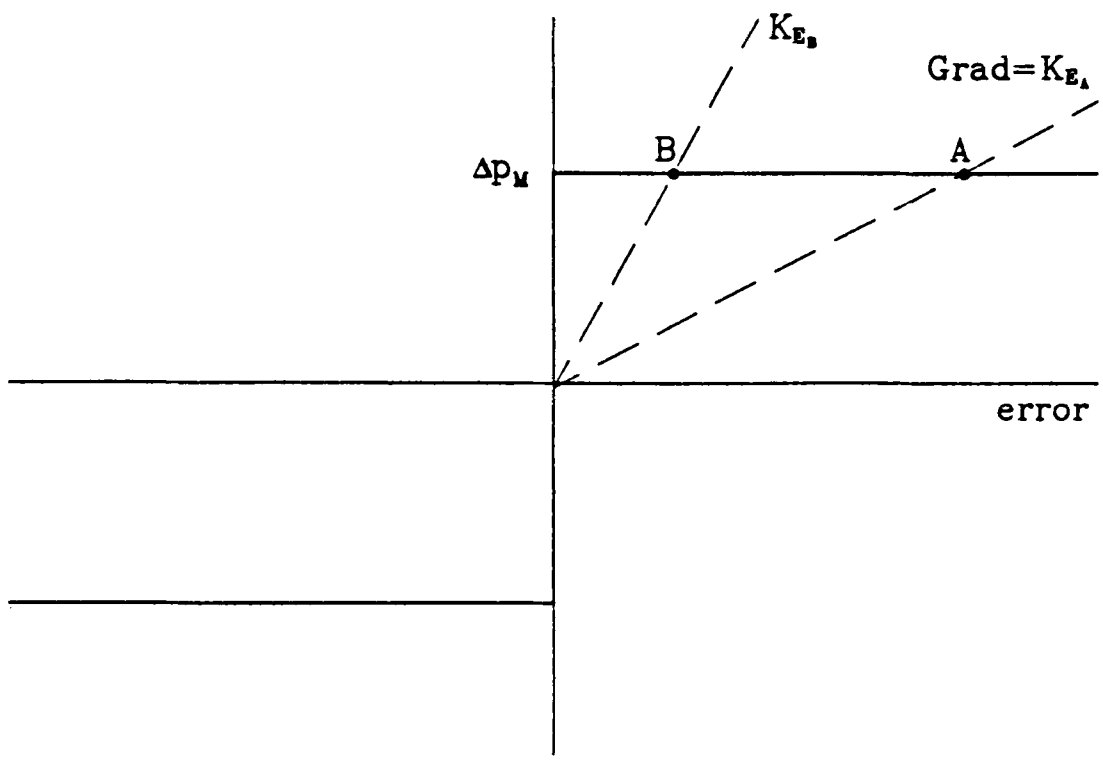

FIGURE 4.7 Solenoid characteristic, showing equivalent gain K_E.

The block diagram in figure 4.6 has the transfer function :

$$\frac{X}{X_d}(s) = \frac{G(s)}{1 + G(s)}$$

where $G(s)$ is the open loop transfer function given by

$$G(s) = \frac{K_E A_P}{ms^2 (1 + \tau_s s)} \qquad [4.5]$$

The characteristic equation is $1 + G(s) = 0$, and the root locus will be a plot of the zeros of this equation as the gain K_E increases.

The values of A_P and m for the real system are easily determined. It is possible to estimate the value of the time constant τ_s from the results of the system modelling of Chapter 3, but again the real system was available so direct measurement was made. With the piston fixed rigidly at a point, measurement of the chamber pressures were made after a step change to one of the valves. The differential pressure was then plotted as a function of time. Comparison of this trace with the exponential function given by :

$$\Delta p = \Delta p_M \left[1 - e^{-t/\tau_s}\right]$$

could then provide an appropriate value of τ_s.

It was found that τ_s varied considerably both with piston position and with the initial chamber pressure. In the position control system a closed mode of pneumatic operation is

used (refer to section 3.2), and so the initial chamber pressure will be supply pressure. However, this control scheme comes into operation some time after the initial step change, and from the simulation studies of Chapter 3 it was found that typical chamber pressures were around 4 *bar gauge*.

The piston was positioned at the mid-stroke position to obtain a mean value of τ_s for this actuator at 4 *bar gauge*, and the result of the test is shown in figure 4.8. This gives a value of

$$\tau_s = 0.35\ s$$

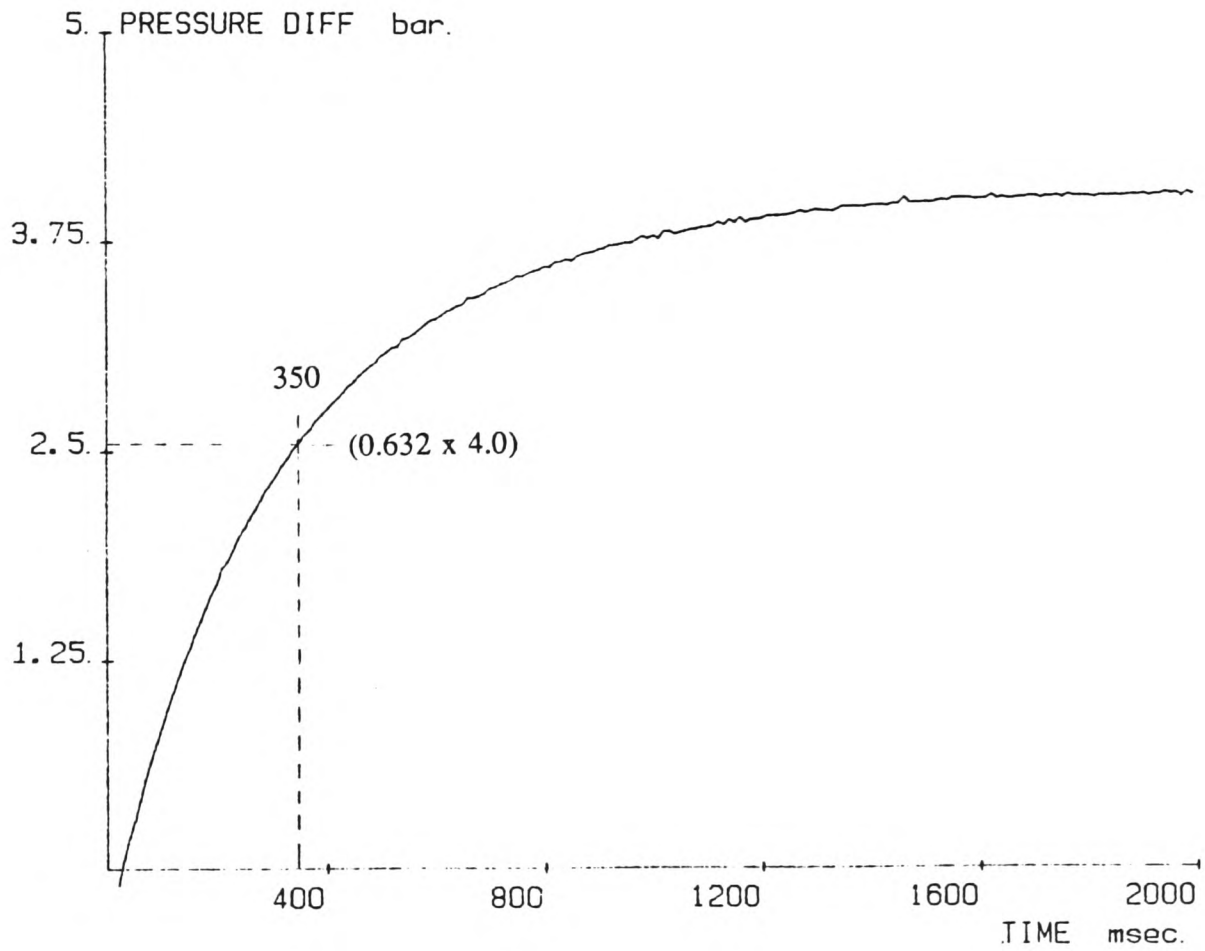

FIGURE 4.8 Measurement of τ_s from experimental test.

This is the value used when plotting the root locus of the system.

A software package for the BBC microcomputer was used for the generation of the root locus diagrams (35). The output is shown in figure 4.9 for control scheme 1 (position feedback only).

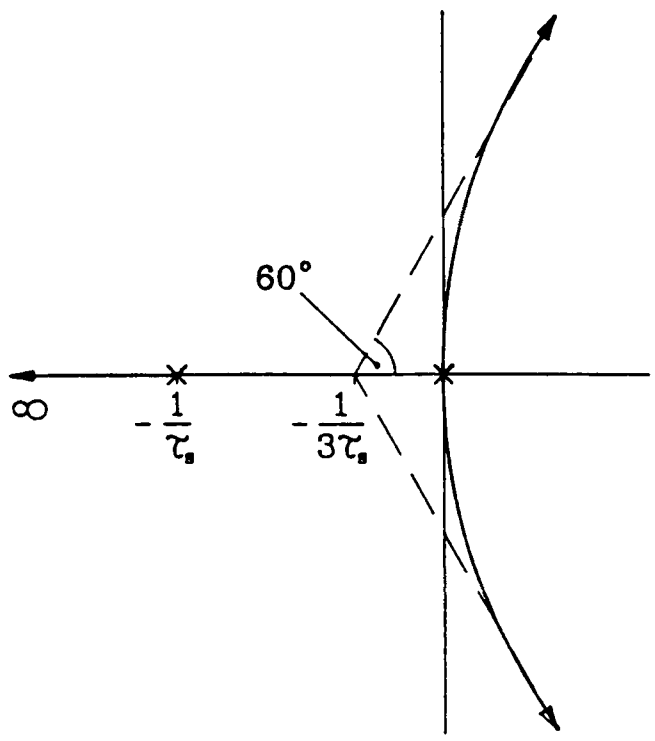

FIGURE 4.9 Root locus diagram for system with position feedback only.

A double open loop pole exists at the origin and another pole at $-1/\tau_s$ on the real axis. As the equivalent gain increases, the locus goes to infinity to the right hand side of the imaginary axis, indicating that the response would be unstable.

A method of stabilising the system is to add a zero on the left hand side of the diagram to 'pull' the locus into the negative real half of the plane. This can be done by adding velocity feedback $\tau_c\dot{x}$. A block diagram of the position plus velocity feedback scheme, termed scheme 2, is shown in figure 4.10.

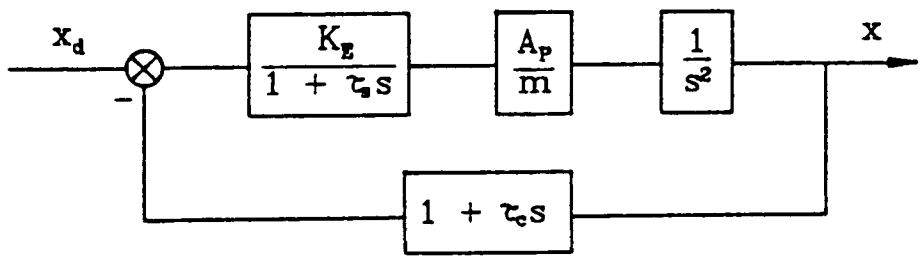

FIGURE 4.10 Simplified system block diagram for position plus velocity feedback.

The revised open loop transfer function is

$$G(s) = \frac{K_E A_P (1 + \tau_c s)}{ms^2 (1 + \tau_s s)} \qquad [4.6]$$

The root locus plot when $\tau_c < \tau_s$ is shown in figure 4.11 and the system is seen to be

unstable. However, the root locus when $\tau_c > \tau_s$ in figure 4.12 shows that the loci are within the left hand half of the *s-plane* so the system is now stable for all values of K_E. The asymptote at $\frac{1}{2}\left[\frac{1}{\tau_s} - \frac{1}{\tau_c}\right]$ shows that the response will be quite slow and oscillatory.

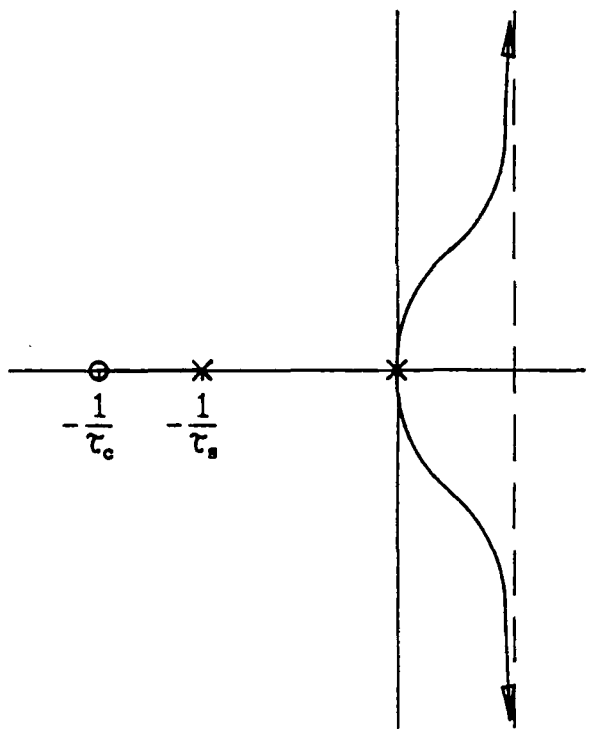

FIGURE 4.11 Root locus diagram for system with $\tau_c < \tau_s$.

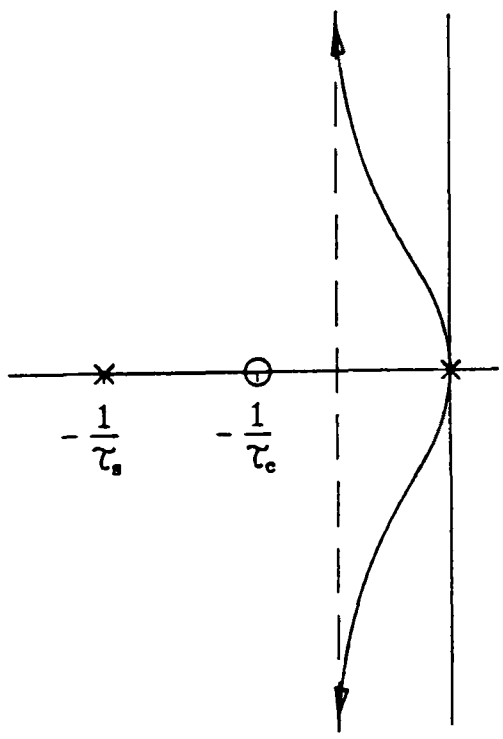

FIGURE 4.12 Root locus diagram for system with $\tau_c > \tau_s$.

A method of increasing the speed of response and increasing the damping would be to introduce further zeros on the negative real half of the *s-plane*. This can be achieved with the feedback of the acceleration of the piston. However, acceleration measurement on the equipment is difficult to achieve to a good degree of accuracy, particularly for the low accelerations near to the target position. The simplified system block diagram in figure 4.5 shows that a linear block of A_P/m relates differential pressure and acceleration and so it is possible to achieve a similar modification to the root locus by feedback of the differential pressure signal which can be measured on the equipment.

The block diagram for this system is shown in figure 4.13, where K_p is the the differential pressure feedback gain.

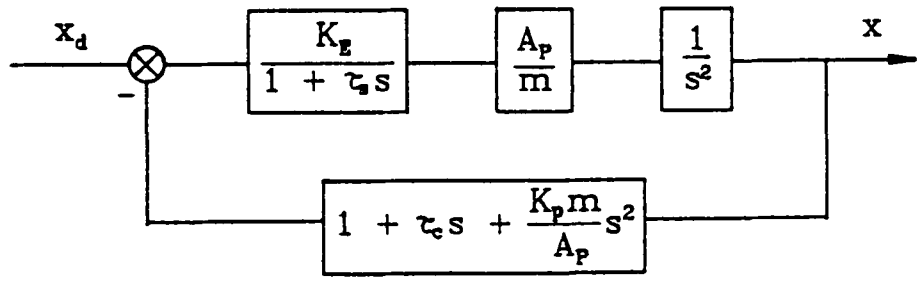

FIGURE 4.13 System block diagram for position plus velocity plus differential pressure feedback.

This control scheme is termed scheme 3, and the revised open loop transfer function is

$$G(s) = \frac{K_E A_P \left[1 + \tau_c s + \frac{K_p m}{A_P} s^2\right]}{ms^2 (1 + \tau_s s)} \qquad [4.7]$$

Again there is a double open loop pole at the origin, and another pole at $-1/\tau_s$ on the real axis. However the two zeros are at positions

$$zero_1 = \frac{A_P}{2K_p m}\left[-\tau_c + \left[\tau_c^2 - \frac{4K_p m}{A_P}\right]^{1/2}\right] \qquad [4.8]$$

$$zero_2 = \frac{A_P}{2K_p m}\left[-\tau_c - \left[\tau_c^2 - \frac{4K_p m}{A_P}\right]^{1/2}\right] \qquad [4.9]$$

Both zeros are in the left hand half of the *s-plane* and their positions can be selected by choosing appropriate values of K_p and τ_c.

For

$$\tau_c^2 > \frac{4K_p m}{A_P}$$

the zeros are real. One possible root locus is shown in figure 4.14.

The segment on the real axis between $-1/\tau_s$ and $zero_1$ will give a real root of the characteristic equation which will dominate the response for high values of K_E. Hence $zero_1$ should be placed as far to the left of the *s-plane* as possible in order to speed up the step response. Even then as $K_E \rightarrow \infty$ all three roots will be real indicating an overdamped system.

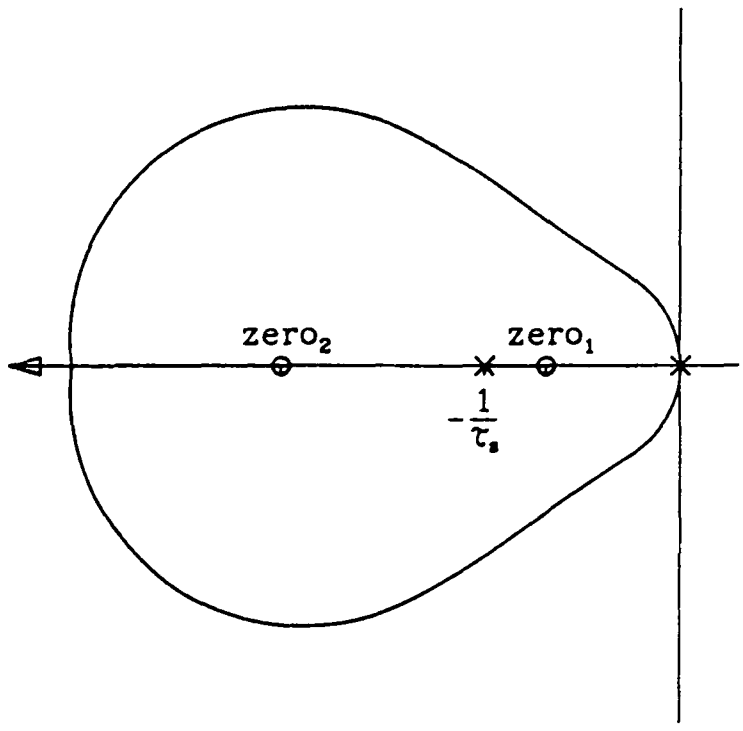

FIGURE 4.14 Root locus plot for system with position plus velocity plus differential pressure feedback with real zeros.

For

$$\tau_c^2 < \frac{4K_p m}{A_P} \qquad [4.10]$$

the zeros form a conjugate complex pair and a typical root locus for this condition is shown in figure 4.15.

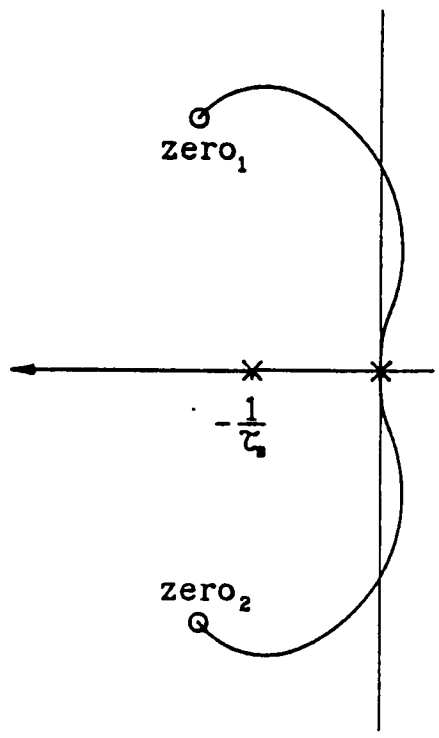

FIGURE 4.15 Root locus for system with position plus velocity plus differential pressure feedback with complex zeros.

It is now possible to make the dominant roots a conjugate complex pair which will approach the zeros as $K_E \rightarrow \infty$ giving a response that will approximate to that of a second order system with damping ratio ζ and undamped natural frequency ω_n determined as shown in figure 4.16.

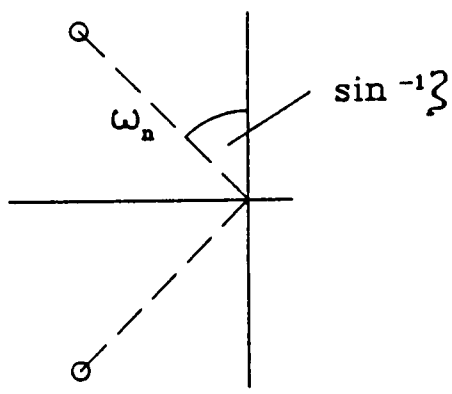

FIGURE 4.16 Conjugate complex pair of roots for a second order system.

To achieve a good fast response ω_n should be as large as possible and $\zeta \approx 1/\sqrt{2}$.

From equations [4.8] and [4.9]

$$zero_{1\,2} = \frac{A_P}{2K_p m}\left[-\tau_c \pm j\left[\frac{4K_p m}{A_P} - \tau_c^2\right]^{1/2}\right]$$

When $\zeta = \frac{1}{\sqrt{2}}$

$$\tau_c = \left[\frac{4K_p m}{A_P} - \tau_c^2\right]^{1/2}$$

$$\tau_c^2 = \frac{4K_p m}{A_P} - \tau_c^2$$

$$\tau_c^2 = \frac{2K_p m}{A_P} \qquad [4.11]$$

Equation [4.11] will provide a relationship between τ_c and K_p for a fast, well damped response of the system under control scheme 3.

4.3.3 State Space Analysis for Mode 2.

The root locus analysis for mode 2 that has been described in section 4.3.2 provided an estimate of the parameter values to be used for control schemes 1 and 2. Further analysis is required to complete the design of control scheme 3.

The state space/phase space analysis was now used. It assumes that the system can be considered as piecewise linear; ie that two linear operating regions exist depending upon the state of the on-off solenoids.

The state variables y_1, y_2 and y_3 are defined in the block diagram of figure 4.17.

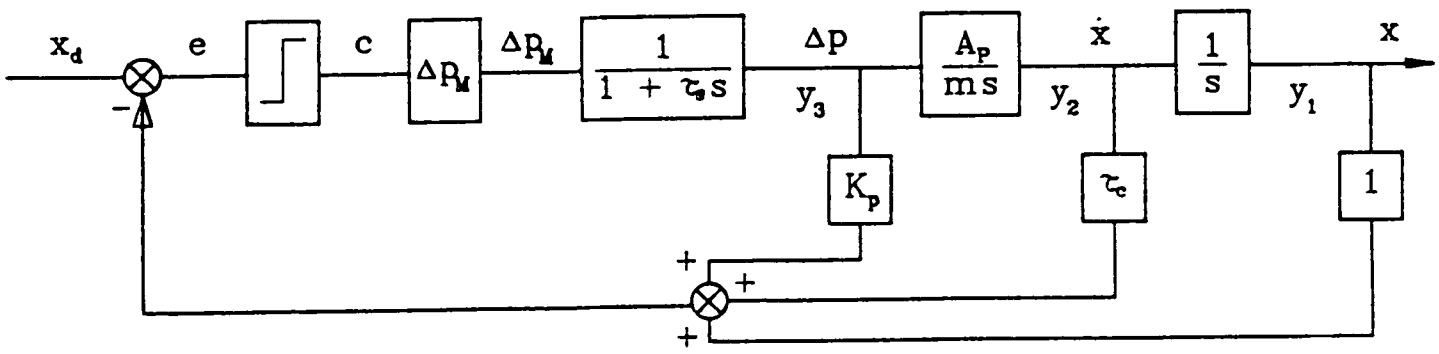

FIGURE 4.17 Block diagram of system showing state variables.

From the diagram it follows that :

$$\dot{y}_1 = y_2 \qquad [4.12]$$

$$\dot{y}_2 = \frac{A_P}{m}\, y_3 \qquad [4.13]$$

$$\dot{y}_3 = -\frac{1}{\tau_s}\, y_3 + \frac{K_L}{\tau_s}\, c \qquad [4.14]$$

where

$$K_L = \frac{\Delta p_M}{c}$$

$$c = \pm 1$$

The switch between $+c$ and $-c$ occurs when $e = 0$, so for a target of zero.

$$0 = -K_p\, y_3 - \tau_c\, y_2 - y_1 \qquad [4.15]$$

This is the equation of the switching plane in the 3D state space of y_1, y_2 and y_3, and this is difficult to depict here.

However, useful results can be obtained by looking at the system trajectories in two dimensions. Direct solution of the trajectories in the two planes of y_1 is not possible, but for the y_3/y_2 plane the following can be obtained.

From equations [4.13] and [4.14]

$$\frac{\dot{y}_3}{\dot{y}_2} = \frac{m}{A_P\, \tau_s}\left[\frac{K_L\, c}{y_3} - 1\right]$$

or

$$\frac{dy_3}{dy_2} = -\frac{m}{A_P\, \tau_s}\left[\frac{y_3 - K_L\, c}{y_3}\right]$$

Therefore

$$\int \frac{y_3}{(y_3 - K_L\, c)}\, dy_3 = -\int \frac{m}{A_P\, \tau_s}\, dy_2$$

And integrating

$$y_3 + K_L\, c \ln (y_3 - K_L\, c) = -\frac{m}{A_P\, \tau_s}\, y_2 + C \qquad [4.16]$$

Referring back to the block diagram in figure 4.17, the value of c switches between +1 and -1 depending upon the sign of the error e. Therefore the two regions of the system response are defined by equation [4.16] with these two values of c. Equation [4.16] defines an infinite number of trajectories in each region, with each trajectory having its own value of C. A few of the possible trajectories are shown in figure 4.18.

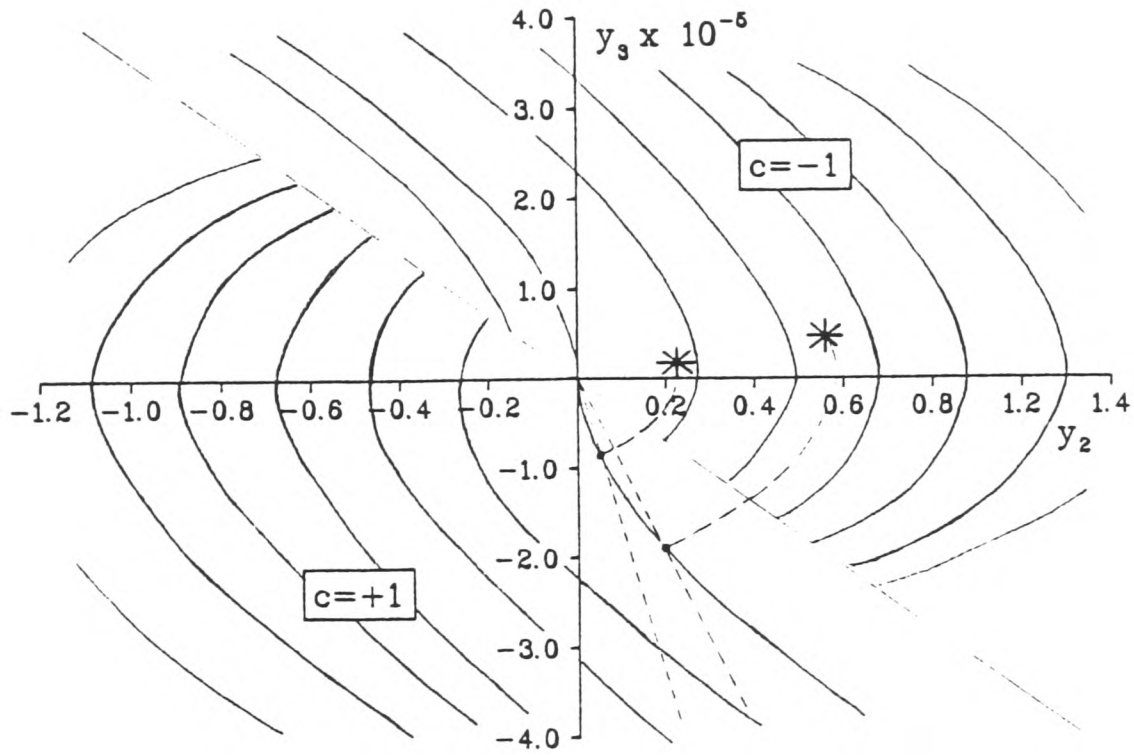

FIGURE 4.18 Phase plane trajectories in the $y_3 - y_2$ space.

Typical initial conditions would be in the range $0.1 < y_3 < 0.5$ *bar* and $0.2 < y_2 < 0.5$ ms^{-1}. Two values of initial condition that represent the likely extremes of the possible trajectories are shown as asterisks in the figure. The trajectory for each is shown as a broken line and the switching point for 'optimal' control is marked. A straight line from the origin through each switch point shows the straight line approximation of the switch line for each condition. The mean of these was used to give a numerical relationship for the switch function relating y_2 and y_3 assuming that y_1 approaches zero (ie that the system reaches the target position).

From equation [4.15]

$$0 = -K_p\, y_3 - \tau_c\, y_2 - y_1$$

$$y_3 = -\frac{\tau_c}{K_p}\, y_2 - \frac{1}{K_p}\, y_1$$

and for $y_1 \rightarrow 0$

$$y_3 = -\frac{\tau_c}{K_p} y_2$$

Therefore, from the gradient of the mean switch line in figure 4.18,

$$\frac{\tau_c}{K_p} = 11.25\times10^5\ Nsm^{-3} \qquad [4.17]$$

Equation [4.17] will set an approximate relationship between τ_c and K_p for control mode 2. Returning to equation [4.10] in section 4.3.2 and substituting K_p from equation [4.17] and the values of $m = 37\ kg$ and $A_P = 2.92\times10^{-3}\ m^2$ gives the condition :

$$\tau_c < 45\times10^{-3}\ s \qquad \text{for complex roots.}$$

For any value of $\tau_c < 45\times10^{-3}\ s$, the corresponding value of K_p can be calculated from equation [4.17] and this will ensure that a reasonable switch line in the y_3/y_2 plane is maintained. The root locus plots for several decreasing values of τ_c, starting at $\tau_c = 45\times10^{-3}\ s$ is shown in figure 4.19.

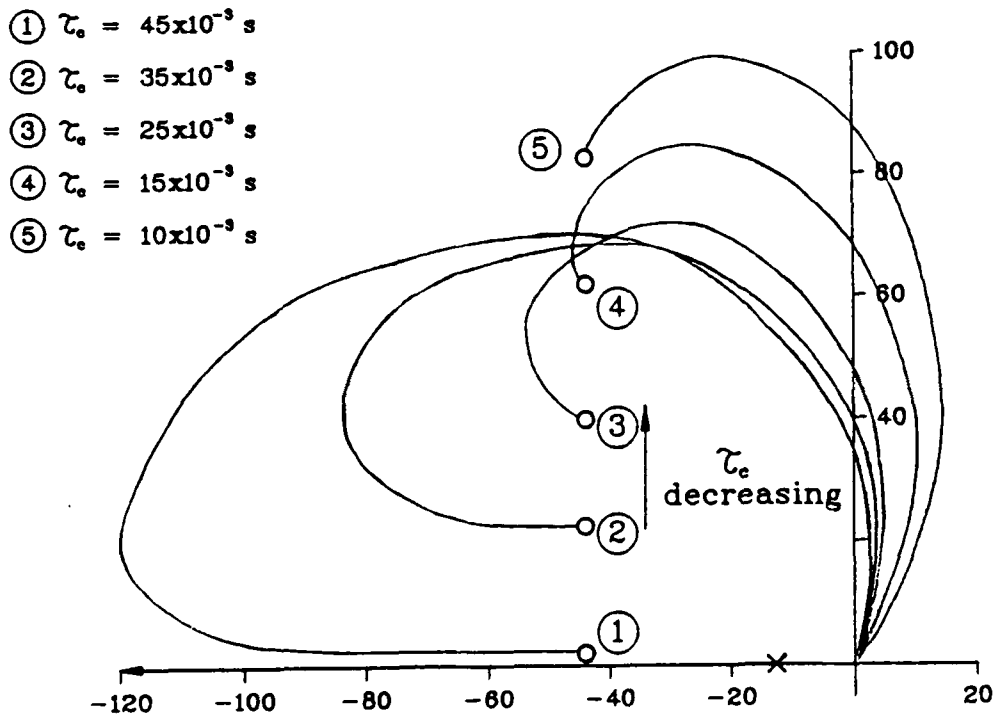

FIGURE 4.19 Root loci for decreasing τ_c with τ_c/K_p a constant.

For $\tau_c = 45\times10^{-3}\ s$ the locus differs little from that obtained with real zeros, however, as τ_c

decreases, the response becomes less damped at the expense of some stability. The locus with $\tau_c = 10\times10^{-3}\ s$ shows conditional stability with the majority of the locus in the right hand part of the s plane. It is not easy to quantify the equivalent gain of this on-off system during a step displacement, so this tendency towards instability should be avoided.

The damping ratio for $\tau_c = 10\times10^{-3}\ s$ is also greater than the desired value of $1/\sqrt{2}$, and this would mean that the system is overdamped. A 'good' value is $\tau_c = 25\times10^{-3}\ s$ with $K_p = 22.2\times10^{-9}\ m^3N^{-1}$. This balances the requirements of stability, speed of response and damping by satisfying equation [4.11], whilst retaining the phase plane requirement of equation [4.17].

Programming considerations for the control scheme 3 were such that certain values of τ_c and K_p were more easily achieved as they required only multiplications by factors of two. Any values could be realised if necessary but this would require more programming effort and a greater time period to complete the interrupt routine. Approximations to the ideal values above were chosen in the light of this. These were :

$$\tau_c = 32\times10^{-3}\ s$$

$$K_p = 46\times10^{-9}\ m^3N^{-1}$$

Higher values of τ_c would exhibit greater damping but at the expense of response speed and lower values of τ_c, although faster in response may show instability with large position errors.

4.4 Computer Simulation of the Control Scheme Proposals.

The computer model that was developed in Chapter 3 was used to carry out simulations of the control schemes that were proposed by the analysis carried out on the simplified system in section 4.3. A listing of the model parameters is given in table 4.2.

PARAMETER	*UNITS*	VALUE
Cylinder Length	*mm*	300
Piston Area A_P	m^2	2.9×10^{-3}
Valve Orifice Effective Area A_{O_1}	m^2	3.1×10^{-6}
Valve Orifice Effective Area A_{O_2}	m^2	4.6×10^{-6}
Mass m	*kg*	37
Coulomb Friction F_C	*N*	22
Coeff of Velocity Related Friction C_{FV}	Nsm^{-1}	75/375
Coeff of Diff Press Related Friction C_{FP}	m^{-2}	30×10^{-5}
Solenoid Dead Time	$s\times10^{3}$	30
Polytropic Exp n		1.27
Gas Temperature T_s	^0K	293
Supply Pressure p_s	*bar*	6.50
Rate of Change of Supply Pressure k_{P_s}	$bars^{-1}$	0.17
Exhaust Pressure p_e	*bar*	1.0
Supply Chamber Pressure p_1	*bar*	6.50
Exhaust Chamber Pressure p_2	*bar*	6.50
Piston Position x	*mm*	30
Piston Velocity $\dot{x}$	ms^{-1}	0
Piston Accn $\ddot{x}$	ms^{-2}	0
Time Increment t	$s\times10^{3}$	1
Duration of Model (approx)	*s*	1.0

TABLE 4.2 Parameters used for the computer simulations.

The system analysis had proposed a number of system control methods. These are listed below:

1. For Mode 1.

Type. Time optimal control from the start to the first switch point.

Controller Task. To monitor the position and velocity of the system and to detect the switch line in the $x/\dot{x}$ phase plane.

Controller Constants. $K_{SW} = 150\times10^{-3}\ s^2m^{-1}$

2. For Mode 2.

i) Scheme 1.

Type. Position feedback control.

Task. To monitor the position of the system and to switch the valves on the sign of the position error detected.

ii) Scheme 2.

Type. Position plus velocity feedback control.

Task. To monitor position and velocity and to switch the valves on the sign of the error, where : $error = x_d - (x + \tau_c\ \dot{x})$

Controller Constant: $\tau_c > 0.35\ s$ for stable response.

iii) Scheme 3.

Type. Position plus velocity plus differential pressure feedback control.

Task. To monitor position, velocity and chamber pressures and to switch the valves on the sign of the error where : $error = x_d - (x + \tau_c\ \dot{x} + K_p\ \Delta p)$

Controller Constants. a) $\tau_c = 32\times10^{-3}\ s$

$K_p = 28.4\times10^{-9}\ m^3N^{-1}$ for 'best' response.

b) $\tau_c > 32\times10^{-3}\ s$

$K_p = \tau_c \times 889\times10^{-9}\ m^3N^{-1}$ for more damped response.

c) $\tau_c < 32\times10^{-3}\ s$

$K_p = \tau_c \times 889\times10^{-9}\ m^3N^{-1}$ for less damped response.

Modification of the model programme was required so that the feedback system could be included. A flowchart of the computer programme used for the simulations of these control schemes is given in Appendix 4.

It would not be representative to evaluate the performance of the schemes for mode 2 without having first used mode 1 for the initial motion. The initial conditions for mode 2 will be provided by the mode 1 control and they will consist of a relatively small position error (< 15 *mm*) plus an approximately constant velocity.

Therefore a simulation of a step displacement was carried out using the dual mode control of :

- Mode 1 control using $K_{SW} = 150\times10^{-3}\ s^2m^{-1}$ followed by
- Mode 2 control using one of the schemes listed above.

The simulation used the following conditions for the step displacement :

1) Initial piston position = 30 *mm*
2) Target position = 130 *mm*
3) Inertia load = 37 *kg*
4) Supply pressure = 5.5 *bar gauge*

A list of the input conditions used in each of the simulations is given in table 4.3.

Simulation	Start Position *mm*	Target Position *mm*	K_{SW} for Mode 1 $\times10^3\ s^2m^{-1}$	Velocity Feedback (τ_c) $\times10^3\ s$	Δp Feedback (K_p) $\times10^9\ m^3N^{-1}$
SIM13	30	130	150	0	0
SIM14	30	130	150	500	0
SIM15	30	130	150	200	0
SIM16	30	130	150	32	92
SIM17	30	130	150	128	114
SIM18	30	130	150	25	28
SIM19	30	130	150	16	23

TABLE 4.3 Initial Conditions and System Feedback Constants for Computer Simulations.

SIM13 was the simulation of the dual mode controller using scheme 1 (position feedback) during mode 2. The result of this simulation is shown in figure 4.20. The response is clearly unstable as predicted by the root locus analysis of the simplified representation of the system in section 4.3.2.

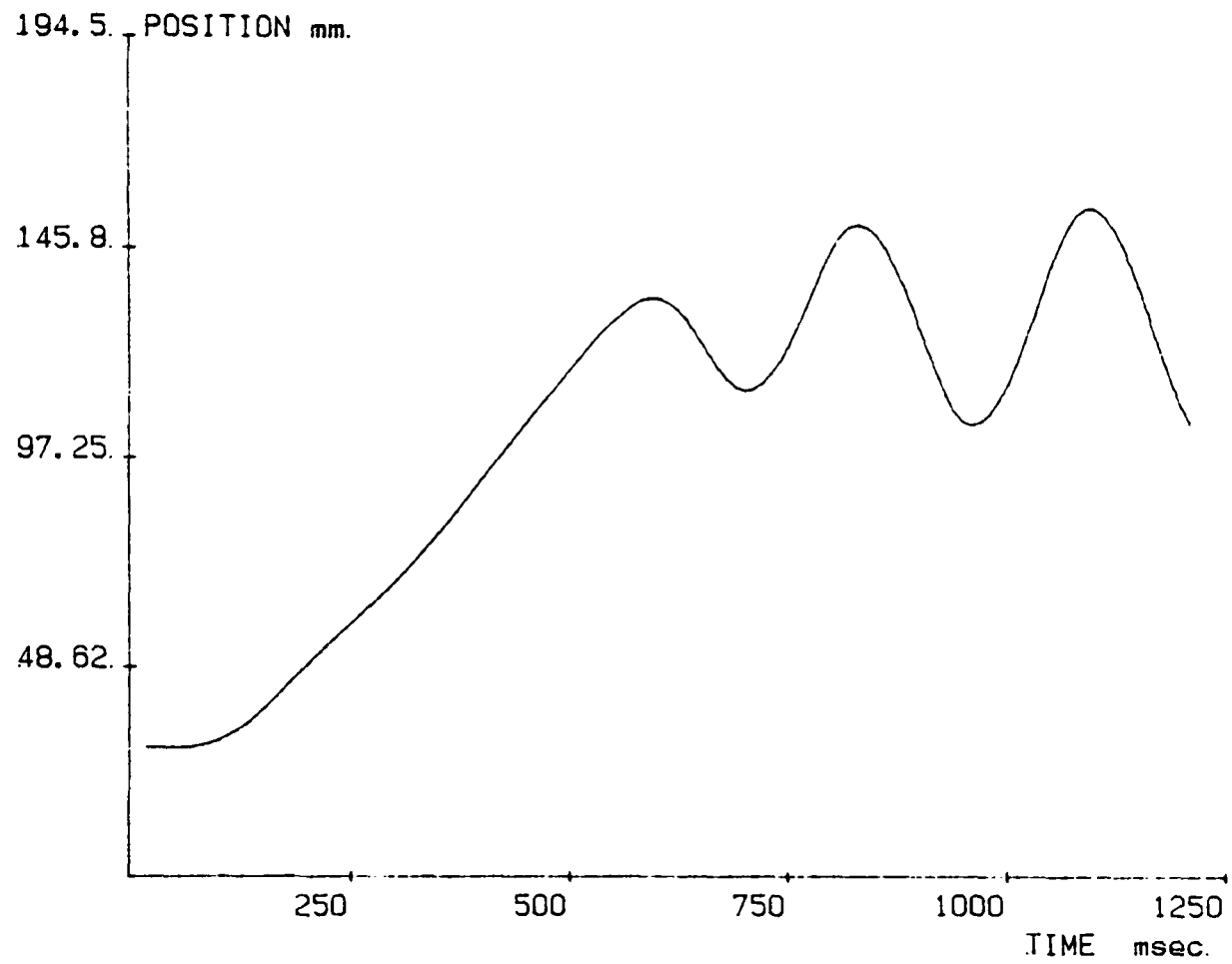

FIGURE 4.20 Simulation of position response of system with position feedback only - SIM13.

The next simulation of the dual mode controller used scheme 2 during control mode 2. The analysis in section 4.3.2 suggested that stable response would be achieved for values of $\tau_c > 0.35$ *s*. SIM14 was the simulation of scheme 2 for $\tau_c = 0.5$ *s*, and the result of this is shown in figure 4.21.

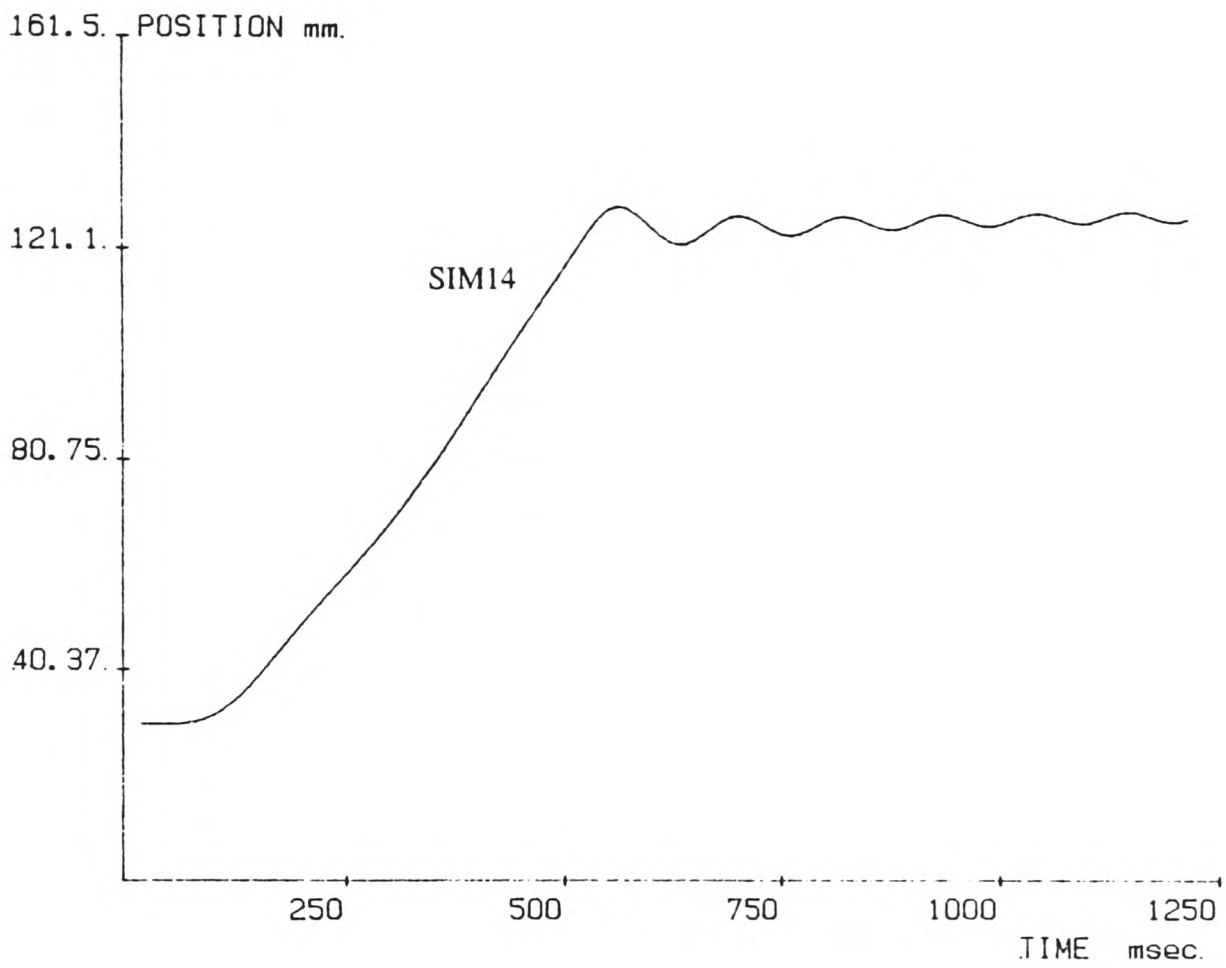

FIGURE 4.21 Simulation of response of system with position and velocity feedback; $\tau_c = 0.5$ *s*.

The system has been stabilised although a small limit cycle with an approximate amplitude of 2 *mm* peak to peak exists. Again the simplified representation of the system and the root locus analysis has predicted a reasonable value of τ_c.

However, the simplified analysis was not as successful at predicting the value of τ_c for unstable response. SIM15 was the simulation of the same control scheme with $\tau_c = 0.2$ *s*. The analysis predicts that this will be unstable, but this was not shown by the computer simulation of the position response in figure 4.22. The response is stable, but the amplitude of the limit cycle has increased to approximately 3 *mm* peak to peak.

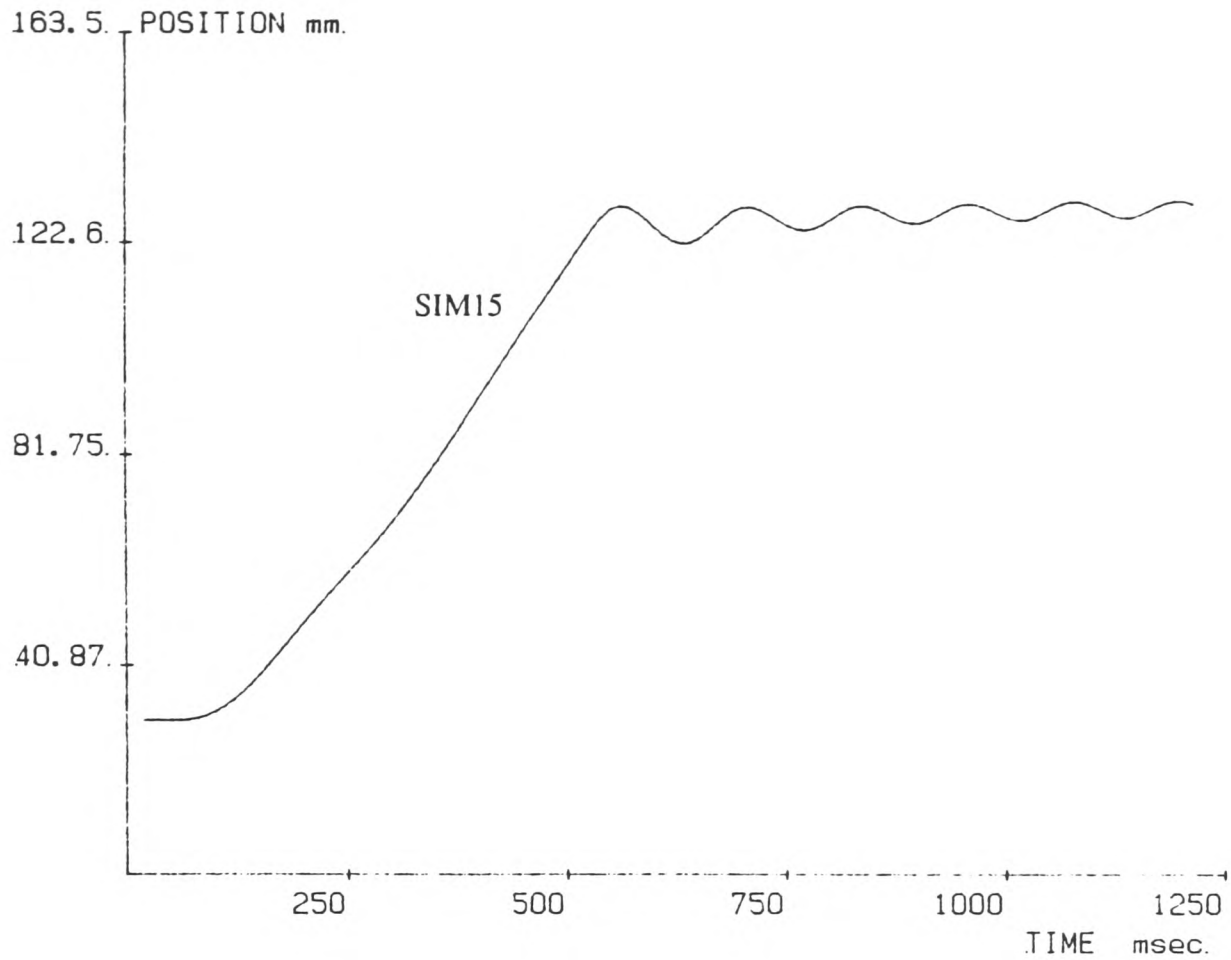

FIGURE 4.22 Simulation of response of system with position and velocity feedback; $\tau_c = 0.2\ s$.

As τ_c is decreased still further the amplitude of the limit cycle is increased. The lower limit on τ_c whilst maintaining a stable limit cycle is approximately 0.4 *s*. It is clear that the simplified analysis could not predict this effect, but it has proved useful in the determination of an initial choice of τ_c to be used in the more complex non-linear computer simulation. This value has also been shown to be a good first approximation of τ_c to combine both a small limit cycle and good damping, with reasonable speed of response.

Control scheme 3, using a combination of position, velocity and differential pressure feedback for mode 2, was now evaluated using the computer simulation. The analysis has predicted good system response with $\tau_c = 32\times10^{-3}\ s$ and $K_p = 46\times10^{-9}\ m^3N^{-1}$. However, after various trial runs with the simulation, it was found that an improved position response was obtained with a change in the ratio of τ_c/K_p from that predicted in the phase plane analysis of section 4.3.2. It was found from the simulation runs that a good choice would be $\tau_c = 32\times10^{-3}\ s$ and $K_p = 92\times10^{-9}\ m^3N^{-1}$.

Referring back to the phase plane trajectories shown in figure 4.18, this ratio corresponds to a switching line that is very close to 45^o, meaning that the trajectory would 'hunt' in a convergent manner until it reached the zero point - ie. rapid switching would occur as the trajectory repeatedly crosses the switching line. The phase plane analysis is a simplification however, and does not account for a finite delay between the switch line detection within the controller and the actual valve reversal. Also, the figure is one view of the 3D phase space at a selected value of position error (in this case with the error = 0) and so it does not give a complete view of the best choice of ratio between τ_c and K_p at all position errors.

The simulation for $\tau_c = 32\times10^{-3}\ s$ and $K_p = 92\times10^{-9}\ m^3N^{-1}$ was termed SIM16 and the position response is shown in figure 4.23. It is clear that the response is a great improvement on the response with scheme 2 control, and that the predictions of the simplified analysis are confirmed.

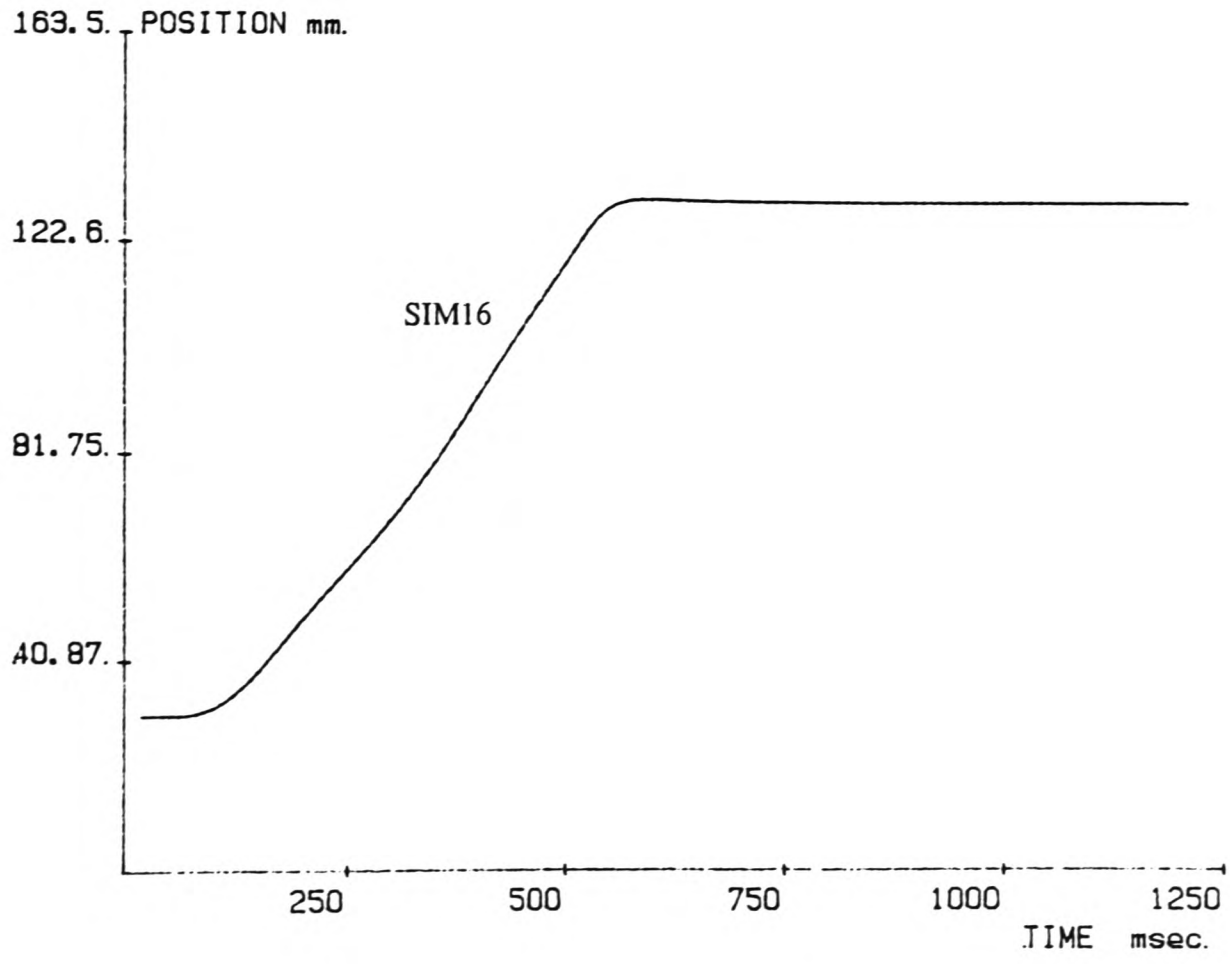

FIGURE 4.23 Simulation of system response with position, velocity and differential pressure feedback; $\tau_c = 32\times10^{-3}\ s$ and $K_p = 92\times10^{-9}\ m^3N^{-1}$.

Simulations were also carried out for values of $\tau_c > 32\times10^{-3}\ s$ and $\tau_c < 32\times10^{-3}\ s$ with corresponding changes in K_p, in order to assess systems that were expected to be more damped and less damped respectively.

SIM17 is the simulation for more damped response and the output is shown in figure 4.24. SIM18 is the simulation for less damped response and the output is shown in figure 4.25. These simulations confirm the predictions of the simplified analysis.

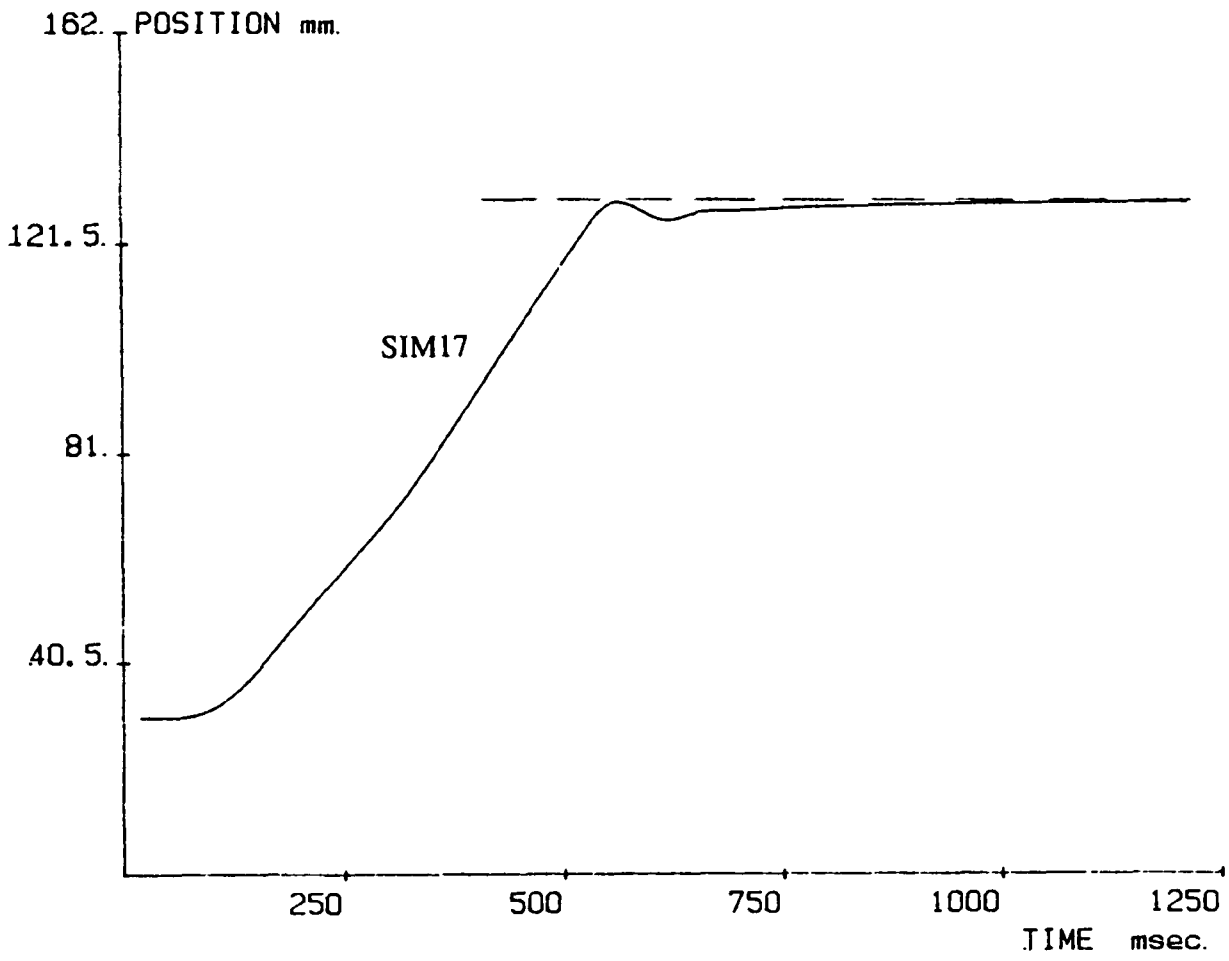

FIGURE 4.24 SIM17 simulation of system response with position, velocity and differential pressure feedback; $\tau_c = 128\times10^{-3}\ s$ and $K_p = 114\times10^{-9}\ m^3N^{-1}$.

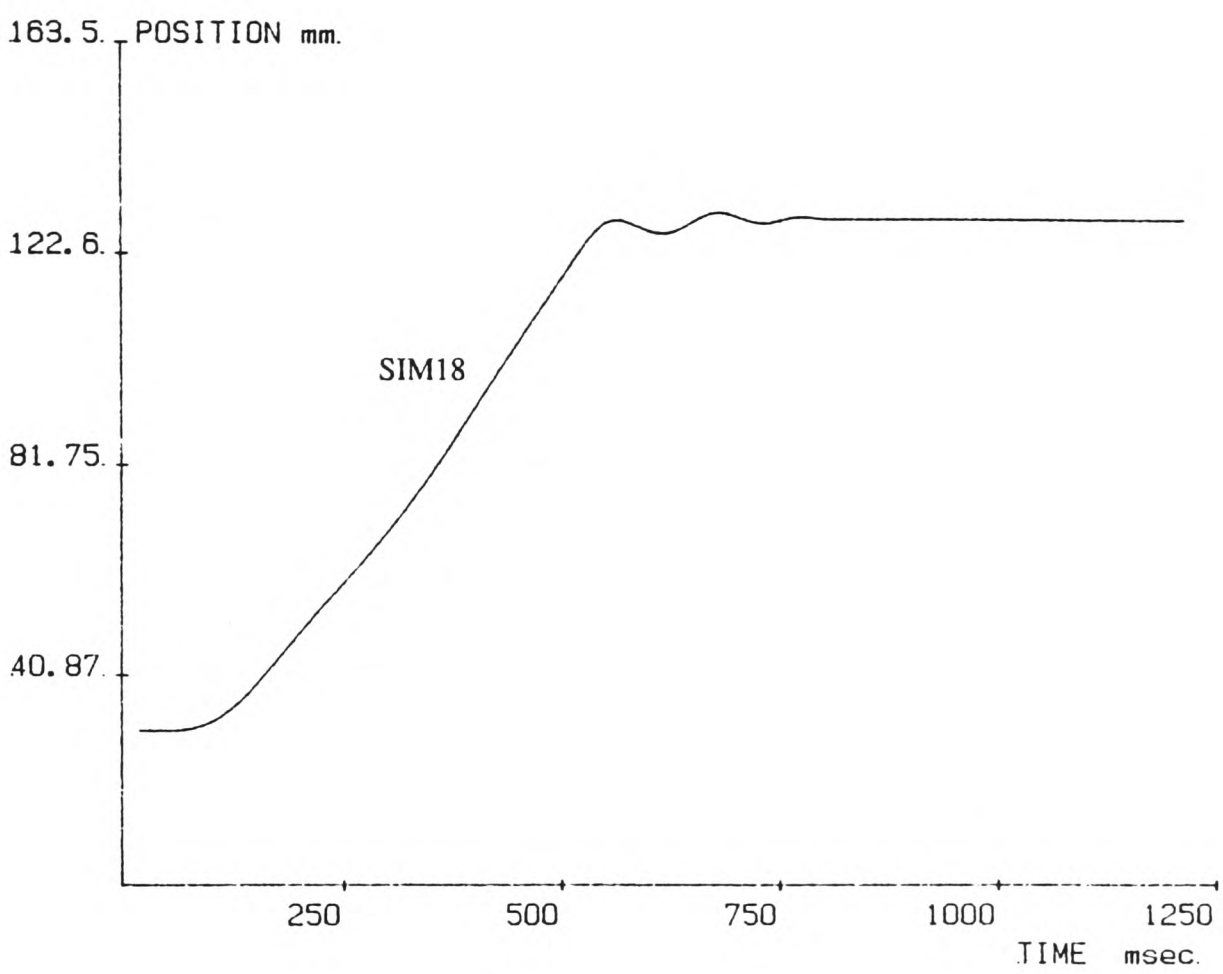

FIGURE 4.25 SIM18 simulation of system response with position, velocity and differential pressure feedback; $\tau_c = 25\times10^{-3}\ s$ and $K_p = 28\times10^{-9}\ m^3N^{-1}$.

The root locus approach also predicted that an instability would occur for very small values of τ_c because the majority of the locus moves through the right hand plane (see figure 4.8). This was also confirmed by a computer simulation - SIM19 - which used control scheme 3 with the following feedback gains : $\tau_c = 16\times10^{-3}\ s$ and $K_p = 23\times10^{-9}\ m^3N^{-1}$. Figure 4.26 is the output of the simulation and it clearly shows the instability in the system for these small values of τ_c and K_p.

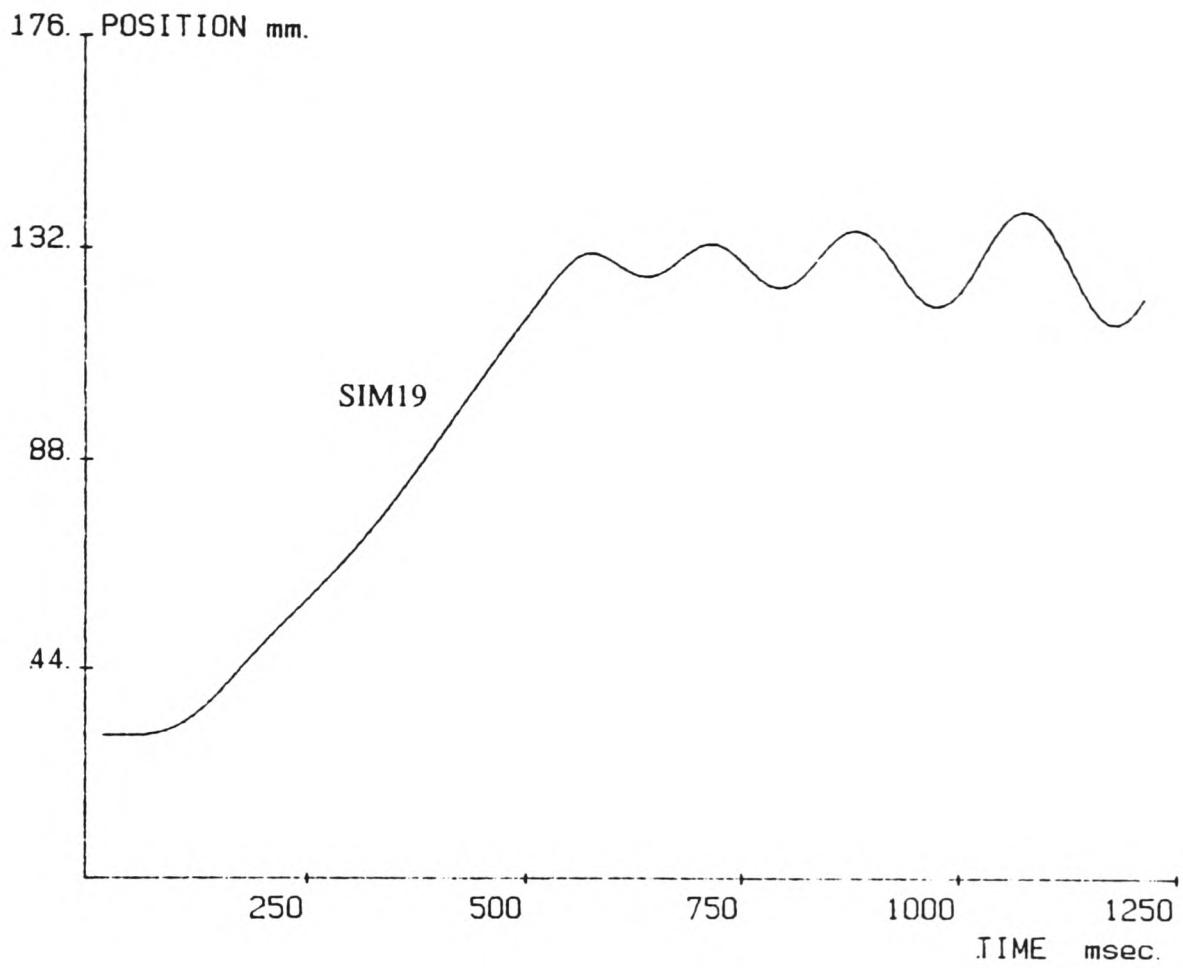

FIGURE 4.26 SIM19 simulation of system response with position, velocity and differential pressure feedback; $\tau_c = 16\times10^{-3}\ s$ and $K_p = 23\times10^{-9}\ m^3N^{-1}$.

4.5 Summary

The highly non-linear system has been analysed using a variety of techniques. Firstly the root locus technique has been used by representing the valve/actuator/load dynamics with a linear transfer function and replacing the non-linear on-off solenoid characteristic with a quasi-linear transfer function of an infinitely variable gain. This enabled the stability of a number of control scheme proposals to be evaluated in an approximate way. A piecewise linear analysis was also carried out to obtain further information on the behaviour of the control scheme using position plus velocity plus differential pressure feedback.

Finally the non-linear computer simulation was used to predict the actual system response for the control schemes proposed by the root locus and the phase plane analysis, and this more complex system representation was used to 'tune' the feedback parameters to obtain an improved response.

5 : EXPERIMENTAL EVALUATION OF CONTROL STRATEGIES

5.1 Introduction

The simulations described in section 4.3.3 have provided information on the likely behaviour of the system under the various control schemes proposed. The result of these simulations suggested that good system response would only be achieved with scheme 3 using a combination of position, velocity and differential pressure feedback. It was also predicted that scheme 2, which used position and velocity feedback, would exhibit a limit cycle for any value of velocity feedback gain. These predictions were now evaluated on the actual system.

Following this, experiments recording the step response of the system for a variety of step sizes were carried out using scheme 3 with the best choice of feedback constants, so that the behaviour of the system for other input conditions could be observed.

All of the tests were carried out using the Type 1 low friction actuator described in Chapter 2. In order to demonstrate the benefits of the use of this low friction actuator in the control system, a final series of experiments were carried out with an added friction load to approximate to a system using an actuator with a high intrinsic friction level.

5.2 Test Equipment

The basis of the test rig used for these experiments was identical to the rig used for the modelling correlation tests in Chapter 3. The sole addition to the equipment was a mechanical brake which enabled a friction load to be added to the piston/load assembly. The arrangement of the brake is shown in figure 5.1.

Two diametrically opposed rubber brake blocks are clamped around the piston rod at the cylinder end using a scissor arrangement. Rotation of the adjustment screw allows the clamping force, and therefore the friction force, to be set. Support of the arms at points A and B was provided to transmit the forces on the scissor mechanism when the rod moves thus reducing axial play in the brake assembly.

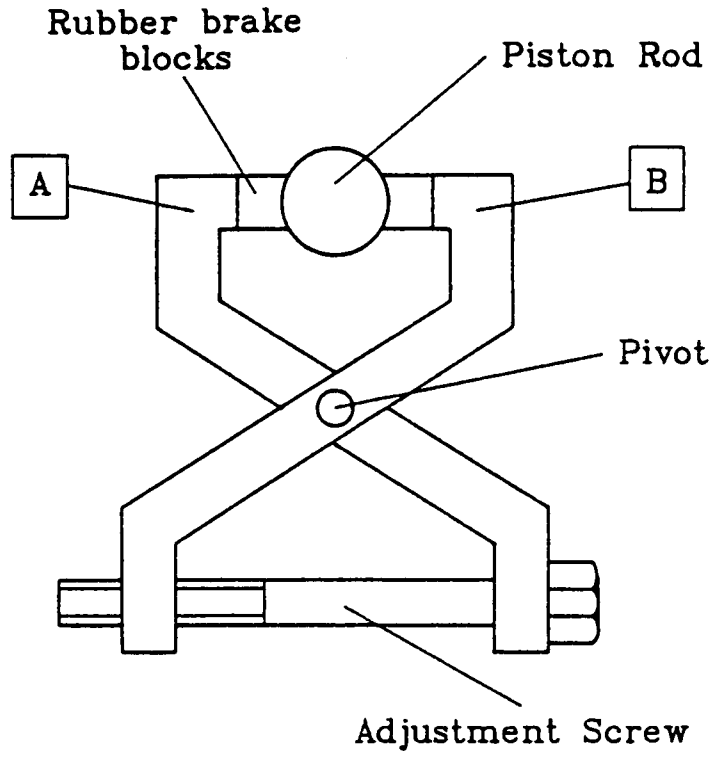

FIGURE 5.1 Schematic Drawing of the Friction Brake Assembly

The computer interface was identical to that used in the model correlation tests of Chapter 3. Modifications to the software used to monitor and record the system data and to control the solenoid valves were required however.

The tasks of the computer programme can be divided thus :

1) To record all data from the transducers and store them in memory.

2) To monitor the system state from a combination of transducer inputs, to evaluate the desired valve states and then to output the solenoid control commands.

These routines are carried out under interrupt as before and this was programmed using the BBC microcomputer BASIC assembler. At each service of the interrupt a set of transducer data is stored in memory. The maximum time duration of the experiment is set by the memory space in the computer and the frequency at which the interrupts are carried out. The maximum interrupt frequency will be determined by the amount of computing required at each interrupt.

For 2) above, the initial task for of the controller is the determination of the time at which the system trajectory crosses the switch line. The calculations require the squaring of the velocity reading and this occupies a considerable proportion of the overall time needed to service the interrupt. The velocity measurement on the system is taken from the tachometer through a 12 bit analogue to digital converter (Section 3.4.3). This 12 bit value is held in two bytes in the computer, the squaring operation results in a 3 byte number being held for comparison with the current position error. It is also necessary to integrate the tachometer

signal during the interrupt in order to monitor the current piston position. This too occupies 3 bytes. A number of conditional branches are required before comparison can be made because the squaring operation will always return a positive number. In fact this feature is exploited in the programme in order to significantly speed up the squaring operation. Any negative twos compliment 16 bit velocity readings are made positive before being squared because the duration of the squaring routine is proportional to the number of ones in the two bytes. With this squaring operation the duration of the interrupt resulted in a maximum frequency of 250 *Hz*, a frequency of 200 *Hz* was used in the programme.

The simulation studies had shown that the response of the system varied with the step size of the computational loop. This is analogous to the sampling frequency of the controller programme and this was confirmed by testing. An optimum step size was found to be around 1 *ms*, or equivalent to an interrupt frequency of 1000 *Hz*. Obviously the mode 1 control which includes the squaring routine could not be carried out at this frequency, but the mode 2 control could be carried out within 1 *ms*, even for the most complicated feedback scheme of position plus velocity plus differential pressure feedback. The dual mode controller was therefore programmed to operate at two frequencies; 200 *Hz* for mode 1, and 1000 *Hz* for mode 2.

The controlling programme took into account the effect of the discontinuity of sampling frequency on the integration routine to obtain the piston position from the velocity readings, and on the time duration between each of the sets of stored data in memory. The controlling programme permitted a choice of mode 2 controller schemes from position feedback only (scheme 1) to position plus velocity plus differential pressure feedback (scheme 3). The programme accounts for the discontinuity in the sampling frequency between the two modes by adjusting the time step in the integration routine and by recording the time duration between each of the sets of stored data in memory. A flowchart of the dual mode controller programme is shown in Appendix 5.

5.3 Test Procedure

For the first series of tests, the initial conditions and the desired step were held constant. The test conditions for each of the simulations that were carried out in sections 4.3.3 were repeated on the test equipment as closely as possible, ie. each of the tests employed dual mode control using one of the three schemes for the second mode of control. The feedback constants τ_c and Kp were approximated to the desired values so that they could be evaluated quickly - ie. they required only multiplications by factors of two and this reduced

the time needed within the interrupt.

The objective of the second series of tests was to evaluate the performance of the 'best' controller parameters for other step sizes and from other points on the stroke. Only the initial position and the step size were varied, all other system parameters remained constant.

The final series of tests were carried out to evaluate the performance of the system with an additional friction load. The brake mechanism would allow a variation in the applied friction. The amount of friction added was dependent on the position of the adjustment screw. A rough calibration of the device was carried out so that the number of turns of the adjustment screw could be related to the approximate values of friction force applied. The accurate determination of the friction/stiction characteristic of the brake system was not carried out at this stage because this was to be an initial investigation only. All tests used control scheme 3 during mode 2 of the dual mode controller, but the mode 1 control period was considerably reduced so that the stability and the positioning accuracy of mode 2 could be observed. This was necessary because for some of the tests, high friction levels caused the deadband of the system to be greater than the system error when mode 2 was entered. The first two tests were carried out to observe the effect of an increasing friction load. These were compared to the result of an identical test without added friction. The third test used adjusted feedback constants to reduce the control damping with a friction load chosen to represent that which might be found on a typical pneumatic actuator of similar size.

All experimental tests were carried out with an inertia load of 37 *kg* and an approximate supply pressure of 5.5 *bar gauge*. A listing of the other test conditions for each of the experiments is given in table 5.1.

Experiment	Mode 2 Control Feedback	Piston Position		MODE 1	MODE 2		Figure Number
		Initial *mm*	Target *mm*	$K_{SW} \times 10^3$ s^{-1}	τ_c *s*	$K_p \times 10^9$ m^3N^{-1}	
EXP8	Position	30	130	160	0	0	5.2
EXP9	Position + velocity	30	130	160	500	0	5.3
EXP10	"	30	130	160	130	0	5.4
EXP11	"	30	130	160	32	0	5.5
EXP12	Position + velocity + diff. press.	30	130	160	32	92	5.6 5.11 5.12
EXP13	"	30	130	160	130	360	5.7
EXP14	"	30	130	160	16	46	5.8
EXP15	"	30	130	160	8	23	5.9
EXP16	"	0	50	160	32	92	5.10a
EXP17	"	0	100	160	32	92	5.10b
EXP18	"	0	150	160	32	92	5.10c
EXP19	"	0	200	160	32	92	5.10d
EXP20	"	0	250	160	32	92	5.10e
EXP21	"	100	200	160	32	92	4.34f
EXP22*	"	30	130	2560	32	92	5.11 & 12
EXP23*	"	30	130	2560	32	92	5.11 & 12
EXP24*	"	30	130	2560	32	92	5.13

* includes friction load.

TABLE 5.1 Test Conditions and Feedback Schemes used for the Control Tests.

5.4 Scheme 1 - Position Feedback Only

This dual mode control method uses the time optimum control for mode 1 followed by position feedback only during mode 2.

The initial conditions for the experiment EXP8 are given in table 5.1. The position response of the system to the step change is shown in figure 5.2. As predicted in the very simple analysis of section 4.3, and the computer simulation of section 4.4, the response is unstable.

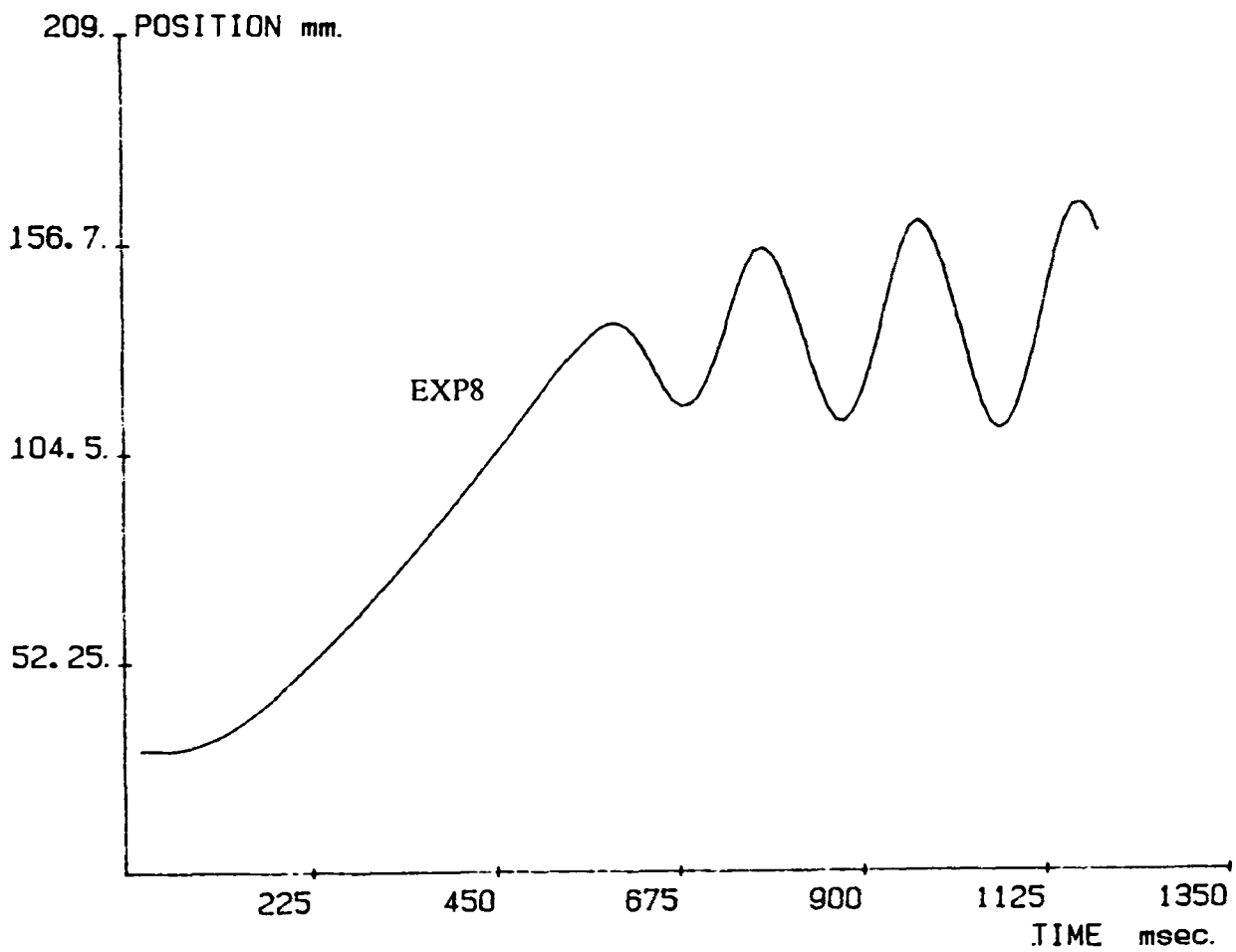

FIGURE 5.2 EXP8 - System response using position feedback only.

5.5 Scheme 2 - Position Plus Velocity Feedback

This dual mode control method uses the time optimum control for mode 1 followed by position plus velocity feedback during mode 2.

The initial conditions for the experiment EXP9 are given in table 5.1. The value of τ_c was chosen to be greater than the estimated system time constant (τ_s), and this was expected to result in a stable system.

The position response of the system to the step change is shown in figure 5.3. Although the system is stable, a limit cycle of approximate amplitude 4 *mm* peak to peak exists. The limit cycling was predicted by the computer simulation, and it could not be eliminated with higher values of τ_c.

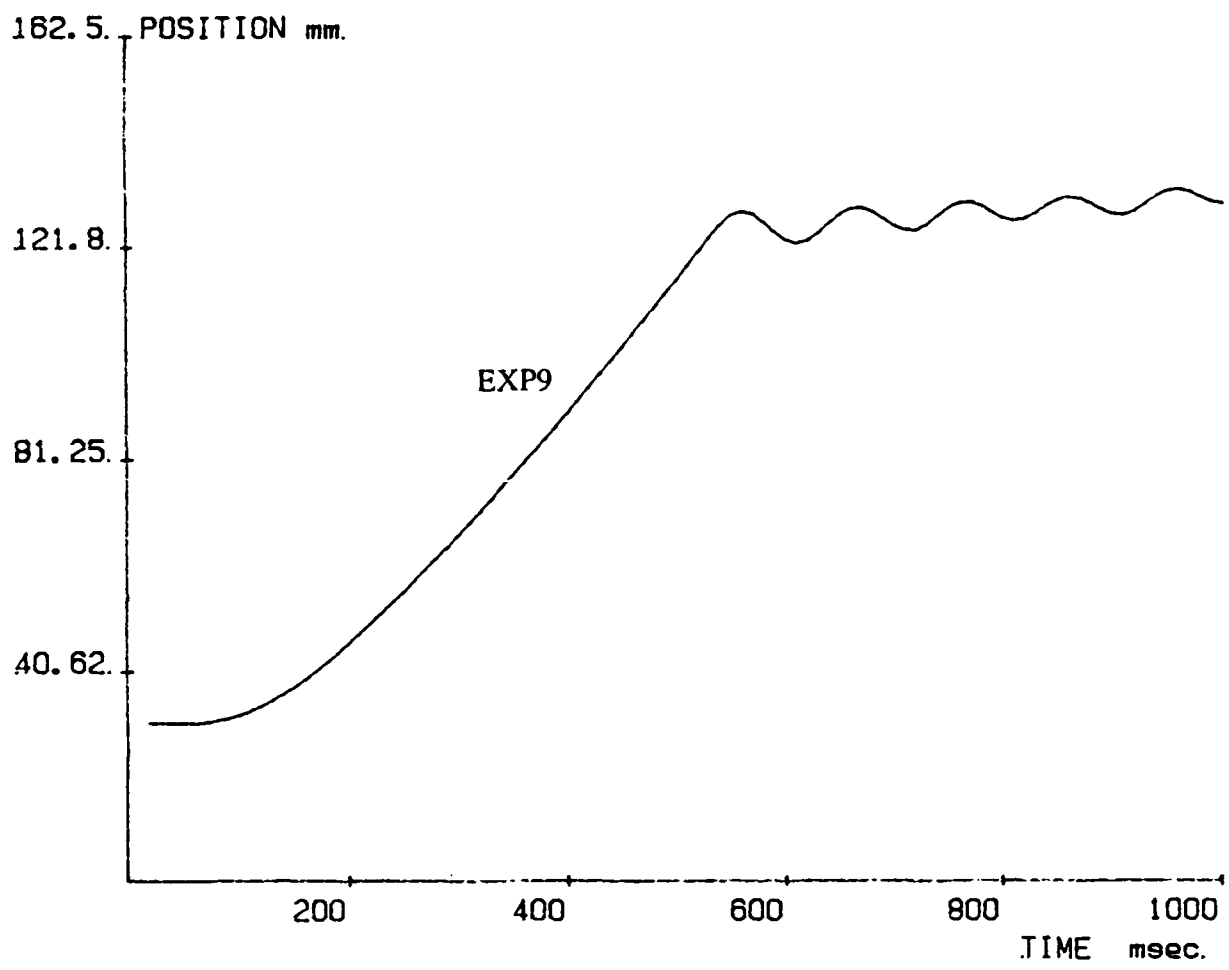

FIGURE 5.3 EXP9 - System response using position plus velocity feedback; $\tau_c = 0.5$ *s*.

The initial conditions for the experiment EXP10 are given in table 5.1. The value of τ_c was now chosen to be smaller than τ_s and this was expected to result in a system with a large limit cycle. Again the computer predictions hold well. Figure 5.4 shows that the limit cycle is increased in size to around 7 *mm* peak to peak, and this was found to increase with smaller τ_c.

Finally, figure 5.5 shows the position response for a test - EXP11 - with $\tau_c = 0.032$ *s*, and now the system is unstable. Performance is similar to the system with position feedback only.

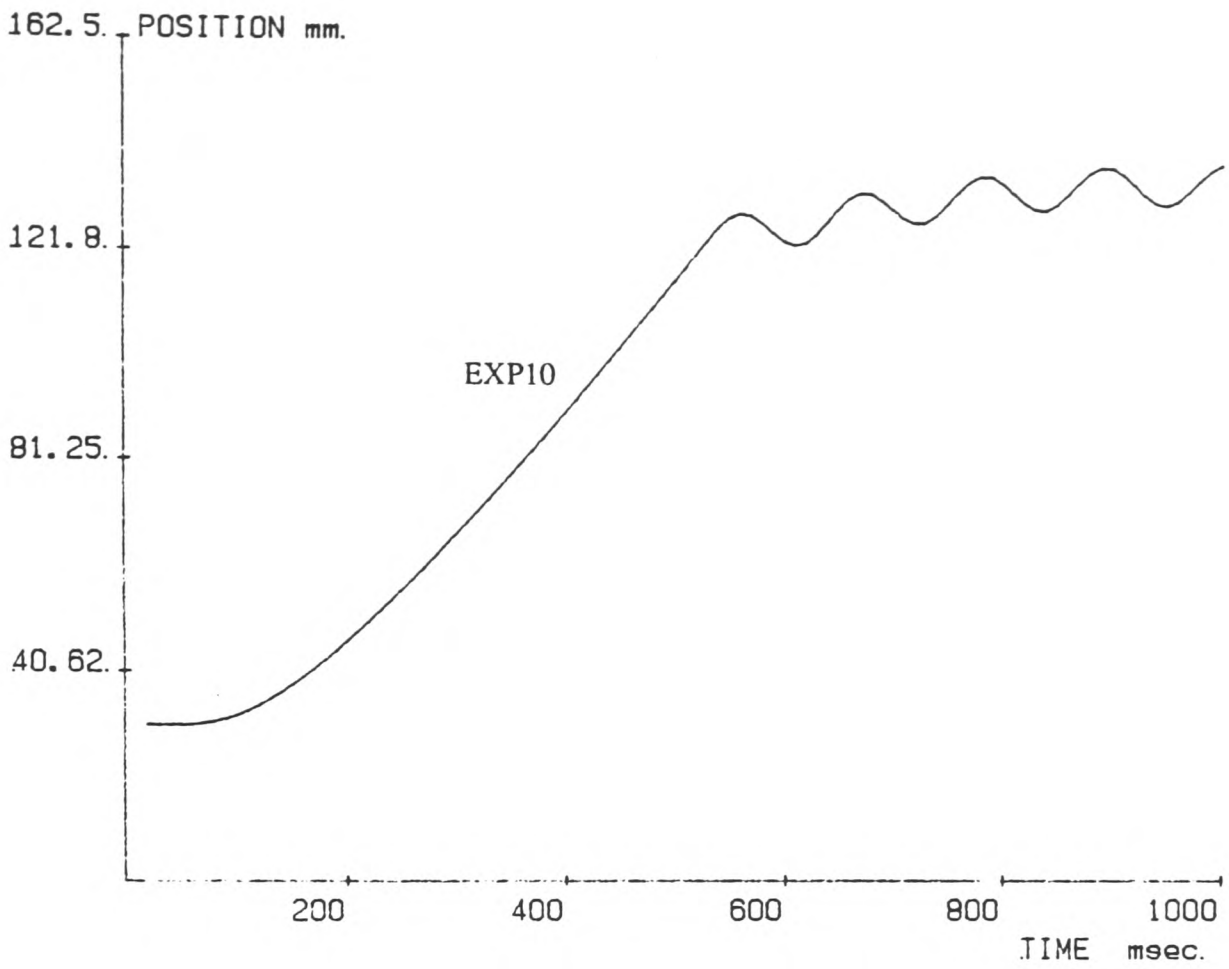

FIGURE 5.4 EXP10 - System response using position plus velocity feedback; $\tau_c = 0.13$ *s*.

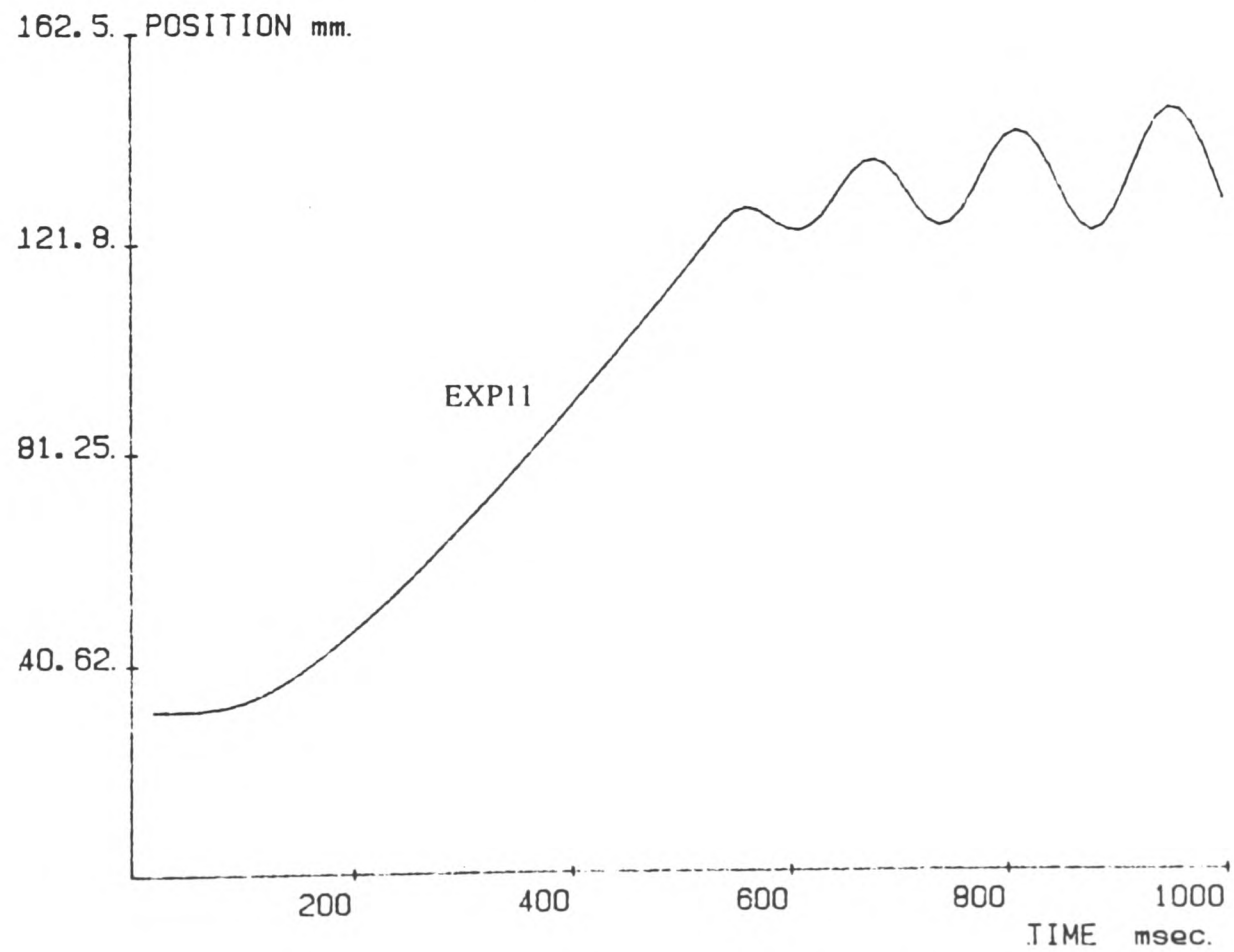

FIGURE 5.5 EXP11 - System response using position plus velocity feedback; $\tau_c = 0.032$ *s*.

These test have demonstrated how the control scheme 2 using position plus velocity feedback successfully stabilises the system, but even with the 'best' choice of τ_c a limit cycle remains with an amplitude of approximately 1.5% of the stroke length.

5.6 Scheme 3 - Position Plus Velocity Plus Differential Pressure Feedback

This dual mode control method uses the time optimum control for mode 1 followed by position plus velocity plus differential pressure feedback during mode 2. The first experiment used the values of τ_c and K_p predicted by the computer simulation to have the best position response ie. $\tau_c = 32\times10^{-3}\ s$ and $K_p = 92\times10^{-9}\ m^3N^{-1}$. The test conditions for EXP12 are given in table 5.1. The position response for the system is shown in figure 5.6.

The step response is vastly improved over that obtained with scheme 2 control, and this has again confirmed that the computer simulation made accurate predictions of the system response.

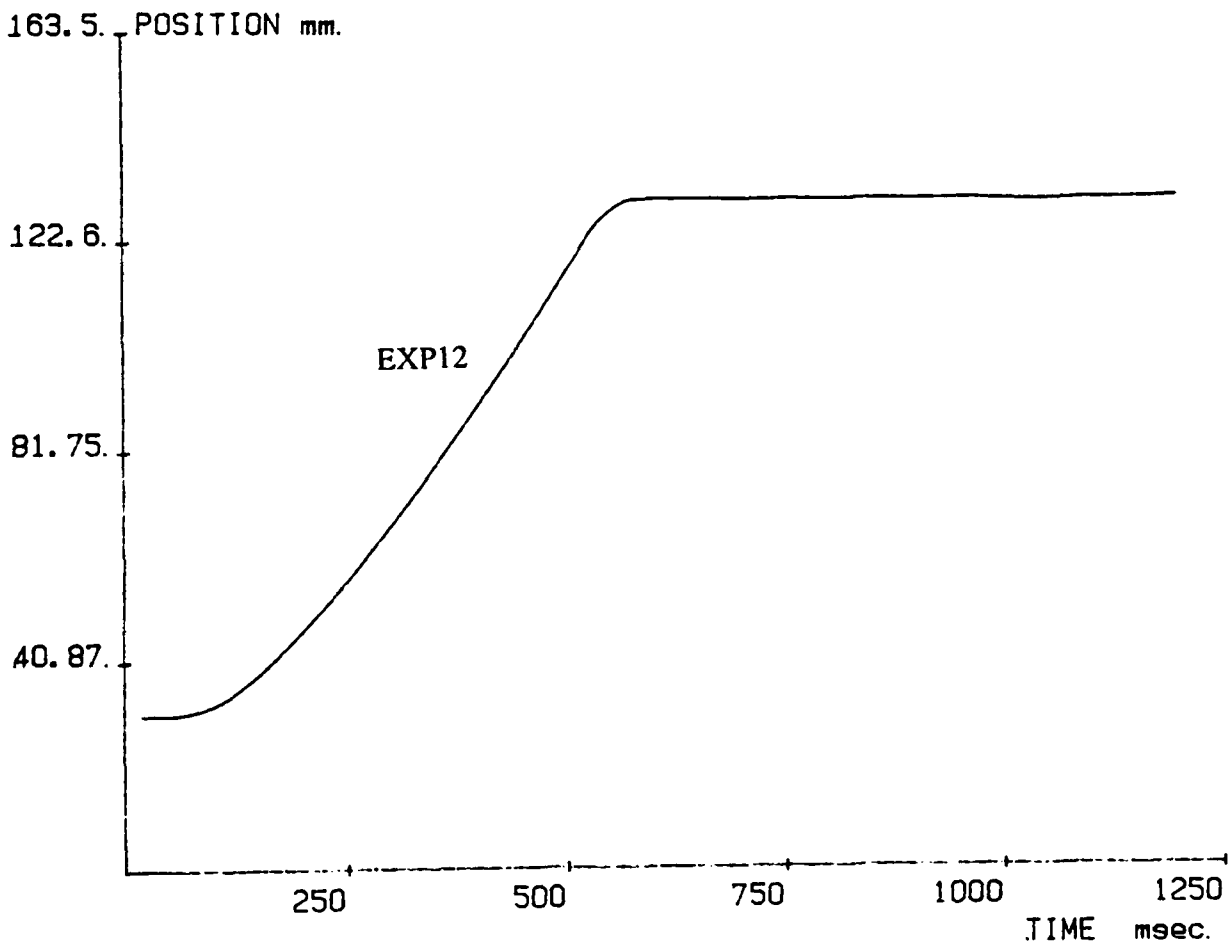

FIGURE 5.6 EXP12 - System response using position plus velocity plus differential pressure feedback; $\tau_c = 32\times10^{-3}\ s$ and $K_p = 92\times10^{-9}\ m^3N^{-1}$.

Three further tests were carried out to demonstrate the system response for a choice of τ_c and K_p to produce a more damped system (EXP13), a less damped system (EXP14) and an unstable system (EXP15). The test conditions for these tests are given in table 5.1. The position response for EXP13, using $\tau_c = 130\times10^{-3}\ s$ and $K_p = 360\times10^{-9}\ m^3N^{-1}$, is shown in figure 5.7. In order to highlight the over-damped response, the final position is marked as a broken line.

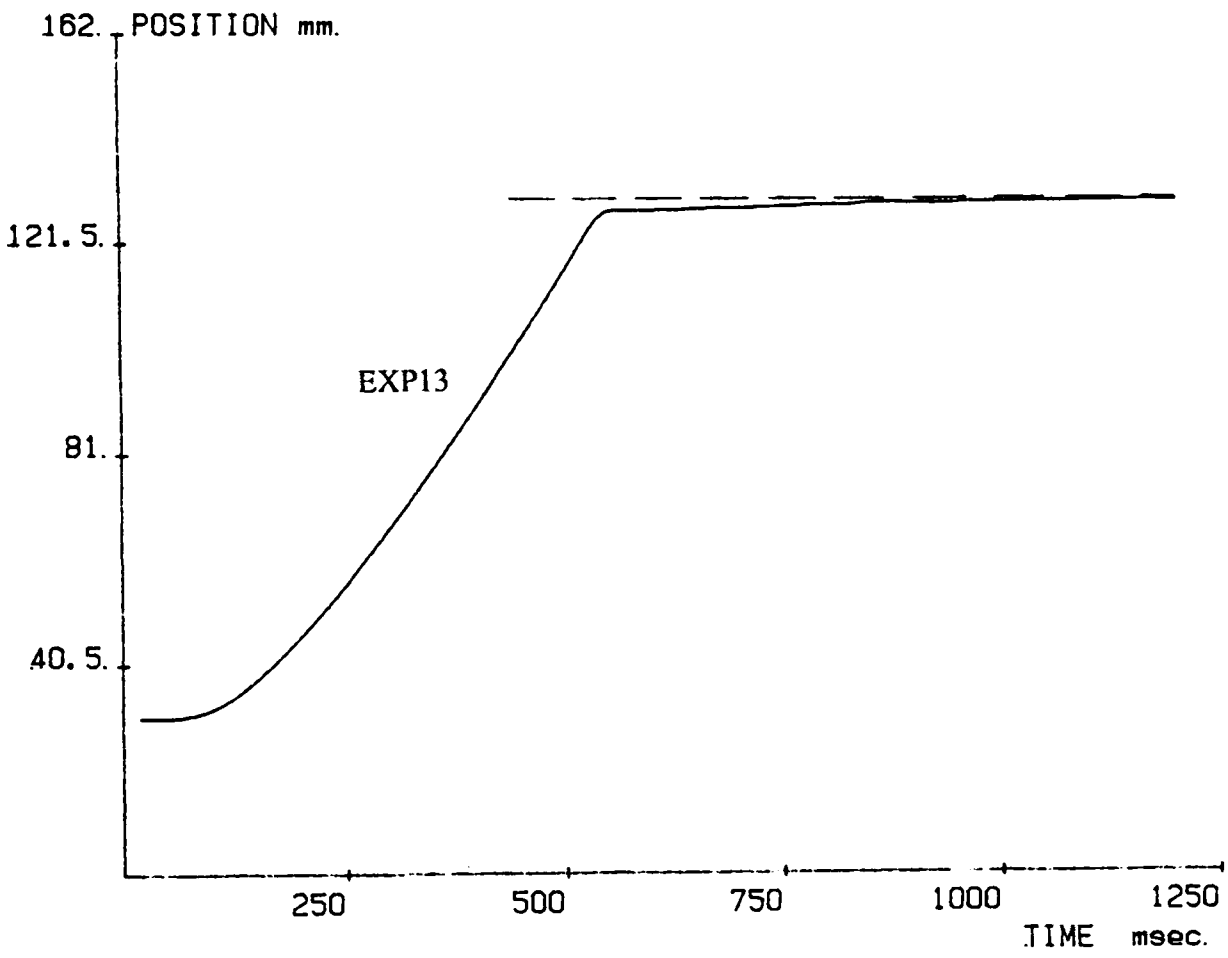

FIGURE 5.7 EXP13 - System response using position plus velocity plus differential pressure feedback; $\tau_c = 130\times10^{-3}\ s$ and $K_p = 360\times10^{-9}\ m^3N^{-1}$.

The position response for EXP14, using $\tau_c = 16\times10^{-3}\ s$ and $K_p = 46\times10^{-9}\ m^3N^{-1}$, is shown in figure 5.8. It is under-damped as expected, with an overshoot of 3.5% of the step size. However, there are not as many oscillations as were predicted in the computer simulation; the actual system incorporates some damping that has not been taken into consideration in the model.

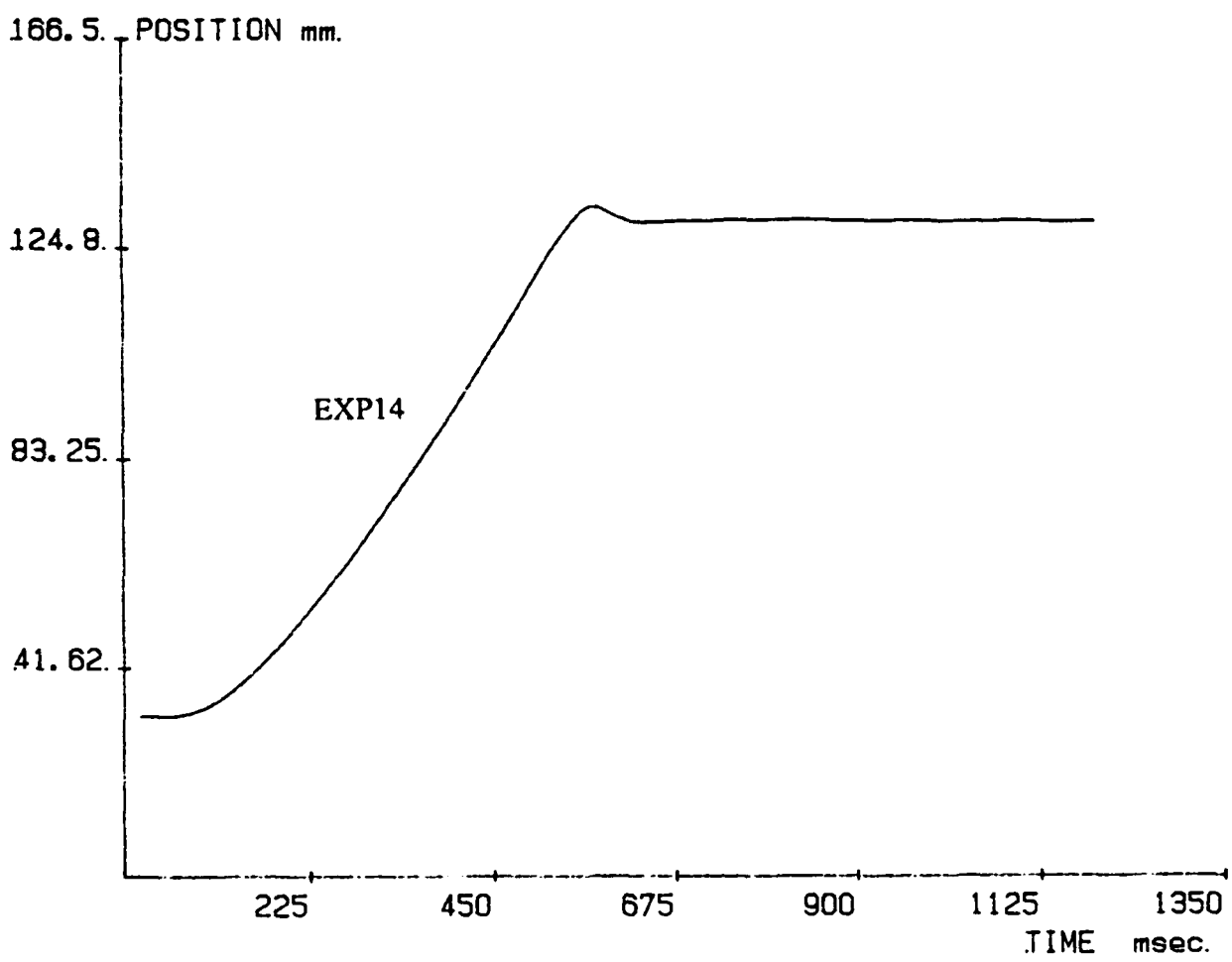

FIGURE 5.8 EXP14 - System response using position plus velocity plus differential pressure feedback; $\tau_c = 16\times10^{-3}\ s$ and $K_p = 46\times10^{-9}\ m^3N^{-1}$.

The position response for EXP15 using $\tau_c = 8\times10^{-3}\ s$ and $K_p = 23\times10^{-9}\ m^3N^{-1}$, is shown in figure 5.9. This shows that the response is unstable for these low values of feedback gain.

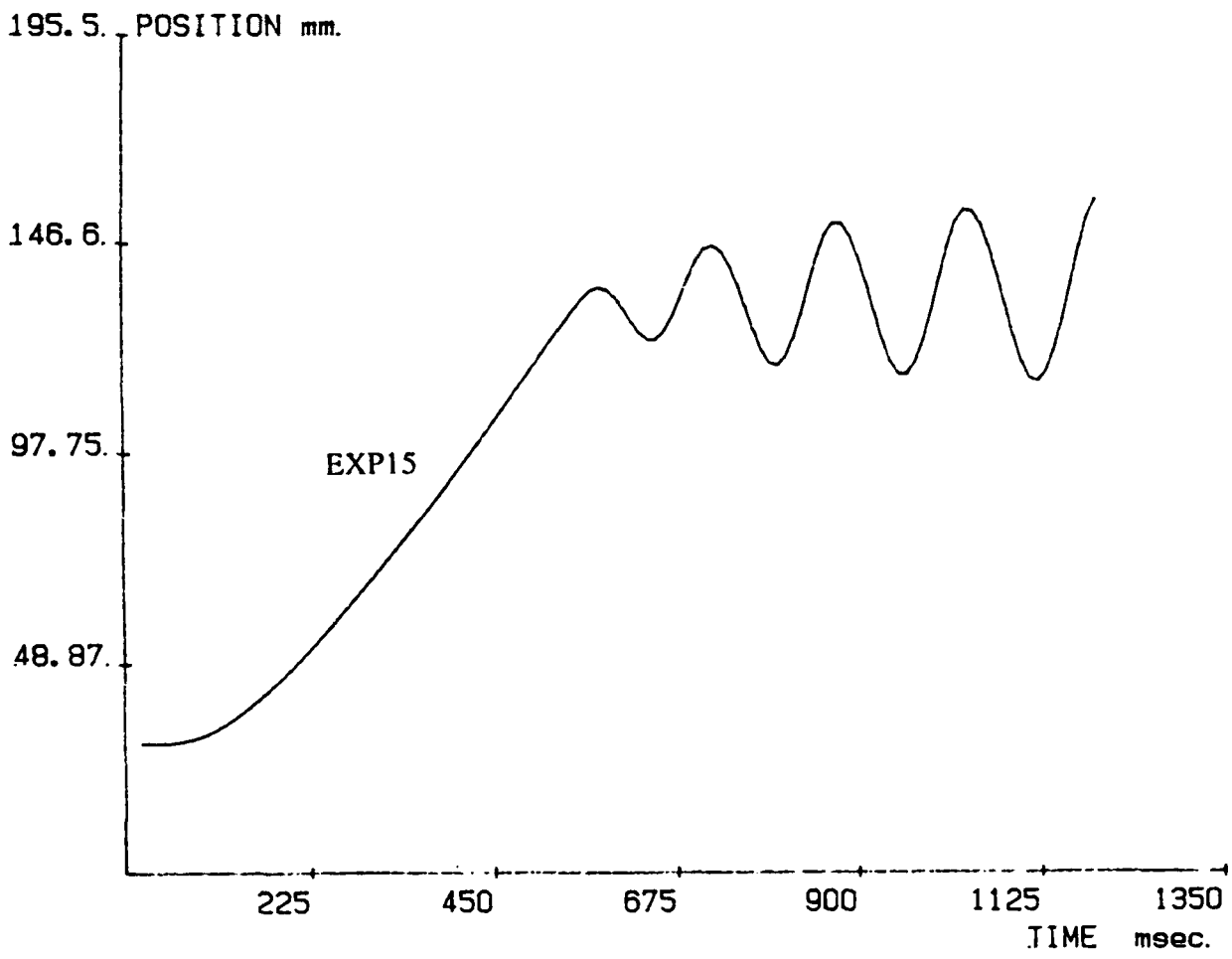

FIGURE 5.9 EXP15 - System response using position plus velocity plus differential pressure feedback; $\tau_c = 8\times10^{-3}\ s$ and $K_p = 23\times10^{-9}\ m^3N^{-1}$.

The final series of tests were carried out to evaluate the performance of the 'best' choice of feedback constant for different step sizes and from different points on the stroke. The feedback constants used were :

$$\tau_c = 32\times10^{-3}\ s$$
$$K_p = 92\times10^{-9}\ m^3N^{-1}$$

The experiments EXP16 to EXP20 were tests of step displacements of increasing size from the end of the stroke. EXP21 was a displacement from 100 *mm* to 200 *mm*. A complete listing of the tests conditions for these experiments is given in table 5.1. The position response for all of the tests is given in figure 5.10a to f.

The response is similar for all step sizes with a very small overshoot only and a good level of damping. On each graph the final position of the piston is printed. These were the result of the individual tests and so are not indicators of the average or likely error for the step response to these positions. They do give some indication however of the current accuracy of the position control system.

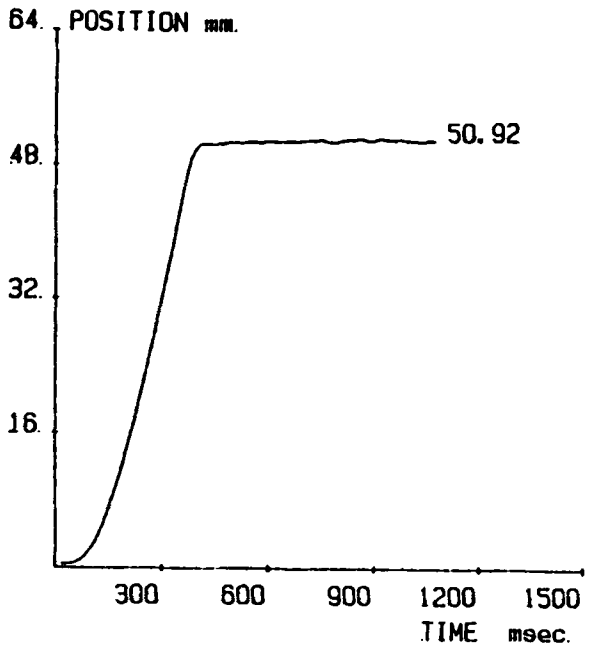

a) EXP16 0 - 50 *mm* step

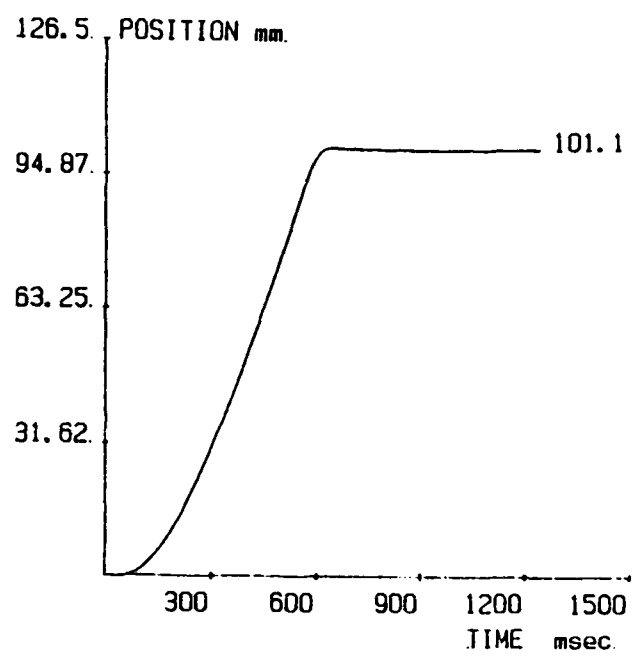

b) EXP17 0 - 100 *mm* step

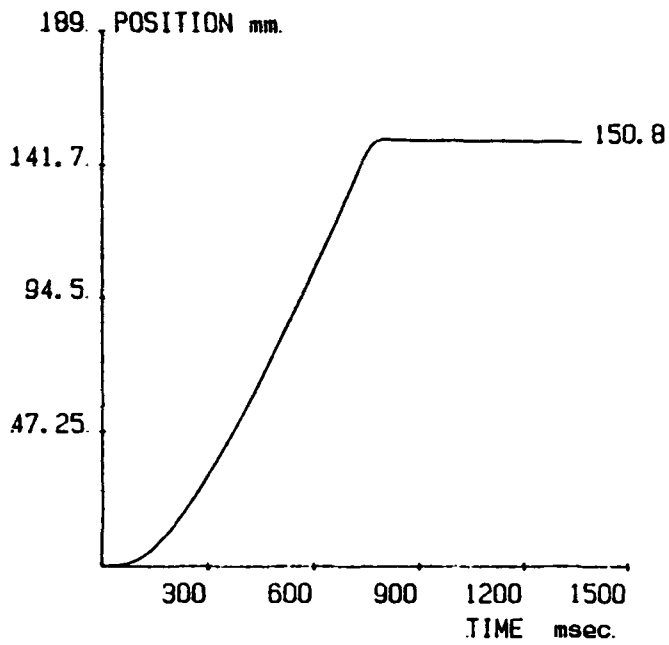

c) EXP18 0 - 150 *mm* step

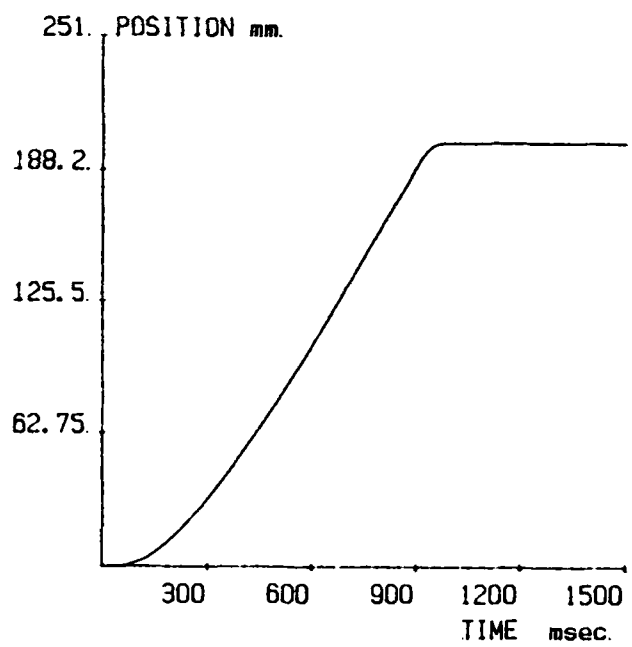

d) EXP19 0 - 200 *mm* step

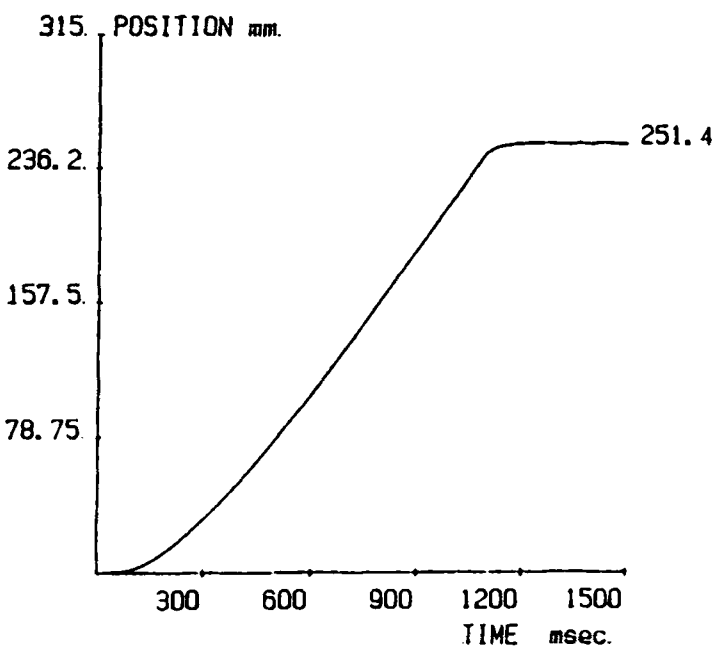

e) EXP20 0 - 250 *mm* step

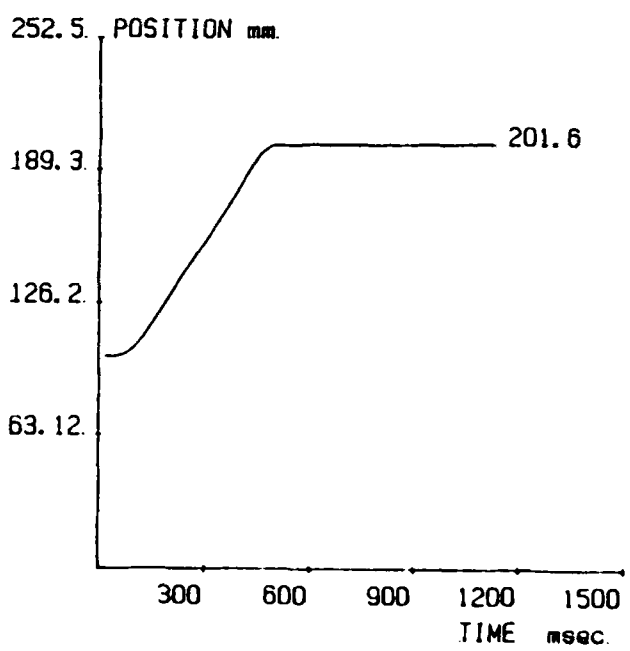

f) EXP21 100 - 200 *mm* step

FIGURE 5.10 Position Response of System for Various Steps Using Position + Velocity + Differential Pressure Feedback.

5.7 System Response with Added Friction Load

The Type 1 low friction actuator that was described in Chapter 2 has been used for all of the control tests. The effect of an added friction load was now to be investigated.

The best control parameters for scheme 3 which were used in section 5.6 were used again here. The initial conditions for two tests with added friction load - EXP22 and EXP23 - are given in table 5.1. The friction load for each of the tests is shown in figure 5.11, together with the friction for a comparison test - EXP12 - which had no added friction load.

The step response for all three tests is shown in figure 5.12.

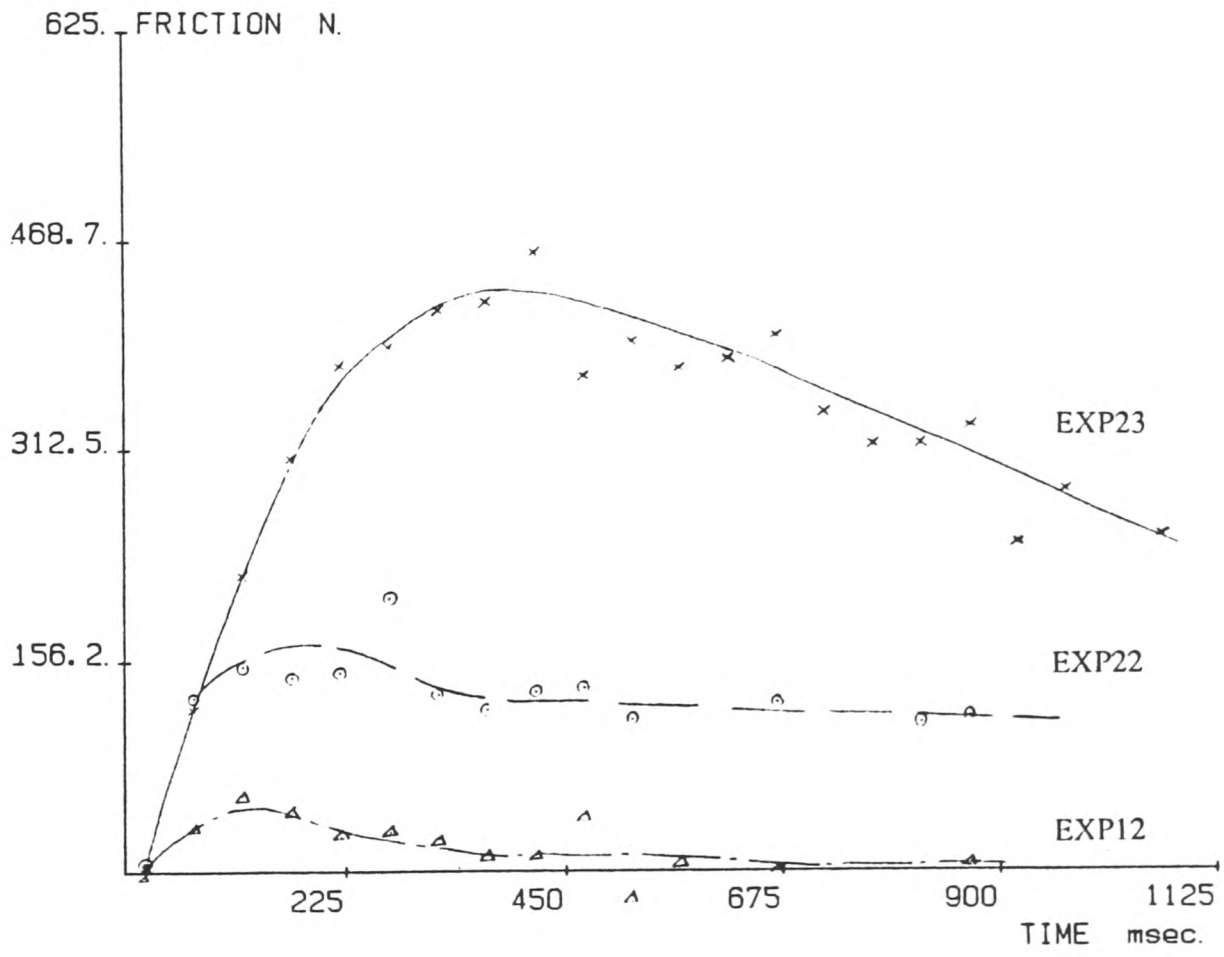

FIGURE 5.11 Measured friction force for EXP12, EXP22 and EXP23.

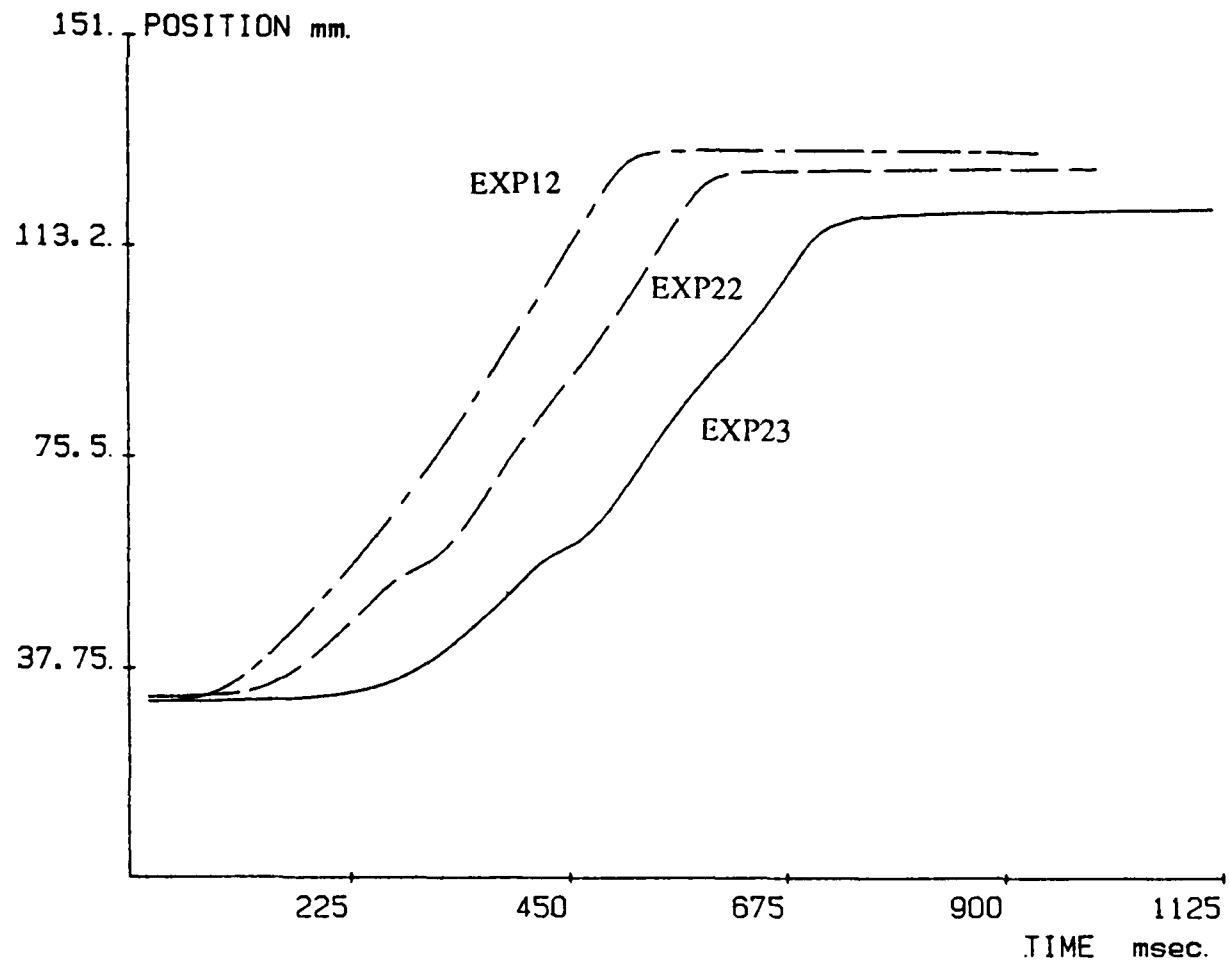

FIGURE 5.12 Step response of system with various friction loads. EXP12, EXP22 and EXP23.

The speed of response is reduced with a higher friction load as expected. The final position error is considerably increased with an increase in added friction load.

The system feedback parameters had been evaluated on the assumption of a negligible friction load and EXP12, which did not have an added friction load, matches this well with only a small position error and a near critically damped response. However, when a friction load is added the step response varies greatly from this prediction. Intuitively it seems that the friction load has added a non-linear damping term and so an improved positioning speed might be achieved by reducing the control damping.

From the simple root locus/state space analysis, the appropriate values for τ_c and K_p can be selected so as to reduce the control damping. A third experiment - EXP24 - used values of $\tau_c = 1\times10^{-3}\ s$ and $K_p = 3\times10^{-9}\ m^3N^{-1}$. These values have been shown to produce an unstable response when used with the low friction actuator (section 4.4). The test conditions for EXP24 are given in table 5.1. The stroking tests described by Bowns (26) had used standard actuators and his measurements of friction had suggested that dynamic

friction for a typical actuator of approximately 50 *mm* diameter may be as much as 300 *N* when driving a large load. A frictional load of about 300 *N* was therefore chosen for EXP24 so that it could represent the friction of a typical pneumatic actuator.

The result of the step response for EXP24 is shown in figure 5.13, together with the low friction actuator response - EXP12 - as a comparison.

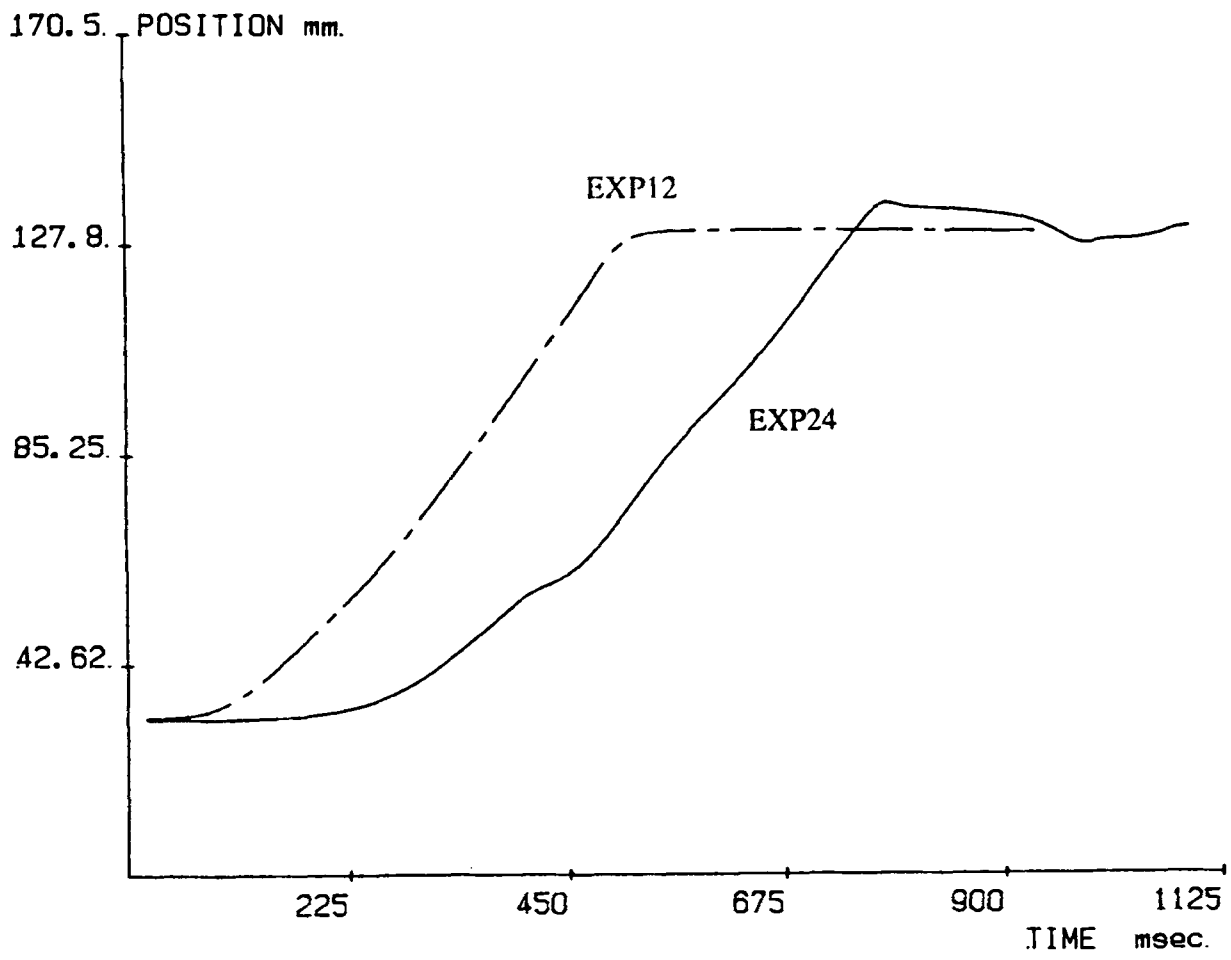

FIGURE 5.13 Comparison of step response of EXP24 which includes 300 *N* friction load and reduced control damping with EXP12.

The step response for the high friction actuator is very poor compared to that of the low friction actuator used for EXP12. The reduced control damping has improved the positioning accuracy of the high friction test, but the motion is no longer smooth. The system with high friction is stable however. The stability may be due to the stiction effect around the target position; the periods during which the piston is stationary act to make the drive 'insensitive' to the control command, thus stabilising a system which would have shown large oscillations in the absence of this.

5.8 Summary

All of the control scheme proposals that were considered in the analysis of Chapter 4 were tested on the actual system and these tests confirmed the accuracy of the computer predictions.

Good system response was demonstrated with a dual mode controller using time optimal response during mode 1, followed by position, velocity and differential pressure feedback during mode 2. The predictions of suitable values of feedback constant from computer simulations were shown to be accurate and provided a good response that approximated to a critically damped second order system. Position errors have not been statistically evaluated but the are typically in the region of $\pm$ 1 *mm*.

The positioning accuracy of the low friction actuator has been shown to be better than for an actuator with a high friction load added; the position error increased with friction force. An initial attempt at improving the positioning accuracy of the high friction system by changing the feedback constants demonstrated the poor response near the target position due to the stiction/friction effect, and showed how high levels of stiction made the system insensitive near to the target where, with low friction, it would have been unstable.

6 : CONCLUSIONS

A summary of the research work described in this thesis is presented in this chapter. Conclusions are drawn and the major achievements are listed. A discussion of the possible routes for the development of the project is then given together with a description of some specific areas of investigation that would provide a more thorough understanding of the system.

6.1 Summary of Research

An accurate, fast pneumatic position control system has been constructed. A theoretical model of the system has been developed and this will enable the accurate analysis of future systems to be undertaken.

Firstly, a review of the previous work in the area of pneumatic position control of rotary or linear actuators was carried out. This revealed the potential benefits that could be gained from the development of a pneumatic position control system which uses computer controlled on-off valves placed near to a low friction actuator. As a first step towards the construction of such a system, two new designs of low friction, symmetrical, double-acting, linear actuators were constructed and the friction of each was measured. The most promising design, which had the lowest measured friction level, was then used as part of the position control system. The level of friction has been shown to be around 10% of that measured in a standard pneumatic actuator of similar dimensions. Air bearings and a PTFE piston seal are used and these proved to be a simple and effective method of reducing the friction at the contact points within the actuator.

Two on-off solenoid operated valves controlled the flow of air into the cylinder chambers. These were switched via a purpose-built interface unit using a BBC microcomputer. An analysis of the behaviour of the system under various feedback control schemes was carried out using ;

i) a non-linear computer simulation of the system,

ii) a quasi-linear model of the system and the root-locus technique,

iii) a piecewise linear model of the system in the phase plane.

The reduction of friction in the pneumatic system has almost eliminated one of the major non-linearities and has allowed the linear root locus and phase plane techniques to provide accurate predictions of the system behaviour. The non-linear computer model was developed from a mathematical model based on thermodynamic expressions for the

actuator charging and discharging process, and is a development of earlier work by other researchers. The digital computer solution was extended to perform a full simulation of the control system and this provided accurate predictions of the system behaviour under the various control schemes considered.

Further investigation of the actuator and load friction, undertaken during the development of the simulation programme, indicated that the friction forces at higher pressures and when driving an inertia load can be represented with a good degree of accuracy by an empirical equation made up of the following ;

- a constant term,
- a velocity related term,
- an acceleration related term,
- a differential pressure related term.

For the closed loop position control a dual mode controller was used with the initial mode following a time-optimal path. Various schemes were investigated for the second mode of control. A simulation of the use of position feedback only showed system instability; the root locus method had also shown this. Analysis of the use of position and velocity feedback showed that the system stability would depend upon the choice of velocity feedback gain; the computer simulation suggested that a stable limit cycle would exist even for the best choice of feedback gain. A scheme using position, velocity and differential pressure feedback was then analysed; greatly improved step response was predicted with an appropriate choice of feedback gains.

Experimental work on the low friction actuator and the evaluation of the control schemes was carried out throughout the project. These tests confirmed the findings of the analysis and clearly demonstrated the accuracy of the simulation predictions. They were also used to show that the step response was considerably worsened when a friction load was applied.

The use of a low friction actuator and load system, combined with a relatively fast computer, has enabled the original on-off pneumatic control system developed by Drazan to be significantly improved upon. The utilisation of on-off valves will enable considerable cost savings to be made over systems using pneumatic servo valves such as the positioning modules developed at Loughborough University of Technology. A fast step response with reasonable positioning accuracy over a broad range of input steps has been achieved even for a system driving a large inertia load. This has laid down a foundation for many possible routes for the future development of the system.

6.2 Achievements

1) An accurate, fast pneumatic position control system has been developed. The use of a low friction actuator, combined with a relatively fast computer has resulted in a much superior system to that developed by Drazan. Positioning of a 37 *kg* inertia load to within ±1 *mm* at any point on a 300 *mm* stroke can be achieved without limit cycling and with little overshoot. Positioning time for a 150 *mm* move is approximately 0.8 *s*.

2) A low friction pneumatic actuator has been designed and built and the friction level has been measured to be around 10% of that found in a standard actuator of similar size. The friction was also found to be almost constant over the stroke of the actuator.

3) The forces acting on the actuator when driving an inertia load at high supply pressures (6 *bar gauge*) has been found to be a function of velocity, acceleration and differential pressure.

4) A non-linear computer simulation of the system has been developed and this can be generally applied to similar systems using a low friction actuator. The simulation provided highly accurate predictions of the system behaviour as the large non-linearity of friction that is normally present in such a system was almost eliminated by the low friction actuator.

5) The step response of a system with a large friction load was shown to be considerably worse than that for the low friction system.

6) An experimental rig has been constructed which features a low friction inertia loading system and the necessary data logging hardware and software including a comprehensive graph plotting programme. This will enable the continuation of this work on pneumatic control systems, or on the testing of low friction actuators.

6.3 Future Work

The development of the project to date has led to the construction of experimental equipment which has shown the potential of this type of system. There are many ways in which this work can be developed further. Specific areas of investigation could be pursued in order to gain a more thorough understanding of the system. At the same time the current system could be developed towards an industrial or commercial application. The various possibilities are discussed here.

6.3.1 Applications Development.

A low friction actuator which incorporates two on-off valves in the cylinder end caps could be developed. The actuator module could also include all of the necessary transducers and a pneumatic lock to hold the piston rod at the desired position. It may also be possible to mount the computer hardware on the actuator making it a self-contained module which, when brought together with other modules, would require supervisory control only. Installation considerations may require that the symmetrical design be changed for a rodless cylinder or an asymmetric design. Further work on friction reduction in these actuator types would be required.

The self-contained pneumatic positioning module could be used in a number of areas ;

1) A programmable robot could be assembled which would use these modules to provide a point-to-point positioning ability. The geometry of the robot could be chosen to compliment the actuator performance, *ie.* improved dynamic stiffness may be achieved by a parallel geometry for the robot rather than a serial.

2) Smaller versions of the module could be developed which may be suitable for prosthetic applications. This may be for an artificial arm or leg, or for a third arm mounted on a wheelchair. The ability to store pneumatic power efficiently would make this module very attractive.

3) A walking robot could use the modules as a leg actuator. Again storage ability and cleanliness would be significant advantages particularly for smaller machines.

4) A small module could be used as the drive for a variable pitch turbo-charger or turbine. This may also be applicable to the control of some aero-engines. The angle of attack of the blades or stators may be controlled using this type of module, where the compressed air power source is readily available.

6.3.2 System Development.

Many questions have arisen from the investigations carried out to date, and there are many opportunities for continued research in various aspects of the project.

Work concerning low friction actuators could continue with a reconsideration of the Type 2 design of actuator using the rolling rubber diaphragm piston seal and air bearings. Actuator friction measurement at higher pressures and with an inertia load could be carried out to assess the current design of the installation of the rolling seal which was established following the manufacturer's guidelines. The guidelines may not be directly applicable to a pneumatic system at these pressures, so a modification of the clearances and perhaps some

control of the intermediate pressure between the two seals may improve the performance of this sealing method.

An air bearing assembly may be fitted to the piston itself in order to reduce the friction at the piston seal even further. This may allow a closer investigation of the friction characteristic that was measured in the tests of Chapter 3, *ie.* it may be possible to deduce what physical effect causes an acceleration dependent friction term.

An alternative approach to research in the area of low friction actuators may be to optimise the cost/reliability/performance of the various low friction sealing methods to move towards the commercial application of a low friction actuator which could be used in a low cost position control module that was proposed in section 6.3.1.

Research on the system hardware could also be carried out. For example, the feedback signals derived from a tachometer and the two pressure transducers could be investigated to determine the accuracy required from them to obtain the desired positioning accuracy. Different types of transducer could be used. At present, position information is obtained from the integration of the tachometer signal so a set point must be established to initialise the system. Drift in the electronics or the integration routine can cause errors to build up with time. This may be avoided with the use of a position encoder which, with differentiation, could also provide velocity information. Error in the differentiation of the encoder signal will reduce the accuracy of the velocity feedback signal and the effect of this on the positioning accuracy of the system must be assessed.

The present use of two pressure transducers is an expensive option for a commercial system. A single differential pressure transducer could provide the feedback signal, but this would introduce time delays due to wave propagation along the transmission pipes as was discussed in Chapter 3. An effective solution to the problem of time delays would be to mount the differential pressure transducer on the piston itself. It would be straightforward to pass the electrical connections along the piston rod, particularly if the design was combined with a piston air bearing.

The present amplification of the pressure transducer signals is contained within the transducer body and has not required modification in the interface unit. In order to allow the system to position an inertia load plus a load force without a steady state error, it will be necessary to add a high pass filter to the interface to eliminate the DC signal from the differential pressure transducer.

The feedback scheme using position, velocity and differential pressure feedback has been shown to work well for certain values of feedback gain. The optimisation of these gains

and perhaps the use of non-linear feedback gains which vary with piston position, load, pressure *etc.* may significantly improve the positioning accuracy. Depending upon the area of application, a learning scheme could be developed which will optimise the values of gain over the first one or two repetitions of a work cycle in order to obtain good response for each of the steps within the cycle.

It may be found that a limitation on positioning accuracy is set by the size of the on-off valve. One method which would overcome this problem would be to use two on-off valves of different size in parallel at each end of the actuator. When near to the target position the large valves would shut and the final positioning would be achieved by the two small valves. A simple design of an integrated pair of on-off valves would still offer a cost advantage over a servo-valve.

Two of the methods of controlling piston motion using two on-off valves are ;

- the open mode where the chamber pressures are initially held at atmospheric pressure,
- the closed mode where both chambers are initially held at supply pressure.

The tests reported in this thesis have used the closed mode in order to limit the piston speed and oscillation and thus ease the control task. It may be possible to use the current control system under open mode with the appropriate choice of feedback parameters, but a brief investigation into this has shown problems with the detection of the first switch point due to the high piston velocities (around 1.2 ms^{-1}).

6.3.3 Modelling and Analysis.

Many of the areas of investigation using the experimental test equipment mentioned in section 6.3.2 could be carried out initially using the digital computer model of the system that was described in Chapter 3. The model could also be used to assess the system performance with a variation in other system parameters. For example ;

- load inertia
- supply pressure
- actuator size/stroke
- transmission pipe length
- valve size
- displacement step size *etc.*

The model programme would require modification to enable an assessment of some other parameters such as load force and stiction/friction effects. It may be possible to include

further terms, such as a variation in chamber temperature and air leakage, in order to improve the model predictions of velocity and acceleration, particularly when near to the centre stroke position.

6.4 Summary

The conclusions from the research into the position control of a low friction pneumatic actuator have been summarised in this chapter. The main achievements have been stated and the possible routes for the development of the system have been discussed. Future work on the system could follow a number of routes towards various application areas. Alternatively, a thorough investigation into the effects of some of the system parameters could be carried out. It is hoped that the work described in this thesis will lay the foundation for a wide variety of future research that will lead to a number of pneumatic position control systems offering significant benefits over systems available at present.

BIBLIOGRAPHY

1. Huhne, G and A Neugebauer, "The Performance of Novel Pneumatic Industrial Robot Drives for Point to Point and Continuous Path Controls," **2nd Conference on Industrial Robot Technology, University of Birmingham**, pp. 73-84, March 1974.

2. Belforte, G, N D'Alfio, and F Quagliotti, "Variable Positioning Systems of Pneumatic Cylinders," **6th International Fluid Power Symposium, Cambridge**, pp. 259-270, BHRA Fluid Engg, Cranfield, Bedford, 8-10 April 1981.

3. Drazan, P J and R Kennett, "An Opto-Pneumatic Manipulating Arm," **Industrial Robot**, vol. 2, no. 1, pp. 7-10, March 1975.

4. Drazan, P J and M F Jeffery, "Microprocessor Control and Pneumatic Drive of a Manipulating Arm," **Proc. of 3rd Conf. on Industrial Robot Technology and 6th Int. Symp. on Industrial Robots, University of Nottingham**, no. D2, pp. 9-20, 24-26 March 1976.

5. Drazan, P J, M F Jeffery, and J M Zarek, "Recent Developments in the Design of a Novel Electro-Pneumatic Robot," **Theory and Practice of Robots and Manipulators, Proc. 2nd Int. CISM IFT-o-MM Symp. Jadwisin, Poland**, pp. 143-150, 14-17 October 1976.

6. Drazan, P J and J M Zarek, "Controllability of an Electro-Pneumatic Manipulator," **3rd CISM IFT-o-MM Symp. Udine, Poland**, pp. 283-300, September 1978.

7. Drazan, P J and V Toulis, "The Use of Interpolation Routines for Path Generation and Control of an Electro-Pneumatic Industrial Manipulator," **Proc. 10th Int. Conf. on Industrial Robots and 5th Int. Conf. on Industrial Robot Technology, Milan**, pp. 313-320, 5-7 March 1980.

8. Drazan, P J and P B Thomas, "Simulation of an Electro-Pneumatic Manipulator System," **5th Int. Fluid Power Symp., Durham**, no. C5, pp. 59-72, BRHA Fluid Engg, Cranfield, Bedford, 13-15 September 1978.

9. Harada, M and O Oyama, "Position Control of Pneumatic Piston and Microprocessor," **9th Triennial World Cong. IFAC. Budapest, July 1984**, pp. 2785-90, Pergammon, Oxford, 1985.

10. Kaiho, F, O Oyama, and M Harada, "Digital Position Control of a Pneumatic Piston," **Papers of the Spring Meeting of Oil-Hydraulics and Pneumatics**, pp. 5-8, 1981. (In Japanese)

11. Moore, P R, F W Ssenkungo, R H Weston, T W Thatcher, and R Harrison, "Control Strategies for Pneumatic Servo Drives," **Int. Jour. Production Research**, vol. 24, no. 6, pp. 1363-1382, 1986.

12. Nagarajan, R and R H Weston, "Front End Control Schemes for Pneumatic Servo Driven Modules," **Proc. Instn. Mechanical Engineers, Part B**, vol. 199, no. B4, pp. 271-277, 1985.

13. Weston, R H, P R Moore, T W Thatcher, and G Morgan, "Computer Controlled Pneumatic Servo Drives," **Proc. Instn. Mechanical Engineers, Part B**, vol. 198B, pp. 175-281, December 1984.

14. Moore, P R, R H Weston, and T W Thatcher, "Control of Pneumatic Servo Drives Using Digital Compensation," **Proc. IASTED Int. Symp. on Telecommunications and Control, Halkidiki, Greece**, pp. 264-268, August 1984.

15. Gavrilovic, M M and M R Maric, "Positional Servo Mechanism Activated by Artificial Muscles," **Medical and Biological Engineering**, vol. 7, pp. 77-82, Pergammon Press, 1969.

16. Bousso, D, "Six Degree of Freedom Experimental Limb for Thalidomide Children," **Biomed. Engineering**, vol. 4, no. 7, pp. 313-321, July 1969.

17. Shearer, J L, "Study of Pneumatic Processes in the Continuous Control of Motion With Compressed Air - 1," **Trans. Am. Soc. Mechanical Engineers**, vol. 78, no. 233, pp. 233-242, February 1956.

18. Shearer, J L, "Study of Pneumatic Processes in the Continuous Control of Motion With Compressed Air - 2," **Trans. Am. Soc. Mechanical Engineers**, vol. 78, no. 233, pp. 243-249, February 1956.

19. Shearer, J L, "Non-Linear Analog Study of a High-Pressure Pneumatic Servomechanism," **Trans. Am. Soc. Mechanical Engineers**, vol. 79, pp. 465-472, April 1957.

20. Davies, R M and T H Lambert, "The Stabilization of Pneumatically Powered Prostheses," **Proc. 23rd Conf. Eng. Med. Biol., Washington Hilton Hotel, Washington DC**, vol. 12, p. 244, 15-19 November 1970.

21. Burrows, C R, D J Martin, and N D Ring, "Responses of a Pneumatically Powered Elbow-joint," **Proc. Conf. Hum. Locomotor. Eng., Sussex**, pp. 136-144, M.E.P, London, September 1971.

22. Lord, M and A Chitty, "Stabilisation of Pneumatic Prosthetic Systems," **Proc. Conf. Hum. Locomotor. Eng., Sussex**, pp. 175-180, M.E.P, London, September 1971.

23. Eun, T, Y J Cho, and H S Cho, "Stability and Positioning Accuracy of a Pneumatic On-Off Servomechanism," **Proc. of Amer. Control Conf. Arlington VA**, pp. 1189-1194, 1982.

24. Burrows, C R and C R Webb, "Simulation of an On-Off Pneumatic Servomechanism," **Proc. Instn. Mechanical Engineers, Part 1**, vol. 182, no. 29, pp. 631-642, 1967-68.

25. Burrows, C R and C R Webb, "Further Study of a Low-Pressure On-Off Pneumatic Servomechanism," **Proc. Instn. Mechanical Engineers, Part 1**, vol. 184, no. 45, pp. 849-857, 1969-70.

26. Bowns, D E and R L Ballard, "Digital Computation for the Analysis of Pneumatic Actuator Systems," **Proc. Instn. Mechanical Engineers**, vol. 186, pp. 881-889, 1972.

27. Sanville, F E, "A New Method of Specifying the Flow Capacity of Pneumatic Fluid Power Valves," **2nd Int. Fluid Power Symp.**, BHRA Fluid Engg., Cranfield, Bedford, January 1971.

28. Horlock, J H and W A Woods, "The Thermodynamics of Charging and Discharging Processes," **Proc. Instn. Mechanical Engineers, Part 3J**, vol. 180, pp. 16-24, 1965-66.

29. Bowns, D E, R L Ballard, and L Stiles, "The Effect of Seal Friction on the Dynamic Performance of Pneumatic Actuators," **3rd Int. Fluid Power Symp., Turin, Italy**, no. G3, pp. 29-48, BHRA Fluid Engg., Cranfield, Bedford, 9-11 May 1973.

30. Bowns, D E and R L Ballard, "Some Aspects of the Dynamic Behaviour of Pneumatic Actuators," **4th Int. Fluid Power Symp., Sheffield**, no. E2, pp. 19-37, BHRA Fluid Engg, Cranfield, Bedford, 16-18 April 1975.

31. Nguyen, H T, E Pachnicke, and P Anders, "Servo Pneumatic Cylinder Drive for Positioning Tasks," **6th Aachen Fluid Tech. Colloquium**, vol. 3, pp. 137-157, 27-29 March 1984. (In German)

32. **Design of Gas Bearings,** 1, Mechanical Technology Inc., 1969.

33. Mannetje, J J, "Pneumatic Servo Design Method Improves System Bandwidth Twenty-fold," **Control Engineering**, pp. 79-83, June 1981.

34. Bognor, I and L F Kazda, "An Investigation of the Switching Criteria for Higher Order Contactor Servomechanisms," **Trans. Am. Inst. Elect. Engrs.**, vol. 73, no. 2, pp. 118-127, 1954.

35. Hahn, D R C, "A Microcomputer Package to Draw Root Locus Diagrams," Honours Project Report, Department of Mechanical Engineering, University of Edinburgh, May 1985.

APPENDIX 1

CIRCUIT DIAGRAM OF INTERFACE UNIT

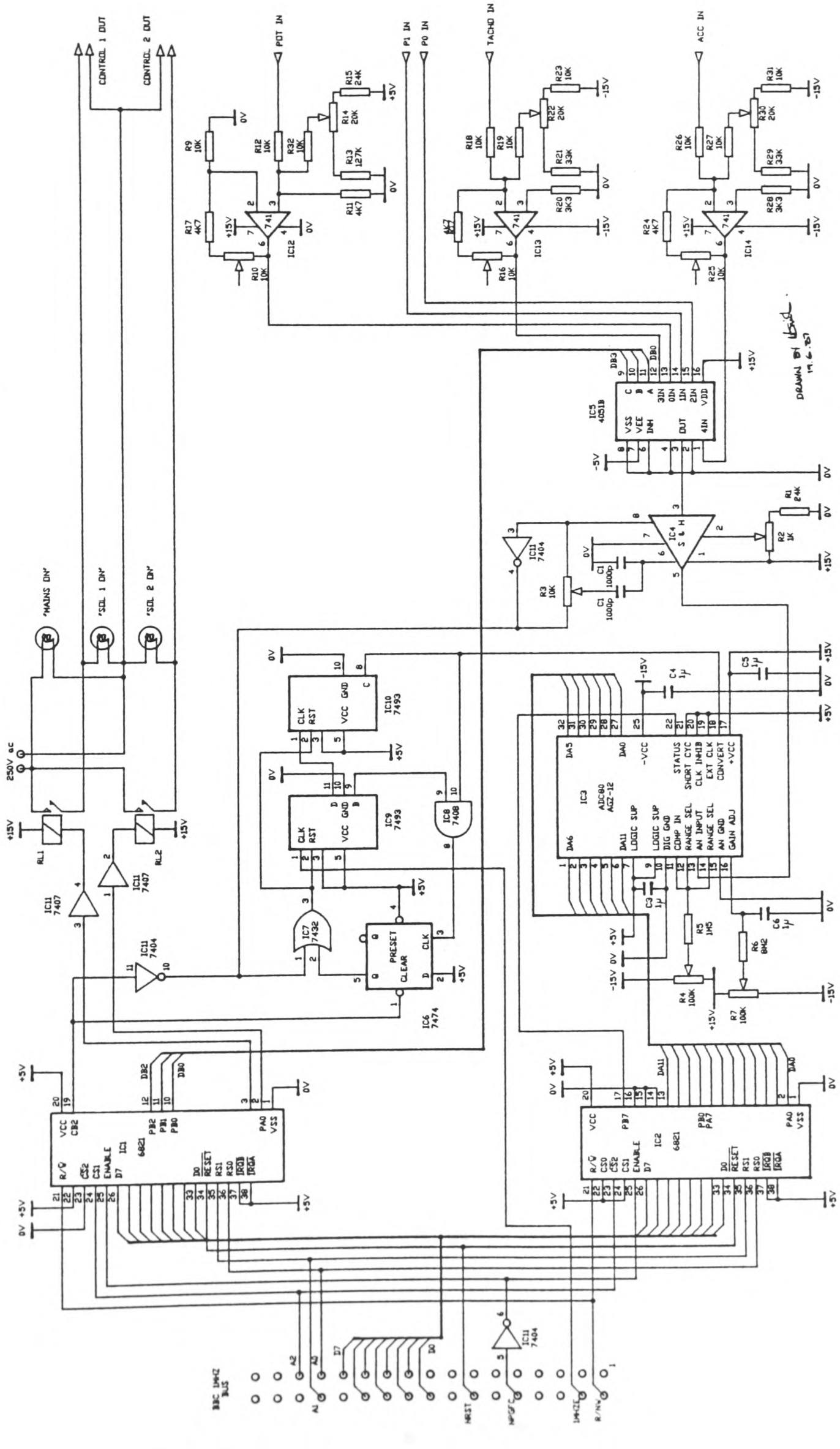

MODEL PROGRAMME FLOWCHART.

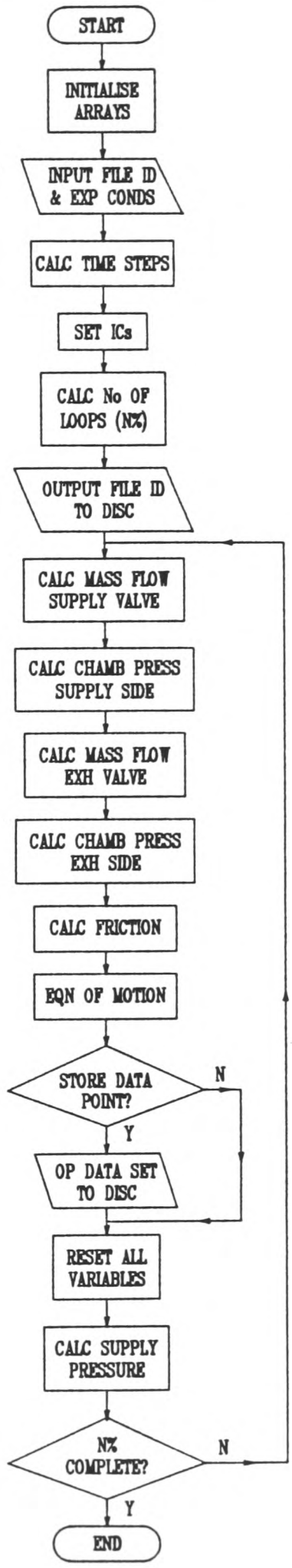

FOR DATA FORMAT ON DISC SEE APPENDIX 6

a) SYSTEM PROGRAMME FLOWCHART - SINGLE STEP.

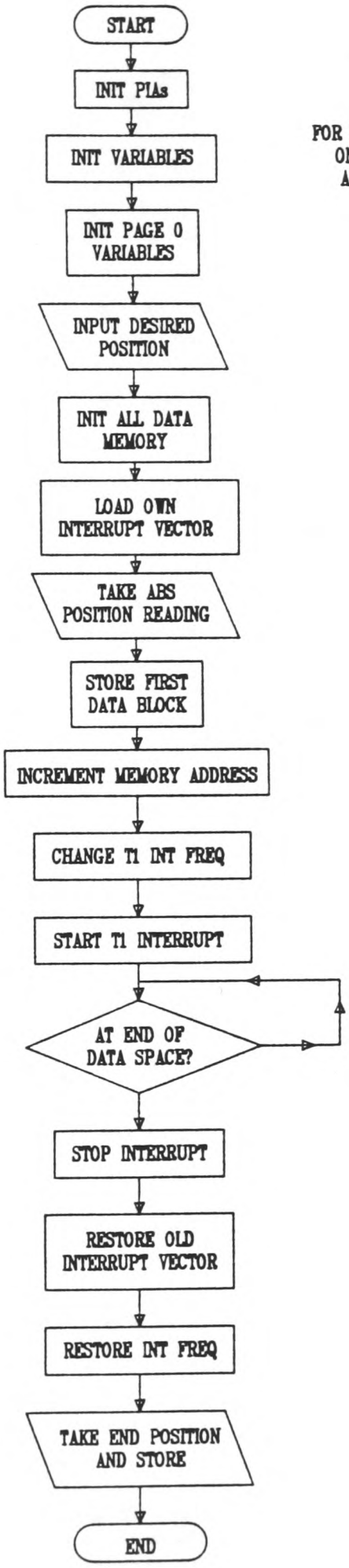

FOR DATA FORMAT ON DISC SEE APPENDIX 6

INTERRUPT ROUTINE

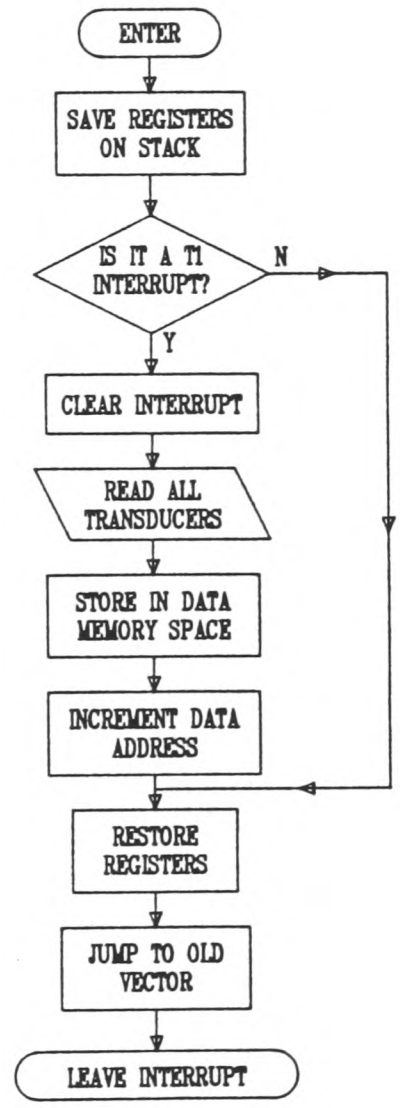

b) SYSTEM PROGRAMME FLOWCHART - MOTION IN TWO DIRECTIONS.

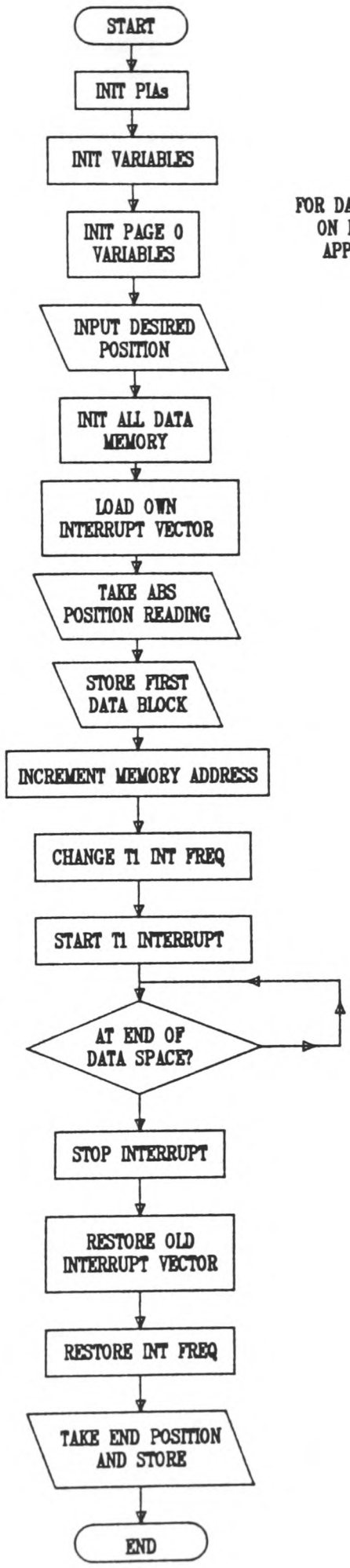

FOR DATA FORMAT ON DISC SEE APPENDIX 6

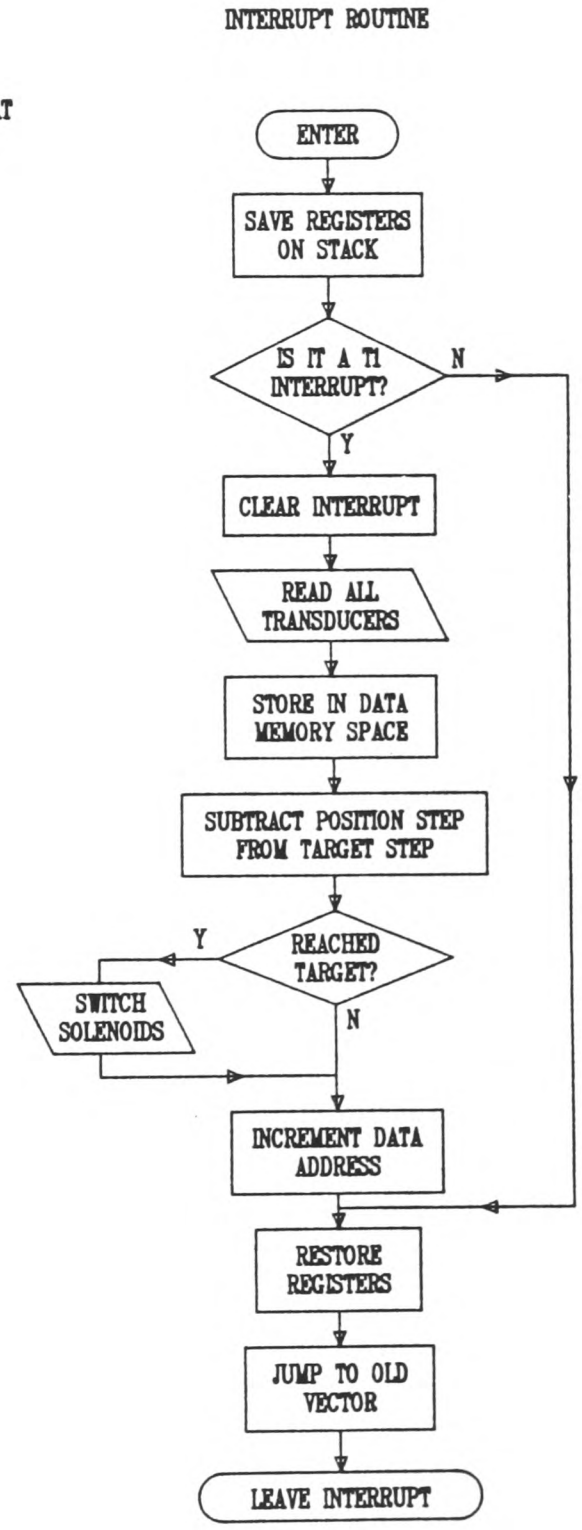

SIMULATION PROGRAMME FLOWCHART.

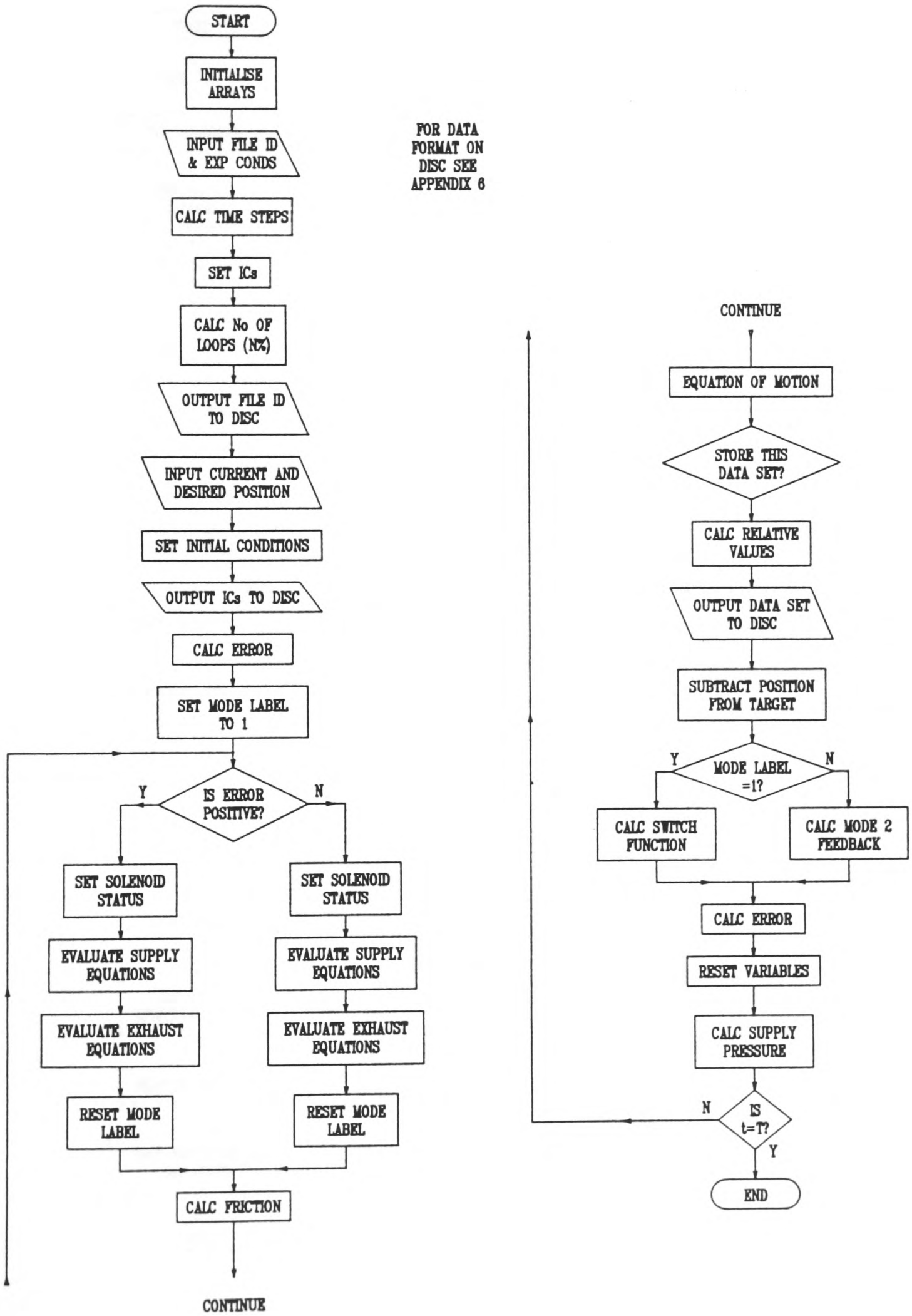

SYSTEM PROGRAMME FLOWCHART - DUAL MODE CONTROLLER.

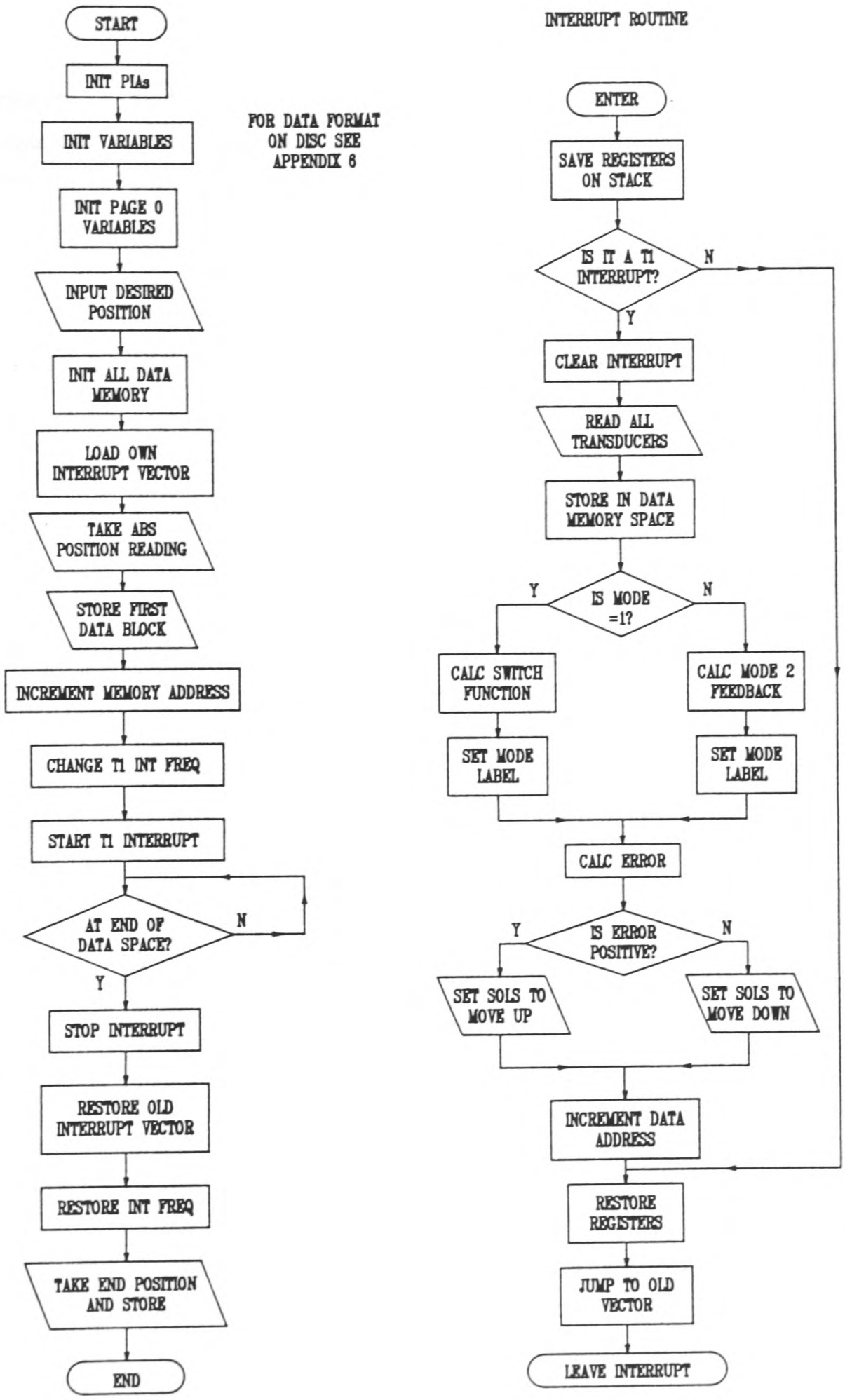

DATA STORE FORMAT ON DISC.

I = INTEGER
V = VARIABLE
S = STRING

I	Number of data points in file (N%)
V	Time step between data sets (ms)
S	Experiment number
S	Date
S	Text string
V	Initial supply pressure
V	Mass
S	Text string
S	Text string
V	Absolute end position
V	Step size
I	Solenoid 0 state
I	Solenoid 1 state
V	Relative position from start
V	Velocity
V	Pressure 0
V	Pressure 1
V	Acceleration
I	
I	
V	
V	
V	
V	
V	

DATA SET 1

V	
V	
I	
I	
V	
V	
V	
V	
V	

DATA SET N%

APPENDIX 7

PUBLICATION - LOW FRICTION PNEUMATIC ACTUATORS FOR ACCURATE ROBOT CONTROL.

Low friction pneumatic actuators for accurate robot control

J A LINNETT, MA, PhD and M C SMITH, BSc, CEng, MIMechE
Department of Mechanical Engineering, University of Edinburgh

SYNOPSIS The performance of two different types of pneumatic cylinder incorporating air bearings is compared with that of a cylinder using conventional seals at the end plates. Friction levels are reduced considerably if a PTFE piston seal is used in addition to the air bearings. This should enable a high accuracy pneumatic position control system to be developed for robot actuators.

1 INTRODUCTION

All of the present generation of precision robots employ either electric or hydraulic actuators. Pneumatic actuators are widely used in pick and place robots, where each actuator can only be driven from end stop to end stop. For this application the inherent problems associated with conventional pneumatic actuators caused by the compressibility of air and the high friction forces compared to the available thrust, are not too important. These problems become very significant if pneumatic actuators are to be used for accurate position control.

On the positive side, pneumatic actuators are cheap, clean and safe for use in hazardous environments. This has encouraged research effort to produce low cost pneumatic servo-drives (1,2, 3,4). The development of microelectronics has enabled complex algorithms to be implemented which can be used to compensate for some of the problems in pneumatic systems such as high friction, little natural damping, long time delays and component non-linearities. This has resulted in much improved system performance and has led to the development of some precision robots (5,6). The control problem should become simpler if the Coulomb friction associated with pneumatic cylinders could be reduced significantly.

The work described in this paper dealing with low friction actuators, is the first part of a research programme aimed at producing a very accurate pneumatic position control system suitable for robotic applications. Air bearings are used in place of conventional seals at the ends of the cylinder. These, together with low friction seals at the piston, have resulted in very low friction levels being achieved.

2 THE REDUCTION OF FRICTION LEVELS

The principal cause of friction in pneumatic cylinders is the seals where the piston rod passes through the end plates. This friction should be reduced considerably if the conventional rubber seals are replaced by air bearings. The remaining friction would then be between the piston and the cylinder. It might be possible to use air bearings here too, but simpler low friction seals were chosen for this first investigation. Two types were selected for comparision; a composite PTFE seal, which appeared to have the lowest friction characteristics of the available conventional seals, and a rolling rubber diaphragm which had the additional advantage of eliminating any air leakage between the two halves of the cylinder.

Two cylinders were designed. Type 1 uses a PTFE composite seal at the piston, fitted as shown in Figure 1. Type 2 uses two rubber diaphragm seals mounted as shown in Figure 2. Both designs incorporated almost identical air bearings where the piston rod passes through the end plates. These air bearings are described in detail in section 2.1

As a comparison to these cylinder designs a typical pneumatic ram of comparable size was bought 'off the shelf'. This design is referred to as Type 0. The specification of the three cylinders is given in Table 1.

2.1 Air bearing design

A drawing of the air bearing assembly used in cylinders 1 and 2 is shown in Figure 3. In order to obtain a statically stable air bearing some form of external restriction is required. This ensures that the bearing load capacity increases with a decrease in bearing film thickness, i.e. that the bearing has 'stiffness'. It can be shown that there is an optimum ratio between the external restriction and the restriction offered by the bearing film in order to obtain maximum bearing stiffness. This was the basis for the choice of design parameters. (7)

2.1.1 Specification

Supply pressure	=	80 lbf/in²
Rod diameter	=	18 mm nom.
Stroke	=	300 mm. max.
Radial clearance	=	0.02 mm
Bleed hole dia.	=	0.2 mm
No. of bleed holes	=	10 in each of 2 planes
Restrictor type	=	Inherrent orifice.

Some variation of straightness and concentricity of the piston and cylinder is certain with a bearing stroke of this length and so the two bushes were mounted on rubber 'O' rings to allow some self alignment.

3. TEST RIG DESIGN

The test equipment is controlled by a BBC B microcomputer interfaced with a solenoid controlled on-off pneumatic valve. The computer can read from three analogue transducers which measure ram position and the two chamber pressures (Table 2). A schematic drawing of the arrangement is shown in Figure 4. The computer interface consists of two 6821 Programmable Interface Adaptors (PIA's), a 12 bit analogue to digital converter (ADC) and an analogue multiplexer. The interface was controlled and read with a machine code program written with the BASIC assembler. The on-off pneumatic valve was chosen for its simplicity and was found to be adequate for this early test work.

4. TEST METHODS

The cylinders were mounted horizontally in all of the tests. Before carrying out any of the tests each of the designs was cycled between the two extremes of their motion 2000 times, in order to bed in the seals.

4.1 Static friction measurement

With the piston in a chosen position, the chamber pressure on one side was slowly increased until movement was detected by the linear potentiometer. The two chamber pressure readings taken immediately prior to this were used to calculate the driving force which equates to the static friction force of the ram assembly in the cylinder.

4.2 Dynamic friction measurement

The ram was driven at a constant velocity and the two chamber pressures were recorded at the desired piston position. These pressures were used to calculate the dynamic friction force.

5 RESULTS

5.1 Static friction

The results of the static friction tests are shown in Figure 5. Type 1 is seen to have the lowest static friction while the comparison cylinder Type 0 has the highest.

There is a variation in friction of over 15N along the stroke for both cylinders 0 and 2. Type 1 shows a much flatter friction characteristic with a slight rise at each end. This rise was probably due to the misalignment of the end caps, cylinder bore, and piston rods. It would be caused by a breakdown of the air bearing film where the '0' ring self alignment was not sufficient. This flatness of the friction curve, except at the ends, may well prove to be as significant as its low absolute value. Large variations along the piston stroke, which are a feature in Type 0 and Type 2, would have to be accounted for in the control algorithm.

In cylinder 0 these large variations of friction are probably due to dimension variations within the cylinder, perhaps in roundness or concentricity, and there will be a variation between 'off the shelf' examples of the same design.

In cylinder 2 the trend is an increase of friction towards the centre of the stroke. This can be explained by the behaviour of the rubber diaphragm as the piston begins to move. At the ends of the stroke the majority of one seal is not trapped in the clearance between piston and cylinder, it is lining some of the wall of the larger chamber volume (see Figures 2a and 2c). This will allow it to 'ripple' as the piston moves a small amount. At the centre stroke position, Figure 2b, both seals are within the piston cylinder clearance where the 'rippling' cannot so easily take place. These effects are emphasised because of the low pressures used during the tests.

5.2 Dynamic friction

The results of the dynamic friction tests are shown in Figure 6. Again, cylinder 1 is seen to have the lowest friction but this time it is cylinder 2 which has the highest. Furthermore the friction levels for cylinder 2 are larger than those obtained in the static test, which is contrary to the normal Coulomb friction characteristic. The explanation must be due to the dynamic behaviour of the rubber seal as the piston is moving. There are two main effects. The first is the hysteresis in the rubber seal. The total length of fold in the 1 mm reinforced rubber diaphragm is approximately 460 mm. These convolutions require some work to roll them up and down the piston. This would account for an overall increase in friction level. The second effect is the physical contact between the two sides of the convolution that must move relative to each other as the piston moves. The rubber is lubricated, but some friction will exist between these surfaces. This will account for the rising friction in the centre stroke position as the area of contact is a maximum at the centre and a minimum of the end of the stroke. (Fig. 2).

Dynamic friction for Type 0 is slightly lower than its static friction as expected, the variation along the length is similar and can be explained in the same way. Type 1 has approximately the same level of dynamic and static friction. Any difference was beyond the accuracy of the test equipment.

6 CONCLUSIONS

The Type 1 cylinder using a combination of air bearings as a piston rod/cylinder seal and a PTFE composite piston ring, has a considerably lower friction level than either the standard Type 0 cylinder or the Type 2 cylinder which also had air bearings but used a rolling piston seal. The performance of the rolling piston seal was particularly disappointing in the dynamic friction case, where it did not perform as well as the standard cylinder. It seems that this type of seal has little to recommend it for lower pressure cylinders. The performance of the Type 1 cylinder was very impressive. Its friction level was only 10% of that of the standard cylinder over the central 90% of the piston travel. Furthermore the friction level is almost constant over this length. It is possible that friction levels could be reduced still further by the use of air bearings at the piston as well as the end seals. This may be investigated at a later stage.

The Type 1 cylinder will enable the next stage of the research to proceed. The low and constant friction level should simplify the control problem so that simple pneumatic valves can

be used to switch the air supply, with compensation being provided by software in real time computer control.

ACKNOWLEDGEMENTS

The authors acknowledge the financial support of the Science and Engineering Research Council, and the invaluable assistance of Mr. A. Thomson, Mechanical Engineering department workshop.

REFERENCES

(1) SHEARER, J. L. Study of pneumatic processes in the continuous control of motion with compressed air. I and II. Trans. Am. Soc. Mech. Engrs., 1956, 78, 233.

(2) CUTLAND, M. J. Response of a pneumatic servomechanism. MSc Thesis, University of London, 1967.

(3) BURROWS, C. R. Effect of position on the stability of pneumatic servomechanisms. J. Mech. Eng. Sci., 1969, 11, 615-616.

(4) CHITTY, A., LAMBERT, T. H. Modelling a two-way pneumatic actuator. J. Measurement and Control, 1976, 9, 19-25.

(5) DRAZAN, P. J., THOMAS, P. B. Simulation of an electro-pneumatic manipulator system. 5th Int. Fluid Power Symp. Durham, 1978, C5-59-72.

(6) WESTON, R. H., MOORE, P. R., THATCHER, T. W., MORGAN, G. Computer controlled pneumatic servo drives. Proc. Inst. Mech. Engrs., Part B, 1984, 198 (14), 275-281.

(7) VOHR, J. H. Restrictor flows. Design Notes. Design of Gas Bearings, Mechanical Technology Inc., 1969, 1, 5.1.1-5.1.21.

Table 1 Specifications of the three cylinder types

		TYPE 0	TYPE 1	TYPE 2
Type		Double acting asymmetric	Double acting symmetric	Double acting symmetric
Nominal bore	mm	57.0	63.5	76.0
Stroke	mm	204	295	120
Piston seal		plastic ring rubber U cups	PTFE composite	rubber diaphragm
Cylinder material		Al. alloy	Al. alloy	Al. alloy
Piston type		solid	split	split
Piston diametral clearance	mm	1.0 max	0.6 max	7.9
Piston rod dia	mm	15.6	18	18
Rod/cylinder seal		rubber wiper bronze bush	air bearings	air bearings

Table 2 Transducer range and digital conversion accuracy

Transducer	Voltage range	Measurement range	Quantisation error
Linear potentiometer	0-10 V	0-450 mm	±0.055 mm
Pressure	0-10 V	0-100 lbf/in² g	±0.013 lbf/in²

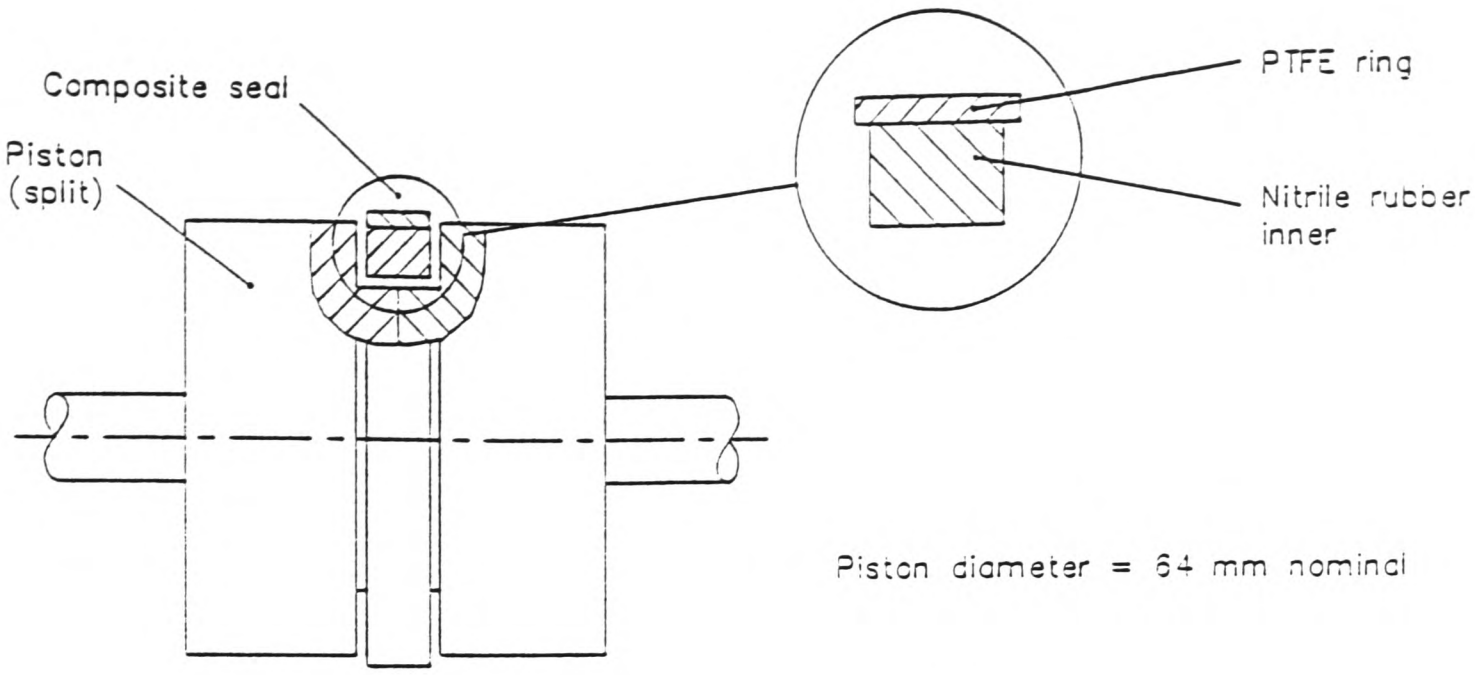

Fig 1 The PTFE composite piston seal used in cylinder 1

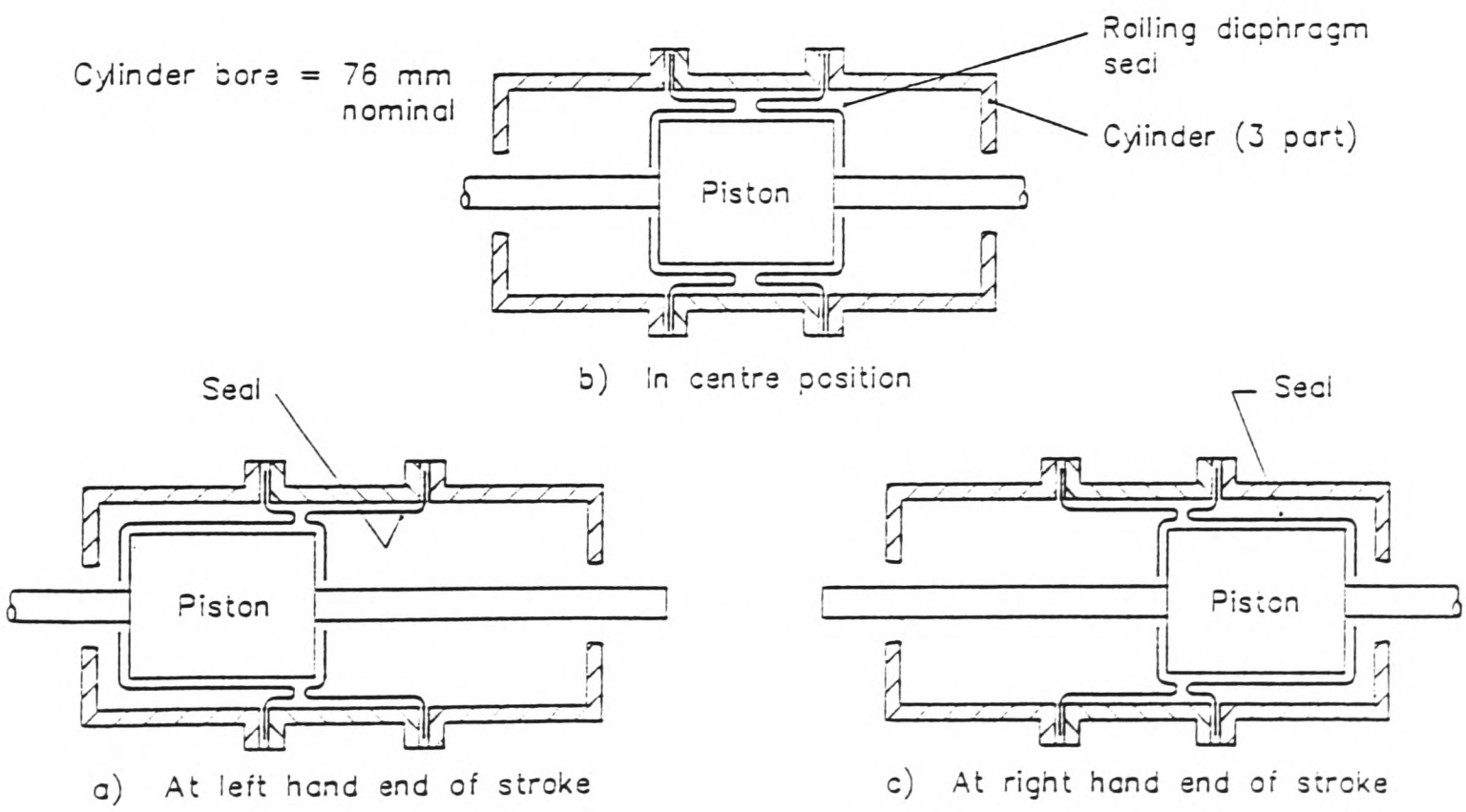

Fig 2 The rubber diaphragm seal assembly used in cylinder 2

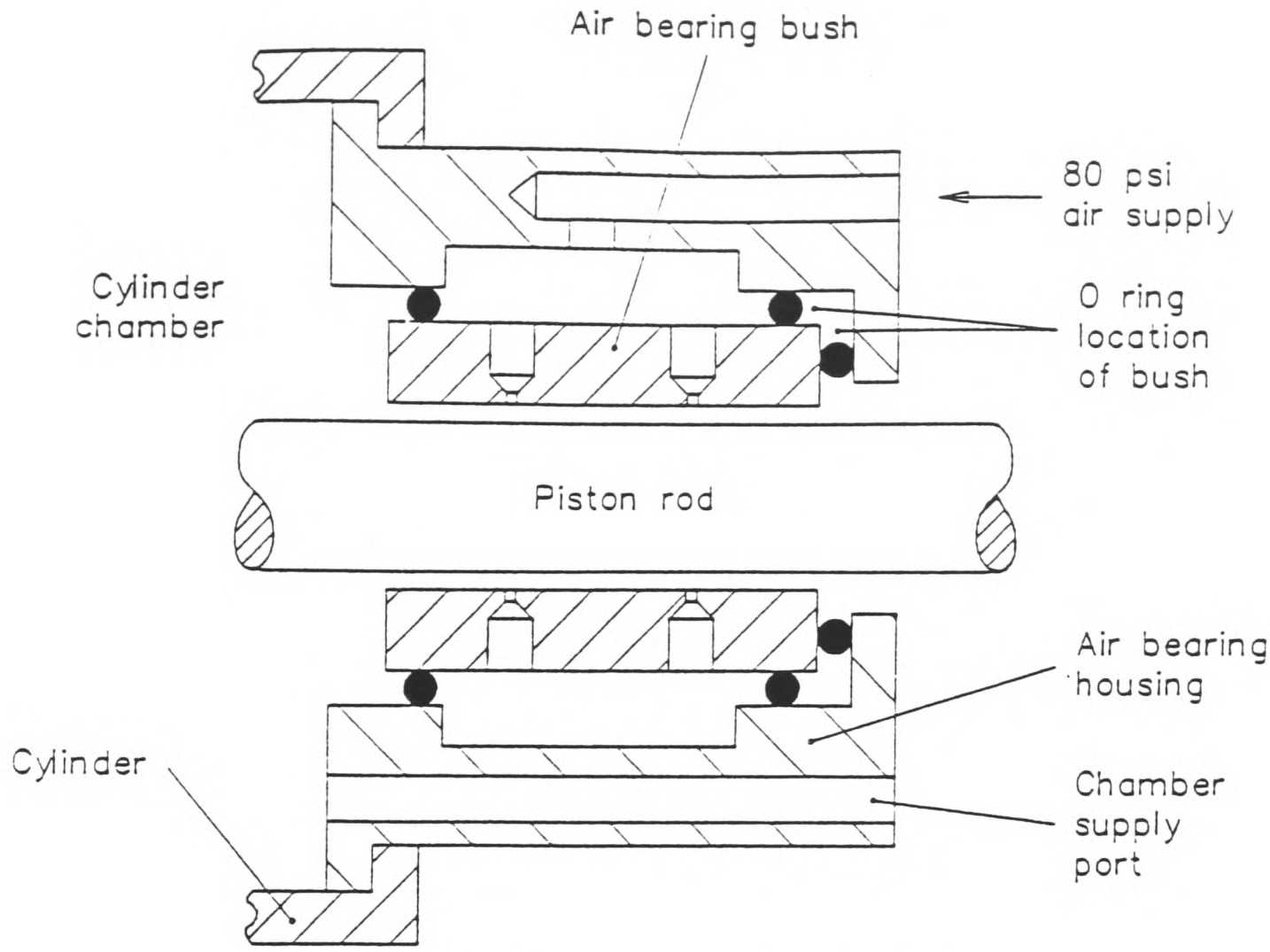

Fig 3 Sketch of air bearing assembly used in Cylinders 1 and 2

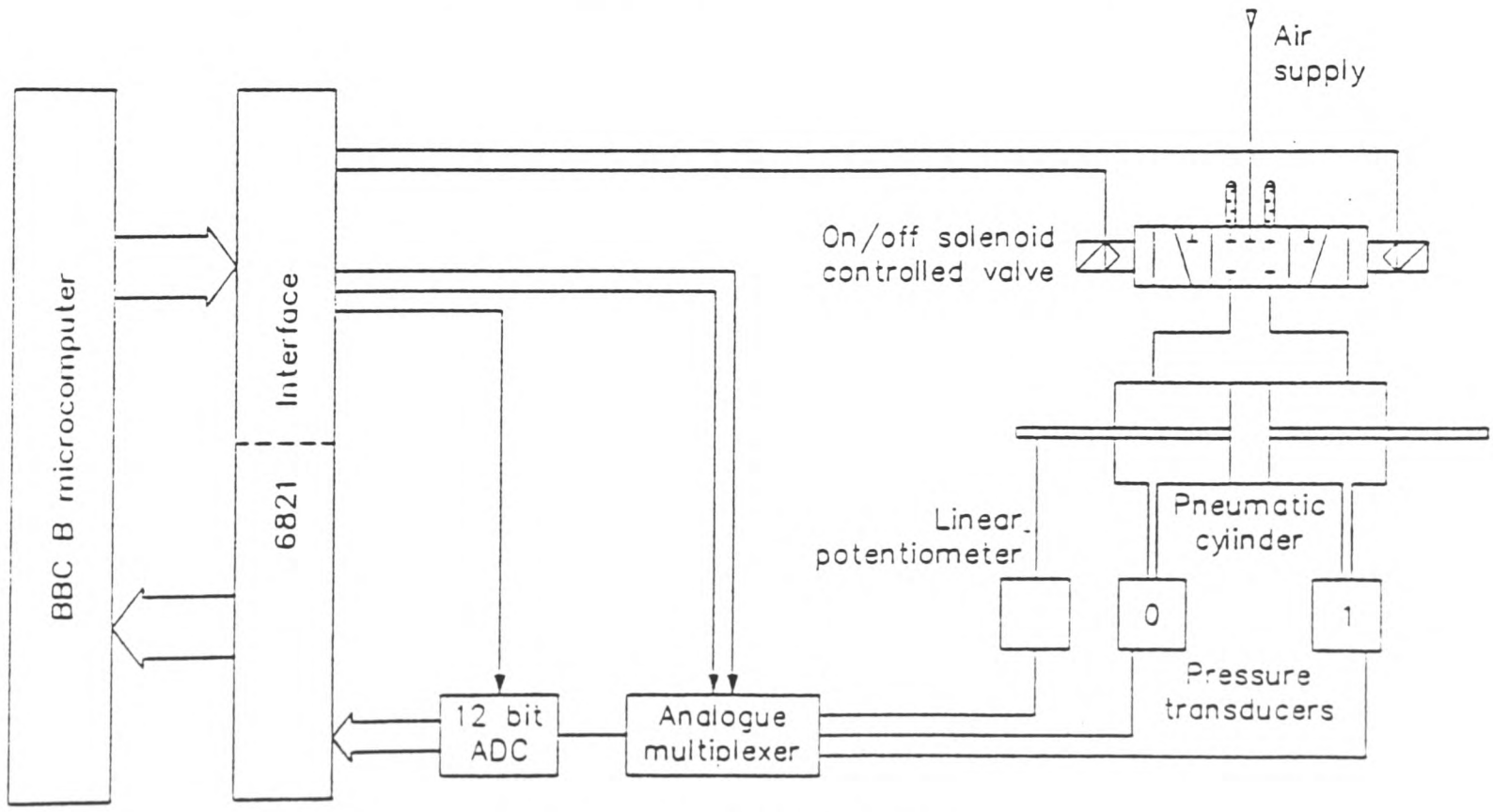

Fig 4 Schematic drawing of test equipment

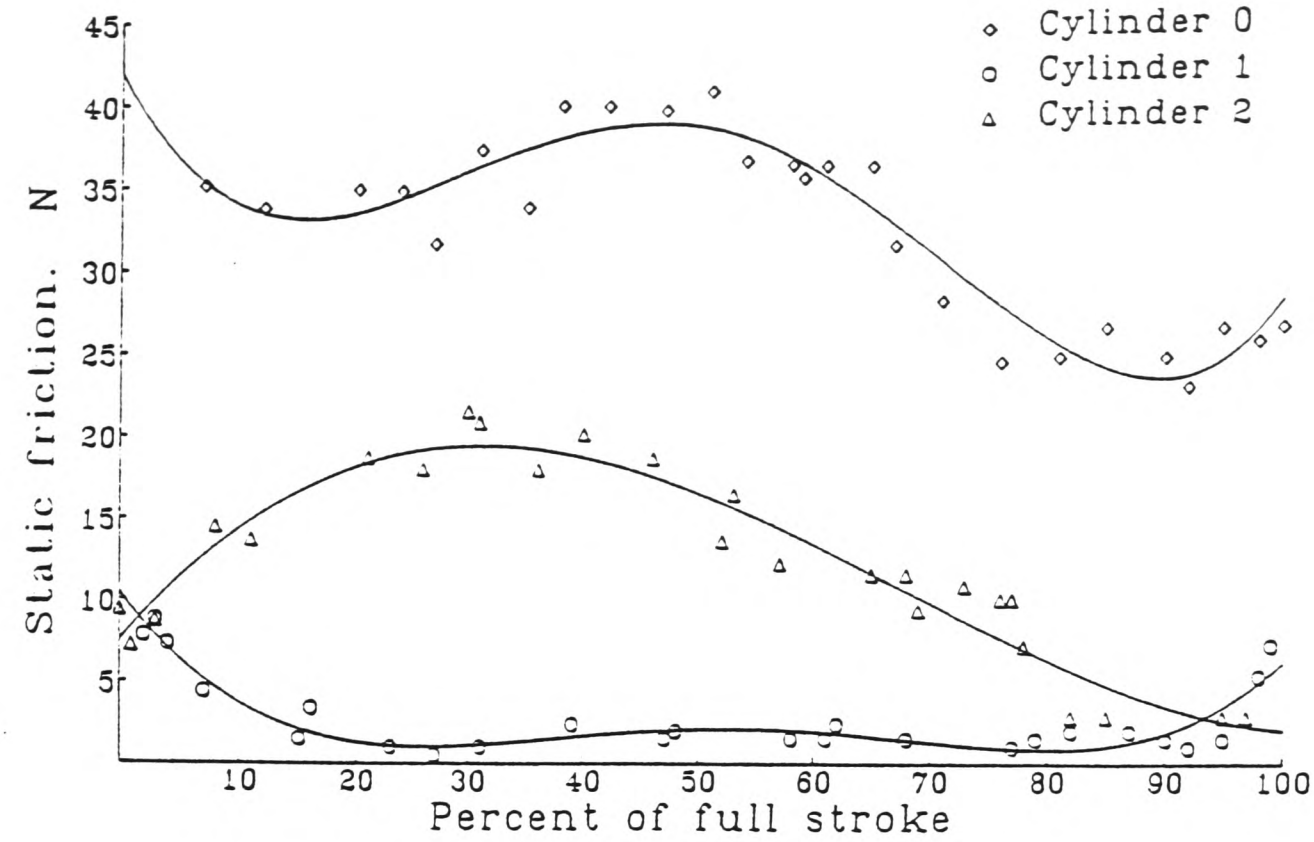

Fig 5 Variation of static friction with piston position

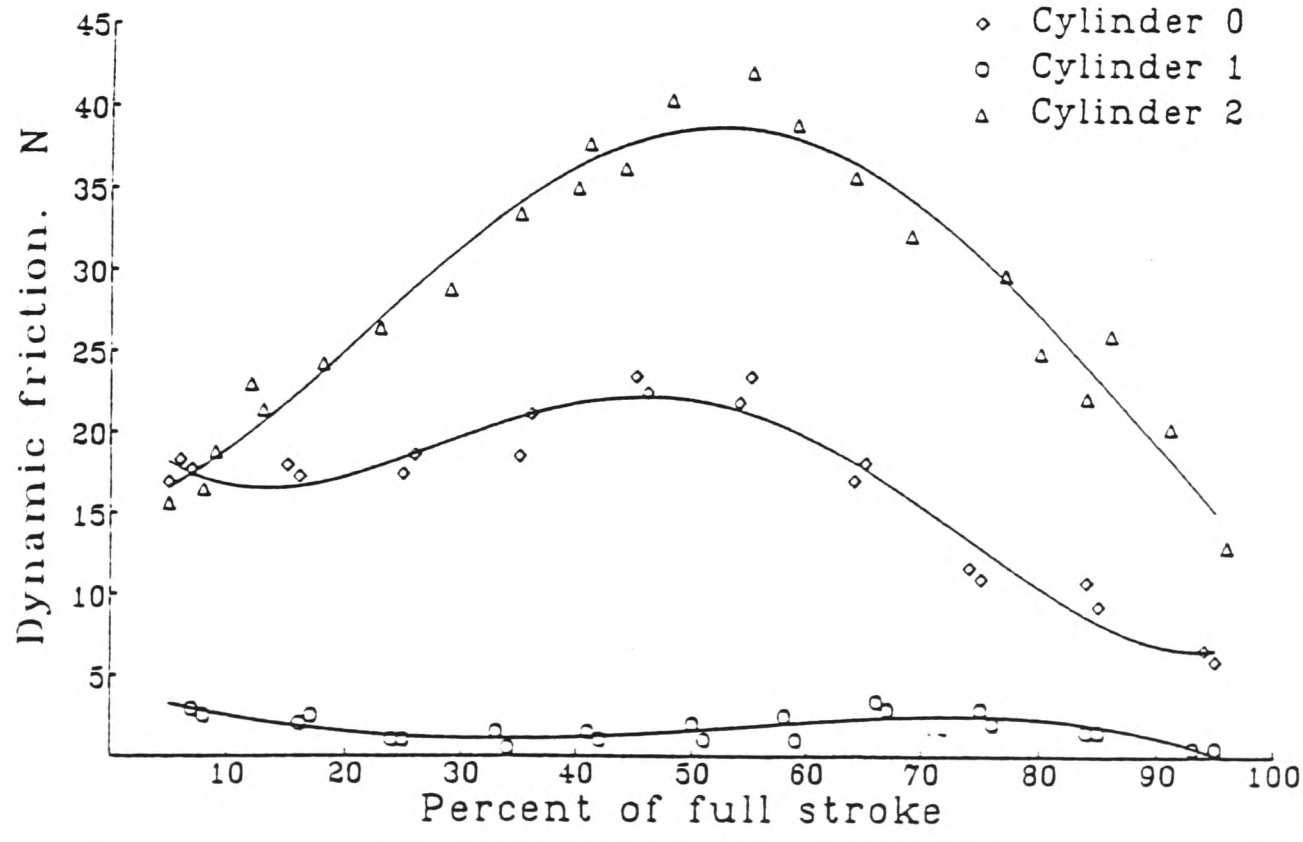

Fig 6 Variation of dynamic friction with piston position

ACKNOWLEDGEMENTS

The author is very grateful to Dr Alan Linnett of the Department of Mechanical Engineering for his keen and helpful supervision and his clear guidance throughout the course of the project. Particular thanks are due also to Mr Alan Thomson of the Mechanical Engineering workshop for his invaluable contribution to the design and construction of the test equipment used. Finally, I would like to acknowledge the financial support of the Science and Engineering Research Council.

DECLARATION

I hereby declare that this thesis was composed
by myself and that it describes my own work.